Colloïdes et compositions élémentaires des solutions de sols

Mathieu Pédrot

N° ordre : 3975 **Année 2009**

THÈSE / UNIVERSITÉ de RENNES 1

sous le sceau de l'Université Européenne de Bretagne

pour obtenir le grade de

DOCTEUR DE L'UNIVERSITÉ DE RENNES 1

Mention : **Sciences de la Terre**

École doctorale : **Sciences de la Matière**

présentée par

Mathieu PÉDROT

Préparée à l'unité de recherche : **Géosciences Rennes**

Composante universitaire : **UFR Structure et Propriétés de la Matière**

Colloïdes et compositions élémentaires des solutions de sols

Soutenue à Géosciences Rennes, le **9 octobre** 2009 devant le jury composé de :

Président	Gérard Gruau	CNRS-Université de Rennes 1
Rapporteurs	Gérard Blanc	Université de Bordeaux I
	Jérôme Viers	Université de Toulouse III
Examinateur	Marc Steinmann	Université de Franche-Comté
Directrices de thèse	Aline Dia	CNRS-Université de Rennes 1
	Mélanie Davranche	Université de Rennes 1

À Jérôme, mon frère Jumeau

À Vanessa et Paméla, mes deux Sœurs

À mes Parents

À Céline !

"Fais de ta vie un rêve

Et d'un rêve, une réalité"

Antoine de Saint-Exupéry

Remerciements

Ce travail, fruit de trois années de recherches, ne serait ce qu'il est sans l'aide et le soutient de nombreuses personnes. Je tiens ainsi à remercier toutes les personnes qui ont suivi de prés ou de loin cette formidable aventure :

Je tiens tout d'abord à adresser mes plus vifs et sincères remerciements à mes deux directrices de thèse, Aline et Mélanie. Elles m'ont accordé toute leur confiance tout au long de ma thèse. Merci pour cette expérience unique et très enrichissante,

Merci aux Messieurs les membres du Jury, Gérard Blanc, Jérôme Viers, Marc Steinmann et Gérard Gruau d'avoir accepté de juger mon travail et pour l'intérêt que vous y avez porté,

Merci au laboratoire Géosciences Rennes, et plus particulièrement à l'équipe Géochimie des Interfaces qui m'on accueilli et soutenu durant ces trois années, merci à Gérard, Émilie, Anne-Catherine, Martine, Odile, Patrice. Vous avez tous participé à l'élaboration de ces 3 années de recherches fructueuses de par vos conseils constructifs et de votre expérience analytique et technique que vous m'avez apportés,

Merci aux stagiaires M2, doctorants et ex-doctorants de l'équipe, Olivier, Mohammad, Morgane, Rémy, Thibault, Ange, Anne... pour l'aide et les conseils que vous m'avez apportés et pour le soutient que vous avez toujours exprimé,

Merci à ma Famille et à mes Amis, Marc, Christophe[2], Mathieu[2], Grég, Stéphanie, Sandrine, Pauline, Yann, Antoine, Sébastien... qui m'ont "supporté", soutenu et exprimé à plusieurs reprises de la curiosité envers mon travail, même si pour vous le sol n'est autre qu'un mélange de terre et de cailloux, voici maintenant l'entrée des colloïdes et des éléments traces !!!

Merci !

Sommaire

Colloïdes et compositions élémentaires des solutions de sols

Résumé :

Ubiquistes, dynamiques et caractérisés par d'importantes capacités de complexation de surface, les colloïdes sont supposés jouer un rôle majeur dans la mobilisation des éléments traces dans les eaux et les sols. Cette étude a pour objectif d'améliorer la compréhension du rôle des colloïdes dans la mobilisation des éléments traces en définissant (a) l'impact de paramètres physico-chimiques sur la composition élémentaire et colloïdale de la phase dissoute d'un sol de zone humide, (b) les modes de genèse de ces colloïdes, ainsi que leur rôle de phases porteuses et vectrices d'éléments traces dans les eaux et les sols.

Les différents travaux accomplis mettent en avant un contrôle colloïdal pour de nombreux éléments traces présents dans la solution de sol. Ainsi, certains éléments sont fortement complexés par le compartiment colloïdal (Al, Cr, U, Mo, Pb, Ti, Th, Fe, et les REE), d'autres le sont plus modérément (Cu, Cd, Co, et le Ni) et une autre partie ne réagit pas avec les colloïdes (Li, B, K, Na, Rb, Si, Mg, Sr, Ca, Mn, Ba et le V). Le pH apparaît être un facteur majeur de contrôle de la composition élémentaire de la phase dissoute ; un changement du pH, à la hausse ou à la baisse impactant fortement les concentrations et la composition colloïdale et élémentaire de la solution de sol. De plus, le pH apparaît un acteur non négligeable de la conformation des substances humiques, principales molécules organiques actives dans la mobilisation des éléments traces dans le milieu naturel, impactant ainsi leur mobilité et celles des éléments associés. Les résultats ont confirmé la présence d'associations supramoléculaires de petites molécules organiques au sein des substances humiques, ainsi que la présence de nanoparticules de Fe intimement liées à la matière organique, et pouvant mobiliser certains éléments traces comme le Pb ou le Ti.

De plus, ce travail a permis de mesurer l'impact des substances humiques sur la vitesse d'oxydation-hydrolyse du Fe, et sur la taille des oxyhydroxydes formés. Les substances humiques tendent ainsi à ralentir et à diminuer les réactions d'oxydation-hydrolyse du Fe, et impactent directement la taille des oxydes de Fe. Le Fe est ainsi présent soit sous forme ionique et complexé aux substances humiques, soit sous forme de nanoparticules et inclus dans la matrice organique. La biodisponibilité de ces nanoparticules de Fe à être utilisée comme accepteur d'électrons par des bactéries *Schewanella putrefaciens* a ensuite été testée en comparaison de celle de particules de Fe formées en absence de substances humiques. Les résultats évoquent une biodisponibilité accrue des nanoparticules de Fe associées aux substances humiques lors de la bioréduction. Ce résultat prouve que les colloïdes mixtes Fe-matière organique représentent dans les zones humides, un stock majeur de fer régulièrement sollicité par la microfaune, bien plus accessible que celui du fonds géochimique.

Mots clés : Colloïdes, substances humiques, nano-oxydes, Fe, éléments traces, complexation, pH, force ionique, bioréduction, *Schewanella putrefaciens*.

Colloids and soil solution elemental compositions

Abstract :

Ubiquitous, dynamic, as well as characterized by important surface complexation ability, colloids are meant to play a key role in trace element sequestration in both waters and soils. This study was aimed on improving the understanding of the role played by colloids in trace element carriage in focusing on: (i) the study of the impact exerted by physico-chemical parameters on the colloidal and elemental composition of the dissolved phase circulating within wetlands, (ii) the colloid genesis ways and their respective role as carriers and vectors of trace elements in waters and soils.

The different performed experiments put forward a colloidal control for a lot of trace elements occurring in the soil solution. Some of these latter are strongly complexed by the colloidal pool such as (Al, Cr, U, Mo, Pb, Ti, Th, Fe, and REE), while others are more little complexed (Cu, Cd, Co, and Ni), and a last part which remains unreactive regards to colloids (Li, B, K, Na, Rb, Si, Mg, Sr, Ca, Mn, Ba and V). pH appears to be one major control parameter on the elemental composition of the soil solution, with any pH increase or decrease putting strong impact on the soil solution colloidal and elemental compositions. Furthermore, pH does largely play on the humic substance conformation, which are the main active organic molecules involved in the trace element sequestration within nature, impacting thus their own mobility and that of associated trace elements as well. This study also evidences the occurrence of supramolecular associations of small organic molecules within humic substances, as well as the presence of Fe-nanoparticles intimately bound to organic matter. These latter can sequestrate specific elements such as Pb or Ti.

This study allowed also to evaluate the impact of the humic substances on both the Fe oxidation-hydrolysis rate and the size of the precipitated oxyhydroxides. Humic substances slow down and decrease the Fe oxidation-hydrolysis reactions and impact directly the Fe oxide size. Iron is therefore, either as ionic state complexed with humic substances, or as nanoparticles included within an organic matrix. The bioavailability of these Fe-nanoparticles to be used as electron acceptor by *Schewanella putrefaciens* bacteria during bio-reduction was then tested compared to that of crystallyzed iron in inorganic medium. Mixed Fe-humic substance colloids showed a more important bioavailablity than did inorganic crystallyzed Fe. This latter result evidences that in wetlands, mixed Fe-organic matter colloids represent a major Fe stock, which is regularly requested by microfauna, since much more available than can be that of the geochemical bedrock/soil.

Keywords: Colloïds, humic substances, nano-oxides, Fe, trace elements, complexation, pH, ionic strength, bio-reduction, *Schewanella putrefaciens*.

Chapitre I : Introduction

I. Contexte de l'étude

Les 68 éléments chimiques constituants de la croûte continentale terrestre, dont la concentration est pour chacun d'entre eux inférieure à 0.1 %, composent le groupe des éléments traces (Baize, 1997). Ces éléments ne représentent que 0.6 % du total des éléments chimiques de la croûte terrestre, cependant leurs effets sur les écosystèmes sont souvent majeurs. Les éléments traces sont naturellement contenus dans les sols (fond pédogéochimique) et sont issus de l'altération des minéraux des roches, des émissions volcaniques et de la diffusion éolienne des aérosols naturels. Les sols reçoivent aussi des flux d'éléments traces d'origine anthropique par les apports industriels, les apports agricoles et domestiques. Certains de ces éléments, appelés oligoéléments, s'avèrent indispensables à l'activité biologique à des concentrations raisonnables : Cu, Zn, Ni, Cr, Co, Mn, V, Mo, Se ou Sn. Cependant, ces éléments peuvent également être toxiques à fortes teneurs ou sous certaines formes chimiques. L'utilisation d'éléments métalliques, et par conséquent leur inévitable dispersion dans l'environnement (eau, sol et atmosphère), n'a cessé de croître au cours du XXe siècle. La contamination des sols qui en découle constitue un enjeu fondamental, non seulement parce qu'elle affecte notre environnement proche, mais aussi et surtout parce qu'elle est susceptible d'affecter notre alimentation en eau potable et en denrées 'propres'.

L'objectif de nombreuses études s'intéressant aux éléments traces est de prévoir *in fine* le devenir des éléments traces dans les sols et les eaux, et de mieux appréhender leur circulation dans les environnements de surface. Différents modèles géochimiques ont permis de simuler la migration des métaux dans les sols (Amoozegar-Fard et al., 1984; Selim et al., 1992), et il s'est avéré que dans certains cas ces modèles sous-estimaient cette migration. Ce manque de concordance entre les valeurs prédites et la migration observée sur le terrain a été attribuée au transport facilité des métaux par les colloïdes, i.e. des nanoparticules très mobiles dans le sol (Seaman et al., 1995). En effet, la plupart des prévisions de transport de contaminants sont basées sur des modèles d'adsorption à l'équilibre entre une phase dissoute et une phase immobile (qualifiée de sorbante). Dans cette hypothèse, la vitesse de mobilité des contaminants est liée à la solubilité des contaminants et à la vitesse de transport de l'eau souterraine. L'apparition inattendue de contaminants très peu solubles à une forte distance de la source a conduit à envisager le rôle joué par des colloïdes mobiles dans le transport des micro-polluants (McCarthy et Zachara, 1989; Penrose et al., 1990 ; Grolimund et al., 1996;

Honeyman, 1999; Kersting et al., 1999; Sen et al., 2002). Des études couplées ou non à de la modélisation suggèrent ainsi qu'une large fraction des éléments, pourrait être associée aux colloïdes (Dai et al., 1995; Karathanasis, 1999). Les colloïdes immobilisent les éléments traces à la suite de leur propre immobilisation ou provoquent leur transfert au sein de l'écosystème à la suite de leur propre migration dans les eaux souterraines ou les eaux de surface. Ainsi, la mobilité des éléments est contrôlée par leur distribution au sein: (a) des phases solides immobiles, (b) des particules colloïdales mobiles et (c) de la phase dissoute (Kretzschmar et al., 1999). Dans le premier cas, les quantités disponibles sont infimes et ont un impact limité sur l'environnement. Mais lorsque les conditions climatiques ou physicochimiques changent de telle manière que les éléments traces métalliques (re)deviennent mobiles, l'augmentation de leur concentration représente alors une menace directe pour l'environnement, du fait de l'augmentation de leur biodisponibilité et donc de leur toxicité potentielle (Zmirou et al. 2000).

Ryan et Elimelech (1996) ont montré que le critère majeur de contrôle du transport colloïdal était la quantité de colloïdes présente en solution. Dans les sols, la concentration de colloïdes mobiles varie de 1 $mg.L^{-1}$ à plusieurs centaines de $mg.L^{-1}$ (Grolimund et al., 1998). Pour prédire le potentiel de transport des colloïdes, il est donc indispensable de définir la quantité et la nature des particules colloïdales présentes dans la zone de sub-surface, elles-mêmes dépendantes des sources et des processus responsables de leur libération (solubilisation).

Les colloïdes sont ubiquistes dans les eaux naturelles. Ils sont présents en concentration importante ($>10^6$ colloïdes.cm^{-3}) dans les eaux de surface, les eaux souterraines, les océans, les interstices de sols (McCarthy et Zachara, 1989; Gounaris et al., 1993; Vilks et al., 1993; Ryan et Elimelech, 1996; Stumm et Morgan, 1996). Par définition, les colloïdes sont des nanoparticules organiques ou inorganiques suffisamment petites pour ne pas sédimenter, en l'absence d'agrégation, pendant un laps de temps assez long (quelques jours) (Buffle et al., 1998). En effet, leur vitesse de décantation est très lente puisqu'elle dépend du carré de leur taille. Leur taille est déterminée par les méthodes d'extractions, mais le plus souvent elle est comprise entre 1 µm et 1 nm au moins dans une dimension (Figure I. 1) (Hayes et Bolt, 1991 ; Stumm et Morgan, 1996 ; Kaplan et al., 1997). La fraction colloïdale, dans les eaux naturelles, est caractérisée par une extrême complexité et diversité de nature. Elle peut être composée d'organismes, de débris biologiques, de macromolécules organiques, de minéraux (argiles et d'oxydes) éventuellement recouverts de matière organique (MO) (Stumm et Morgan, 1996). Du fait de leur surface spécifique importante (entre 10 et 800 $m^2.g^{-1}$), les

colloïdes sont extrêmement complexants. Les éléments se lient aux colloïdes principalement par adsorption (spécifique ou non spécifique), échange d'ions et co-précipitation.

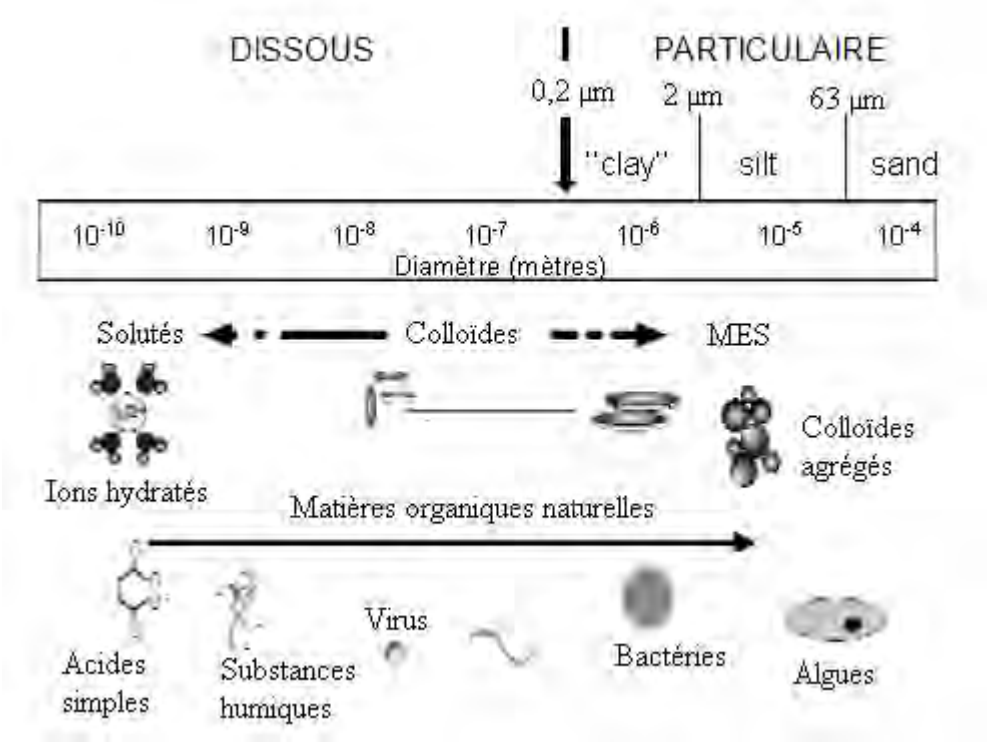

Figure I 1. Classification en fonction de la taille des composants organiques et inorganiques des milieux aqueux (Weber, 2006 ; adaptée de Ranville et Schmiermund, 1999)

Les colloïdes sont générés par divers mécanismes : (a) lors de l'altération de la roche mère et/ou néoformation de phases minérales, (b) lors des processus d'humification de la matière organique (formation et dégradation), (c) par dissolution de la matrice et précipitation de minéraux en fonction des changements des paramètres physico-chimiques du milieu (ex : dissolution des carbonates par acidification ou précipitation de Fe(II) en Fe(III) en milieu oxydant) (Schwertmann and Cornell, 2000), (d) durant les processus d'érosion, de libération et de dégradation de particules de sols (Citeau, 2004), (e) par la mobilisation de biocolloïdes (Kurek et al., 1982) ou encore (f) par l'introduction de colloïdes exogènes au sol ayant pour origine des apports anthropiques (ex : épandage de déchets). Quatre types de colloïdes peuvent être ainsi définis dans le milieu naturel : (1) les colloïdes organiques qui proviennent de la dégradation de la flore et de la faune, (2) les colloïdes minéraux composant le sol, (3) les biocolloïdes comme les bactéries et les virus (4) et les colloïdes mixtes. Les caractéristiques et propriétés des colloïdes dépendent de leur composition chimique (organique ou minérale), de leur taille et de leur forme, des caractéristiques de leur surface (surface spécifique, charge de surface et capacité de sorption). Ces caractéristiques sont interdépendantes et variables dans

l'environnement. Dans ce travail, nous ne discuterons que des colloïdes de la phase dissoute (<0.2 µm).

II. Les colloïdes organiques

La MO est une composante ubiquiste des milieux terrestres (sols, sédiments (McCarthy, 2001)), aquatiques (eaux de surface (Violleau, 1999) et eaux souterraines (Artinger et al., 2000) et anthropiques (stations d'épuration (Imai et al, 2002), décharges (Kang et al., 2002)), mais dont l'origine et la composition restent propres à chaque environnement. La richesse de cette répartition souligne les multiples possibilités de cette matrice organique à réagir ainsi que les nombreux mécanismes la régissant.

Comme l'ont démontré Bryan et al. (2002) dans une étude sur la complexation du cuivre par la matière organique, environ 65 % du Carbone Organique Dissous (COD) est considéré comme actif (complexant). Les colloïdes organiques, les plus complexants vis-à-vis des métaux sont identifiés comme étant les substances humiques (SH) ; des biopolymères naturels, comparables à des ligands polyfonctionnels (Logan et al., 1997), formés à partir de résidus de végétaux par des processus biochimiques intégrant l'activité microbienne. Ce sont de larges composés moléculaires, de compositions atomiques hétérogènes constituées principalement de carbone, d'oxygène, d'hydrogène, d'azote et occasionnellement de soufre et de phosphore. Selon Thurman (1985), dans les zones humides, 70 à 90 % du COD sont représentés par des substances humiques. Les substances humiques sont classées sur la base de leur solubilité en milieu aqueux et de leur taille moléculaire. Les substances humiques de la phase dissoute sont représentées par :

-les acides humiques (AH) d'un poids moléculaire compris entre 3 et 1000 kDa, solubles en milieu basique et insolubles en milieu acide (Sparks, 1995).

-les acides fulviques (AF) d'un poids moléculaire compris entre 0,5 et 5 kDa, solubles à la fois en milieu basique et acide (Drever et Vance, 1994; Sparks, 1995).

Les acides humiques constituent une quantité importante du carbone organique dissous dans la solution du sol, alors que les acides fulviques, plus mobiles, constituent la majeure partie du carbone organique dissous des eaux naturelles. Ces substances humiques forment des classes de composés relativement homogènes malgré la grande diversité du matériel dont elles proviennent. Davies et Ghabbour (1998) ont ainsi trouvé des formules empiriques extrêmement similaires pour des acides humiques d'origines très différentes (litière de forêts, sols de prairies, podzols, aridisols…).

1. Formation et décomposition

Dans la plupart des environnements, la majorité de la biomasse morte est convertie en dioxyde de carbone, lors du processus de minéralisation. Cependant, la minéralisation est rarement complète. L'humification est le processus qui permet à la matière organique faiblement biodégradable de subir une lente métabolisation, conduisant à la formation de molécules complexes de type substances humiques. Ces substances humiques, une fois formées, résistent à la dégradation. Elles sont réfractaires et s'accumulent. Ceci est dû à l'hétérogénéité chimique et physique qui inhibe l'évolution des enzymes de dégradation (Tipping, 2002). L'ampleur de l'accumulation dépend de la vitesse du turn-over de la matière organique, du climat, de la végétation, de la roche mère, de la topographie et des entrées-sorties (Stevenson, 1994). Les substances humiques sont notamment très présentes dans les sols de zones humides. Plusieurs théories expliquent la formation des substances humiques. Ainsi, Stevenson (1994) propose que les processus d'humification suivent quatre voies différentes, comme représentées sur la figure I. 2.

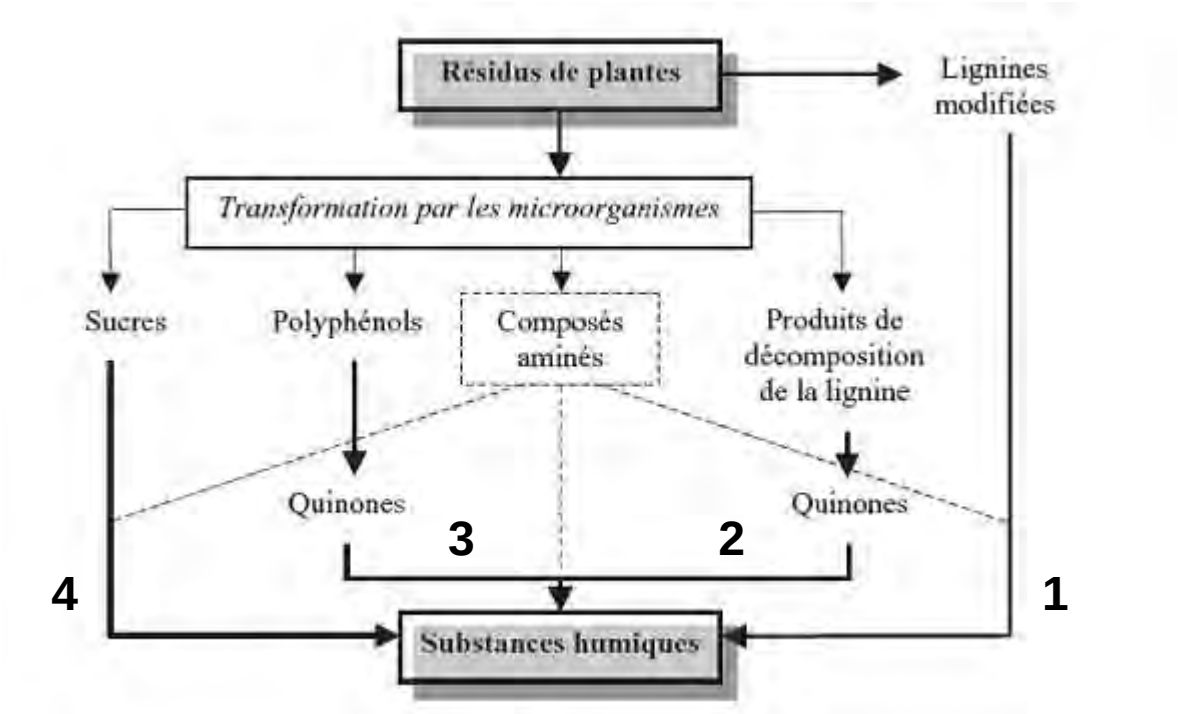

Figure I. 2. Mécanismes de formation des substances humiques du sol (d'après Stevenson, 1994).

La voie 1 reprend la théorie ligno-protéique. En effet, L'origine des SH a longtemps été liée à la dégradation de la lignine des résidus de plantes (Waksman, 1932). La lignine est un groupe de composés chimiques, difficilement biodégradables, appartenant aux composés phénoliques. Seconds biopolymères en abondance après la cellulose, les lignines résistantes à

la dégradation microbienne sont partiellement dégradées par les microorganismes dans le sol et s'oxydent pour former des unités structurales primaires de l'humus de sol. Felbeck (1971) souligne la formation de substances humiques de hauts poids moléculaires (acides humiques et humines) dans les premiers temps de l'humification. L'hypothèse de formation des SH à partir de la lignine repose sur les nombreuses similitudes existantes entre ces deux composés telles que leur faible dégradabilité, leur propriété de solubilité, la nature acide de leurs constituants ou leur réactivité chimique.

La théorie impliquant des polyphénols, représentée par les voies 2 et 3, considère les polyphénols et les quinones, comme principaux précurseurs des SH (Stevenson, 1994). Les polyphénols sont synthétisés, soit à partir de lignine, soit à partir des sources de carbone non ligneuses, par des microorganismes. Ils constituent une source majeure des unités aromatiques présentes dans les molécules humiques. Les phénols synthétisés par ces bactéries sont oxydés et transformés en quinones. Les quinones se polymérisent ou se recombinent en présence de composés aminés pour former des molécules humiques par des réactions enzymatiques et des réactions d'auto-oxydation. Flaig (1964) précise que les polyphénols, résultants de l'attaque microbiologique de la lignine, sont transformés en quinones par des enzymes de type polyphénoloxydase qui enlèvent un atome d'hydrogène au groupement OH phénolique.

Enfin, les processus d'humification peuvent suivre la voie de la théorie de la condensation amino-saccharidique (voie 4). En effet, les polysaccharides synthétisés par les microorganismes ont longtemps été considérés comme précurseurs des fractions humiques (Kononova, 1966). Selon ce concept, les sucres réducteurs et les composés aminés issus du métabolisme microbien et de la dégradation des matières organiques se polymérisent par condensation abiotique pour former des polymères azotés bruns. Tous ces composés sont fortement réactifs et se polymérisent aisément en présence de composés aminés pour former des substances humiques. Les changements énergétiques fréquents de l'environnement du sol (gel et dégel, sécheresse et humidification), ainsi que les propriétés catalytiques de la matière minérale, peuvent faciliter leur condensation.

L'ensemble de ces voies de synthèse peut être considéré comme des mécanismes probables de la formation des substances humiques. La formation des substances humiques reste ainsi encore énigmatique au même titre que la structure des molécules les composant (McCarthy et al., 1990). De plus, leur ordre de formation (humine - acides humiques - acides fulviques) lors des processus d'humifications n'est pas toujours clairement défini. En effet, les substances humiques ne constituent pas des composés bien spécifiques, mais correspondent à l'ensemble des composés d'un milieu possédant certaines propriétés chimiques identiques.

Par conséquent, il est très difficile de distinguer les SH résultant des processus de dégradation de la lignine des SH résultant des processus de néosynthèse. Dans le cadre de la théorie ligno-protéique de Waksman, la dégradation des lignines conduit à la formation de composés de type humines, puis acides humiques qui en se décomposant donnent des composés de type acides fulviques, qui se décomposent à leur tour en plus petites molécules organiques. Cette dernière fraction organique, définie fréquemment comme de la MO labile (Stevenson, 1994), est alors directement minéralisée ou bien impliquée dans les processus de néosynthèse. Dans le cas des théories relatives à des phénomènes de néosynthèse, l'ordre de formation des substances humiques est inverse. L'évolution des produits de dégradation de la lignine ou résultant de l'activité microbienne se fait vers l'obtention de poids moléculaires élevés par condensation croissante, sous l'influence des facteurs physico-chimiques (pH, Eh, température).

2. Réactivité

Même si la structure des substances humiques reste jusqu'à présent mal définie, les groupements fonctionnels responsables de leur réactivité, quelle que soit l'origine de la matière organique, sont essentiellement des groupements carboxyliques, phénoliques, alcooliques, quinoniques, des cétones et au sein de certaines fractions, des fonctions amines. Le C et l'O sont les deux éléments principaux. Les concentrations en C avoisinent les 50 %, bien que les acides fulviques en contiennent un peu moins. Les concentrations en O sont de 30 à 40 %, les valeurs les plus basses étant détenues pour des eaux souterraines. La composition élémentaire en H est d'environ 5 % pour des échantillons extraits de sols ou de rivières, mais elle est un peu plus importante pour des échantillons d'eau marine, reflétant leurs natures aliphatiques (Tipping, 2002). Les substances humiques des sols ont ainsi une charge variable due à la déprotonation de ces groupements fonctionnels de surface très diverses (fonctions carboxylate, phénolate, énolate, amine,…).

Exemple pour la fonction carboxylate : $\equiv COOH \rightleftharpoons \equiv COO^- + H^+$

Dans le milieu naturel, en milieux non extrêmes, les substances humiques se trouvent toujours chargées négativement pour des pH > 3 puisque leur charge de surface est globalement nulle pour un pH d'environ 3 (Sparks, 1995). La charge de la substance humique permet ainsi de retenir les ions par des interactions électrostatiques ou de coordination. Les

acides fulviques possèdent en général la plus grande teneur en groupements fonctionnels –COOH et –OH et la plus forte réactivité chimique. Ces groupements fonctionnels constituent un ensemble de charges variables, dont l'état de dissociation est dépendant du pH du milieu. Les acides fulviques ont des groupements acides qui restent dissociés à des pH plus bas que les acides humiques. Pour les milieux d'acidité forte à très forte, les groupements carboxyliques et phénoliques ne sont pas dissociés et les composés humiques sont floculés-condensés. En milieu alcalin, ils seront dispersés et les groupements fonctionnels seront dissociés (Girard et al., 2005).

III. Les colloïdes inorganiques

D'origine minérale, il s'agit d'argiles, de carbonates, d'oxydes de fer, d'oxydes de manganèse, de phosphates… Leurs propriétés complexantes varient selon le degré de cristallisation, les impuretés associées, la taille, la présence de co-précipités, le degré d'altération des oxydes et les paramètres physico-chimiques du milieu (Warren et Haack., 2001).

Les colloïdes inorganiques de nos régions se composent donc d'une part, d'"oxydes", terme désignant le plus souvent dans les sols l'ensemble des oxydes, oxyhydroxydes et hydroxydes. Le degré de solubilité des oxydes de fer est conditionné par le degré de cristallinité, dépendant de leurs conditions de formation. On peut distinguer les composés bien cristallisés comme la gibbsite $Al(OH)_3$, la goethite αFeOOH, l'hématite αFe_2O_3, des composés mal cristallisés ou amorphes tels que la boehmite αAlOOH, la lépidocrocite γFeOOH ou la ferrihydrite $5Fe_2O_3.9H_2O$. La réactivité du minéral sera d'autant plus élevée que la cristallinité sera faible.

Les oxydes de fer peuvent être fortement substitués par des cations de rayons ioniques voisins sans modification de la structure (substitution isomorphique) dont notamment l'Al, Mn, Cr and V (Al^{3+}, Mn^{3+}, Cr^{3+} and V^{3+} à la place de Fe^{3+}) et développeront donc peu de charges permanentes (Schwertmann and Cornell, 2000). Le Fe(III) dans l'hématite, la goethite ou la ferrihydrite peut respectivement présenter un taux maximal de substitution alumineuse de 16 %, 33 %, 15 % (Girard et al., 2005). D'autres cations, comme Ni^{2+}, Co^{3+}, Zn^{2+}, Cd^{2+}, Pb^{4+} and Cu^{2+} peuvent aussi être incorporés dans la structure de l'oxyde, particulièrement dans la goethite (Gerth, 1990). Ainsi, les oxydes de fer peuvent être de véritables puits et/ou sources de métaux (Al, Cr, Ni, Co, …). Les oxydes de fer sont des minéraux finement divisés de très petite taille, 10 à 100 Â, leurs conférant de grandes surfaces spécifiques de 60 à 600

$m^2.g^{-1}$ des hématites aux ferrihydrites et potentiellement une forte densité de fonctions de surface. Ceci leur permet de présenter des charges de surface variables, déterminées par le pH et la nature électrolytique de la solution du sol (cf. Tableau I. 1).

Les oxydes d'aluminium sont très peu affectés par la substitution de l'ion Al^{3+} ou d'autres cations et sont de plus grande taille que les oxydes de fer. Ils ne développent donc pas de charges permanentes et peu de charges variables (Girard et al., 2005). Dans la plupart des sols, les oxydes de Fe et d'Al sont chargés positivement car ils présentent de fortes valeurs de pHzpc (zero point charge, valeur de pH où la charge de surface est globalement nulle) (Tableau I. 1). Puisque les substances humiques sont chargées négativement et les oxydes positivement, ils sont souvent associés les uns aux autres dans le milieu naturel (Girard et al., 2005).

Tableau I. 1. Surface spécifique (Sa) et pH zpc de différents oxydes d'après la littérature (Stumm et Morgan, 1996; Langmuir, 1997; Schwertmann et Cornell, 2000).

	Sa (m^2/g)	pH_{ZPC}
Ferrihydrite $Fe(OH)_3 . nH_2O$	250-600	8.5-8.8
Goethite (α-FeOOH)	45-169	5.9-6.7
Hématite (α-Fe_2O_3)	3-160	4.2-6.9
Oxydes de Mn (MnO_x)	≈ 180	1.5-7.3
Gibbsite (α-$Al(OH)_3$)	≈ 120	8-10
Bayerite (γ-$Al(OH)_3$)	≈ 155	8-10

Les oxydes de manganèse sont peu abondants dans les sols et très complexes d'un point de vue minéralogique. Ils présentent des arrangements et compositions octaédriques plus diversifiés que les oxydes de fer et d'aluminium avec par exemple des couches octaédriques contenant de l'aluminium et du lithium, des structures en feuillets ou en tunnels qui peuvent contenir de gros cations (K^+, Pb^{2+}, Ba^{2+}). Aux valeurs de pH de la plupart des sols, ils ont la capacité d'échanger des cations et ainsi de fixer divers éléments traces métalliques (Cu, Zn, Ni, Pb, …) disposant de valeurs de pHzpc autour de 5-7. La fixation de métaux peut dépasser la capacité d'échange des oxydes de manganèse par incorporation dans le réseau cristallin de métaux, comme par exemple le cobalt (Girard et al., 2005).

Les colloïdes inorganiques sont également composés de phases siliceuses et de fragments d'argiles résultants des produits d'altération, soit hérités des minéraux primaires, soit néoformés. Ils sont constitués par une structure en feuillets : superposition de couches

tétraédriques (te) de silicium et de couches octaédriques (oc) d'aluminium. La réactivité en termes de charges et sites d'échanges de la structure argileuse sera dépendante du nombre de feuillets constituant l'argile. Les argiles sont des minéraux sujets aux substitutions isomorphiques, en raison de la coprécipitation d'ions de valence inférieure au sein de la maille cristalline (Al^{3+}/Fe^{2+} ou Mg^{2+}, Si^{4+}/Al^{3+}), qui leur permettent de développer une charge permanente. Cependant, certains minéraux argileux présentent également des fonctions de surface de type silanol au niveau des ruptures des feuillets qui leur confèrent une charge variable. Ainsi, les argiles type 2 :1 (te/oc/te) seront plus réactives que les argiles de type 1 :1. La kaolinite (type 1 :1) possède ainsi une faible surface spécifique et une faible capacité d'échange cationique. Les illites, vermiculites et les smectites (type 2 :1) possèdent des surfaces spécifiques plus développées et des capacités d'échanges cationiques plus importantes (Tableau I. 2). Pour les minéraux argileux ne possédant que peu ou pas de charges permanentes (comme la kaolinite) et donc de faibles capacités d'échange cationique, les sites silanol (≡Si-OH) contrôlent la charge de surface et se dissocient en $\equiv Si\text{-}O^-$ aux pH de la plupart des sols (<7). Les minéraux argileux peuvent être présents sous divers états : dispersés, agrégés et floculés qui sont liés à la nature et à la concentration des cations (force ionique), notamment du Na^+ et Ca^{2+} et à la présence de substances humiques (formation du complexe argilo-humique) (Girard et al., 2005).

Tableau I. 2. Surface spécifique (SA), pH zpc et CEC de différents minéraux argileux d'après la littérature (Langmuir, 1997; Girard et al., 2005).

	Sa (m^2/g)	pH_{ZPC}	CEC (meq/100g)
Kaolinite	10-40	≤ 2-4.6	3-15
Illites	65-150		10-40
Vermiculites	300-500		100-150
Smectites	600-800	≤ 2-3	80-150

La charge de surface des colloïdes inorganiques peut ainsi être permanente (substitutions isomorphiques), mais elle peut également être variable par ionisation des fonctions de surfaces ou adsorption d'ions (Sigg et al., 2000). Les colloïdes inorganiques participent ainsi, à des réactions d'adsorption spécifiques ou non spécifiques, permettant la fixation de cations, d'anions et, à la formation de colloïdes mixtes en s'associant avec la matière organique.

IV. Phénomène de sorption

La charge des colloïdes dans les sols provient ainsi d'une multitude de sources, passant par des petits minéraux argileux, des produits de décomposition organique, jusqu'aux micro-organismes vivants comme des bactéries. Les colloïdes peuvent être considérés comme des particules chargées, interagissant fortement avec les constituants du sol à travers une variété de réactions de surface. Outre les substitutions isomorphiques, la charge de surface est généralement dépendante du pH. Une caractéristique importante du transport colloïdale est donc la nature et la variation de la valeur de la charge de surface des solides des sols (Brady et Weil, 1996).

La sorption est le processus par lequel les substances réactives se fixent à la surface des solides. Les sites de sorption dans les sols sont localisés à la fois dans la matrice statique du sol et sur les particules mobiles du sol. La charge effective d'une particule peut différer de sa charge réelle du fait de la présence d'ions en solution qui adhèrent plus ou moins fermement à la particule (Figure I. 3). La distribution des ions autour d'une particule chargée n'est pas uniforme et peut être représentée par différents modèles. Ces derniers se distinguent essentiellement par le nombre de couches considérées dans la subdivision de l'interface particule/solution : le modèle à capacité constante (CCM), le modèle à couche diffuse (DLM), le modèle à triple couche (TLM), le modèle Donnan ou encore le modèle multi-sites (CD-MUSIC). Le modèle à capacité constante (CCM) ne considère qu'une seule couche, caractérisée par une relation linéaire entre la charge de surface et le potentiel électrique (Schindler et Kamber, 1968; Lützenkirchen, 1999). Le modèle à couche diffuse (DLM) résulte de l'arrangement spatial des ions dissociés à partir de la surface chargée. Ces ions sont soumis à deux forces opposées: une force d'adsorption provenant du champ électrique généré par la surface chargée ainsi qu'une force de diffusion provenant des gradients de concentration à l'équilibre des ions dans l'ensemble de la solution (Davis et Kent, 1990; Brady et Weil, 1996). Les ions les plus proches de la particule sont fortement retenus par attraction électrostatique. Ils constituent la couche fixe ou adhérente délimitée par le plan de Stern. La concentration de ces ions diminue rapidement lorsque l'on s'éloigne de la particule. Il existe une deuxième couche, diffuse celle-ci, délimitée par le plan de Gouy, qui n'adhère pas à la particule, mais forme un nuage de charges autour d'elle puis s'estompe et devient nulle à une certaine distance. Les cations s'accumulent de façon exponentielle pour une charge négative de surface, et la concentration en anions diminue de la solution vers la surface du solide. Le modèle de triples couches (TLM) met en jeu une couche supplémentaire entre la couche fixe

et la couche diffuse pour prendre en compte les ions faiblement adsorbés (Brown, 1990; Stumm et Morgan, 1996). Le modèle Donnan diffère des modèles précédents par sa géométrie (Miyajima et al., 1992; Van Beinum et al., 2005). En effet, il suppose que les ions sont distribués dans un volume et non sur un plan. Le modèle CD-MUSIC repose sur une approche cristallographique de la surface et conduit à la détermination de la charge résiduelle portée par les différents types d'atomes d'oxygène présents en surface du solide (Hiemstra et al., 1989; 1996; Hiemstra et Van Riemsdijk, 1996). La compensation de la charge de l'oxygène par le métal va dépendre de la longueur de liaison entre ces deux éléments. Ainsi, plus la distance métal-oxygène sera courte, plus la compensation de la charge portée par l'atome d'oxygène sera importante et donc plus sa charge résiduelle sera faible.

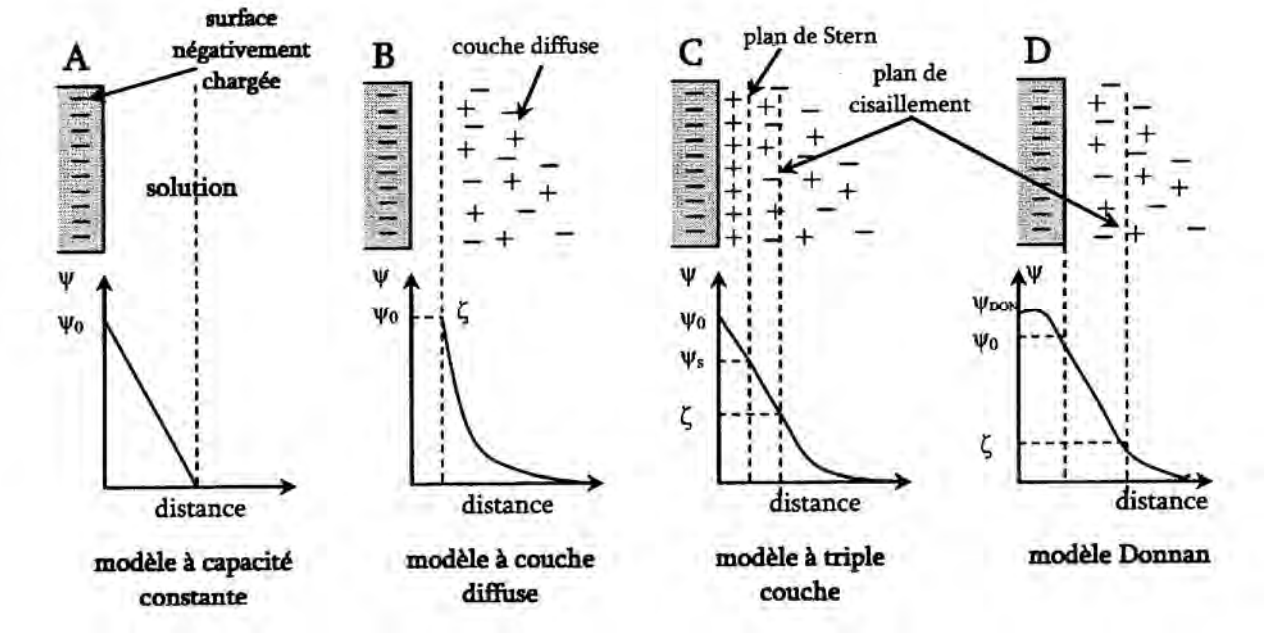

Figure I. 3. Représentation schématique de la distribution des ions sur une surface chargée négativement. A : modèle à capacité constante (ψ_0 : potentiel de surface), B : modèle à couche diffuse (ζ : potentiel Zêta), C : (ψ_s : potentiel de Stern), D : modèle de Donnan (ψ_{DON} : potentiel de Donnan) (d'aprés Warren et Haack, 2001, Yee et al., 2004).

Une caractéristique importante de ces modèles est l'étendue du domaine d'influence de la surface chargée sur la distribution des ions, qui peut être déterminée par exemple pour le modèle DLM par trois variables : le logarithme de la plus grande concentration de la solution du sol, de la valence des cations et de la teneur en eau du sol. L'épaisseur de la couche est grande (10 nm) pour les cations monovalents combinés à de faibles concentrations d'électrolytes sous des conditions saturées. Par contraste, cette couche est mince (0,1 nm) pour des ions multi-valents, des concentrations élevées d'électrolytes et des conditions insaturées (McGechan et Lewis, 2002). Dans ces modèles, les métaux et/ou les éléments

nutritifs peuvent être séquestrés, et libérés lentement en cas de besoin par échange de cations au sein de la solution du sol.

V. La formation et la libération de colloïdes

La libération de colloïdes mobiles dans les sols et les eaux souterraines est couramment induite par les changements de la chimie de la solution et lors de perturbations dans les écoulements hydrauliques (Ryan et Elimelech, 1996; Roy et Dzombak, 1996; Kretzschmar et Sticher, 1998; McCarthy et McKay, 2004), notamment les changements du potentiel redox, de pH et/ou de force ionique ou encore une rapide infiltration lors d'un fort événement pluvieux (Kaplan et al., 1993; Ryan et al., 1995). Pour que la mobilisation colloïdale des éléments traces soit notable, trois critères doivent être réunis : (a) des colloïdes doivent être générés ; (b) des contaminants doivent être associés aux colloïdes et (c) les colloïdes doivent être mobiles (Ryan et Elimelech, 1996). La zone la plus propice satisfaisant à ces critères à l'échelle du bassin versant est constituée par les zones hydromorphes de fond de vallée. Elles abritent, principalement lors des crues à la suite de fortes précipitations, le lit majeur de la rivière y circulant potentiellement et/ou une remontée de la nappe souterraine libre, générant des zones saturées temporaires. Ainsi, ces zones humides de bas de versant sont des écosystèmes particuliers à l'interface entre le milieu terrestre et aquatique. Les périodes d'immersion qui peuvent être plus ou moins longues leur confèrent des caractéristiques chimiques très différentes des autres écosystèmes. Elles représentent de véritables réacteurs biogéochimiques où les réactions aux interfaces Sol/Eau sont catalysées et amplifiées. Elles contrôlent également les flux d'éléments traces exportés hors de bassins versants, notamment par la fraction colloïdale. Ces zones sont soumises à des changements fréquents des paramètres physico-chimiques, liés aux changements de l'état de saturation hydrique du sol notamment, et représentent ainsi des zones privilégiées de libération de colloïdes et d'éléments associés.

Prenons l'exemple des oxydes de fer. Le fer en solution est contrôlé par les équilibres de réduction/oxydation et de dissolution/précipitation (Bourrié et al., 1994). Il existe sous deux formes impliquées dans les équilibres redox (Todorova et al., 2005) :

- Le fer ferreux Fe(II) est la forme réduite du fer. Sa plus forte solubilité facilite sa mobilité et le rend plus facilement disponible pour les microorganismes (Mitsch et Gosselink, 2000).

- Le fer ferrique Fe(III) est la forme oxydée. Peu soluble, le Fe(III) est relativement immobile (Mitsch et Gosselink, 2000). Il peut précipiter sous la forme d'oxyhydroxydes de fer (Todorova et al., 2005).

Le Fe(II) est généralement produit *in situ* dans une zone humide par réduction microbienne du Fe(III) (Todorova et al., 2005). La réduction dissimulatrice du fer (Eq. 1) correspond à une réduction du fer avec un substrat organique comme donneur d'électrons (Lovley et al., 1987; Lovley et Phillips, 1988; Roden et Lovley, 1993; Drever, 1997, Lovley, 2000, Zachara et al., 2001; 2002; Roden, 2006).

$$CH_2O + 4\ Fe(OH)_3 + 8\ H^+ \leftrightarrow CO_2 + 4\ Fe^{2+} + 11H_2O \qquad (1)$$

La réduction du fer est un mécanisme bien connu dans les zones humides compte tenu des conditions réductrices du milieu liées à la submersion et à l'abondance de substrats organiques. Cette réaction est réalisée grâce aux bactéries ferro-réductrices et dépend du type d'oxyde, de sa cristallinité et de son degré de substitution. Les bactéries utilisent préférentiellement les oxyhydroxydes de fer mal cristallisés (lépidocrocite) aux formes cristallisées (goethite, hématite) (Lovley et Phillips, 1986; Ehrlich, 1990).

L'alternance de conditions oxiques et anoxiques, liée à la fluctuation de la saturation hydrique du sol, influence les conditions redox, la solubilité et la spéciation du fer (Steinmann et Shotyk, 1997). Pendant la phase désaturée, le fer solide est stable et particulièrement immobile dans le sol. Quand les conditions deviennent saturées, le milieu devient anoxique et le fer se transforme en Fe(II) soluble par réduction dissimilatrice. Puis, le Fe(II) est oxydé sous forme solide lors du passage au milieu aquatique ou lors du retour à la phase désaturée. La MO peut alors complexer le Fe(III) et ainsi accroître sa solubilité et sa stabilité (Stumm et Morgan, 1996). De plus, de récentes études ont mis en évidence l'impact de la présence des substances humiques sur la taille des oxydes de fer (Gaffney et al., 2008). En effet, la présence de colloïdes mixtes substances humiques-Fe(III) a été précédemment supposée dans plusieurs études dans des milieux riches en MO (Rose et al., 1998; Pokrovsky et al., 2005; You et al., 2006; Dahlqvist et al., 2007). Les substances humiques inhiberaient la formation des oxydes de fer et permettraient la formation de nanoparticules de fer associées à la MO. Ainsi, les phases de réductions-oxydations permettraient la formation de colloïdes mixtes substances humiques-Fe(III) mobiles dans les sols. Des observations par microscopie électronique à transmission (MET) conduites sur des échantillons d'eaux de rivières (Allard et al., 2004) et de solution de sol soumis à des alternances redox (Thompson et al., 2006) supportent cette hypothèse. De plus, la réduction du fer en produisant du Fe(II) stimule la

décomposition de la MO (Todorova et al., 2005; Van Bodegom et al., 2005). En effet, la présence du Fe(II) stimule l'activité d'une enzyme la phénol-oxydase, cet enzyme oxyde les composés phénoliques dont la présence est un facteur limitant de la dégradation de la MO (formation de quinones et ainsi de substances humiques).

La réduction du fer conduit à un accroissement du pH (Eq. I) et peut ainsi conduire à la désorption/solubilisation de la MO (Hagedorn et al., 2000; Grybos et al., submitted 2009). En effet, la désorption des substances humiques par augmentation du pH est également un mécanisme susceptible de libérer des colloïdes et les éléments associés dans la phase dissoute (Murphy et al., 1992; Avena et Koopal, 1998; Zuyi et al., 2000). Il a été démontré que la sorption était dépendante du pH, diminuant avec l'augmentation du pH, en raison des effets électrostatiques (surface minérale de plus en plus électropositive) et des interactions stériques spécifiques. L'augmentation du pH peut aussi favoriser la désorption de matières organiques, et notamment des substances humiques, forme prépondérante du COD présent dans les zones humides (Thurman, 1985), des différentes surfaces minérales du sol. En effet, les 'oxydes' du sol sont chargés négativement à pH basique et positivement à pH neutre ou acide (Tableau I. 1). Les matières organiques, négativement chargées s'adsorbent ainsi préférentiellement lorsque le pH est neutre ou acide (Stumm et Morgan, 1996). La capacité d'un sol à adsorber des substances humiques sera donc plus importante en milieu légèrement acide. En conditions plus basiques, ou lors d'une augmentation du pH, le bilan des charges mènera à un transfert des substances humiques vers la solution, par désorption des phases solides.

De plus, les différences intrinsèques de volume molaire et de nombre de moles de groupements carboxyliques impliquent que les acides humiques sont plus adsorbés à la surface des phases inorganiques que les acides fulviques (Murphy et Zachara, 1995). La relation entre l'augmentation de la sorption de substances humiques et les propriétés, telles qu'une haute aromaticité, une polarité faible et un haut poids moléculaire, suggère que les acides humiques sont probablement plus liés que les acides fulviques aux sites hydroxylés des surfaces minérales. McCarthy et al. (1993) suggèrent que les substances humiques, durant leurs transferts des sols aux hydrosystèmes, se fractionnent par des phénomènes de sorption, et ce qui tend à enrichir la phase solide en acides humiques et le carbone organique dissous des eaux souterraines en acides fulviques. Ce fractionnement peut ainsi enrichir la phase solide en acides humiques, fortement complexants, et provoquer une libération importante de colloïdes vecteurs d'éléments traces lors d'un changement de la chimie de la solution du sol.

VI. Objectifs de l'étude

Cette étude vise à améliorer la compréhension du rôle des colloïdes dans la mobilisation des éléments traces en définissant (a) l'impact de paramètres physico-chimiques sur la composition élémentaire et colloïdale de la phase dissoute d'un sol de zone humide, (b) les modes de genèse de ces colloïdes, ainsi que leur rôle de phases porteuses et de vecteurs d'éléments traces dans les eaux et les sols. Une attention particulière sera portée aux zones humides et notamment à la zone humide du Mercy dans le bassin versant expérimental de Kervidy/Coët-Dan (Morbihan), appartenant au réseau de bassins versants suivis dans le cadre des travaux de l'Observatoire de Recherche en Environnement AgrHys. Les études menées préalablement sur ce bassin versant nous ont apporté une bonne connaissance, à la fois, du contexte hydro-pédo-climatique (Mérot et al., 1995; Durand et Juan Torres, 1996; Curmi et al., 1998) et hydro-géo-chimique (Jaffrézic, 1997; Dia et al., 2000; Molénat et al., 2002; Pourret et al., 2007a). Nous avons donc choisi de travailler lors de nos expérimentations avec du sol issu de cet environnement bien contraint, connu pour sa réactivité, sa richesse en MO et éléments traces et sa propension à générer et libérer des colloïdes lors d'interaction Eau/Sol.

Les principaux objectifs de ce travail de recherche étaient donc ainsi de :

- décrire le rôle des colloïdes dans la mobilisation des éléments traces dans une zone humide et déterminer la nature des colloïdes complexants mis en jeu;
- de déterminer le rôle du pH et de la force ionique sur la conformation des substances humiques et par voie de conséquence sur la distribution des éléments traces associés;
- d'étudier l'influence du pH sur le détachement des colloïdes et sur la composition en éléments dans la phase dissoute;
- d'étudier l'influence des substances humiques sur l'état d'oxydation et la taille des oxydes de fer;
- de comparer lors d'expériences de bioréduction mettant en jeu des bactéries ferro-réductrices, la biodisponibilité du fer engagé, soit dans des oxydes de fer cristallisés, soit dans des colloïdes mixtes Fe-MO.

VII. Organisation de la thèse

Ce mémoire composé d'articles publiés, soumis ou en préparation, se décompose en cinq parties ordonnées dans l'ordre des objectifs ci-dessus définis :

Le mémoire commence classiquement par une *introduction* présentant le contexte, les objets cibles de l'étude et les objectifs.

Le *chapitre 2* intitulé : **'Transport colloïdal des éléments traces à l'interface sol/eau : une nouvelle contribution'** est consacré à la réalisation d'une étude cinétique expérimentale de lessivage de sol dans le but de préciser le rôle des nanoparticules sur la mobilisation des éléments traces. Il correspond à un article publié en 2008 dans la revue Journal of Colloid and Interface Science - Pédrot, M., Dia, A., Davranche, M., Bouhnik-Le Coz, M., Henin, O., Gruau, G., 2008. 'Insights into colloid-mediated trace element release at the soil/water interface'. Journal of Colloid and Interface Science 325, 187-197.

Le *chapitre 3* intitulé : **'Structure dynamique des substances humiques et impact sur la distribution en solution des terres rares associées'** est focalisé sur l'étude de l'influence du pH et de la force ionique sur la conformation spatiale des substances humiques et l'impact qui en résulte sur la distribution des terres rares (REE) dans la phase dissoute. Il correspond à un article soumis pour publication à la revue Chemical Geology - Pédrot, M.; Dia, A.; Davranche, M. 'Dynamic structure of humic substances and its impact on sequestrated Rare Earth Element distribution'.

Le *chapitre 4* intitulé : **'Double contrôle du pH sur la distribution des substances humiques et des éléments traces associés dans les solutions de sols : apport de l'ultrafiltration'** présente une étude expérimentale sur le double rôle exercé par le pH sur le détachement des colloïdes et sur la composition en éléments traces de la phase dissoute. Ce volet correspond à un article soumis pour publication à la revue Journal of Colloid and Interface Science - Pédrot, M.; Dia, A.; Davranche, M. 'Double pH control on humic substance-borne trace element distribution in soil waters as inferred from ultrafiltration'.

Le *chapitre 5* intitulé '**Interactions fer-matière organique et biodisponibilité des nanoparticules de Fe'** traite de l'influence des substances humiques sur l'oxydation et la taille des particules de fer et ainsi de la possibilité de la présence de nanoparticules de fer dans la phase dissoute. Il comporte également un volet consacré au rôle majeur joué par les colloïdes mixtes Fe-SH en tant que source de fer pour les bactéries ferro-réductrices, et donc par voie de conséquence sur le contrôle exercé par ces colloïdes mixtes sur la dynamique du fer et la dynamique bactérienne ferro-réductrice dans des zones riches en MO comme les zones humides par exemple.

Enfin, la dernière partie de ce manuscrit se décompose en une *conclusion* qui résume les principaux résultats de ce travail et des *perspectives* de travaux futurs axés sur la levée de certains verrous rencontrés durant ces trois années de thèse.

Chapitre II : Transport colloïdal des éléments traces à l'interface sol/eau : une nouvelle contribution

Insights into colloid-mediated trace element release at the soil/water interface

Ce chapitre correspond à un article publié dans la revue : 'Journal of Colloid and Interface Science' : Pédrot, M., Dia, A., Davranche, M., Bouhnik-Le Coz, M., Henin, O., Gruau, G., 2008 : 'Insights into colloid-mediated trace element release at the soil/water interface'. Journal of Colloid and Interface Science 325, 187-197.

Résumé : Les colloïdes organiques ou inorganiques jouent un rôle majeur dans la mobilisation des éléments traces dans les sols et les eaux. Les paramètres physicochimiques environnementaux (pH, potentiel redox, température, pression, force ionique...) sont les facteurs de contrôle de la mobilisation colloïdale. Cette étude était dédiée à la réalisation, par une approche expérimentale, d'un suivi cinétique de la dynamique colloïdale et des éléments traces associés à l'interface sol/eau. Les expériences ont été réalisées par percolation de solution synthétique dans des colonnes de sol. Les percolats ont été ultrafiltrés avec plusieurs seuils de coupure pour séparer les différentes phases colloïdales par poids moléculaires. Les concentrations en carbone organique dissous et en éléments traces ont ensuite été mesurées dans ces différentes fractions. Les principaux résultats qui découlent de cette étude sont les suivants: (a) Les données permettent de séparer en plusieurs groupes les composés organiques (métabolites microbiens, acides fulviques, acides humiques) en fonction de leur aromaticité et de leur masse moléculaire respective. (b) Trois groupes d'éléments ont pu être distingués en se basant sur leurs relations avec les phases colloïdales : le premier correspond aux éléments membres du groupe 'dissous vrai' et comprend le Li, B, K, Na, Rb, Si, Mg, Sr, Ca, Mn, Ba et le V. Le second peut être considéré comme un groupe intermédiaire avec le Cu, Cd, Co, et le Ni, tandis que le troisième groupe rassemble l'Al, Cr, U, Mo, Pb, Ti, Th, Fe, et les terres rares (REE) mobilisés par le compartiment colloïdal organique. (c) Les données ont démontré que les acides fulviques semblaient être une phase organique porteuse majeure pour des éléments traces comme le Cu, Cd, Co, et le Ni. En revanche, les éléments traces appartenant au compartiment colloïdal seraient surtout mobilisés par les acides humiques contenant des nanoparticules de fer. Le Pb, Ti, et U seraient mobilisés par les nanoparticules de fer liées à ces acides humiques. Ainsi, les acides humiques permettent directement ou indirectement le transport colloïdal de nombreux éléments traces insolubles, soit en les complexant, soit en stabilisant la phase ferrique porteuse. (c) Enfin, les données expérimentales ont aussi montré que les REE étaient surtout mobilisées par les acides humiques. Les spectres normalisés des REE ont montré une forme concave. Par conséquent, comme précédemment démontré dans d'autres études, les substances humiques exercent un contrôle majeur sur la spéciation et le fractionnement des REE, puisque le rapport Substances Humiques/Métaux serait un paramètre clé de contrôle de la forme du spectre des REE dans les environnements organiques.

Abstract : Organic or inorganic colloids play a major role in the mobilization of trace elements in soils and waters. Environmental physicochemical parameters (pH, redox potential, temperature, pressure, ionic strength, etc.) are the controlling factors of the colloidal mobilization. This study was dedicated to follow the colloid-mediated mobilization of trace elements through time at the

soil/water interface by means of an experimental approach. Soil column experiments were carried out using percolating synthetic solutions. The percolated solutions were ultrafiltrated with various decreasing cutoff thresholds to separate the different colloidal phases in which the dissolved organic carbon and trace element concentrations were measured. The major results which stem from this study are the following: (i) The data can be divided into different groups of organic compounds (microbial metabolites, fulvic acids, humic acids) with regard to their respective aromaticity and molecular weight. (ii) Three groups of elements can be distinguished based on their relationships with the colloidal phases: the first one corresponds to the so-called "truly" dissolved group (Li, B, K, Na, Rb, Si, Mg, Sr, Ca, Mn, Ba, and V). The second one can be considered as an intermediate group (Cu, Cd, Co, and Ni), while the third group gathers Al, Cr, U, Mo, Pb, Ti, Th, Fe, and rare earth elements (REE) carried by the organic colloidal pool. (iii) The data demonstrate that the fulvic acids seem to be a major organic carrier phase for trace elements such as Cu, Cd, Co, and Ni. By contrast, the trace elements belonging to the so-called colloidal pool were mostly mobilized by humic acids containing iron nanoparticles. Lead, Ti, and U were mobilized by iron nanoparticles bound to these humic acids. Thus, humic substances allowed directly or indirectly a colloidal transport of many insoluble trace elements either by binding trace elements or by stabilizing a ferric carrier phase. (iv) Finally, the results demonstrated also that REE were mostly mobilized by humic substances. The REE normalized patterns showed a middle REE downward concavity. Therefore, as previously shown elsewhere humic substances are a major control of REE speciation and REE fractionation patterns as well since the humic substance/metal ratio was the key parameter controlling the REE pattern shape.

I. Introduction

For 10 years, many studies were dedicated to elemental dynamics in rivers or groundwaters (Shiller, 1997; Dia et al., 2000; Pokrovsky and Schott, 2002; Dahlqvist et al., 2007, Grosbois et al, 2007; Pourret et al., 2007a). Waterborne elements are carried out through groundwater aquifers, vadose zone, and soils by the particulate, colloidal, or "truly" dissolved phase. Colloids, either organic or inorganic, are microscopic phases in a size range of 1 nm to 1 μm in at least one direction (Stum and Morgan, 1996; Kaplan et al., 1997; Kretzschmar and Sticher, 1998). Because of their small size, they do not tend to settle down out of suspensions, being influenced by Brownian motion and minor currents in the bulk solutions. The solid–water interface established by these micro-particles plays a key role in regulating the concentrations of most reactive elements and of many pollutants in soils and natural waters (Stumm and Morgan, 1996). Colloids adsorb heavy metal ions and waterborne pollutants and therefore govern—via their movements in aqueous systems and

soils—the fate of reactive elements and/or pollutants. They can be the main vehicle for their transport (McCarthy and Zachara, 1989; Kalbitz et al., 2000).

Recent studies coupled or not with speciation calculations suggest that a large fraction of trace elements are closely associated with dissolved organic carbon (DOC) including colloidal organic matter in many natural waters (Dia et al., 2000; Pokrovsky and Schott, 2002; Dahlqvist et al., 2007; Tanizaki et al., 1992; Dai et al., 1995; Eyrolle et al., 1996; Logan et al., 1997; Viers et al., 1997; Dupré et al., 1999; Oliva et al., 1999; Ingri et al., 2000; Donisa et al., 2003; Gruau et al., 2004; Johannesson et al., 2004; Pokrovsky et al., 2006). Organic matter (OM) can either (i) adsorb trace elements and immobilize them in the soil within organomineral complexes or (ii) migrate with the soil solution and induce trace element transfer within the ecosystem toward groundwaters or surface waters. Since most waters undergo more or less prolonged passage in soils, soil organic horizons play a major role in the acquisition of the chemical signature of waters. Soil/water interactions generate various medium-dependent type colloids in the different environments. As carbon-rich colloids likely derive from the uppermost soil horizon, it appears that many trace elements (e.g., Co, Ni, Cu) usually associated to carbon colloid have their origin here (Dahlqvist et al., 2007). It is therefore important to study OM-trace element interactions to understand lixiviation/cheluviation phenomena occurring both within soils and at the soil/water interface.

However, these interactions strongly depend on physicochemical parameters such as pH, redox potential, temperature, pressure, and ionic strength (Chuan et al., 1996; Grolimund et al., 1996; Kedziorek and Bourg, 1996; Logan et al., 1997; Tyler and Olsson, 2001). These parameters control both the amount and the speciation of waterborne elements. It is then required to estimate their role in order to define their respective impacts in the OM–trace element interactions. As an example, redox conditions do control the dynamics and fate of some toxic and/or redox-sensitive elements at the soil/water interface. However, it is not clear whether trace metals are directly bound to the oxyhydroxides and complexed by organic matter when the oxyhydroxides are dissolved during reduction, or whether they are directly bound to dissolved organic matter and controlled by the organic matter dynamics throughout the entire redox cycle. The true respective roles of organic matter and Fe–Mn oxyhydroxides as elemental carriers remain thus still poorly understood.

Such studies dedicated to the understanding of the respective role of the environmental physicochemical parameters were little carried out in situ, since it appears rather difficult to control the external environmental parameters and therefore to identify the key factors. Batch experimental approaches were undertaken for modeling soil–water interactions (Gerritse, 1996; Shi et al., 2007; Wong et al., 2007). However, batch systems are known to strongly disturb the medium by destroying aggregates and thus not represent truly the natural conditions. In order to minimize disturbance of

soil, we designed experimental systems using columns. Column leaching experiments were shown to be appropriate for providing information about heavy metal release and associated transport in soil (Kedziorek et al., 1998; Voegelin et al., 2003). They were also tested for possible soil remediation, stabilization treatments, to assess heavy metal binding and desorption kinetics, or to study processes such as colloid-facilitated metal transport at the laboratory scale (Grolimund et al., 1996; Kedziorek et al., 1998; Kretzschmar and Sticher, 1998).

The aim of this work was to realize a kinetic experimental study of OM-trace element relationships to provide evidence that in a natural wetland organic-rich soil, colloidal organic particles are major trace element carriers. Leaching and release dynamics of organic colloids and associated trace elements were followed through time as well as the aromaticity of the carbon-rich solute phase to identify whether C-rich or Fe-rich colloids are the major carrier phases in wetland soils and how the distribution of elements in between evolved through time with special care of the molecular weight of the involved carriers.

II. Materials and methods

1. Soil sample location

Soil/water interactions were carried out in a laboratory using a wetland organic-rich soil and a synthetic solution. The soil sample was collected from the upper soil horizons located in the Mercy wetland in January 2006. The Mercy wetland is located in the Kervidy/Coet Dan catchment (Northwestern Europe) (Figure II. 1). The Kervidy/Coet Dan catchment has been monitored since 1991 to investigate the effects of intensive agriculture on water quality. Detailed information regarding its soil types, hydrology, and geomorphology can be found elsewhere (Mérot et al., 1995; Durand and Torres, 1996; Curmi et al., 1998). The region is marked by a humid temperate climate with a mean annual rainfall of 909 mm. The water table reaches the organic-rich upper soil horizons in the wetlands. Wetland waters are colored, DOC-rich and exhibit variable nitrate concentrations (Durand and Torres, 1996; Jaffrézic, 1997). In addition, these waters are characterized by the development of periodic reducing conditions - mostly in late winter and spring - which are a direct consequence of the waterlogging of the uppermost soil horizon (Jaffrézic, 1997). The vegetation is represented by a wet meadow. See Section S1 of Supplementary material for more details (see also Nelson and Sommers, 1982).

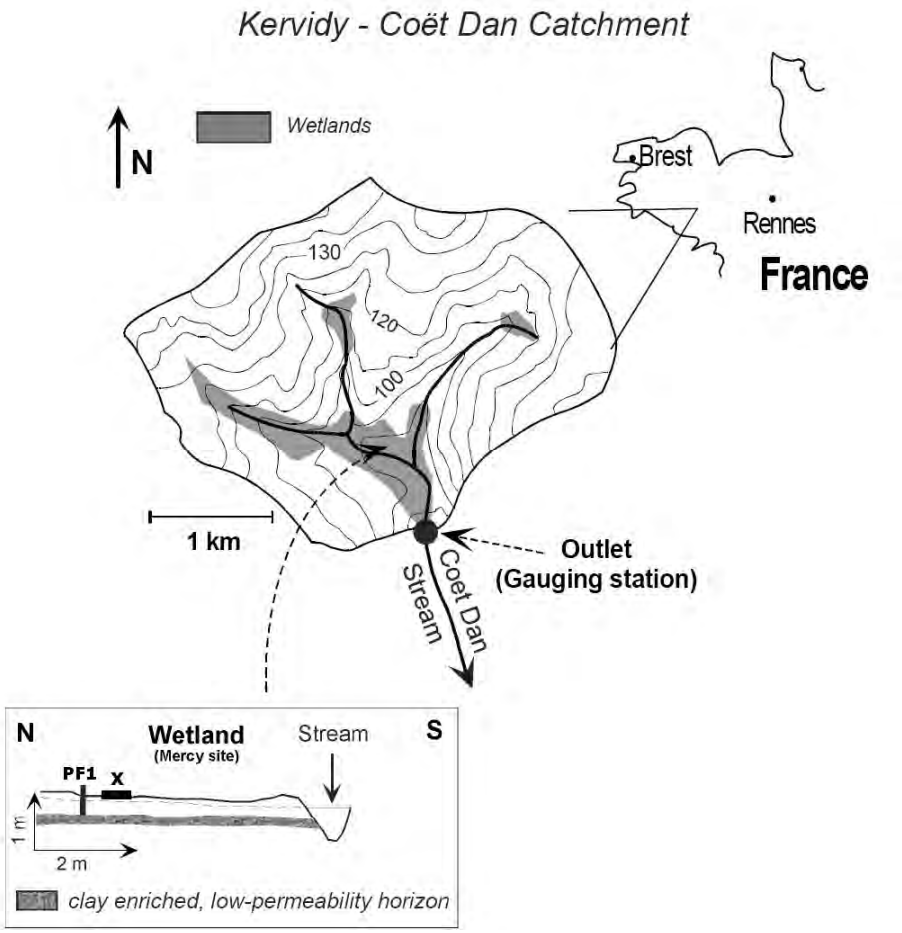

Figure II. 1. Sketch showing the (a) topography, channel network geometry, and geographical location of the Kervidy–Coet Dan subcatchment, and (b) sampling point location as evidenced by X. Discontinuous patterned areas located close to the channel network indicate the location of wetland zones.

2. Experimental setup

Leaching experiments were conducted with dynamic column systems (Figure II. 2). The release of DOC and major and trace elements from the organic-rich soil was followed through time. The column system consisted of several reservoirs connected together by a flexible 0.2-mm internal diameter hose tygon. A synthetic percolating solution was placed in the solution reservoir. This solution reservoir was formed by a 1500-ml polypropylene bottle equipped with an output for solution circulation and several air vents. The soil was placed in three soil columns formed by a Plexiglas tube. Each 21-mm inner diameter and 37-cm-long Plexiglas column contains 50 g of soil (equivalent to 67.23 cm3). The size of the columns was selected to compensate for the spatial variability, especially that concerning the soil hydraulic conductivity. The total porosity in the soil columns (i.e., pore water volume) was 56%, while the effective porosity was 2.9% as estimated from data displayed in Section S2 of Supplementary material. The calculated effective porosity is very

close to the natural field porosity of the soil. Each Plexiglas column was equipped with an input and an output for solution circulation. A horizontal perforated Teflon disk (<100-µm pore size) was inserted at its bottom. The disk allowed soil particles to stay in the column, while allowing percolation of the solution into the lower reservoirs called "sample reservoir." This sample reservoir was formed by a 500-ml polypropylene bottle equipped with a syringe to sample the percolating solution. The solution was continuously flowing from the solution reservoir to the columns driven by a peristaltic pump (Ismatec Ecoline) during the experiment (Figure II. 2). The solution gently percolated through the soil sample and returned back to the sample reservoir by the mean of a peristaltic pump. The percolation rate was set at about 1.1 ml/min to optimize the soil–solution interface reactions. Air vents-on top of the solution reservoir and on top of the soil reservoir-allowed the preservation of aerobic conditions during the experiments. The synthetic solution consists of a $1.88*10^{-3}$ M NaCl solution, which corresponds to the ionic strength of the soil waters within the investigated wetland organic-rich horizon.

3. Ultrafiltration

All collected waters were filtered using 0.2-µm-pore-size cellulose acetate filter capsules (polyether sulfone membrane Sartorius Minisart). Ultrafiltration experiments were then performed to separate the different phases following the decreasing pore size. This was done using 15-ml centrifugal tubes (Vivaspin) equipped with permeable membranes of decreasing pore sizes (30, 5, and 2 kDa). Each centrifugal filter device was washed and rinsed with HCl 0.1 N and Milli-Q water three times before use. Centrifugations were performed using a Jouan G4.12 centrifuge with swinging bucket at about 3000*g* for 20 min for 30-kDa devices, and 3500 and 3750*g* for 30 min, for 5 and 2-kDa devices, respectively. These small volume ultrafiltration cells allow a quick and easy molecular weight-dependent separation of the colloidal fraction with consuming only little solution (15 ml). All procedures (sampling, filtration, and analysis) were carried out in order to minimize contamination. Blank tests were performed during this study to determine possible contamination due to the filtration and analysis.

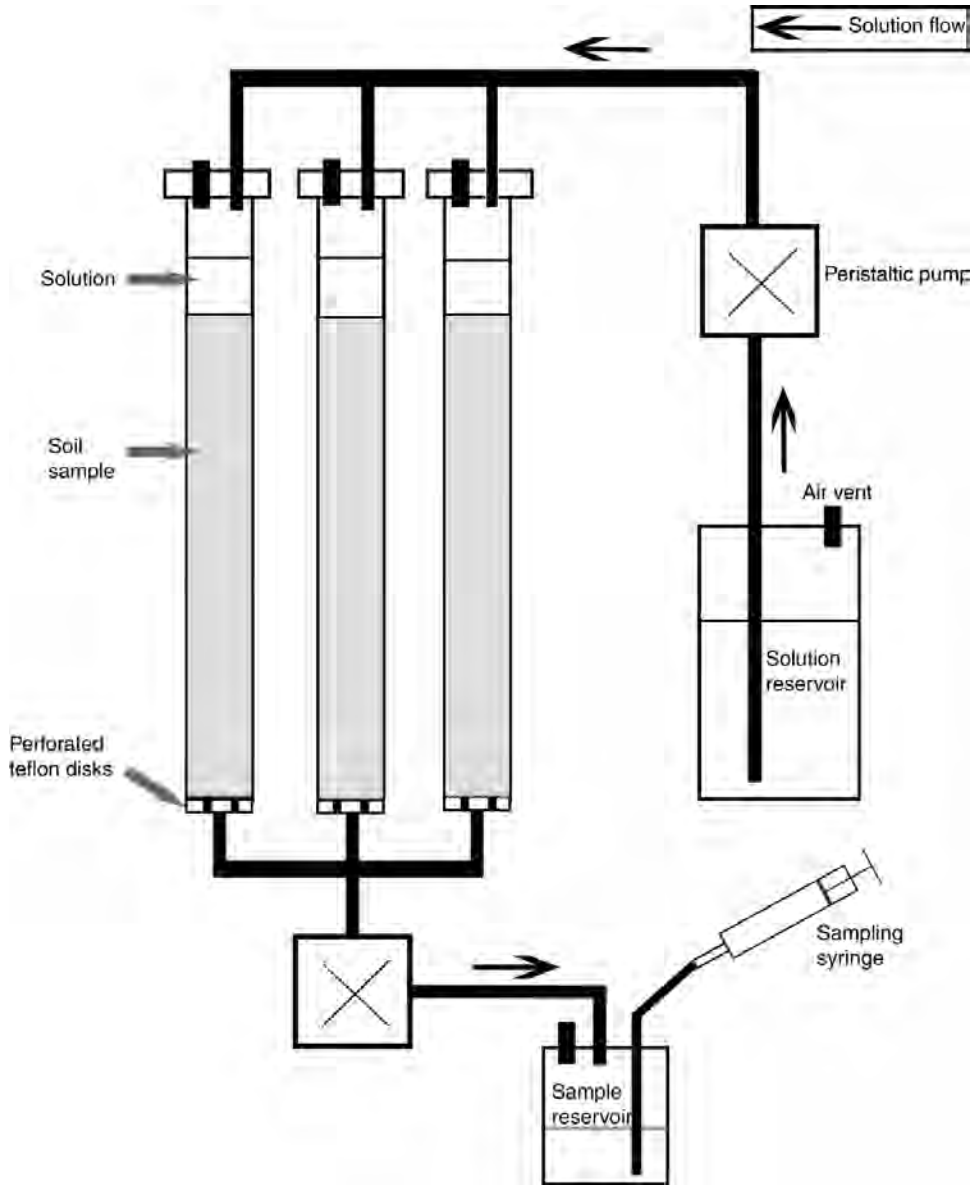

Figure II. 2. Scheme of the experimental setup involving the soil columns. The synthetic solution is conveyed to the soil reservoirs by a peristaltic pump (ISMATEC, ecoline). Soil was irrigated at low flow intensity (1.1 mlmin−1).

4. Chemical analyses

The pH was measured with a combined Mettler InLab electrode after a calibration performed with WTW standard solutions (pH 4.01 and 7.00 at 25 ◦C). The accuracy of the pH measurement is ±0.05 pH units. Dissolved organic carbon was analyzed with a Total Organic Carbon analyzer (Shimadzu TOC-5050A). The accuracy of DOC measurement was estimated at ±3% (by using standard solution of potassium hydrogen phtalate). SUVA (Specific UltraViolet Absorbance)-strongly correlated with degree of aromaticity of organic matter (aromaticity = 6.52 * SUVA + 3.63) (Weishaar et al., 2003)-was used as an indicator of the chemical composition and reactivity of

dissolved organic carbon. Major anions (Cl^-, SO^{2-}_4, and NO^-_3) concentrations were measured by ion chromatography (Dionex DX- 120): the uncertainty was below 4%. Major cation and trace element concentrations were determined by ICP-MS (Agilent 4500), using indium as an internal standard. The international geostandard SLRS-4 was used to check the validity and reproducibility of the results. Typical uncertainties including all error sources were below ±5% for all the trace elements, whereas for major cations, the uncertainty lay between 2 and 5%, depending on the concentration (Yéghicheyan et al., 2001; Davranche et al., 2004).

5. Data treatment

Ascending hierarchical classification (Lebart and Morineau, 2000) using Ward criterion was performed on data through Lumiere, version 5.30. This method is based on squared Euclidian distances between individuals in the space formed by the available variables. The initial sample is partitioned into several classes of individuals so as to maximize interclass inertia (i.e., to maximize variability between groups) and minimize intraclass inertia (i.e., to maximize homogeneity in each group). The input data are the whole set of ultrafiltrates after each cutoff for all considered elements.

III. Results and discussion

The whole dataset is reported in Section S3 of Supplementary material.

1. Dissolved organic carbon release through time and associated aromaticity variations

Dissolved organic carbon concentrations decreased quickly at the beginning of the experiment, and then more slowly after 9 pore water volumes (Figure II. 3). The high DOC concentration at the beginning of the experience resulted from an important leaching of the fine fraction (below 2 kDa).

Humic substances - including humic and fulvic acids formed by degradation of biogenic organic matter - are the main components of the dissolved organic carbon in aquatic systems and soils (Kalbitz et al., 2000; Mercier et al., 2001). They are composed of mixtures of organic macromolecules displaying a broad spectrum of functional groups (carboxylic acids, phenols, amines, etc.), structures, and molecular weight distributions. All of them are strongly dependent on their origin and genesis and can be viewed as polyfunctional ligands. We can gain information on the nature of the different groups of dissolved organic matter released by comparing their respective aromaticity as elsewhere reported (Chin et al., 1994; Tipping, 2002). Simple organic molecules and microbial metabolites are aromatic carbon depleted, and thus show lower aromaticity values. By

contrast, humic substances are aromatic carbon enriched and display high aromaticity values (Chin et al., 1994; Tipping, 2002). Moreover, the relative amount of aromatic moieties in humic substances increases with increasing molecular weight (Chin et al., 1994). Thus, simple organic molecules have the lowest aromaticities, and within the humic substance group, humic acids heavier than fulvic acids display higher amounts of aromatic moieties than fulvic acids.

Three groups of organic matter corresponding to three different degrees of aromaticity were identified during this study (Figure II. 4). (i) The first group, corresponding to the first collected samples, displayed the lowest values of aromaticity (less than 14%) and corresponded to the smallest size organic molecules. These materials were the fastest leached species at the beginning of the experiment. These simple organic molecules or compounds were very labile. Then, later during the experiment, compounds characterized by different aromaticity were leached. They can be divided into two groups to which we refer as the second and the third group. (ii) The second group—corresponding to the fractions lower than 5 kDa—displayed average values of aromaticity (about 20%) which increased little during the experiment as shown in Figure II. 4. This group was probably composed by a small fraction of simple organic molecules and a larger amount of fulvic acids since aromaticity increased (Chin et al., 1994; Tipping, 2002). These results support those of Drever and Vance (1994) who reported a molecular range of about 0.5 to 5 kDa for the fulvic acids. (iii) The third group included fractions higher than 5 kDa. Organic molecules characterized by a strong aromaticity (higher than 20%) such as that corresponding to humic acids (Weishaar et al., 2003) belong to this group. These organic ligands were especially concentrated in the fraction between 5 and 30 kDa because the values of aromaticity were higher in the fraction below 30 kDa than in the fraction below 0.2 μm. Chemical, spectroscopic, and Py-GC-MS analyses showed in a study carried out by Li et al. (2004) that, as apparent molecular size increases, the humic acid fraction becomes less polar and less aromatic as well. Humic acid fractions with smaller molecular weight have much greater O/C and lower H/C ratios, and higher contents of oxygencontaining functional groups (Li et al., 2004). By contrast, the humic acid fraction with larger molecular weight has lower O/C but higher H/C atomic ratios and lower contents of oxygen-containing functional groups.

To summarize, the aromaticity of the released organic compounds increased through time throughout the experiment and increased with the organic compound size, to decrease afterward with the largest compounds. Simple organic compounds were leached at the beginning of the experiment and then followed by humic substances as a whole with different aromaticities depending on the considered sampled compound size.

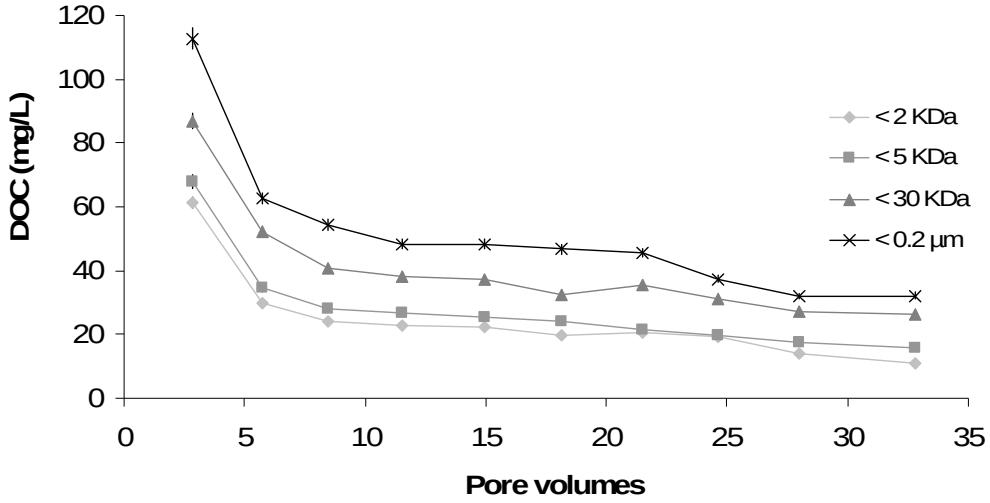

Figure II. 3. DOC kinetics during the experiment for the four cut thresholds (black stars correspond to the fraction below 0.2 µm; gray triangles correspond to the fraction below 30 kDa; gray squares correspond to the fraction below 5 kDa, while gray diamond-shape symbols correspond to the fraction below 2 kDa).

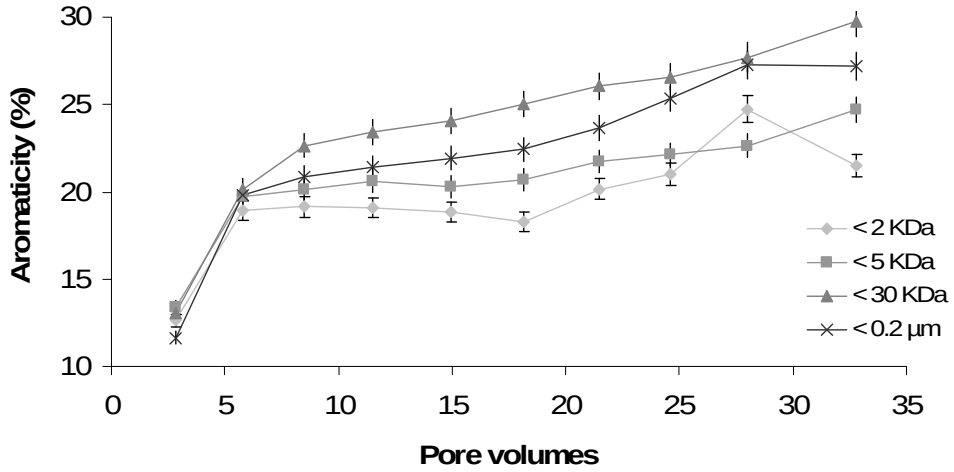

Figure II. 4. Aromaticity (%) is reported versus DOC (mg/L) (black stars correspond to the fraction below 0.2 µm; gray triangles correspond to the fraction below 30 kDa; gray squares correspond to the fraction below 5 kDa, while gray diamond-shape symbols correspond to the fraction below 2 kDa).

2. Trace element behaviour

An ascending hierarchical classification was carried out in order to determine different groups of elements behaving in the same way within each group. Cluster analysis data are presented as a dendogram, where the similarity of behaviour of two elements is conversely proportional to the linkage distance (Figure II. 5). Both ascending hierarchical classification (Figure II. 5) and ultrafiltration data (reporting the distribution of elements in the major colloidal phase—higher than 2-kDa molecular weight) (Figure II. 6) showed different groups of elements on the basis of their behavior with regard to the leaching process. The first group is composed of alkaline and alkaline

earth metal elements and other trace element such as Mn, Si, and B. These elements were either (i) strongly leached during the experiment or (ii) not (or little for Ca, Sr, Mn, and Ba) fractionated with decreasing pore-size cuts and there is no relationship between these elemental concentrations and associated DOC concentrations (Figure II. 7). So, they were easily leached but not mobilized by organic colloids. They have been often described as occurring at a “true” dissolved state (Pokrovsky et al., 2007; Pourret et al., 2007a), since almost not mobilized by the colloidal phase. Si concentrations were relatively low in the different fractions. They decreased during the experiment and there was no fractionation of Si concentration with decreasing pore-size cuts. Thus, Si was not trapped by small-size clay minerals and/or by organic colloids as elsewhere evidenced by ultrafiltration of organic-rich natural waters (Viers et al., 1997), solubility, and potentiometric measurements (Pokrovski and Schott, 1998). This point clearly demonstrates that Si–humic acid complexes were here negligible. Silicium occurred as “truly” dissolved species in the soil solution. Thus, Si was rather labile and was present in compounds of low molecular weight such as silicic acid. In this case, the role of aluminosilicates in the colloidal pool generated in this experiment must be extremely limited. This clearly prevented them from being good candidates for trace element complexation in such context.

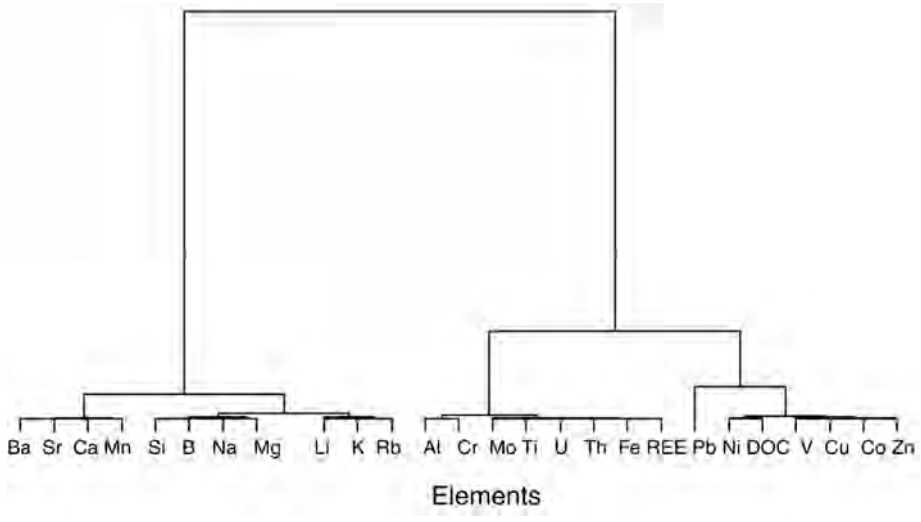

Figure II. 5. Ascending hierarchical classification of elements following the ward criterion (Lebart and Morineau, 2000).

Mobilization via organic colloids for Ca and Mg in organic-rich environments was however elsewhere observed (Eyrolle et al., 1996; Viers et al., 1997, Dupré et al., 1999). This contrasted behavior can be explained by the fact that such mobilization was mainly carried out via vegetable remains and phytolithes in soils (Eyrolle et al., 1996). This study did not allow their analyses, as all the leachates were filtered before measurement with a 0.2- μm filter. The weak mobilization observed for Ca, Sr, Mn, and Ba is comparable to other studies undertaken in organic-rich environments (Pokrovsky and Schott, 2002; Dahlqvist et al., 2004; Pokrovsky et al., 2005). Van

Hees and Lundstrom (2000) estimated that about 14% of Ca and Mg can be bound to low molecular weight organic ligands (such as citric and oxalic acids) in soil solution of a podzolic organic horizon, while complexation was generally negligible in other horizons.

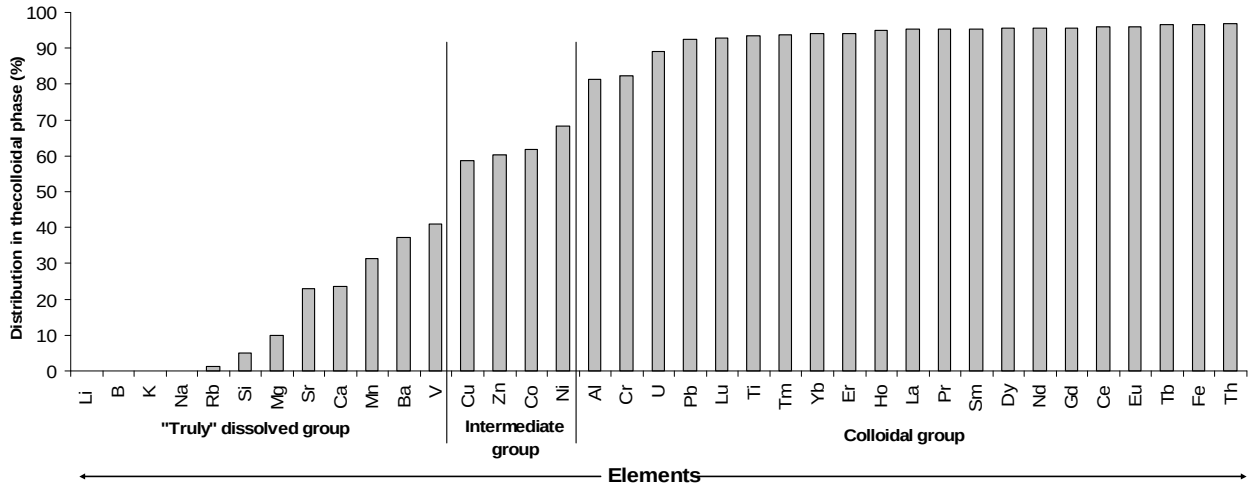

Figure II. 6. Distribution of elements in major colloidal phase (higher than 2 kDa) at the end of the experiment. Three groups are identified with respect to contrasted behaviour with regard to the colloidal phase: (i) the "trully" dissolved group, (ii) the intermediate group, and (iii) the colloidal group.

The second group is composed of all the other elements recognized in several publications as being more or less strongly mobilized by the organic and/or inorganic colloidal phase (Pokrovsky and Schott, 2002; Oliva et al., 1999; Bradl, 2004). Two subgroups can be formed within this group depending on the mobilization characteristics. The first subgroup is composed of Cu, Zn, Co, V, and Ni. These latter elements appeared to be only moderately mobilized by organic colloids and to have a significant fraction occurring as truly dissolved species (Figure II. 8). These elements form an intermediate group. Dissolved organic carbon appeared to have the same behaviour with regard to the leaching process than these elements since the below 2-kDa fraction, which was released all over the experiment, was important (about 30%) (Figure II. 3). This DOC release is similar to those recorded in a temperate peat and podzol soil solution (Pokrovsky et al., 2005) where the proportion of thin-size organic colloids (<1 kDa) can be as high as 40%. The second subgroup is composed of Al, Cr, Mo, Ti, U, Th, Fe, and REE. These elements evidenced a strong fractionation with decreasing pore-size cuts with a very low concentration in the lowest fraction and showed strong interactions with DOC (Figure II. 9) (see Section S3 in Supplementary material). Figure II. 10 shows that these elements belonging to the colloidal group were mobilized at more than 80% in the fraction higher than 5 kDa and at about 60% in the fraction in between 5 and 30 kDa. They were thus strongly mobilized by organic colloids and more precisely by humic acids considering the molecular weight of the involved organic pool. Similar estimations of Al and Fe complexation were observed by Van Hees and Lundstrom (2000) where 85 and 95% of the Al and Fe, respectively, were organically

bound. Lead exhibited a comparable behaviour. However, the ascending hierarchical classification put aside this element from this latter group because the major colloidal fraction mobilizing this element was different. It appeared especially mobilized by large colloids in the fraction heavier than 30 kDa. A previous study conducted on field samples close to the sampling site of the used soil sample showed the same trace element distribution (Pourret et al., 2007a). Thus, trace elements such as Cu, Zn, Co, Ni, Al, Cr, Mo, Ti, U, Th, Fe, Pb, and REE were moderately or strongly mobilized by humic substances. But, humic acids are enriched in iron nanoparticles and thus, the presence of a second possible carrier phase leads to the debated following question: What are the respective roles of the organic and inorganic carrier phases involved in the sorption and/or carrying of these trace elements?

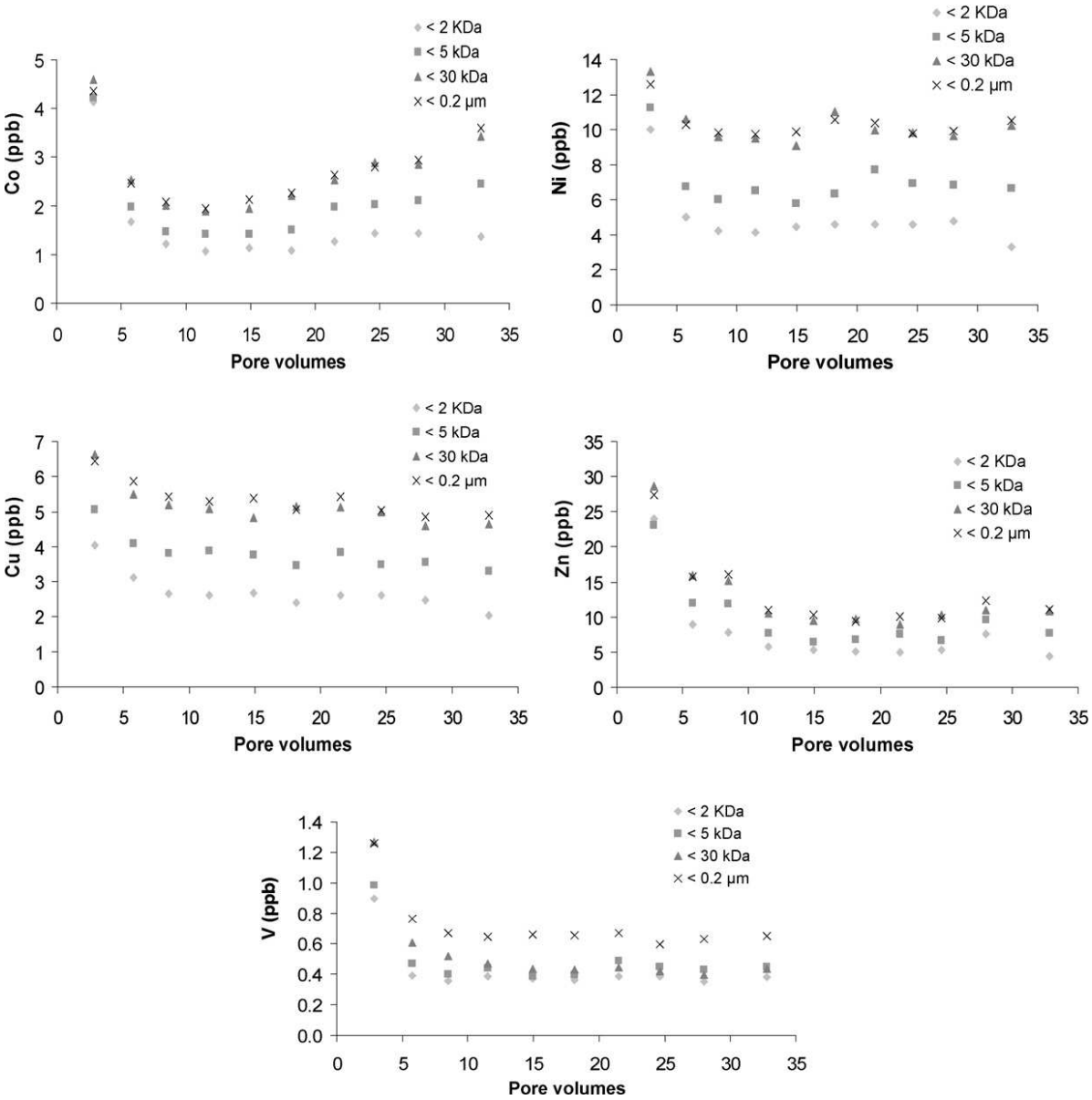

Figure II. 7. Elemental concentration distribution, of the "truly" dissolved group all along the experiment (black stars correspond to the fraction below 0.2 µm; gray triangles correspond to the fraction below 30 kDa; gray squares correspond to the fraction below 5 kDa, while gray diamond-shape symbols correspond to the fraction below 2 kDa).

3. Organic and inorganic colloidal carrier phases

Data indicate a lack of Fe in the fractions lower than 2 kDa, and then a distribution of the concentration of Fe correlated with DOC (see Section S3 in Supplementary material). We should mention that we did not observe any distinct Fe increase in the fractions higher than 30 kDa, which is the molecular weight range where iron oxides were previously identified in the Mercy wetland (Pourret et al., 2007a). This latter point suggests the lack of iron oxide senso stricto but the possible occurrence of iron nanoparticles closely related to organic matter as elsewhere evidenced (Pokrovsky et al., 2005). Aluminum oxides cannot be present in the various fractions since they are of micrometric size (Girard et al., 2005). Thus, Al did also occur as closely associated with the so-called organic colloidal pool. This point probably explains why the distribution of Al concentrations displays a positive relationship with the concentrations of both DOC and Fe (see Section S3 in Supplementary material). Fulvic acids were thus present in the fractions lower than 5 kDa, while humic acids occurred in the fractions between 5 kDa and 0.2 μm which were probably mixed (Al, Fe-rich) fractions. The presence of the combined occurrence of Fe and Al associated to humic substances has previously been reported in organic-rich soil (Van Hees and Lundstrom, 2000; Tyler, 2004; Pokrovsky et al., 2005) and in several rivers of organic-rich environment (Lyven et al., 2003; Pokrovsky et al., 2006; Dahlqvist et al., 2007; Pourret et al., 2007a). In these studies, the nature of the colloidal carrier phases which have been observed was either variable or similar according to the considered trace elements and organic versus inorganic compound ratio.

In this contribution, the two major carrier phases displayed time-linked releases through time characterized by contrasted shapes. The most striking point when looking at the release is the elemental concentration distribution in the different phases. This point allows suggesting that the associations between the carrier phases and the elements occurred when the potential carrier phases and the elements display comparable release through time. During the experiment, the Fe concentrations were mostly localized in fractions higher than 30 kDa. The Fe concentration distribution was different from that of DOC which displayed more uniform concentrations whatever the considered fraction was. These data suggest the presence of iron nanoparticles in the fraction higher than 30 kDa. To reinforce this hypothesis, a “reduction–oxidation” test was made on the same soil. Most part of the precipitated iron nanoparticles were characterized by size ranging between 30 kDa and 0.2 μm.

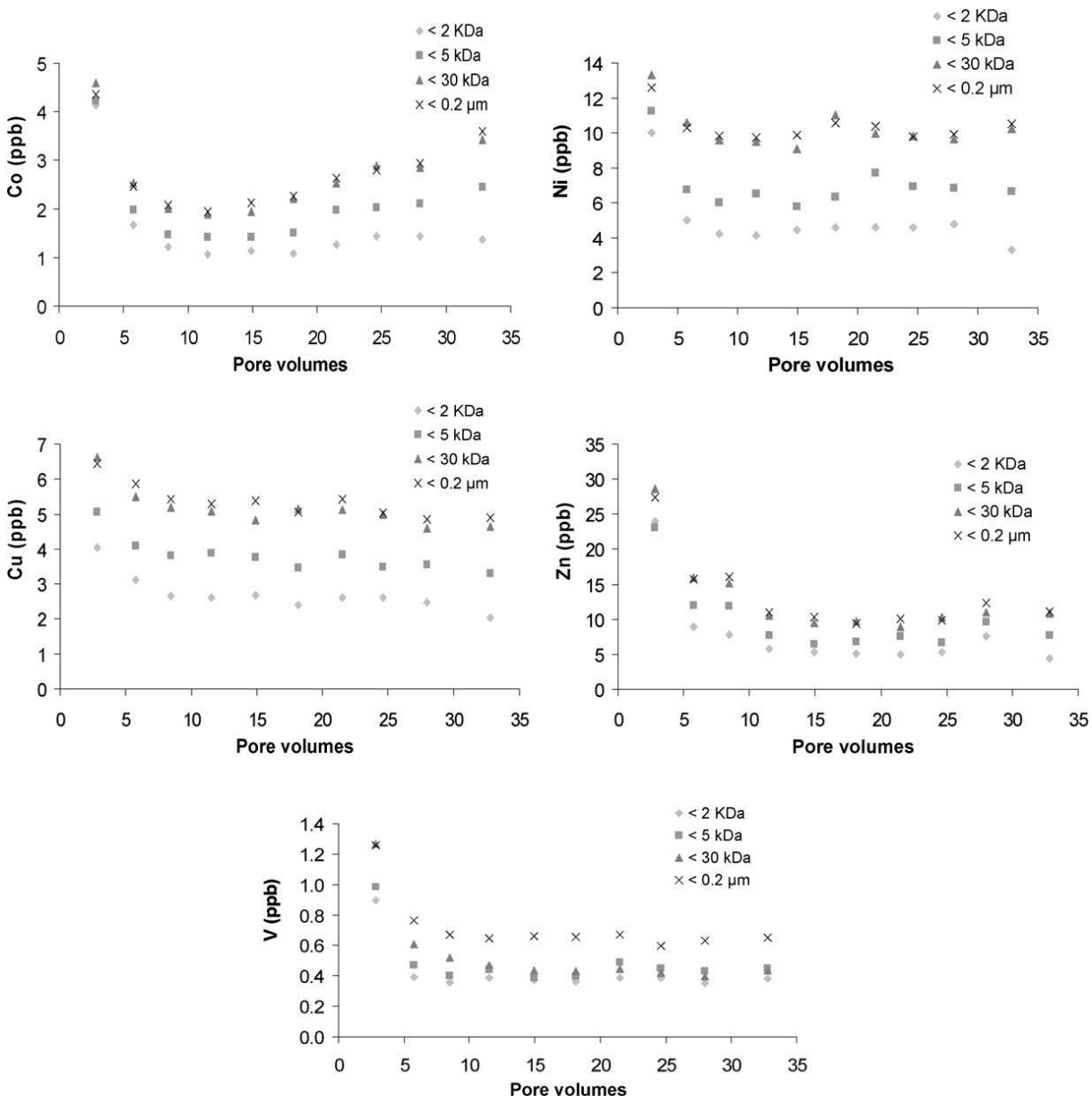

Figure II. 8. Elemental concentration distribution of the intermediate group all along the experiment experiment (black stars correspond to the fraction below 0.2 µm; gray triangles correspond to the fraction below 30 kDa; gray squares correspond to the fraction below 5 kDa, while gray diamond shape symbols correspond to the fraction below 2 kDa).

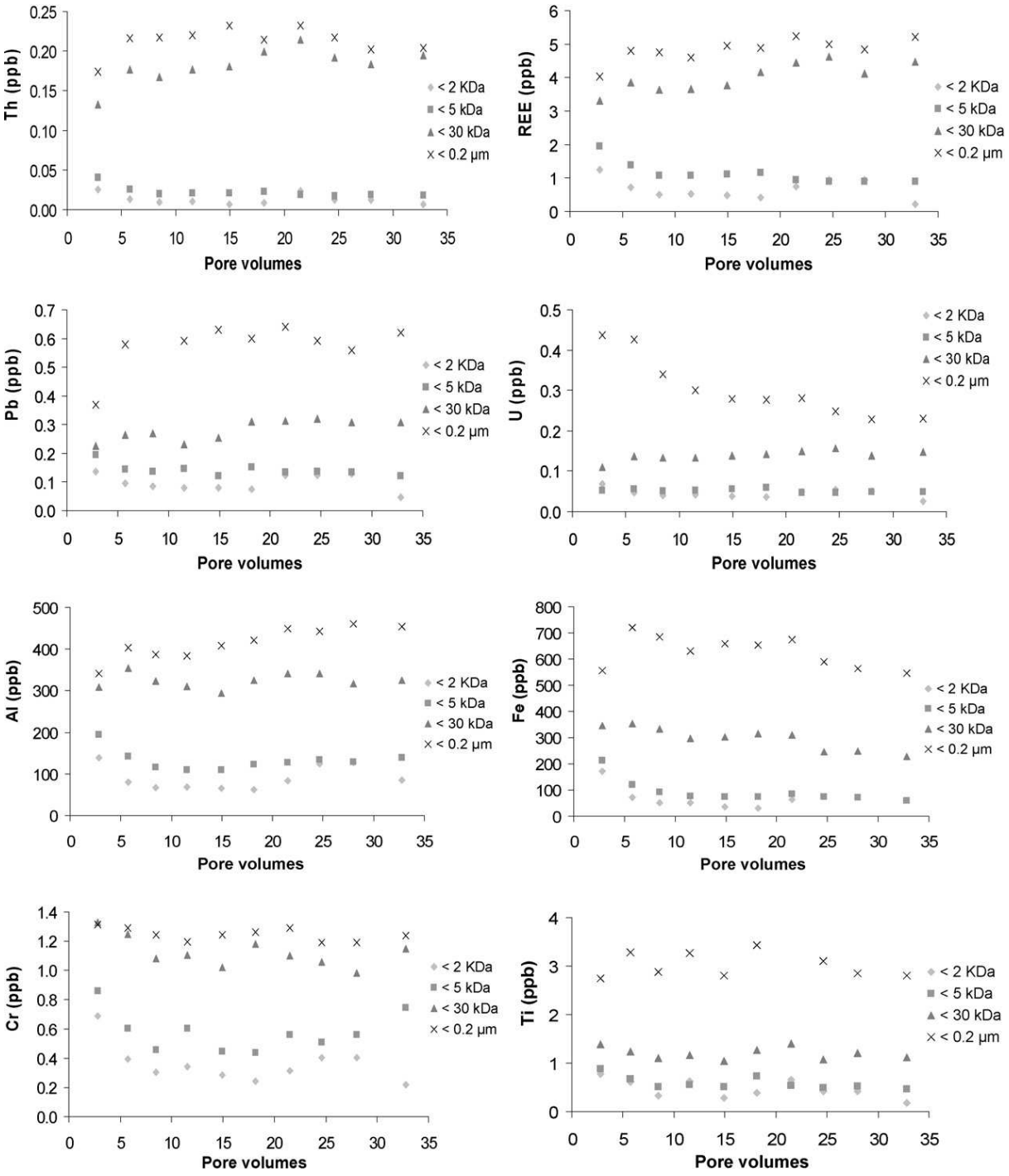

Figure II. 9. Elemental concentration distribution of the colloidal group all along the experiment (black stars correspond to the fraction below 0.2 µm; gray triangles correspond to the fraction below 30 kDa; gray squares correspond to the fraction below 5 kDa, while gray diamond shape symbols correspond to the fraction below 2 kDa).

Cobalt, nickel, copper, zinc, and vanadium (Figure II. 8) displayed the same kinetic pattern as that of DOC, suggesting that they followed DOC release in solution. This point has been previously reported elsewhere (Table II. 1). For example, Tyler (2004) showed a mobilization of Ni, Cu, Zn, and V by DOC. The data also established that the mobilization of these elements was made for a

significant part by organic compounds of small molecular weight (lower than 5 kDa) such as fulvic acids, as elsewhere observed (Pokrovsky et al., 2005; 2006). This differs for some trace elements strongly bound to colloids, which displayed more contrasted release patterns with regard to that of DOC. This is true for Ti, U, and Pb (Figure II. 9), whose release patterns followed that of Fe. This latter point suggests that these trace elements were mostly bound to iron-rich nanoparticles, however, possibly associated with humic acids. The corresponding samples displayed release patterns for trace elements which followed the shape of that of iron. This suggests that a mobilization of these elements by iron nanoparticles occurred in fractions higher than 5 kDa, while an organic colloid-mediated mobilization had to occur in fractions lower than 5 kDa. This hypothesis was confirmed by the calculation of the available surface sites of these iron nanoparticles with the hypothesis that they were under an amorphous hydrous ferric oxide form characterized by a concentration of the available surface sites of 1.8 to 16 * 10^{-3} mol g^{-1} (Langmuir, 1997). The concentration of the available surface sites of iron nanoparticles was higher than the total concentration of these trace elements in fractions higher than 5 kDa. Therefore, there were enough iron nanoparticles in organic colloids higher than 5 kDa to allow their adsorption. The mobilization of these trace elements by iron was also previously observed elsewhere (Table II. 2). To summarize, humic substances and more precisely humic acids are iron-rich nanoparticular compounds which significantly complex part of trace elements. Thus, by stabilizing these ferric carrier phases humic substances can be involved either directly as trace element carriers or indirectly by the formation of a mixed organic/inorganic colloidal phase in the transport of many relatively insoluble trace elements.

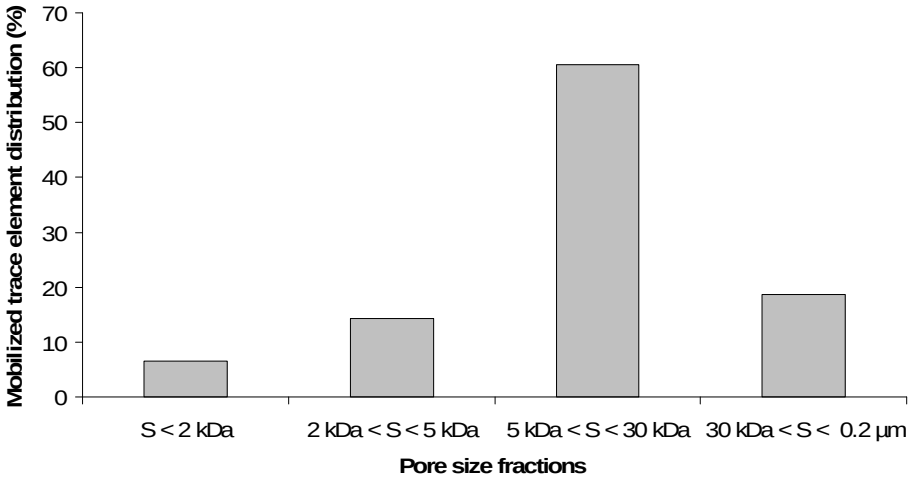

Figure II. 10. Distribution of the mobilized trace elements belonging to the colloidal group in the different cut thresholds at the end of experiment (*S* corresponds to the molecular weight of the sample compounds).

4. Dissolved organic matter and humic substances/metal ratio: the key parameters to understanding REE patterns in organic-rich environment

Rare earth element patterns for each cut threshold are displayed in Figure II. 11. The REE patterns were normalized to the upper continental crust (UCC) (Taylor and McLennan, 1985). REE data indicated the presence of a middle rare earth element downward concavity fractionation and the occurrence of Ce anomalies (0.56) for each cut threshold. But, there was no significant pattern difference between each fraction. The REE pattern shape remained constant through time whatever the considered cut threshold. In addition, the REE concentration levels of the fractions below 2 and 5 kDa on one side, and of the fractions below 30 kDa and 0.2 μm on the other side, were comparable. The fractions below 2 and 5 kDa were REE depleted while those below 30 kDa and 0.2 μm were relatively REE rich. Thus, the occurrence of REE fractionation with decreasing pore-size cutoff indicated that REE were mostly mobilized by high molecular weight colloids and, more precisely, by between 5- and 30-kDa molecular weight assemblages.

This dataset showed that REE were significantly bound to humic substances as evidenced by a release dynamics comparable to that of DOC (Figures III. 3 and 9). Furthermore, the concave shape of the REE pattern (Figure II. 11), which remained unchanged through the experiment, reflects an organic matter-mediated complexation as previously evidenced (Pourret et al., 2007b). Indeed, it has been previously observed that this pattern shape was quite typical of such interaction between organic matter and REE when organic interaction with REE took place (Viers et al., 1997; Dia et al., 2000; Gruau et al., 2004; Grybos et al., 2007). This point reinforces the hypothesis of REE mobilization by the organic pool, and more precisely by humic substances. These experimental data are comparable to those previously published by Yamamoto et al. (2005) and Pourret et al. (2007b) but differ from another one performed under significantly different experimental conditions (Sonke and Salters, 2006). This study showed an increase in log $K_{C,LnHs}$ (conditional binding constants), with a decrease in the ionic radius for REE-Leonardite HA complexes on the considered pH range (Sonke and Salters, 2006). This continuous increase of log $K_{C,LnHs}$ values from La to Lu has been ascribed to a lanthanide contraction effect, and was quantified as the numerical difference between the Lu and the La binding constants (Sonke and Salters, 2006; Stern et al., 2007). In this case, the REE pattern showed a linear increased from La to Lu, and thus a heavy rare earth element enrichment. However, these experiments were performed in a different analytical window (especially when considering the metal loading) than that undertaken in this contribution. The metal loading can have a strong effect on metal–humic complexation (Bidoglio et al., 1991; Hummel et al., 2000). The humic substances/metal (HS/metal) ratio is often used to define the metal loading. In this case, HS is the molar concentration of total carboxylic binding sites and metal is the molar concentration of total

metal ion binding with humic substances. Humic substances are composed of different binding sites, namely the weak and the strong sites. The weak sites determine the behavior of humic complexation at high metal concentrations (low HS/metal ratio) (Yamamoto et al., 2005; Hummel et al., 1995).

Table II. 1. Trace element mobilization by organic carrier phases as evidenced from the literature.

Authors	C-rich carrier
Dahlqvist et al., 2007	Co, Ni and Cu
Lyvén et al., 2003	Co, Ni and Cu
Pokrovsky et al., 2006	Co, Ni, Cu and Zn
Pourret et al., 2007	Co, Cu
Tyler, 2004	Co, Ni, Cu, Zn and V

Table II. 2. Trace element mobilization by either iron inorganic phases or iron-rich organic phases as evidenced from the literature.

Authors	Fe-rich carrier	(C/Fe)-rich carrier
Dahlqvist et al., 2007		REE, Pb, U and Th
Pokrovsky et al., 2005		REE, Pb, Ti, Th and U
Pokrovsky et al., 2006	REE, Pb, Ti, Th and U	
Pourret et al., 2007	Al and Th	REE
Tyler, 2004	Al, Th, Ti, REE and U	

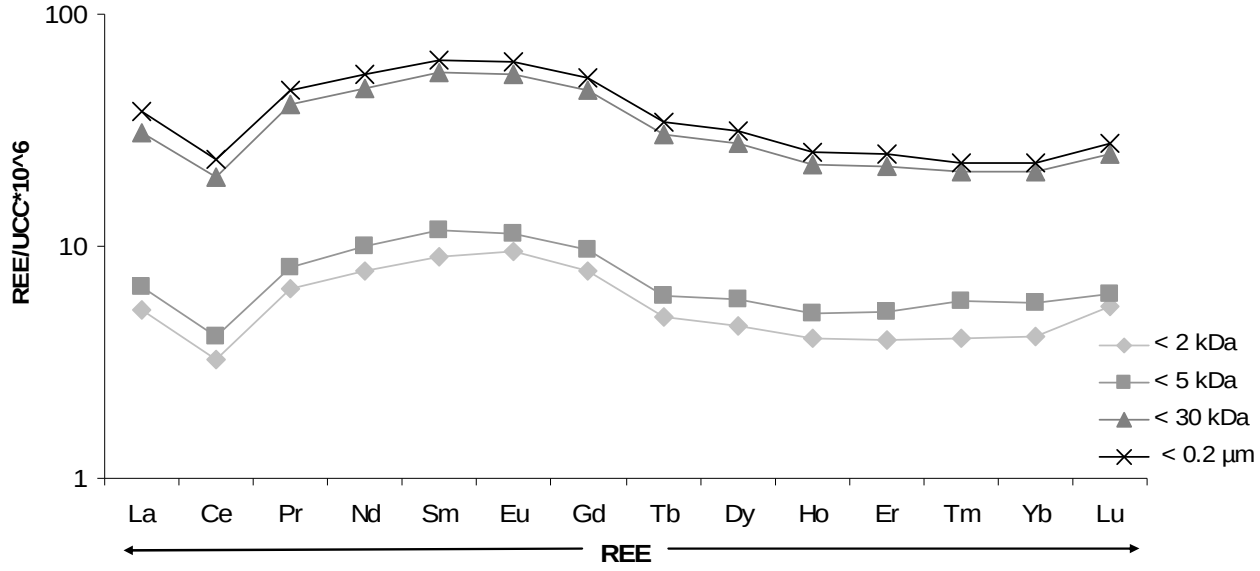

Figure II. 11. Upper continental crust (UCC) normalized (Taylor and McLennan, 1985) patterns of soil solution (black stars correspond to the fraction below 0.2 µm; gray triangles correspond to the fraction below 30 kDa; gray squares correspond to the fraction below 5 kDa, while gray diamond-shape symbols correspond to the fraction below 2 kDa).

Although characterized by concentrations in a range of a few percent, the strong sites determine the complexation strength of humic substances at low trace metal concentrations (high HS/metal ratio) (Hummel et al., 1995). In this study, HS/metal ratios were ranging between 30 and

40, whereas they were between 5 and 20 in Pourret et al. experiments (2007b), close to 80 in Yamamoto et al. experiments (2005) and between 500 and 600 in Sonke and Salters (2006) and Stern et al. (2007). Thus, this strongly suggests that different metal loading led to the use of different binding sites in the humic substances resulting in variations in the REE fractionation and the resulting REE pattern. Consequently, the main point which stems from this new REE dataset is that such REE pattern type (Figure II. 11) could be expected in all natural systems characterized by a high metal loading itself significantly bound to humic substances.

IV. Conclusions

Although characterized by small size, colloids are mobile and offer diverse surface functions allowing interactions with trace elements. Colloids play a key role in the distribution of trace elements as established through this experimental study and elsewhere. The mobility of trace elements is strongly increased via the genesis and transfer of the colloidal pool in hydrosystems. But, all trace elements do not behave and interact in the same way with the surrounding medium. Some of them are only slightly prone to a colloidal complexation, whereas others are much more involved in such colloid-controlled complexes.

This experimental dataset reveals three groups of elements with regard to their mobilization via colloids. First, there is the truly dissolved group with alkaline, alkaline-earth metal elements, and other trace element such as Mn, Si, B, and V which are little mobilized by colloids and quickly leached. Secondly, the intermediate group includes Cu, Zn, Co, and Ni partly mobilized by colloids, thus evidencing different release behaviors. Humic substances of small molecular weight (lower than 5 kDa) and medium aromaticity, such as fulvic acid, complex a significant part of these trace elements. The third group is characterized by trace element mobilities depending on the involved colloid types. This latter group includes Al, Cr, U, Mo, Pb, REE, Fe, Ti, and Th.

These experimental data reveal that fractions higher than 5 kDa, and particularly the fraction ranging in between 5 and 30 kDa which is very aromatic, are very efficient complexing agents for trace elements. Thus, the major carrier phase for these trace elements results from an assembling among Fe, Al, and humic substances, especially humic acids. However, the data suggest that a ferric phase is bound to several trace elements of the third group (such as Pb, Ti, and U). As a consequence, humic acids can be indirectly involved in a colloidal transport of many insoluble trace elements by stabilizing these ferric carrier phases. This study demonstrated also that humic substances play a major control onto REE speciation. However, the metal loading and, more precisely, the humic substances/metal ratio must be considered as a major controlling parameter of the REE fractionation pattern in organic-rich environments.

Chapitre III : Structure dynamique des substances humiques et impact sur la distribution en solution des terres rares associées

Dynamic structure of humic substances and its impact on associated Rare Earth Element distribution in waters

Ce chapitre correspond à un article soumis (Mai 2009) à la revue 'Chemical Geology' : Pédrot, M.; Dia, A.; Davranche, M. : 'Dynamic structure of humic substances and its impact on sequestrated Rare Earth Element distribution'.

Résumé : Bien que les substances humiques soient connues pour jouer un rôle clé dans le contrôle de la spéciation des métaux et de la mobilité des éléments traces dans les sols et les eaux, la nature de leur structure reste un sujet de débat. Plusieurs modèles structuraux de substance humiques ont été proposés ; les substances humiques seraient composées soit de : (a) polyélectrolytes macromoléculaires susceptibles de former des agrégats moléculaires avec des molécules organiques de haut poids moléculaire, soit, (b) d'assemblages supramoléculaires (agrégats moléculaires) de petites molécules, réunies par des forces attractives de faible intensité. Cette étude expérimentale a été conçue pour suivre : (1) l'évolution de la taille des molécules organiques, selon la force ionique ou le pH au moyen de l'analyse combinée de données d'ultrafiltration, d'aromaticité et de teneurs en terres rares, et (2) l'impact du pH et de la force ionique sur la distribution des terres rares associées dans la solution de sol. Cette étude confirme la présence d'associations supramoléculaires de petites molécules, et probablement également la présence de macromolécules dans la majeure partie de la matière organique dissoute. Contrairement à la force ionique, le pH semble être le paramètre majeur jouant sur la stabilité structurale des substances humiques. Les substances humiques révèlent donc une structure dynamique, qui évolue selon le pH. De faibles pH induisent une déstabilisation de la structure des substances humiques. Cette déstabilisation a un impact sur la distribution des éléments traces dans la solution de sol, comme l'atteste la distribution des terres rares, et inversement, le degré de déstabilisation des substances humiques semble être influencé par la charge en ions métalliques présente dans la solution.

Abstract : While humic substances are known to play a key role in controlling metal speciation and mobility of trace elements within soils and waters, the understanding of their structure is still unclear and remains a matter of debate. Several models of humic substance structures have been proposed, where humic substances were composed of either, (i) macromolecular polyelectrolytes that can form molecular aggregates with heavy organic molecules or, (ii) supramolecular assemblies (molecular aggregates) of small molecules without macromolecular character, joined together by weak attraction forces. This experimental study was designed and dedicated (i) to follow the size of organic molecules versus ionic strength or pH by the combined means of ultrafiltration and aromaticity data and Rare Earth Element (REE) fingerprinting, and (ii) to investigate the pH and ionic strength effect on the distribution of associated rare earth elements in soil solution. This study supports the presence of supramolecular associations of small molecules and probably the presence of macromolecules in the bulk of the dissolved organic matter. By contrast to ionic strength, pH appeared to be the major parameter playing on the stability of the humic substance structure. Humic substances displayed dynamic structure, which evolved regards to pH. Low pH led to a destabilization of the humic

substance conformation. This destabilization had an impact on the trace element distribution in soil solution, as assessed by Rare Earth Element data, and reversely, the destabilization degree of humic substances seemed to be influenced by the metal ion charge.

I. Introduction

Soil organic matter represents nearly three times the mass of all aboveground life. The Earth's carbon pool is vital to terrestrial life, influencing soil ecology, food production, quality of water, carbon sequestration, and the mobility and fate of anthropogenic chemicals and heavy metals. Dissolved Organic Carbon (DOC) is composed of mixtures of organic molecules, displaying a broad spectrum of functional groups (carboxylic acids, phenols, amines, etc.), structures, and molecular weight distributions. Humic substances - including humic and fulvic acids - are the main components of the dissolved organic carbon in aquatic systems and soils (Kalbitz et al., 2000; Mercier et al., 2001) and are probably the most abundant naturally occurring organic molecules. Humic and fulvic acids are usually considered to be the most reactive humic substances involved in cation and slightly polar (such as pesticides) organic contaminant binding. Their structures carry a large diversity of functional groups, with the majority being carboxilic (-COOH) and phenolic (-OH) groups allowing the adsorption of multivalent ions (Tipping, 2002; Martyniuk and Wieckowska, 2003). Therefore, humic substances play a key role in controlling speciation and mobility of metal and organic contaminants in soils and aqueous environments (Tipping, 2002).

Further information on the nature of the different groups (microbial metabolites - fulvic and humic acids) of DOC can be gained by comparing their respective aromaticity (Chin et al., 1994; Tipping, 2002). Microbial metabolites have the lowest aromaticities, while humic acids display higher amounts of aromatic moieties than fulvic acids. But, the knowledge of the humic substance molecular size and shape is still a large matter of debate. Several humic substance structural models have been proposed, where structure of humic substances was either, (i) macropolymeric with heavy organic molecules considered to be flexible linear synthetic polyelectrolytes or, (ii) supramolecular with an association of a complex mixture of different molecules held together by dispersive weak forces. Indeed, many authors defined humic substances as linear macromolecular polyelectrolytes that can form molecular aggregates under specific experimental conditions, principally acid pH and high ionic strength (Senesi, 1999; Swift, 1999). Other authors proposed defining humic substances as supramolecular assemblies (molecular aggregates) of small molecules without macromolecular character, joined together by weak attraction forces (Piccolo et al., 1996; Wershaw, 1999; Piccolo et al., 2001; Simpson et al., 2001). To reconcile these two hypotheses, more recently Baigorri et al.

(2007) showed that macromolecules, small molecules and supramolecular associations all seemed to coexist in the humic substances.

It is well known that physicochemical parameters such as pH and ionic strength can significantly influence the behaviour of humic substances (Dehaan et al., 1987; Murphy et al., 1994; Benedetti et al., 1996; Gonet and Wegner, 1996; Avena et al., 1999; Cooke et al., 2007; Weng et al., 2007). Thus, the humic substance structure seems to be dynamic regards to environmental conditions. Therefore, these hereabove apparently opposing hypotheses concerning the humic substance structure could be both true, depending on the prevailing physico-chemical conditions. It becomes then most important to determine the impact of any parameter change on the humic substance structure, and their ability to sequestrate or release trace elements. Tombacz and Meleg (1990) showed a dependence of molar masses and coagulation according to pH and ionic strength. On the basis of model calculations, it was thus expected that the repulsion between the humic particles decreases with decreasing pH and increasing electrolyte concentration, which both increase the degree of aggregation (Tombacz and Meleg, 1990). Kipton et al. (1992) suspected that different humic molecular size fraction might dominate the trace element binding at different pH and ionic strengths. Environmental conditions could influence the size and shape of humic substances, and therefore, affect the distribution and the mobility of associated trace elements, especially trace elements known to be strongly bound to humic substances. As an example, the Rare Earth Elements (REE) are known to be mainly bound to organic matter in natural waters (Viers et al., 1997; Dia et al., 2000; Tang and Johannesson, 2003; Pourret et al., 2007b). Their complexation to humic substances involves the development of typical pattern shapes in solution, characterized by Middle Rare Earth Element (MREE) downward concavity (Davranche et al., 2005; Yamamoto et al., 2005; 2006; Pourret et al., 2007c; Yamamoto et al., 2008). A previous study on the organic colloids release from the same soil sample showed a strong interaction between humic substances and REE and the development of this specific MREE downward concavity (Pédrot et al., 2008). Thus, since closely associated to humic substances in organic-rich waters, REE can be used as a tracer to investigate the impact of pH and ionic strength on the humic substance structure and how this latter plays on the associated trace element distribution.

In this context, the aim of this work was to evaluate experimentally both the humic substance molecular-weight distribution as a function of pH and ionic strength, and its impact on the REE distribution. Thus, the size fractionation of organic molecules in the dissolved fraction (less than 0.2 µm) was investigated according to pH and ionic strength by coupling ultrafiltration at different cut-offs, analysis of the aromaticity, and using REE as tracer of humic substances. Rare earth elements patterns were discussed regards to the size range of the associated organic matter pool.

II. Materials and Methods

1. Soil Sample

The soil sample was collected from the upper soil horizons located in the Mercy wetland in January 2006. The Mercy Wetland (France), located in the Kervidy/Coët Dan experimental catchment, has been intensively surveyed for hydrological, pedological and geochemical issues (Mérot et al., 1995; Durand and Juan Torres, 1996; Curmi et al., 1998; Dia et al., 2000; Olivié-Lauquet et al., 2001). The organic-rich soil was dried at 40 °C for 72 h and sieved at 2 mm. Further details can be found in section S1 of the supporting information and in reference (Nelson and Sommers, 1982).

2. Experimental set up

The experimentation involved two steps. Firstly, a DOC-rich solution was prepared. For this purpose, batch-equilibrium soil experiments were conducted at pH = 7.5 to allow organic matter release in the soil solution. Ninety-five g of soil were added in a polypropylene container to 1900 ml of a $2*10^{-3}$ M NaCl solution. pH was maintained at 7.5 using an automatic pH stat titrator (Titrino 794, Metrohm) with a 0.1 M NaOH solution. The soil solution was continuously stirred. After 48 hours (at steady state), soil solution was filtered at 0.2-µm with a cellulose acetate filter (polyether sulfone membrane Sartorius Minisart). Then, pH and ionic strength of various aliquots of the organic-rich solution recovered from the batch experiment were modified to reach pH ranging from 3 to 7.5 (Exp1: pH = 3; Exp2: pH = 3.5; Exp3: pH = 3.9; Exp4: pH = 6; Exp5: pH = 7.5) and ionic strength ranging from 10^{-3} to 10^{-1}M (Exp4: I = 10^{-3} M; Exp6: I = 10^{-2} M; Exp7: I =10^{-1} M). Selected pH was monitored using an automatic pH stat titrator (Titrino 794, Metrohm) with 0.1 M NaOH or HCl solutions. We checked that NaOH or HCl additions to change pH did not drastically affect the ionic strength, since it only varied between 1 to $2*10^{-3}$ M in the 'pH' experiments. Sodium chloride was used to fix the ionic strength in each experiment. All experiments were made in triplicate.

All collected soil solution were filtered using 0.2-µm-pore size cellulose acetate filter capsules (polyether sulfone membrane Sartorius Minisart). Ultrafiltration experiments were performed to separate organic molecules following decreasing pore-size cuts. Fifteen-mL centrifugal tubes (Vivaspin) equipped with permeable membranes of decreasing pore sizes were used. Each centrifugal filter device have a vertical membrane of 2, 5 or 30 kDa and was washed and rinsed with HCl 0.1 N and MilliQ water three times before use. Centrifugations were performed using a Jouan

G4.12 centrifuge with swinging bucket at about 3000g for 20 minutes for 30 kDa devices, and 3500 g and 3750 g for 30 minutes, for 5 kDa and 2 kDa devices, respectively (Pourret et al., 2007a; Pédrot et al., 2008). All procedures (sampling, filtration and analysis) were carried out in order to minimize contamination. Blank tests were performed during this study to determine possible contamination due to filtration and analysis and were always negligible.

Dissolved organic carbon was analysed on a Total Organic Carbon analyser (Shimadzu TOC-5050A). Specific UltraViolet Absorbance (SUVA) - strongly correlated with degree of aromaticity of organic matter (Aromaticity = 6.52 * SUVA + 3.63) (Weishaar et al., 2003) - was used as an indicator of the chemical composition and reactivity of dissolved organic carbon (Grybos et al., 2007). Major anions (Cl^-, SO_4^{2-} and NO_3^-) concentrations were measured by ion chromatography (Dionex DX-120). Major cation and trace element concentrations were determined by ICP-MS (Agilent 4500). See section S2 of the supporting information for further details (Yéghicheyan et al., 2001; Davranche et al., 2004).

III. Results and discussion

1. Humic substance aromaticity and size distribution regards to pH and ionic strength

Different degrees of aromaticity were identified in the size-fractions according to pH or ionic strength (Figures III. 1a, III. 1b). However, all fractions displayed aromaticity higher than 30 %, suggesting that the main components were humic substances. Indeed, the aromaticity values are similar to those noted for humic substances from many environments (Malcolm, 1990; Tipping, 2002; Weishaar et al., 2003). The results followed two trends regards to pH: (i) the aromaticity degree was similar in the fractions <30 kDa and <0.2 µm, but changed in the fractions <5 kDa (Figure III. 1a). Dissolved organic carbon aromaticity in the fractions <5 kDa was strongly dependent on pH, displaying a decreasing aromaticity with the increasing pH. (ii) By contrast, according to the ionic strength, the aromaticity was similar in the fractions <30 kDa and <0.2 µm (less than 1 % and 2 % of differences, respectively) and slightly dissimilar in the fractions <5 kDa (between 6 and 9 % of differences for fractions <5 and <2 kDa, respectively). Figures III. 2a and III. 2b display the DOC concentration versus the size fraction range regards to pH (a) or ionic strength (b). Figure III. 2a shows that pH fractionated DOC according to the decreasing pore-size. At high pH values (pH 7.5 and 6), 76 % (10.2 ppm) of DOC was contained in the 5 kDa <fractions< 0.2 µm, 62 % (8.4 ppm) in the 5 kDa<fraction<30 kDa and 24 % (3.2 ppm) in fractions <5 kDa. At low pH (pH 3-3.5), the DOC concentration decreased from 8.4 to 3.75 ppm in the 5 kDa<fraction<30 kDa, while

it increased from 1.4 to 3.8-4.25 ppm in the fraction <2 kDa. At low pH, the fraction <2 kDa represented 30 % of the DOC, while it represented 10 % at high pH. The DOC increased by a factor of 50 % (1.7-2 to more than 3 ppm) in the fraction >30 kDa. A slight change in the DOC distribution was observed regards to the ionic strength (Figures III. 1b and 2b). Dissolved organic carbon concentration decreased weakly in the 5 kDa<fraction<30 kDa, when conversely it slightly increased in the fractions <5 kDa at a high ionic strength.

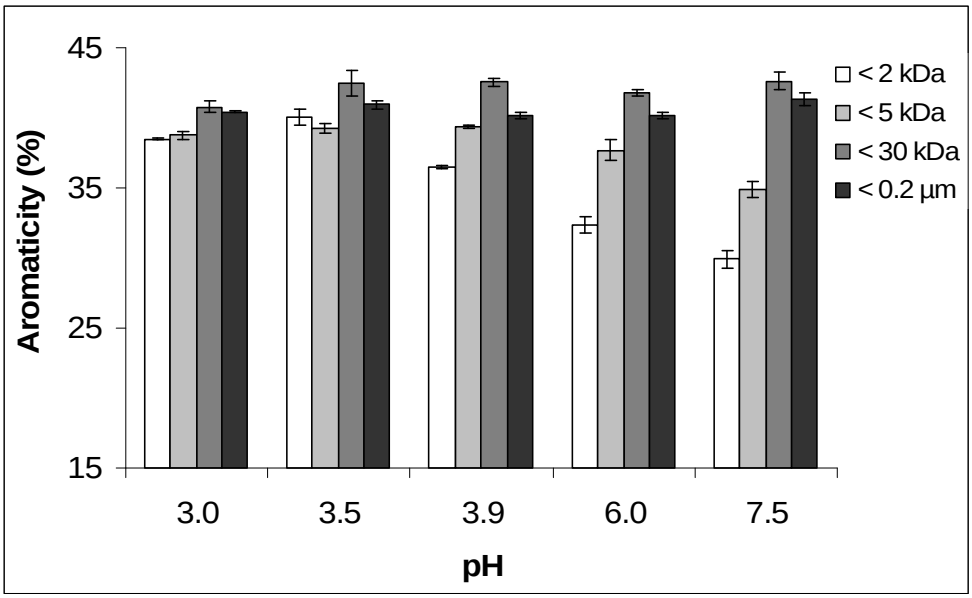

(a)

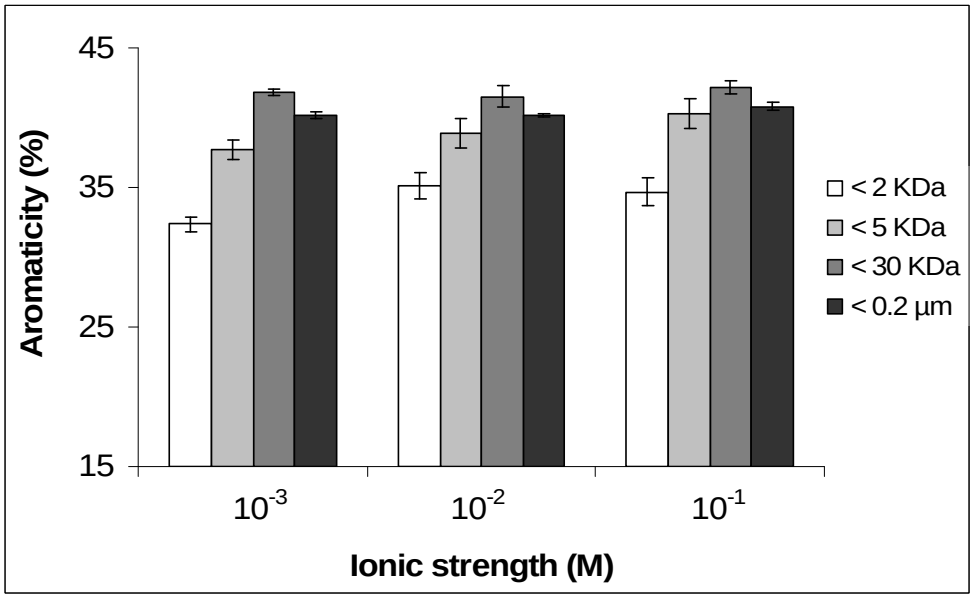

(b)

Figure III. 1. Aromaticity (%) is reported versus pH (a) or versus ionic strength (b). Ionic strength was fixed at $I = 10^{-3}$ M for all the 'pH' experiments, while pH = 6 for all the 'Ionic strength' experiments.

Therefore, the aromaticity of the organic compounds <5 kDa increased with the decreasing pH, to reach the aromaticity degree of fractions <30 kDa and <0.2 µm. Moreover, the DOC increased strongly in the fractions <5 kDa and decreased in the 5 kDa<fraction<30 kDa with decreasing pH.

The humic substance size was therefore controlled by pH. The ionic strength had far less impact than pH. At high ionic strength (10^{-1}M), the organic compound size decreased slightly, to increase the proportion of humic molecules present in fractions <5 kDa. The difference between a 'high ionic strength' and a 'low pH' experiment lied in the distribution of the small molecules. At high ionic strength, the increase of the amount of molecules (or associations of molecules) ranging in between 2 and 5 kDa was similar to the increase of the amount of molecules of sizes lower than 2 kDa. At high and low pH, the amount of molecules ranging in between 2 and 5 kDa was similar, while the amount of molecules lower than 2 kDa increased strongly with decreasing pH.

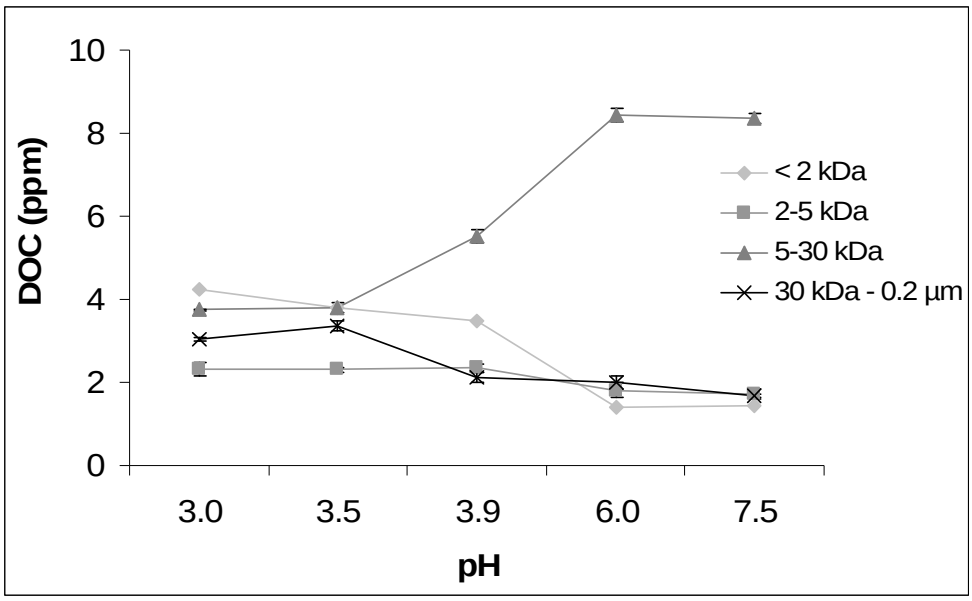

(a)

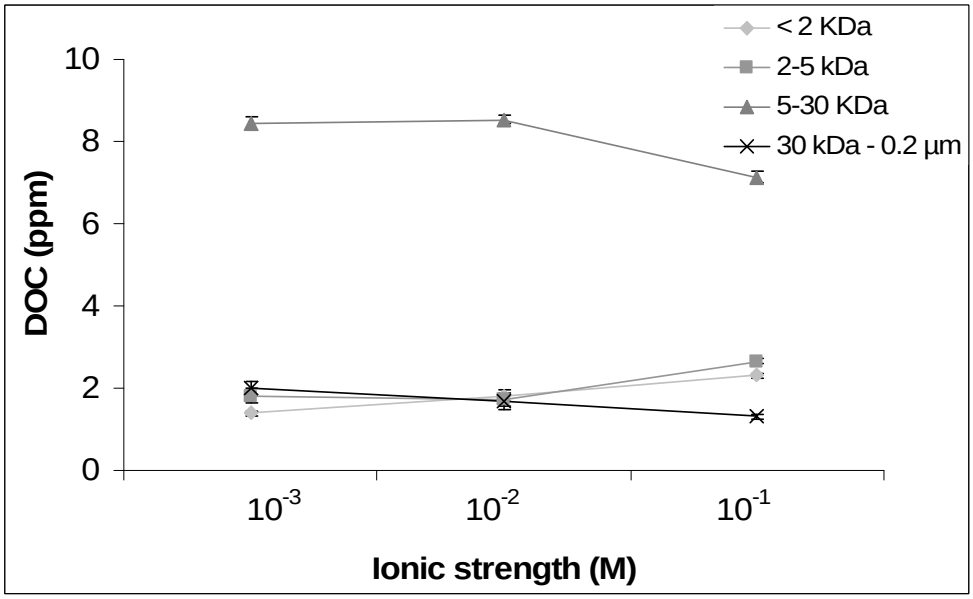

(b)

Figure III. 2. Dissolved organic carbon (DOC) (ppm) is reported versus pH (a) or versus ionic strength (M) (b) in the different fractions of cut-thresholds

2. The rare earth element fingerprinting

The REE patterns (normalized to the Upper Continental Crust (Taylor and McLennan, 1985) indicated the presence of a MREE downward concavity fractionation for each cut threshold and remained unchanged through the different experiments (Figures III. 3a, III. 3b and III. 3c). This concave shape reflects an organic matter complexation as previously evidenced with the same soil (Pédrot et al., 2008) and elsewhere (Viers et al., 1997; Tang and Johannesson, 2003). This pattern shape is quite typical to the complexation between humic substances and REE (Davranche et al., 2005; Yamamoto et al., 2005; Pourret et al., 2007b; Yamamoto et al., 2008). Consequently, since this pattern is not modified regards to pH, ionic strength, and cut-threshold, we might considered that REE could be used as a humic substance tracer. Figure III. 4 presents the REE concentration variations versus pH (a) or ionic strength (b) for the different size-fractions. The REE distribution followed that of DOC respective to the size fractions. The concentrations increased in the fraction <5 kDa with the increasing ionic strength or decreasing pH, but the REE enrichment was stronger when promoted by pH than by ionic strength. The strong ionic strength increase enhanced mostly the proportion of REE occurring in the 2 kDa<fraction<5 kDa, as compared to the fraction <2 kDa. An enrichment of humic molecules was thus provided in the 2 kDa <fraction<5 kDa, in agreement with DOC ultrafiltration and aromaticity data (Figures III. 1 and III. 2), suggesting a humic association and contraction. By contrast, the pH decrease induced a significantly REE concentration increase in the fraction <2 kDa and in the 30 kDa<fraction<0.2 µm. These fractions were thus enriched in humic molecules, following ultrafiltration and aromaticity DOC data (Figures III. 1 and 2). The pH decrease led to an enrichment of small and large organic- and REE-rich molecules in solution.

3. Ionic strength as a less controlling factor

The impact of ionic strength on the size or shape of humic substances seems to be limited in this study. The rheological behaviour of polyelectrolytes in salty medium has been often considered as the result of equilibrium between (i) the electrostatic repulsion shielding, related to the ionic strength increase, which leads to contract the hydrophilic-hydrophobic moieties and, (ii) the consolidation of hydrophobic interactions from a hydration decrease (Esquenet, 2003). A number of studies have shown that in macromolecular systems, the ionic strength rise decreased inter-molecular and intra-molecular repulsion forces favouring molecules contraction and exclusion of solvating solvent molecules from the molecular domain (Swift, 1999). Thus, Kipton (1992) showed that the proportion of large molecules decreased with the increasing ionic strength. Ren et al. (1996) showed that hydrodynamic radius from dynamic light scattering measurements decreased to 50 % (from 95

nm to 48 nm) when ionic strength increased from 0.001 to 0.1 M at pH 9. Tombacz et al. (1999) explained this size decrease by a significant decrease in the electrical potential of the outer layer which reduced the repulsion between charged sites of the humate nanoparticles. Avena et al. (1999) and Weng et al. (2007) also proposed the hypothesis that humic acids might have a more compact structure at higher ionic strength. Moreover, several studies, which have shown that humic substances behaved as molecular association, demonstrated that ionic strength enhance could decrease the hydration of humic substances, which involves a compacting-reducing of the humic acids molar volume and thereby the volume-size (Dehaan et al., 1987; Piccolo, 2001). In this study, a weak humic acid size decrease was observed according to the increase of ionic strength. Therefore, these organic molecules were slightly sensitive to important ionic strength increases, and thus presented probably a weak macromolecular behaviour and an aggregation structure weakly dependent on any ionic strength increase. We can explain these findings by the fact that these humic substances occurring in solution were trace element-enriched. Trace elements potentially screened the humic substance surface charge. Indeed, when cations are bound to humic substances, changes may occur in the conformation of the humic molecules themselves such as: (i) the formation of multidentate complexes leading to a more compact structure or (ii) by reducing the net humic charge (Tipping, 2002). The cation binding leads to the reduction of repulsive interactions, again leading to compaction (Tipping, 2002). Thus, in the followed experimental conditions, the net potential of destabilization or compaction of humic substances aggregates was decreased by the associated trace elements.

To summarize, the impact of the ionic strength rise remained weak in this soil solution sample. A high increase of ionic strength becomes thus necessary for screening the remaining humic molecules charges, which slightly destabilized the aggregated structure and weakly decreased the size by compaction.

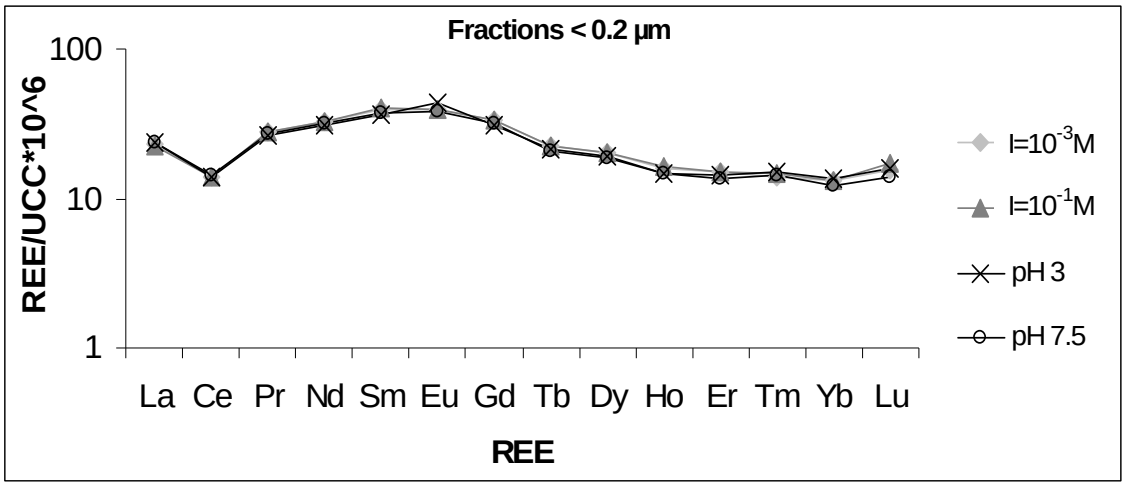

(a)

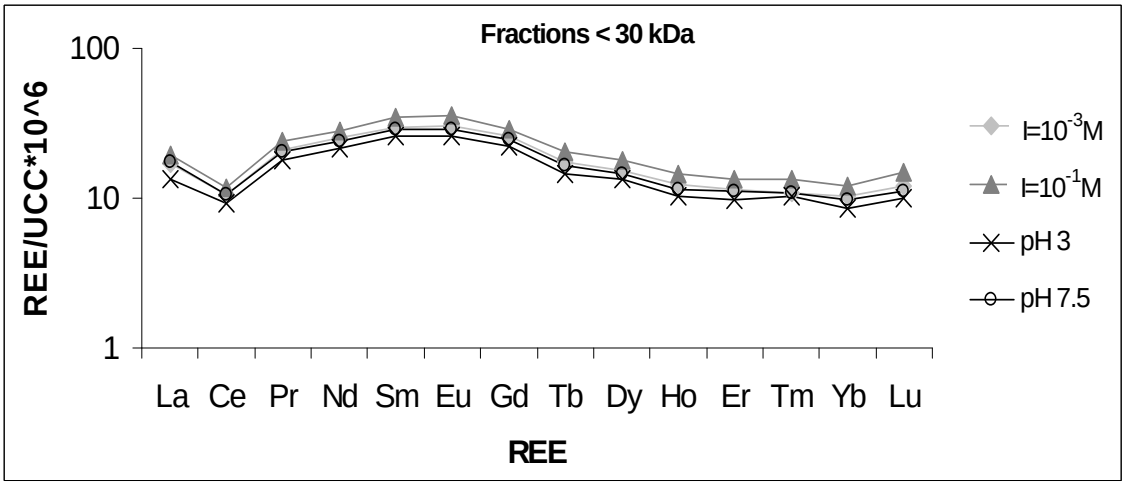

(b)

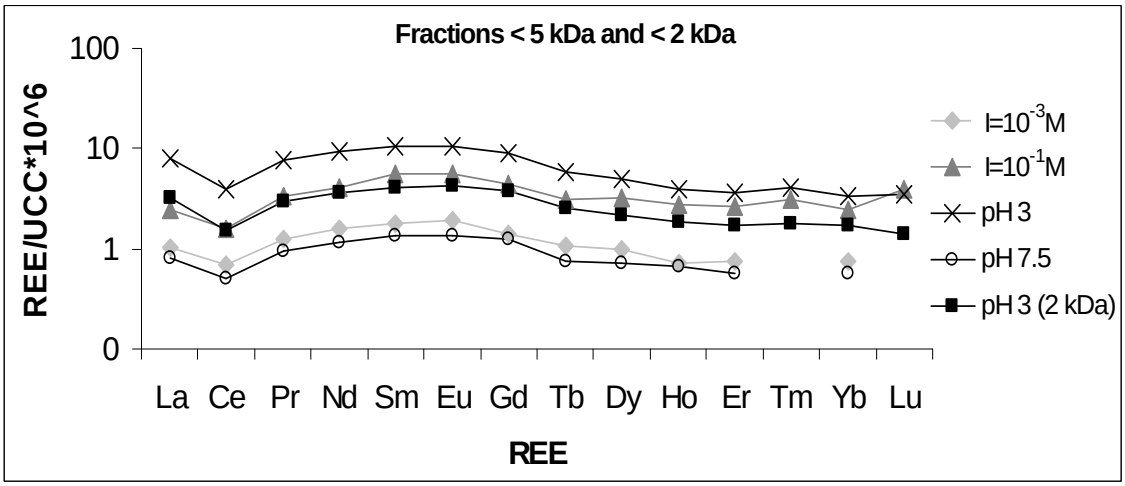

(c)

Figure III. 3. Upper continental crust (UCC) (Taylor and Mc Lennnan, 1985) normalized REE patterns recovered through the different experiments for the fraction <0.2 µm (a), the fraction < 30 kDa (b) and the fraction <5 and <2 kDa (c). Experiments at pH = 3 was the alone experimental modality, where REE concentrations were high enough to be determined in fractions lower than 2 kDa.

4. pH as the key parameter playing on the molecular aggregation of humic substances

pH appeared to be the parameter which most strongly modified the couple size/configuration of humic substances. Figures III. 1 and III. 2 showed a strong increase of the amount of molecules <5 kDa, and principally of molecules <2 kDa characterized by high aromaticity. Moreover, as shown in Figure III. 4, the pH decrease led to an enrichment of small REE-rich organic molecules in solution. These results demonstrated the presence of supramolecular assemblies and thus, agree with the hypothesis that humic substances can behave as molecular association of small molecules, associated at high pH values. The humic molecules distribution change promoted by the pH decrease might be due to a disruption of larger molecular-weight humic associations (Figure III. 2a). At pH = 3, hydrogen ions protonated humic carboxylic functions, which were dissociated at pH = 6 or 7.5. A number of negative charges were then neutralized, and hydrogen bonds were concomitantly formed among the complementary functions of humic molecules. The spatial arrangement existing at higher pH was thereby altered. Miano et al. (1992) showed that the increase of formation of H bonds, stronger than the hydrophobic forces stabilizing the original conformation, led to a disruption of the humic supramolecular associations.

A significant fraction of DOC was not affected by pH change. Indeed, nearly 30 % of DOC remained in the 5<fraction<30 kDa and were thus, potentially, not impacted by pH variation. A first hypothesis can be that this fraction could be composed of macromolecules characterized by a slight shrink process at low pH not allowing a strongly decrease of humic size. Indeed, Avena et al. (1999) showed that humic substances can be internally structured. The internal structure limits the shrink of molecules when the pH is decreased. Another hypothesis is that this fraction could be composed of supramolecular assemblies characterized by stable molecular aggregates possibly resisting to acidification (down to pH = 3). Therefore, these results showed the possible presence of different moleculars behaviors (macromolecular and supramolecular) in these humic substances. Similar results were previously evidenced by Baigorri et al. (2007), which showed in humic solution the coexistence of macromolecules, small molecules and supramolecular associations and thus, as in this study, an increase of humic substances in fractions lower than 5 kDa after acidification to pH = 2 and re-alkalinized to the initial pH (pH = 10).

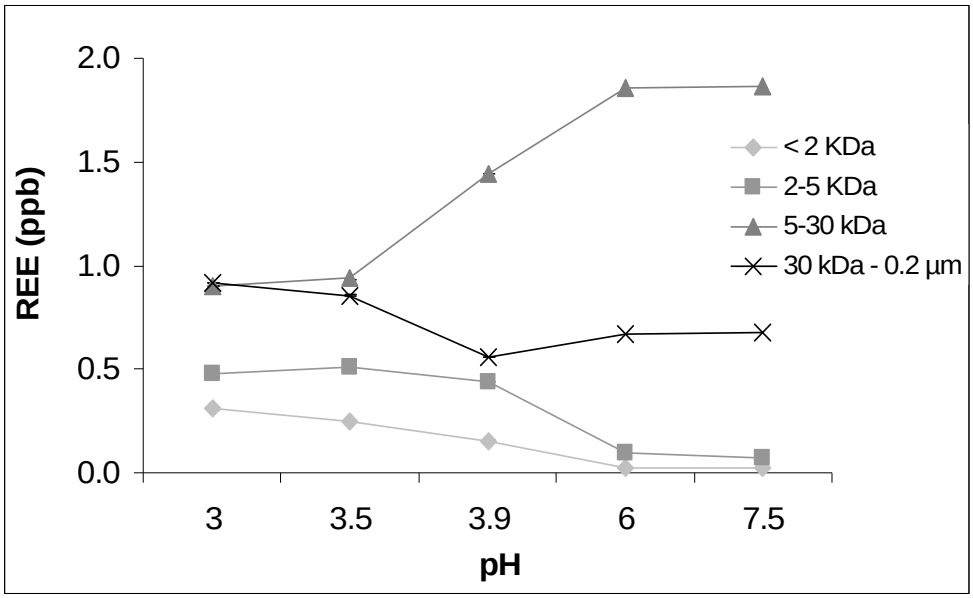

(a)

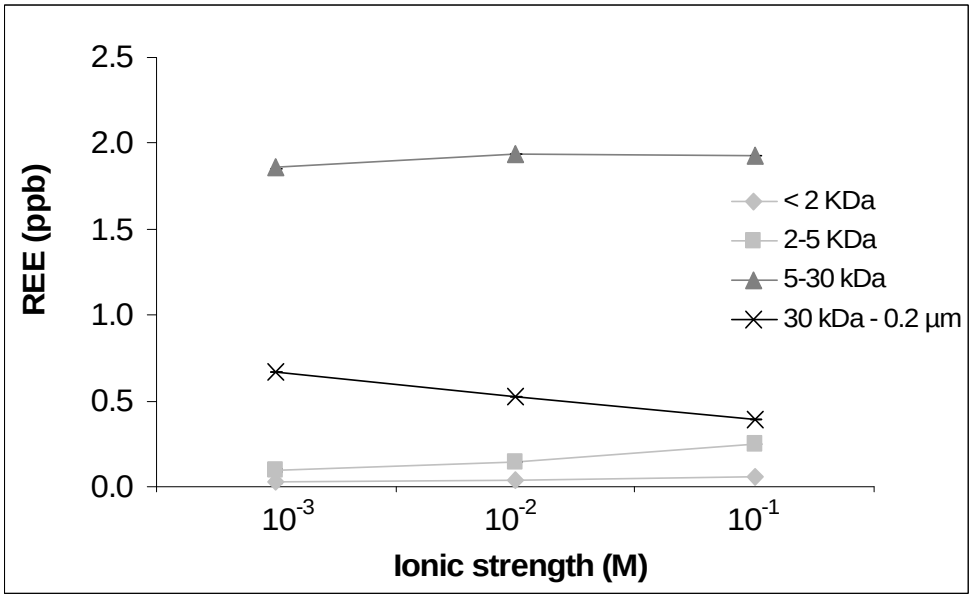

(b)

Figure III. 4. Rare earth elements concentrations (ppb) are reported versus pH (a) or versus ionic strength (b) in the different fractions of cut-thresholds.

5. Impact on associated trace element distribution

The REE/DOC ratios in the various fractions (Figure III. 5) allowed assessing the REE amount bound to a given DOC fraction. These ratios were different regards to pH or ionic strength in each fraction. At neutral pH, and almost regardless of the ionic strength, REE were in higher concentration in fraction >5 kDa. With the decreasing pH, REE/DOC ratio became homogeneous within each size fraction. As a consequence, the fractions <2 kDa were enriched in REE. However, this fraction <2 kDa enrichment remained low regards to the DOC rise. The REE/DOC ratio in

fraction <2 kDa reached only the value of 0.07. As established, the 5 kDa<fraction< 30 kDa displayed a larger DOC and REE concentration decrease (Figures III. 2a and III. 4a). The average REE/DOC ratio of these fractions was about 0.21 when the pH preserved the humic substance aggregation. If the DOC release from the supramolecular structure would not have been selective, the input of 2.85 ppm of DOC would have provided 0.6 ppb of REE into the fraction <2 kDa. Therefore, considering that in fraction <2 kDa, 0.6 ppb of REE and 4.25 ppm of DOC should be present; the REE/DOC ratio should have reached 0.14. However, the REE/DOC ratio was only 0.07 (Figure III. 5a). Therefore, the additional low-molecular weight DOC was less complexing regards to REE. It probably displayed lower density of functional groups able to complex REE. These small REE-depleted organic molecules might also be released easier from the supramolecular structure of humic substances. Consequently, the humic substances metallic ion charge must be significant to support the supramolecular structure. The existence of such metal-induced humic agglomeration has been visualized even at trace metal concentrations by flow-field flow fractionation studies (Geckeis et al., 2002; Suteerapataranon et al., 2006). Suteerapataranon et al. (2006) showed that Th(IV)-humate complexes displayed a size of about the double of the hydrodynamic diameter of humic acids alone. They suggested the bridging unit formation between metal ion and more than one humic acid entity. Another hypothesis could be that complexed metal ions screened the humic acid surface charge and thus favoured the humic acid units agglomeration. Consequently, the humic substances degree of agglomeration might be a function of the occurring metal ion charge.

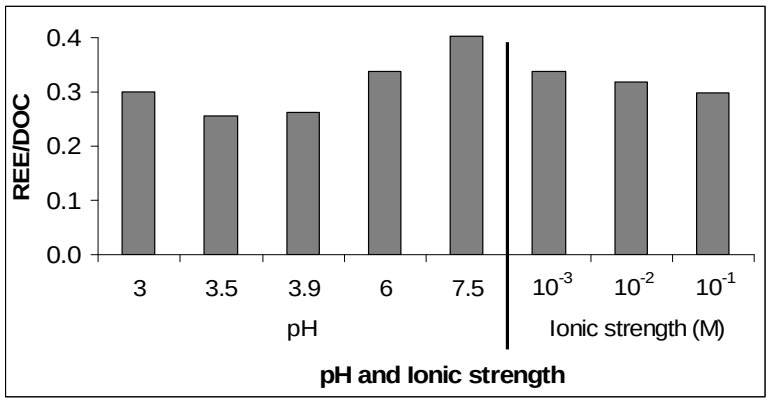

(a)

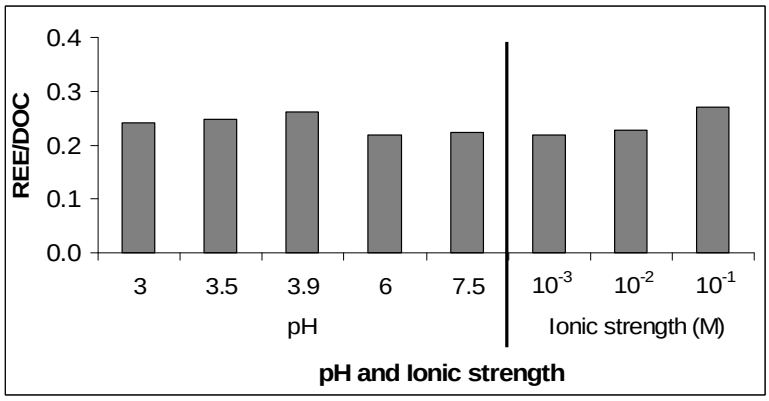

(b)

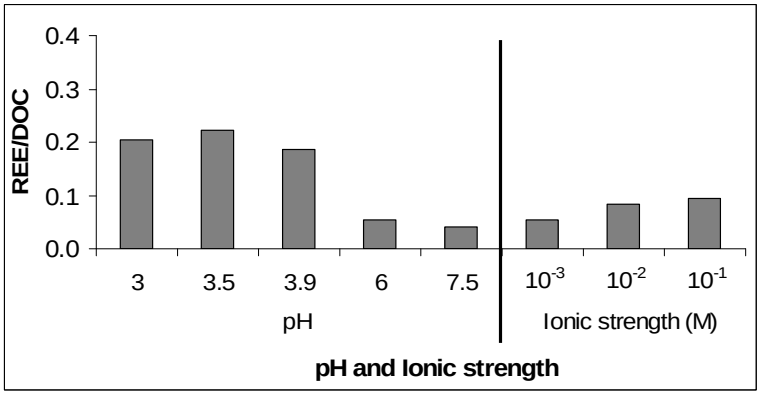

(c)

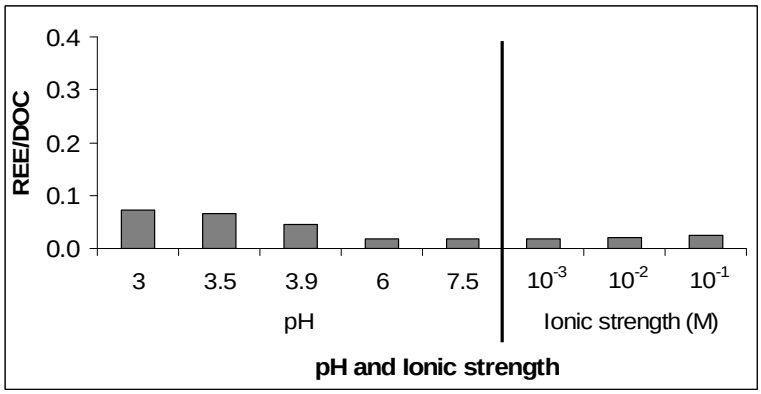

(d)

Figure III. 5. REE/DOC ratio is reported versus pH or versus ionic strength in the different fractions of cut-thresholds : 30 kDa - 0.2 µm (a), 5-30 kDa (b), 2 - 5 kDa (c) and <2 kDa (d).

IV. Conclusions

Data recovered from the conducted experiments suggested that the dissolved organic pool was slightly sensitive to ionic strength, probably partly because of the trace elements carried by humic substances. By contrast, pH seems to play a key role in the size distribution of humic substances involving the combined occurrence of small molecules and supramolecular associations. A pH decrease destabilized the humic association and led to an enrichment in small molecules resulting from the disruption of the supramolecular assemblies. This disruption seems to be higher for organic molecules less trace element complexing. Consequently, the metallic ions charge of humic substance must be significant to support the supramolecular structure. The presence of molecules with macromolecular behaviour was suspected but the net potential of humic substance aggregation was decreased by the associated trace elements. This study provided evidence that the humic substance aggregation is dynamic notably regards to pH. The understanding of the humic substance structure as dynamic supramolecular associations put further implications for the understanding of the mobility of associated trace elements. Moreover, the structure destabilizing at acid pH enhances potentially the mobility of humic acids by the production of labile and trace element-rich small molecules. Change of the humic conformational structure regards to pH can be thus a key factor controlling the mobility of the trapped and/or complexed cations. This latter point might be one major issue of concern since local (anthropogenic pressure) and/or global (climatic) warming not only consists in rising temperature, but also in acidification of soil and waters.

Chapitre IV : Double contrôle du pH sur la distribution des substances humiques et des éléments traces associés dans les solutions de sols : apport de l'ultrafiltration

Double pH control on humic substance-borne trace element distribution in soil waters as inferred from ultrafiltration

Ce chapitre correspond à un article soumis (version révisée : corrections mineures et soumises Juillet 2009) à la revue 'Journal of Colloid and Interface Science' : Pédrot, M.; Dia, A.; Davranche, M. : 'Double pH control on humic substance-borne trace element distribution in soil waters as inferred from ultrafiltration'.

Résumé : Le Carbone Organique Dissous (COD) colloïdal représente une phase porteuse majeure pour les éléments traces (ET) dans les environnements de sub-surface. Comme le suggèrent des observations de terrains précédemment publiées, la sorption préférentielle de COD sur les surfaces minérales tend à enrichir la phase solide en acides humiques. Ce fractionnement du COD peut affecter la mobilité des ET. Cette étude est consacrée à l'étude de l'influence du fractionnement du COD sur la mobilité des ET. Une extraction séquentielle a été utilisée pour fournir des informations sur les phases porteuses en ET dans le sol (fraction échangeable, soluble via un acide faible, réductible, oxydable et la fraction métallique non extractible). Le pH étant connu pour jouer un rôle majeur sur la stabilité des colloïdes, des expériences en batch ont été réalisées pour étudier l'influence du pH sur le détachement des colloïdes et des ET associés. Différents groupes d'éléments ont été ainsi identifiés en fonction du comportement des ET vis-à-vis des phases colloïdales lors des changements de pH. Plusieurs éléments chimiques révèlent une augmentation de leurs concentrations avec une diminution du pH. Ces concentrations peuvent représenter une fraction importante de la concentration totale du sol. En revanche, d'autres éléments révèlent une augmentation des concentrations lors de l'augmentation du pH, en association avec une augmentation de la quantité de colloïdes dans la solution de sol. En ce qui concerne ce dernier groupe, deux phases porteuses colloïdales ont été identifiées au cours de l'augmentation du pH: (a) la première correspond à des substances humiques remises en solution et véhicule la majorité des éléments associés à une phase colloïdale, et (b) la deuxième est constituée de nano-oxydes. Par conséquent, le fractionnement du COD joue un rôle clé sur la concentration en ET dans la solution de sol lors de changements de conditions de pH.

Abstract : Colloidal dissolved organic carbon (DOC) is an important carrier phase for trace elements (TE) in subsurface environments. As suggested by previously published field observations, preferential sorption of DOC onto mineral surfaces tends to enrich the solid phase in humic acids. This DOC fractionation may affect the mobility of TE. pH is known to play an important role on the stability of colloids. This study was therefore dedicated to identifying the influence of DOC fractionation on TE mobility. Sequential extraction has been used to provide information on the possible TE carriers within soil (as exchangeable, weak acid soluble, reducible, oxidizable, and non-extractible metal fractions). Batch experiments were carried out to investigate the influence of pH on the detachment of colloids and associated TE. Different groups of elements were identified according to TE behaviour during pH changes. Several elements displayed increasing concentrations with decreasing pH. These concentrations can represent an important fraction of the total soil concentration. By contrast, other elements showed increasing concentrations following increasing pH, in association with an increasing amount of colloids in soil solution. Concerning this latter

group, two colloidal carrier phases were identified during the pH increase: (i) the first one concerned the majority of elements, which was associated to humic substances remaining in solution, and (ii) the second one involved several TE rather associated with nano-oxides. Therefore, DOC fractionation plays a key role on the TE concentration in soil solution during pH changes.

I. Introduction

Ubiquitous in soils and waters, colloids are known to play a key role in major biogeochemical cycles of elements. A large fraction of trace elements (TE) is indeed closely associated with colloids (Karathanasis, 1999; Dia et al., 2000; Pokrovsky and Schott, 2002; Dahlqvist et al., 2004; 2007; Strobel et al., 2005; Thompson et al., 2006; Ohno et al., 2007) especially with colloidal dissolved organic carbon (DOC) and/or iron-rich nanoparticles. Colloids, either organic or inorganic, are microscopic TE adsorbent phases and therefore govern, via their mobilisation in both aqueous systems and soils, the fate of reactive elements. Trace elements mobility in soils and aquatic environments is thus mainly controlled by their respective distribution between immobile solid phases, mobile colloidal particles and 'truly' dissolved species (Kretzschmar et al., 1999). Colloidal particles are composed of minerals with amphoteric surface (e.g. iron, aluminum and manganese oxides, carbonates) and fixed surface charges (phyllosilicate faces as fragments of clay minerals), organic matter possibly coated onto minerals, and bacteria (Sen and Khilar, 2006). Among the elements, cations are known to be the most affected by colloid-mediated transport (Kersting et al., 1999; Bradl, 2004).

The high abundance of Fe-particles or clays, their large specific area and charge, as well as their surface functional hydroxyl groups make of mineral particles the most important sorbents of metal cations. However, metal speciation and mobility are also strongly controlled by dissolved organic carbon (DOC). Dissolved organic carbon is composed of a mixture of organic molecules displaying a broad spectrum of functional groups (carboxylic acids, phenols, amines, etc.), structure, and molecular weight distributions. Humic substances are usually considered to be the most reactive fraction of DOC. They also represent the most important fraction of DOC involved in colloid-mediated transport for TE and hydrophobic organic compounds in subsurface environments (Stevenson, 1999; Tipping, 2002). Humic substances are persistent nanoparticles of molecular weights ranging between 1 and 200 kDa (Tipping, 2002) and composed of various organic molecules. Moreover, humic substances frequently coat onto a large extent on reactive mineral surfaces (Sposito, 1984). When humic substances bind to mineral surfaces, their net particle charge, zeta potential, and colloidal stability are modified as previously shown (Amal et al., 1992; Tiller and O'Melia, 1993; Kretzschmar and Sticher, 1997; Tombácz et al., 1998), inducing major changes

regards to adsorption properties especially concerning cations (Murphy and Zachara, 1995; Schroth and Sposito, 1998; Vermeer et al., 1999; Christl and Kretzschmar, 2001; Heidmann et al., 2005). Aggregation/disaggregation and coating/detachment of humic substances are highly dependent on environmental conditions (Avena and Wilkinson, 2002; Sutton and Sposito, 2005). Globally, (i) ion exchange (electrostatic interaction), (ii) ligand exchange surface complexation, (iii) hydrophobic interaction, (iv) entropic effect, (v) hydrogen bonding, and (vi) cation bridging are the mechanisms governing organic matter coating onto mineral surfaces (Sposito, 1984). Specific adsorption by ligand exchange is considered to be the most important mechanism (Gu et al., 1994; Schlautman and Morgan, 1994). Field investigations suggested a preferential sorption of humic acid onto mineral surfaces, which tends to enrich both the solid phases in humic acids and the groundwaters in fulvic acids (Murphy et al., 1989; McCarthy et al., 1993). Such organic matter fractionation resulting from coating onto mineral surfaces has been previously observed (Vermeer et al., 1998; Meier et al., 1999; You et al., 1999; 2006; Balcke et al., 2002; Hur and Schlautman, 2003). In most investigations, the fractions with higher molecular weights, aromatic moieties, and more hydrophobic compounds were preferentially bound to the mineral surfaces. Organic matter coated to mineral surface may thus influence the distribution and the size of the organic matter released in solution (Meier et al., 1999). Thereby, this humic substance fractionation may affect the (bio)availability and mobility of TE, especially if their binding capacity is more important in these higher fractions.

pH is likely to be the most important physicochemical parameters controlling metal speciation. Even though the stability of colloids according to pH is well documented, little studies were dedicated to the understanding of the detachment of organic colloids and associated TE release from soils regards to pH change. In these studies, pH was evidenced to control the mobilization of organic colloids in soils (Tyler and Olsson, 2001; Klitzke et al., 2008). This mobilization enhance might be explained by the increasing negative surface charges of colloids with increasing pH (Kretzschmar et al., 1993; Avena and Koopal, 1998; Kretzschmar and Sticher, 1998; Tipping, 2002). pH affects the dissociation of functional groups, and put constrains on both the humic substance structure and the cation binding ability changes. Their respective solubilities allowing the formation of aggregates at the mineral surface are also modified following pH evolution (Liu and Gonzales, 1999; Tipping, 2002; Pédrot et al., submitted 2009a).

This study is thus an attempt to identify the influence of pH on the detachment of colloids and fractionation of humic substances and on the availability and mobility of TE through the following main objectives: (i) to identify the distribution and chemical speciation of TE in this soil, (ii) to investigate the pH impact on the detachment of colloids and associated TE, and (iii) to determine the nature and the size distribution of the carrier colloidal phase. In this context, soil/water interactions conducted through batch system experiments, were carried out with an organic-rich wetland soil.

Ultrafiltration experiments were performed to separate the colloidal phases following decreasing pore sizes and identify the various TE-colloidal phase associations. Moreover, sequential extraction procedure was performed on the wetland soil sample to determine the major carriers of the TE pools.

II. Materials and methods

1. Soil sampling and characterization

The soil/water interactions were carried out in laboratory with wetland organic-rich soil. Soil was sampled in January 2006 within the uppermost organo-mineral horizon (Ah) from a planosol (according to the WRB international classification) of the Mercy wetland located in the Kervidy/Coët-Dan experimental subcatchment in Brittany, Western France. The Kervidy/Coët-Dan catchment has been monitored since 1991 to investigate the effects of intensive agriculture on water quality (Mérot et al., 1995; Durand and Torres, 1996; Curmi et al., 1998). The water table regularly reaches the organic-rich upper soil horizons and soil solutions are DOC-enriched as usually in the wetlands (Durand and Torres, 1996; Jaffrézic, 1997).

Table IV. 1. Granulometric composition, pH, cationic exchange capacity (CEC) of soil expressed in meq/100 g, total iron concentration and organic carbon content.

Clay (<2 µm)	33.5 %
Silt (2-20 µm)	46 %
Coarse Silt (20-50 µm)	14.7 %
Sand (50-200 µm)	3.4 %
Coarse Sand (> 200 µm)	2.4 %
pH Water	5.9
CEC meq/100g	4.7
Fe_2O_3	2.61 %
Total Organic Carbon	5.87 %

The soil was dried at 40 °C during 72 h and the agglomerates were broken by hand. Particles larger than 2 mm were removed by sieving. The here below described experiments were conducted using the soil fraction smaller than 2-mm-size. The granulometric composition of the soil was determined at the INRA laboratory in Arras (France) (Table IV. 1). The organic carbon content was determined at the SARM laboratory in Nancy (France), using an oxygen combustion method with a CS Analyser (LECO SC 144DRPC) (Table IV. 1). The soil organic matter content was estimated by

multiplying the organic carbon concentration of the analysed soil sample by the Van Bemmelen factor of 1.724 (Nelson and Sommers, 1982). The upper soil in the Mercy wetland is considered as an organic acid soil dominated by silt with total silt corresponding to 60.7%. The organic matter concentration equals 10.12%. The soil pH was 5.9. This soil contains more humic acids than fulvic acids, characterized by a humic acid versus fulvic acid ratio of 1.85.

The sample was sequentially leached in three steps following the modified BCR extraction scheme used for determining operational speciation of metals (Mossop and Davidson, 2003). The protocol is described in Table IV. 2. The BCR sequential extraction procedure was applied in three times to 1 g of dried soil sample and the extractions were conducted in ultra-cleaned 50-mL polypropylene centrifugal tubes.

Table IV. 2. The modified BCR sequential extraction scheme used for operational speciation of metals.

Step	Soil phases	Extractant	Shaking time and temperature
F1	Water and acid soluble and exchangeable	40 mL 0.11 M CH_3COOH	16 h at room temperature
F2	Reducible	40 mL 0.5 M $NH_2OH.HCl$ (pH 1.5)	16 h at room temperature
F3	Oxidizable	10 mL 8.8 M H_2O_2(pH 2)	1 h at room temperature
		10 mL 8.8 M H_2O_2(pH 2)	1 h at 85 °C
		50 mL 1 M NH_4Oac (pH 2)	16 h at room temperature
F4	Residual	15 mL aqua regia	Heating to dryness
		10 mL aqua regia	

2. Experimental set up

Batch experiments are commonly used to determine the genesis and stability of colloids. Experiments were thus conducted through batch to investigate DOC, major and trace elements release through time at pH equal to 7.2 and 4. The experimental set up consisted of a 2000 ml polypropylene bottle equipped with a syringe to sample the soil solution and several air events which allowed the preservation of aerobic conditions. Ninety-five g of soil were mixed with 1900 ml of a 1.88 10^{-3} M NaCl electrolyte solution, whose ionic strength corresponded to the ionic strength of the soil solution circulating within the organo-mineral horizon in the Mercy wetland. The pH was monitored using an automatic pH stat titrator (Titrino 794, Metrohm) equipped with burettes of 0.1 M NaOH and HCl solutions. pH monitoring did not drastically affect the ionic strength, since ionic strength varied from 4 to 5 10^{-3} M. The soil suspension was continuously stirred. The sampling of soil solution was made through time until steady state was reached. All experiments were made in duplicate.

3. Ultrafiltration

All collected soil solutions were filtered trough a 0.2-µm-pore size cellulose acetate filter capsules (polyether sulfone membrane Sartorius Minisart). Ultrafiltration experiments were performed to separate organic molecules following decreasing pore size cuts. Fifteen-mL centrifugal tubes (Vivaspin) equipped with permeable membranes of decreasing pore sizes (30 kDa, 5 kDa and 2 kDa) were used. Each centrifugal filter device was washed and rinsed with HCl 0.1 N and ultra-pure water three times before use. Centrifugations were performed using a Jouan G4.12 centrifuge with swinging bucket at about 3000g for 20 minutes for 30 kDa devices, and 3500 g and 3750 g for 30 minutes, for 5 kDa and 2 kDa devices, respectively (Pourret et al., 2007a; Pédrot et al., 2008). All procedures (sampling, filtration and analysis) were carried out in order to minimize contamination. Blank tests were performed during this study to determine possible contamination due to filtration and analysis and were always negligible.

4. Chemical analyses

pH was measured with a combined Mettler InLab® electrode after a calibration performed with WTW standard solutions (pH= 4.01 and 7.00 at 25 °C). The accuracy of the pH measurement was ± 0.05 pH units. Dissolved organic carbon was analysed on a Total Organic Carbon analyser (Shimadzu TOC-5050A). Accuracy of DOC measurement was estimated at ± 3 % (by using standard solution of potassium hydrogen phtalate). Specific Ultra Violet Absorbance (SUVA) - strongly correlated with degree of aromaticity of organic matter (Aromaticity = 6.52 * SUVA + 3.63) (Weishaar et al., 2003) - was used as an indicator of the chemical composition and reactivity of dissolved organic carbon. Major anion (Cl^-, SO_4^{2-} and NO_3^-) concentrations were measured by ion chromatography (Dionex DX-120) with an uncertainty below 4%. Major cation and TE concentrations were determined by ICP-MS (Agilent 4500), using indium as an internal standard. The international geostandard SLRS-4 was used to check the validity and reproducibility of the results. Before measurements of major cation and TE concentrations to avoid interferences with DOC during mass analysis, DOC-rich samples were digested with sub-boiled nitric acid (HNO_3 14.6 N) at 85°C, and then resolubilized in HNO_3 0.37 N after complete evaporation. All measurements were made in triplicate. Typical uncertainties including all error sources were below ± 5 % for all TE, whereas for major cations, the uncertainty lied between 2 % and 5 %, depending on the measured concentrations (Yéghicheyan et al., 2001; Davranche et al., 2004).

III. Results

1. Sequential extraction data

Although extractions are known to be not fully selective (e.g. Rauret et al., 1989; Nirel and Morel, 1990; 1991; Mossop and Davidson, 2003; Cornu et al., 2004), results remain qualitatively informative with respect to the main phase(s) extracted during each step of the procedure. Figure IV. 1 displays the proportions of elements according to each fraction. Significant proportions of Ba, Mg, Mn, Ca, Co, Zn, Sr and Ni occurred in the exchangeable fraction. Residual fraction presented high concentrations of Ba, Rb, Li, Al, Th, REE, U, Y, Ti and V. This group of elements is therefore mainly linked to refractory soil minerals such as well-crystallized clays or primary minerals provided by the alteration of the bed rock. Around 10 % of Co, Ni, Zn, Th, Cr, REE, U and Pb occurred in the organic fraction. Iron is distributed at about 23% in the reducible fraction (probably as Fe-oxyhydroxides), 24% in the oxidizable fraction (as organic complexes or as sulphides), while the remaining part lied in the residual fraction (crystallized Fe(III)-oxides, clays and/or primary minerals). The reducible fraction provided also a significant proportion (≥15%) of Mn, Ca, Co, Ni, REE and Pb concentrations This group of elements were thus, probably, either complexed with Fe-oxyhydroxides, or carried by mixed Fe/C-rich complexes as elsewhere evidenced (Rose et al., 1998; Pokrovsky et al., 2005; Dahlqvist et al., 2007; Pédrot et al., 2008).

The proportions of elements released from the solubilization experiment at pH = 4 and pH = 7.2 regards to total soil concentration (determined at the Nancy SARM laboratory) are reported in Table IV. 3. Two groups of elements can be evidenced: (i) the first group is composed of alkaline and alkaline earth metal elements and Co, Mn, Ni and Zn, which were more released at acidic pH than at pH = 7.2. The proportion solubilized at pH = 4 represented between 3% and 50% of soil total concentration. This first group matches with elements occurring in the F1 fraction of the selective extractions (exchangeable an acid soluble elements). Consequently, the elements belonging to the first group were probably mainly solubilized in our pH experiments as inorganic soluble complexes or free ions. (ii) The second group of elements is composed of Al, Fe, Th, REE, U, Cr, Y, Ti, V and Pb, which corresponds to the group of elements solubilized at less than 0.5% of their total amounts These elements were also from 4 to 19 times more solubilized at pH = 7.2 than at pH = 4. However, the solubilization of cations is not supposed to be promoted at pH = 7.2. Therefore, the unique hypothesis, which allows to explain their release, is their binding to strong anionic ligands, such as organic ligands, themselves supposed to be released in solution at pH = 7.2. This hypothesis is reinforced by their occurrence in both the F3 (organic) and F2 fraction (reducible fraction composed of Fe/C-rich complexes) of the soil selective extraction.

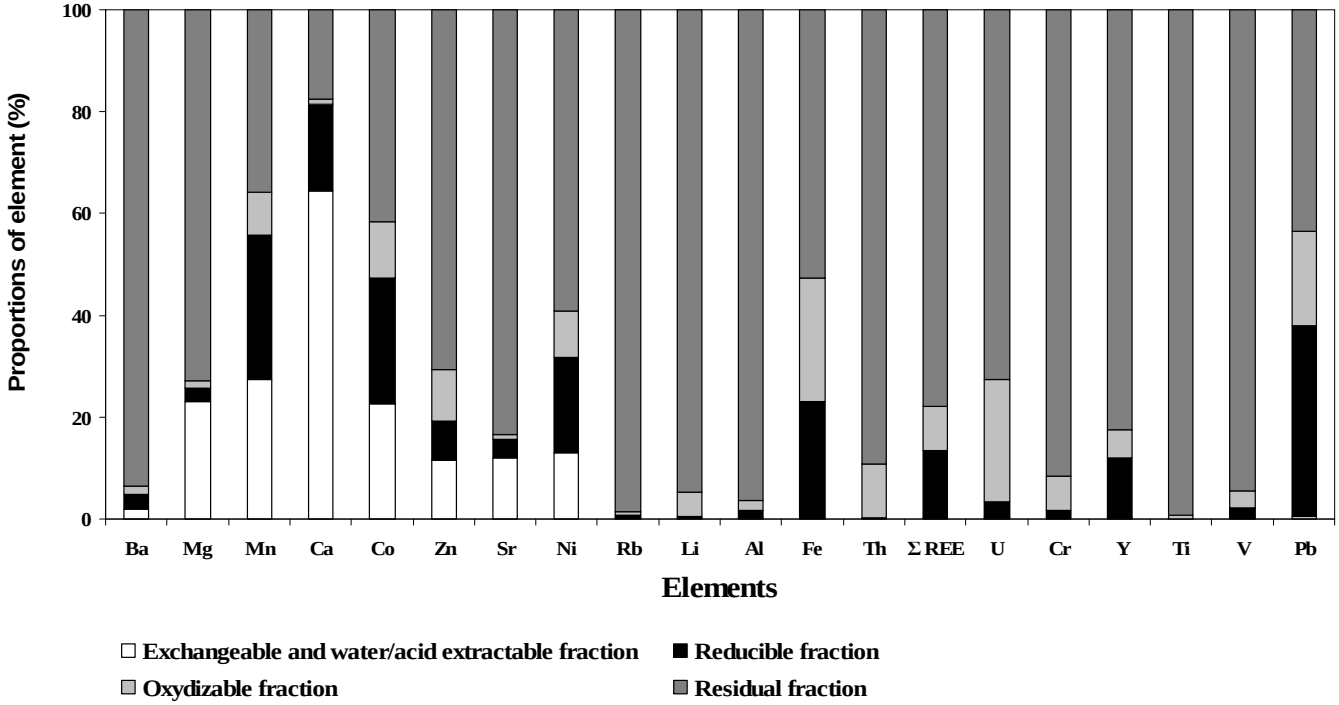

Figure IV. 1. Proportion of elements (%) in each fraction recovered after the selective extraction procedure (Exchangeable fraction - Reductible fraction - Oxydizable fraction and Residual fraction).

Table IV. 3. Proportion of released element at pH = 4 and pH = 7.2 regards to total soil concentration.

	Ba	Mg	Mn	Ca	Co	Zn	Sr	Ni	Rb	Al
pH 4 Fraction / Total fraction (%)	0.79	17.74	18.53	39.90	9.53	4.11	7.72	2.81	0.23	0.01
pH 7.2 Fraction / Total fraction (%)	0.05	1.01	0.13	1.91	0.49	0.36	0.28	1.47	0.13	0.05

	Fe	Th	REE	U	Cr	Y	Ti	V	Pb	Ga
pH 4 Fraction / Total fraction (%)	0.02	0.01	0.02	0.03	0.04	0.02	0.00	0.01	0.04	0.00
pH 7.2 Fraction / Total fraction (%)	0.22	0.22	0.17	0.33	0.10	0.09	0.00	0.04	0.12	0.06

2. *Dynamics of the organic and inorganic fractions*

The occurrence and the nature of colloids were investigated regards to the variation of DOC size distribution and associated TE concentrations against pH.

a. Dissolved organic carbon release kinetics and aromaticity dynamics

The DOC concentration (a), and the aromaticity (b) evolution trough time versus the size fraction are displayed at pH = 4 and pH = 7.2 in Figure IV. 2 and IV. 3, respectively. At pH 4, DOC concentrations increased during the first hours whatever the cut-threshold, and then decreased to reach a value of 9 ppm. The fraction <2 kDa represented more than 50% of the total solubilized DOC and even more than 65% of DOC in the first sample (recovered after 1 h) (Figure IV. 2a). At the first stage of the experiment, DOC was weakly aromatic in each size-fraction (Figure IV. 2b). Afterwards, DOC aromaticity increased differently regards to the size-fraction, slightly in fractions <30 kDa and <0.2 µm and more strongly in fractions <5 and <2 kDa. Surprisingly, this aromaticity increase followed the DOC decrease.

At pH = 7.2 (Figures IV. 3), two DOC trends related to the size-fractions were observed: (i) in fractions <5 kDa, the DOC concentration increased very slightly to reach a steady concentration of 8 or 13 ppm in fractions <2 kDa and <5 kDa, respectively. (ii) By contrast, in fractions >5 kDa, DOC was strongly solubilized during the first twenty hours and next slightly increased to reach 36 or 49 ppm in fractions <30 kDa and <0.2 µm, respectively. The aromaticity increased in all the fractions, but more rapidly in the first stage of the experiments. It then increased according to the increasing molecular weight with similar values in fractions <30 kDa and <0.2 µm. This comparable trend could be explained by polarity and aromaticity reductions following the increasing apparent molecular size (Shin et al., 1999). Small humic acids display, indeed, high O/C ratio, low H/C ratio, and high density of oxygen-containing functional groups. By contrast, large humic acid fractions presented low O/C ratio, high H/C ratios and low density of oxygen-containing functional groups (Li et al., 2004). Moreover, the aromaticity was more important at pH = 7.2 than pH = 4 (25-35% against 19-25%, respectively), except at the beginning of experiment where aromaticities displayed comparable values. This low aromaticity corresponded probably to simple organic molecules and/or microbial metabolites. Therefore, a significant DOC solubilization occurred at pH = 7.2 with a preferential release of heavy size (>5 kDa) and strongly aromatic (>30 %) organic molecules, which were probably humic acids. By contrast, at pH = 4, the soil organic matter was weakly solubilized (DOC >40 ppm and <10 ppm at pH = 7.2 and pH = 4, respectively). Most part (75%) of this organic

matter <5 kDa was slightly aromatic (less than 25%) and could correspond to fulvic acids. Humic substances may indeed occur in soils in several forms: (i) as dissolved molecules in aqueous solution, (ii) as adsorbed molecules or adsorbed aggregates at mineral surfaces or (iii) as humic substance particles or solid aggregates (Hayes et al., 1989; Stevenson, 1994). pH did here thus strongly influence the solubilization and nature of the humic substances occurring in the soil solution by controlling their chemical properties.

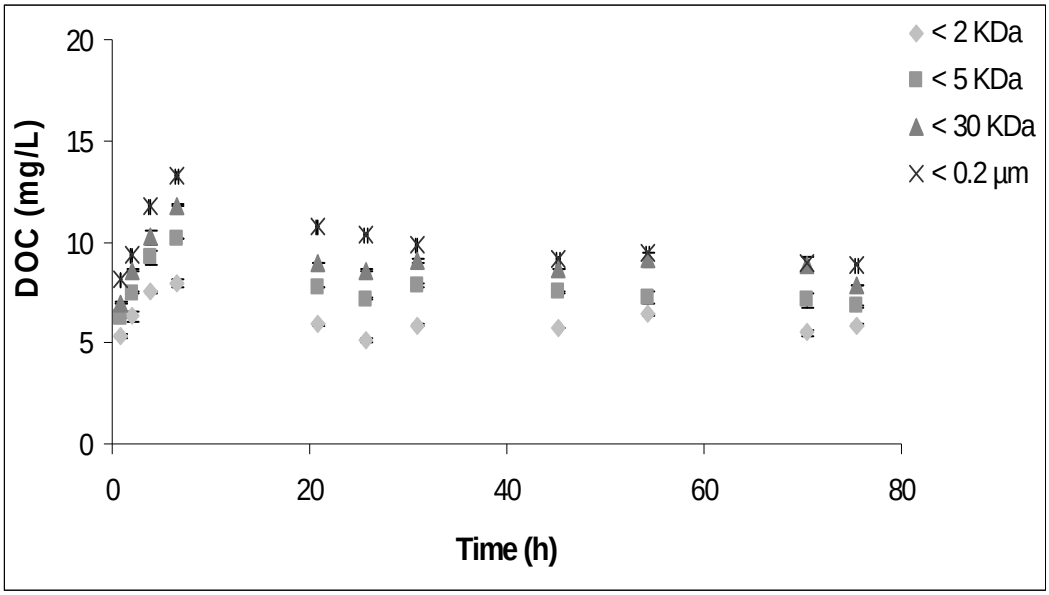

(a)

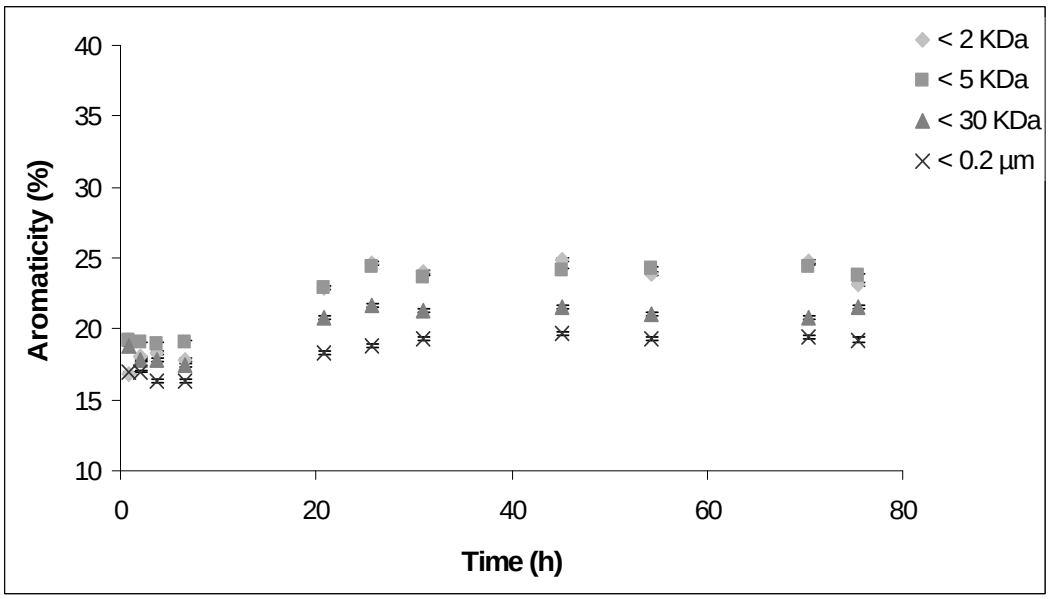

(b)

Figure IV. 2. Dissolved organic carbon kinetics (a) and aromaticity kinetics at acid pH (pH = 4) for the four cut thresholds (black stars correspond to the fraction below 0.2 µm; grey triangles correspond to the fraction below 30 kDa; grey squares correspond to the fraction below 5 kDa, while grey diamond-shape symbols correspond to the fraction below 2 kDa).

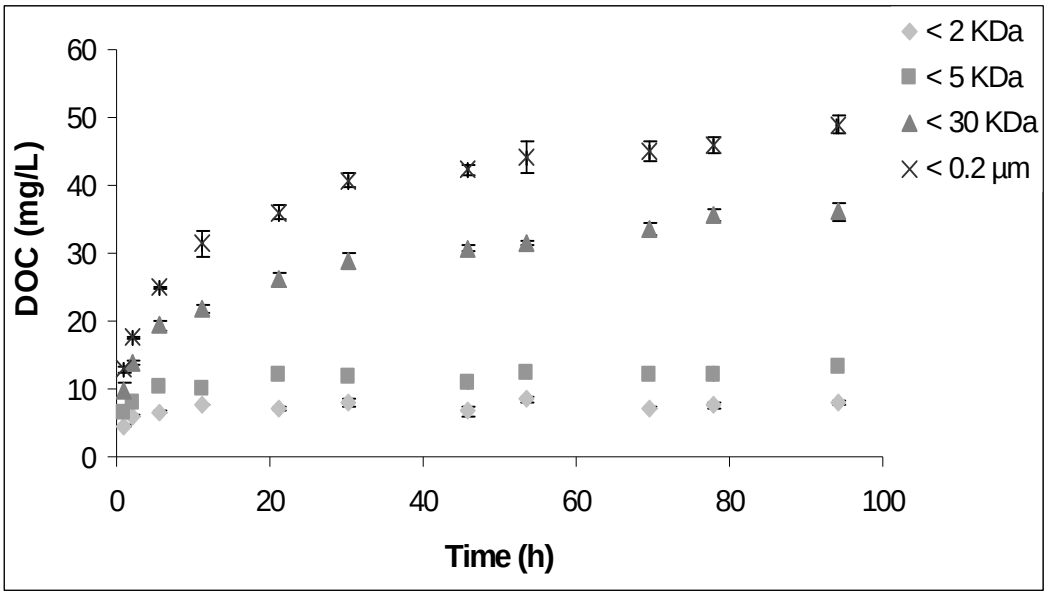

(a)

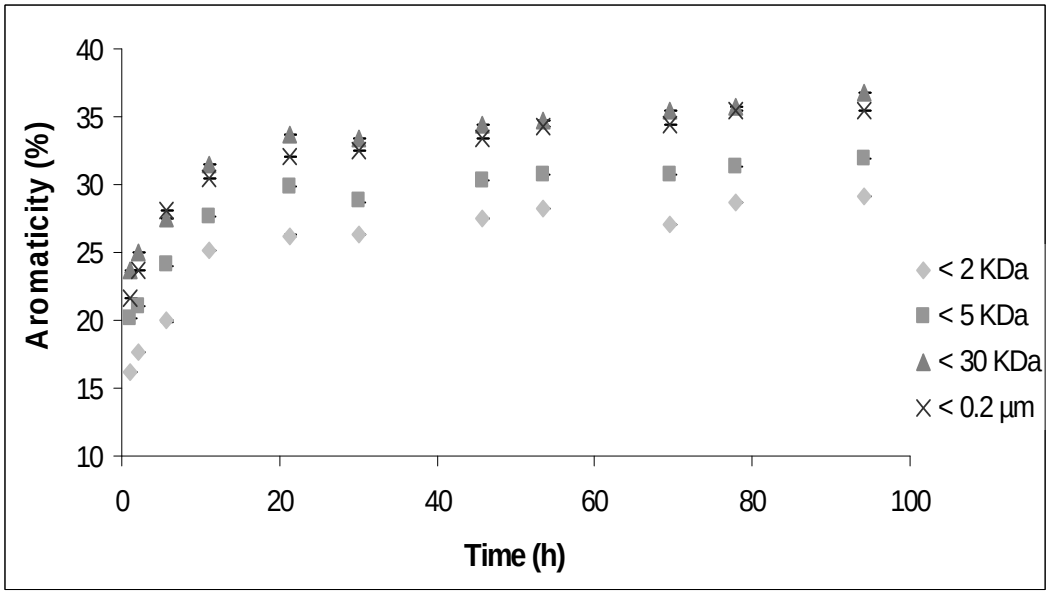

(b)

Figure IV. 3. Dissolved organic carbon kinetics (a) and aromaticity kinetics at neutral pH (pH = 7.2) for the four cut thresholds (black stars correspond to the fraction below 0.2 µm; grey triangles correspond to the fraction below 30 kDa; grey squares correspond to the fraction below 5 kDa, while grey diamond-shape symbols correspond to the fraction below 2 kDa).

b. Dynamics of the inorganic fraction

When looking at both Fe and Al concentrations and distributions regards to the different pore size cuts and pH (Figure IV. 4), significant contrasted behaviours can be observed. At pH = 7.2, the samples displayed higher Fe and Al concentrations than at pH = 4. The strong Fe and Al concentrations displayed a strong decrease in fraction < 30 kDa at pH = 7.2. More than 80 and 90% of Fe and Al occurred in the fraction >30 kDa, respectively. Iron and Al distributions were therefore

different from that of DOC, which was uniformly distributed relative to the size-fraction. Iron and Al might therefore be released as Fe-Al nanoparticles at pH = 7.2. Recently, Pédrot et al. (2008) from experiment of reduction/re-oxidation of the same wetland soil estimated Fe-Al nanoparticles size range in between 0.2µm and 30 kDa. Moreover, by simulating the binding of Al and Fe to humic substances in organic-freshwater in equilibrium with $Al(OH)_3$ and $Fe(OH)_3$, Tipping et al. (2002b) demonstrated that the maximal concentration of Fe(III) that could be bound to humic substances was ca. 1.10^{-4} $mol.g^{-1}$ of C at pH 7. In this study, the concentration of Fe, in the 0.2 µm<fraction <30 kDa reaches 10^{-3} $mol.g^{-1}$ of C at pH 7.2. Thus, a large fraction of Fe may be present as colloidale Fe-oxyhydroxides in this fraction. The combined occurrence of Fe, Al and humic substances in the colloidal fractions was previously supposed in several studies dealing with organic-rich samples (Rose et al., 1998; Pokrovsky et al., 2005; You et al., 2006; Dahlqvist et al., 2007; Pédrot et al., 2008). Moreover, Fe-Al nanoparticles-organic matter associations were evidenced by TEM observations conducted on river samples (Allard et al., 2005) or soil samples submitted to redox alternations (Thompson et al., 2006). Such mixed Al-Fe-C rich colloids may therefore be present in our experiments. Their occurrence agrees with the here above described sequential extraction data (see paragraph 3.a.), recording strong Fe amounts in the oxidizable fraction (Figure IV. 1). The Si solubilization kinetics is reported in Figure IV. 5 at pH = 4 (a) and pH = 7.2 (b). Silicon concentrations remained low and steady (nearly 2 ppm at the end of the experiment) whatever the pH, suggesting that clay nanoparticles were probably not forming the major inorganic colloidal pool. None fractionation was observed for Si distribution regards to the different pore-size cuts at pH = 4. Silicon occurred thus as truly dissolved ionic species. However, at pH = 7.2, Si concentrations were fractionated with nearly 50% of Si located in fraction >30 kDa, suggesting that Si might be trapped in Si-rich nano-oxides.

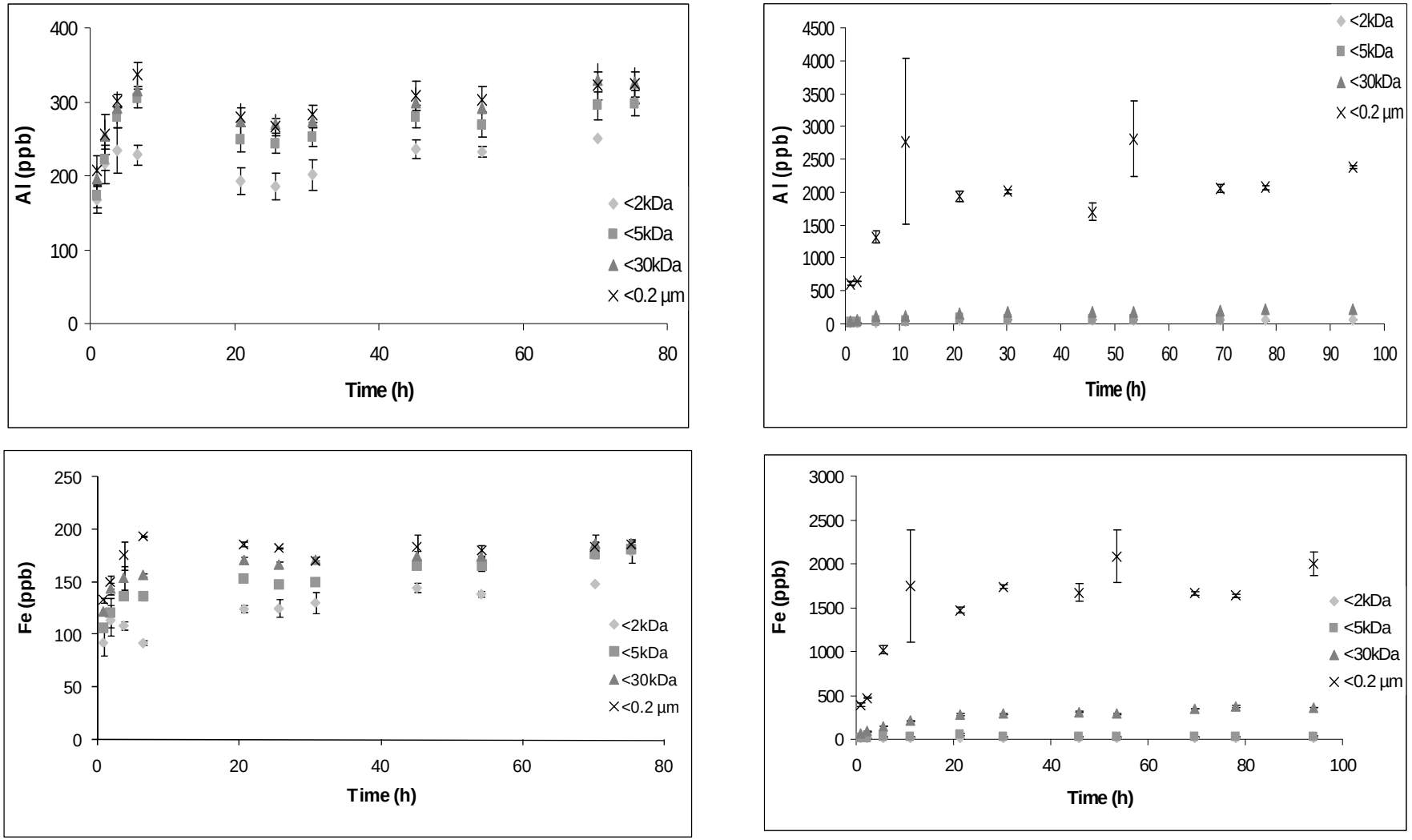

(a) (b)

Figure IV. 4. Iron and Al concentrations at acid pH acid (pH = 4) (a) and at neutral pH (pH = 7.2) (b) for the four cut thresholds (black stars correspond to the fraction below 0.2 µm; grey triangles correspond to the fraction below 30 kDa; grey squares correspond to the fraction below 5 kDa, while grey diamond-shape symbols correspond to the fraction below 2 kDa).

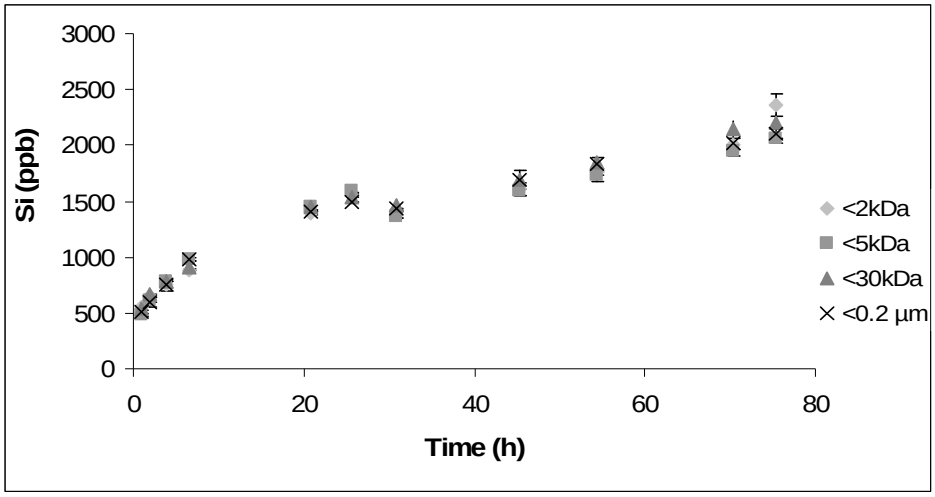

(a)

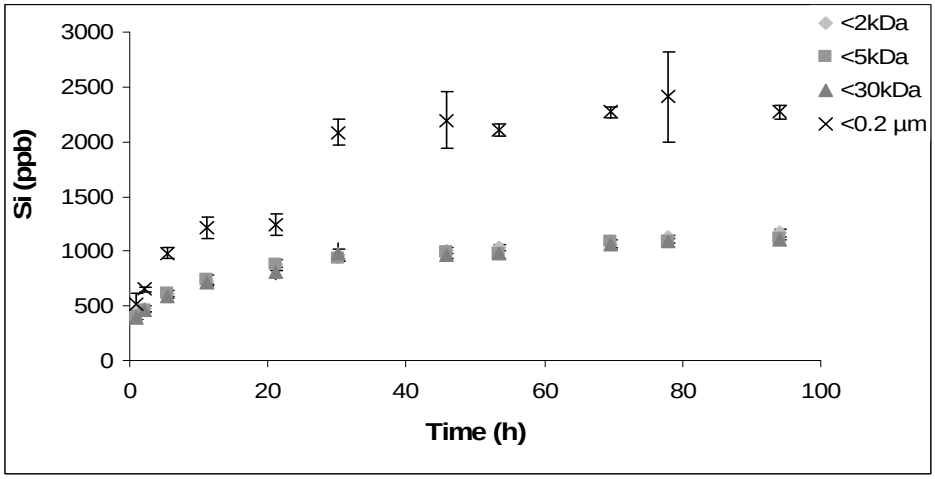

(b)

Figure VI. 5. Silicon concentrations at acid pH (pH = 4) (a) and at neutral pH (pH = 7.2) (b) for the four cut thresholds (black stars correspond to the fraction below 0.2 µm; grey triangles correspond to the fraction below 30 kDa; grey squares correspond to the fraction below 5 kDa, while grey diamond-shape symbols correspond to the fraction below 2 kDa).

3. Trace elements solubilization

As inferred from the data, the element solubilization kinetics allows dividing elements into three groups regards to their pH dependency.

(i) ***Element concentrations increasing <u>strongly</u> with decreasing pH***. Calcium, Sr, Ba, Mn, Mg, Co and Zn concentrations versus pH are reported in Figure IV. 6. Their concentrations strongly increased as the pH decreased (with an increasing factor from 10 for Zn to 150 for Mn). None elements distribution fractionation was observed in between the different pore-size cuts at pH = 4. These elements occurred therefore as a dissolved state and were not mobilized by colloids as previously hypothesis from selective extraction. By contrast, at pH = 7.2, a strong fractionation developed with the decreasing pore-size cuts. The

fraction <2 kDa exhibited low concentrations suggesting that these elements could be released from soil with DOC. Baryum behaved differently with a majority of Ba present in fraction >30 kDa suggesting that Ba might be solubilized from soil with DOC but also with Fe-and Al-nanoparticles. It is important to note that concentrations of these elements at pH = 7.2 were lower than at pH = 4, representing at pH = 7.2 less than 10% for Ba and Zn, 5% for Ca, Sr, Mg and Co and 1% for Mn compared to pH = 4.

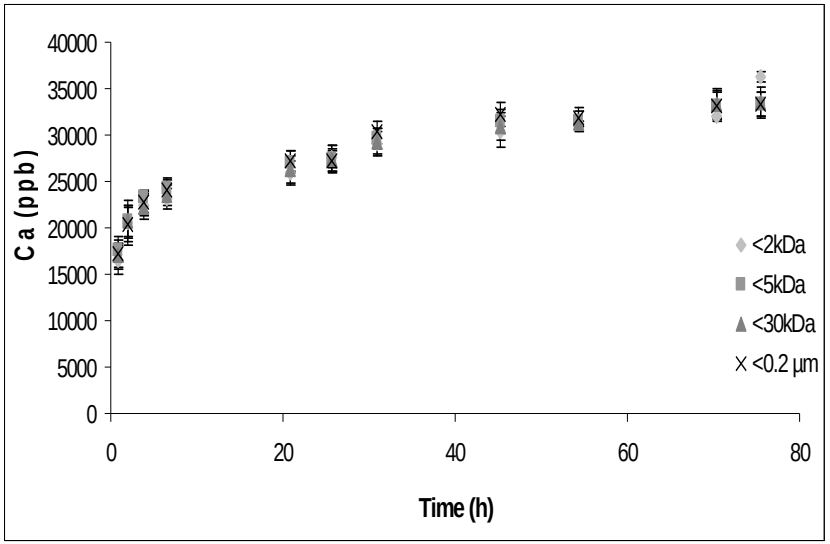
Ca (ppb)
Time (h)
<2kDa
<5kDa
<30kDa
<0.2 µm

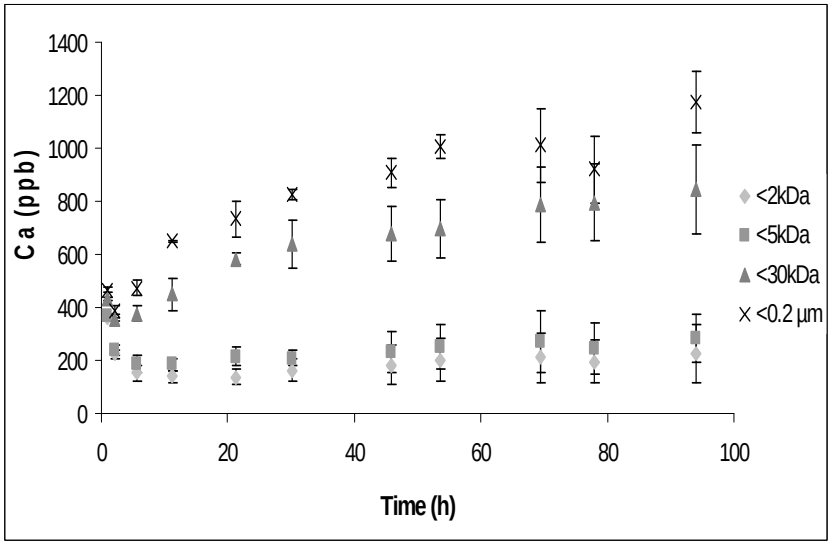
Ca (ppb)
Time (h)
<2kDa
<5kDa
<30kDa
<0.2 µm

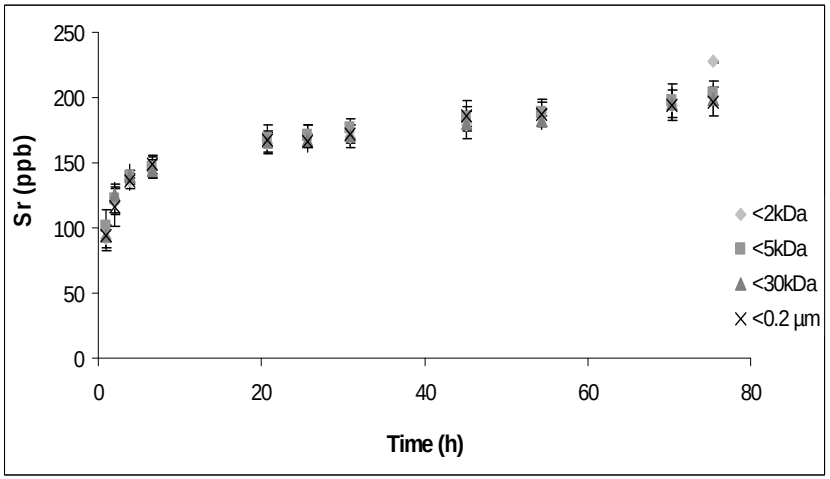
Sr (ppb)
Time (h)
<2kDa
<5kDa
<30kDa
<0.2 µm

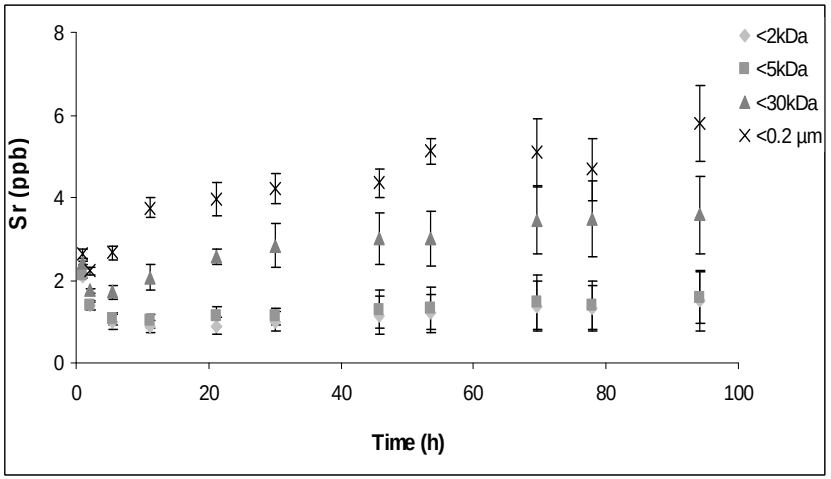
Sr (ppb)
Time (h)
<2kDa
<5kDa
<30kDa
<0.2 µm

(a) (b)

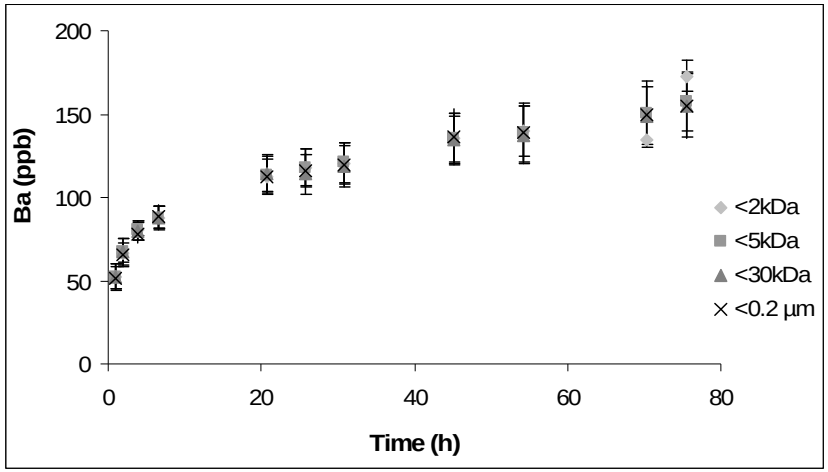
Ba (ppb)
Time (h)
<2kDa
<5kDa
<30kDa
<0.2 µm

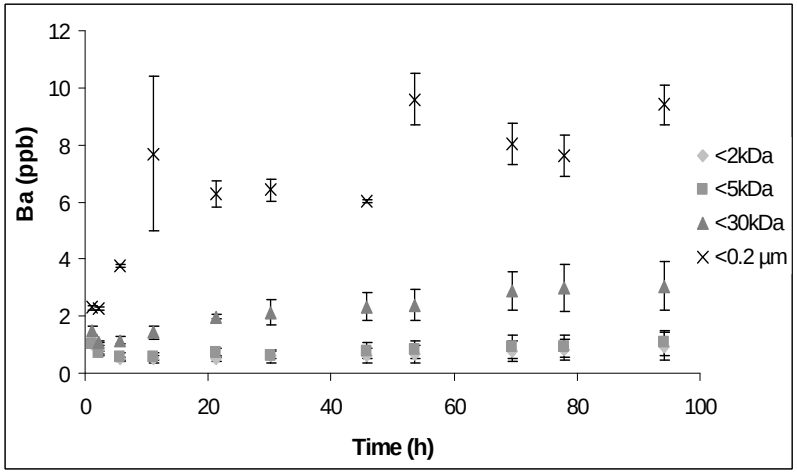
Ba (ppb)
Time (h)
<2kDa
<5kDa
<30kDa
<0.2 µm

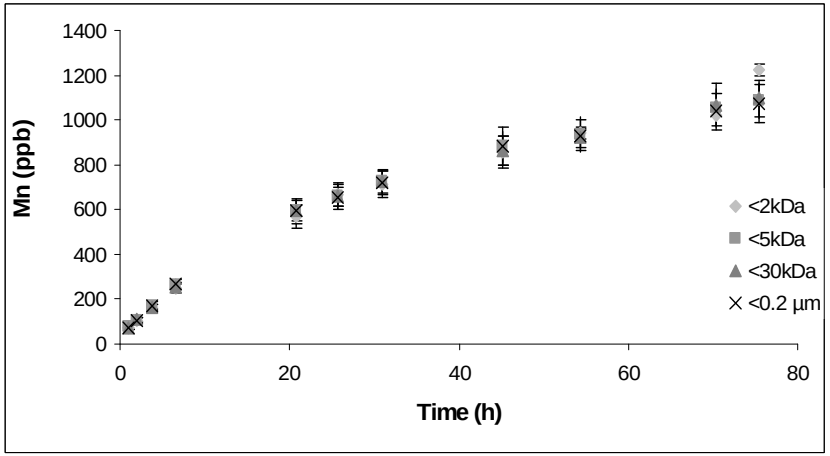
Mn (ppb)
Time (h)
<2kDa
<5kDa
<30kDa
<0.2 µm

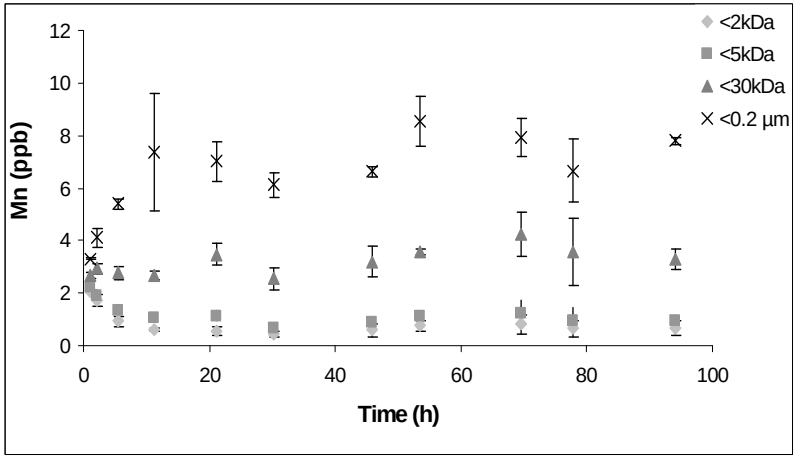
Mn (ppb)
Time (h)
<2kDa
<5kDa
<30kDa
<0.2 µm

(a) (b)

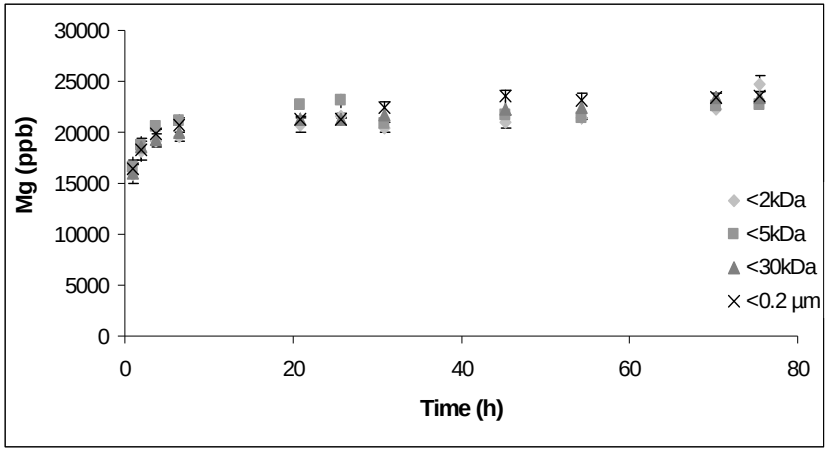
Mg (ppb)
Time (h)
<2kDa
<5kDa
<30kDa
<0.2 µm

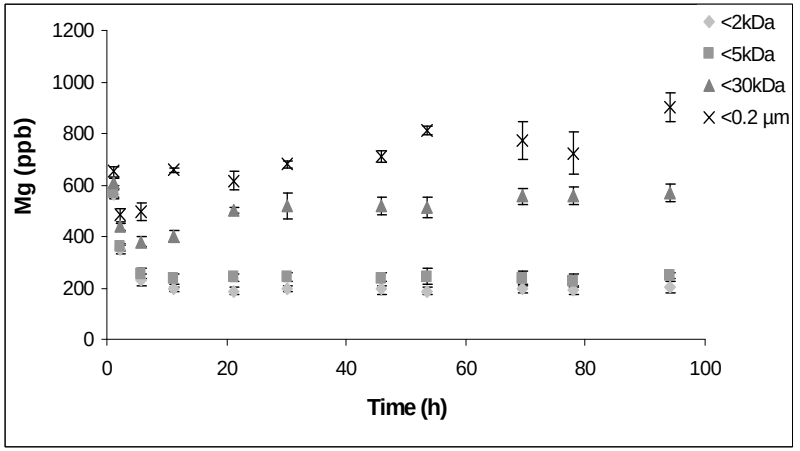
Mg (ppb)
Time (h)
<2kDa
<5kDa
<30kDa
<0.2 µm

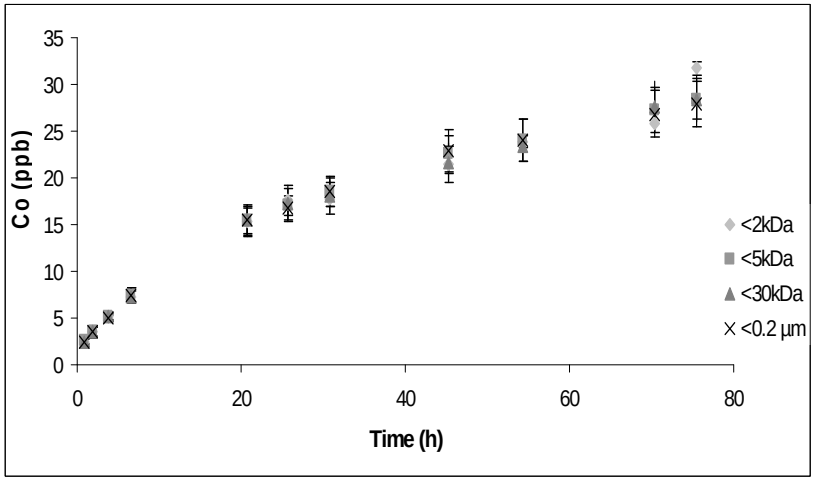
Co (ppb)
Time (h)
<2kDa
<5kDa
<30kDa
<0.2 µm

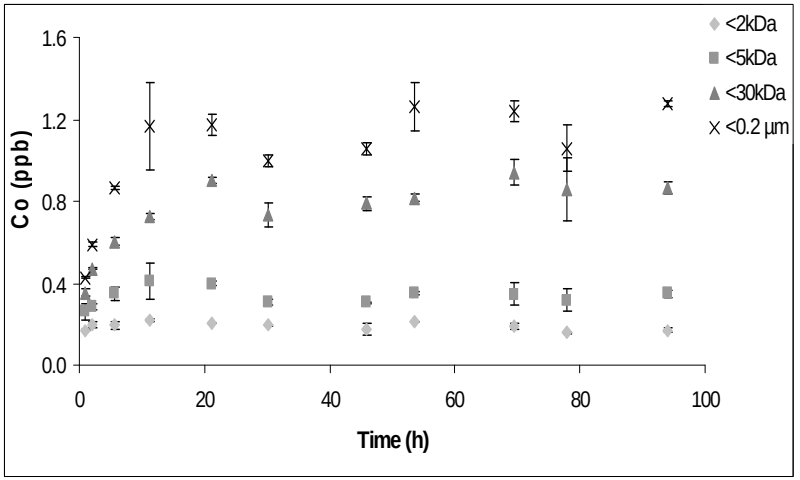
Co (ppb)
Time (h)
<2kDa
<5kDa
<30kDa
<0.2 µm

(a) (b)

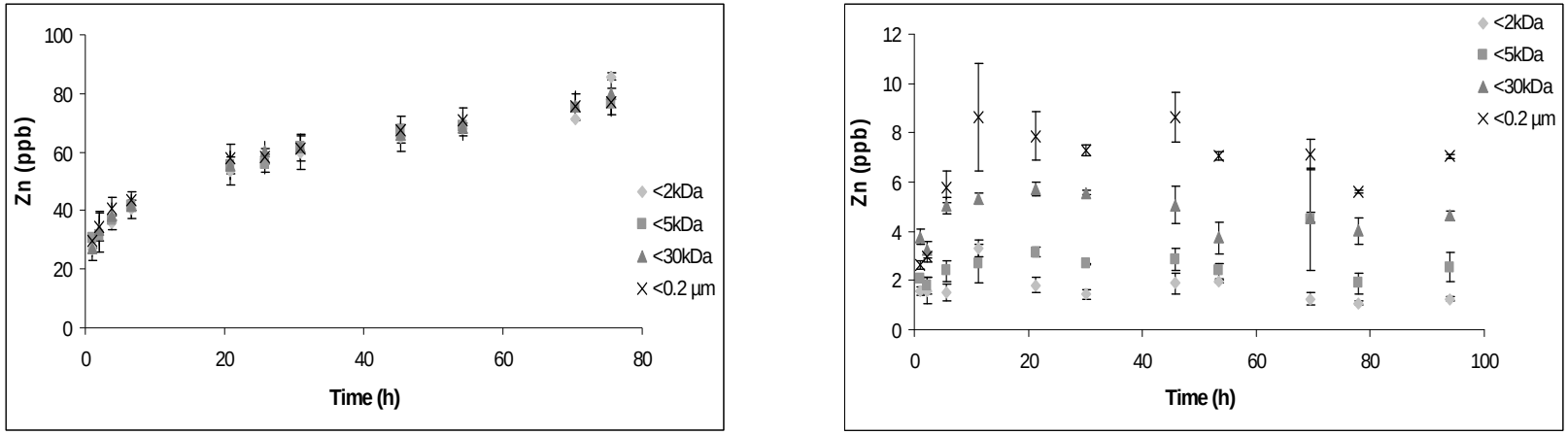

Figure IV. 6. Calcium, Sr, Ba, Mn, Mg, Co and Zn concentrations at acid pH (pH = 4) (a) and at neutral pH (pH = 7.2) (b) for the four cut thresholds (black stars correspond to the fraction below 0.2 µm; grey triangles correspond to the fraction below 30 kDa; grey squares correspond to the fraction below 5 kDa, while grey diamond-shape symbols correspond to the fraction below 2 kDa).

(ii) Element concentrations increasing slightly with decreasing pH. Rubidium, Li and Ni concentrations regards to pH are reported in Figure IV. 7. Their concentrations increased at pH = 4, with an increase factor ranging between 2 and 2.4. Moreover, at pH = 4, none significant difference was observed for the concentrations measured in the fractions below 2 kDa regards to that measured in the other fractions. These elements were thus released as soluble ions or molecules. By contrast, at pH = 7.2, their concentrations decreased with decreasing pore-size cuts suggesting their possible release as colloids. Nickel showed strong interactions with DOC. Lithium and Rb displayed also interactions with Fe-Al, with 90% of Li, located in the fraction between 30 kDa and 0.2 µm. Lithium and Rb were therefore tightly associated with Fe-Al oxides (Figures IV. 4b and IV. 7b).

(iii) Element concentrations increasing significantly with increasing pH. Thorium, REE, Y, U, Cr, Ti, Pb, V, and Ga belong to the group for which their concentrations increased significantly with increasing pH (Figure IV. 8). At pH = 7.2, most solid surfaces were negatively charged implying that metal cations might remain bound to soil solids. However, in the present experiment, significant amounts of these element were released into solution at pH = 7.2 (Figure IV. 8). Since cation desorption cannot occur, the released TE were probably bound to anionic ligands themselves in solution at pH = 7.2. Thorium, REE, Y, U and Cr concentrations decreased strongly with the pore-size cuts at pH = 7.2 and were correlated with the DOC distribution. They were therefore associated to the organic pool. By contrast, Ga, Ti, V and Pb concentrations displayed variable fractionation regards to the pore-size cuts. Nearly 80% of Ti, V and Pb, and more than 90% of Ga, were located in fraction >30 kDa at pH = 7.2. Gallium, Ti, V and Pb were probably associated to mineral colloids, considering that at pH = 7.2, the colloidal pool was mostly inorganic in this size fraction.

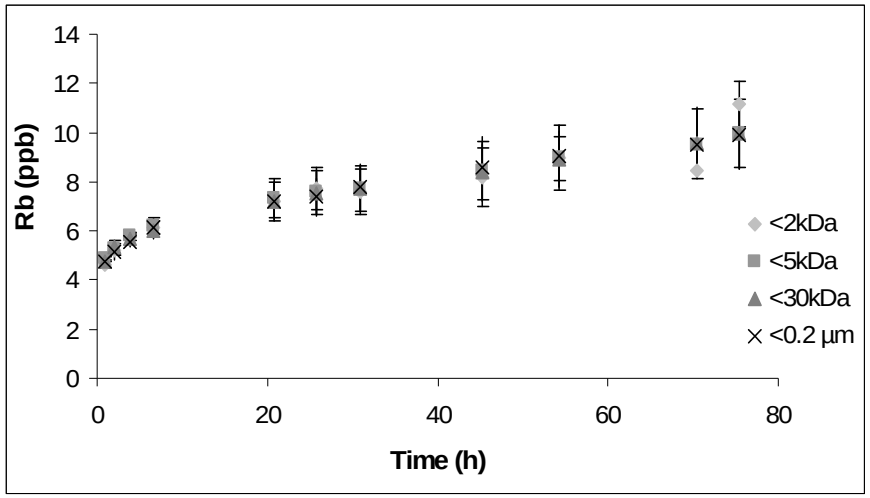
Rb (ppb)
Time (h)
<2kDa
<5kDa
<30kDa
<0.2 µm

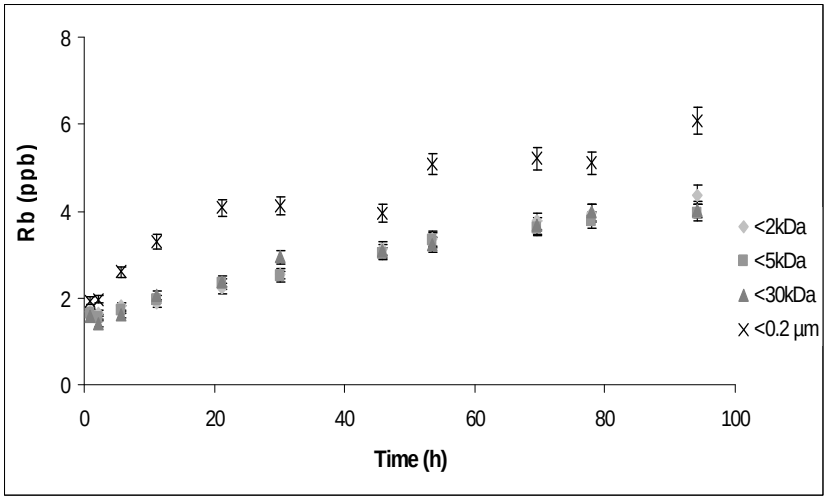
Rb (ppb)
Time (h)
<2kDa
<5kDa
<30kDa
<0.2 µm

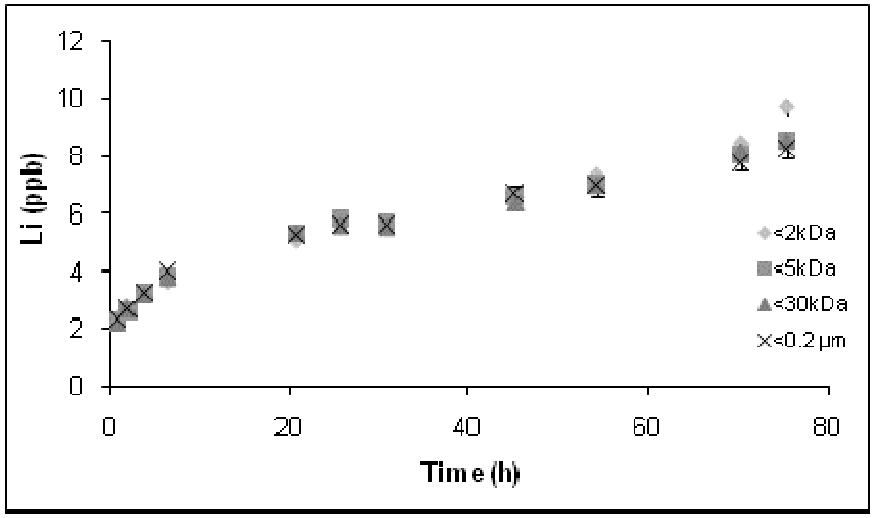
Li (ppb)
Time (h)
<2kDa
<5kDa
<30kDa
<0.2 µm

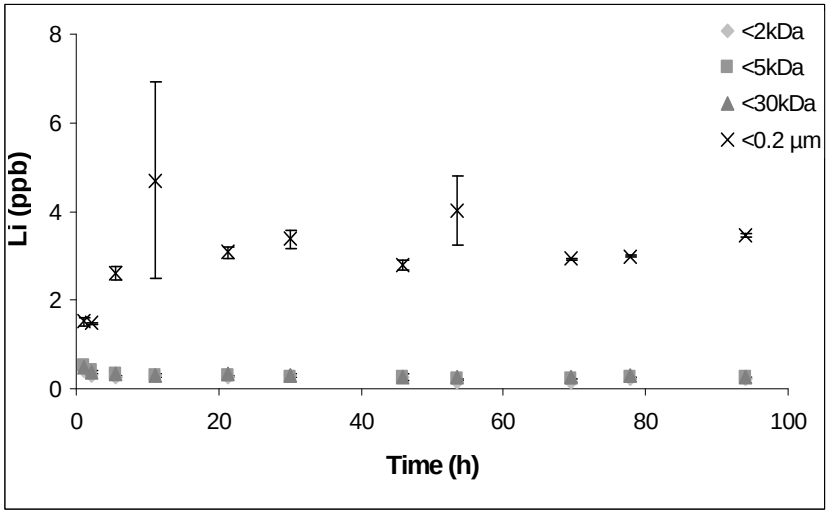
Li (ppb)
Time (h)
<2kDa
<5kDa
<30kDa
<0.2 µm

(a) (b)

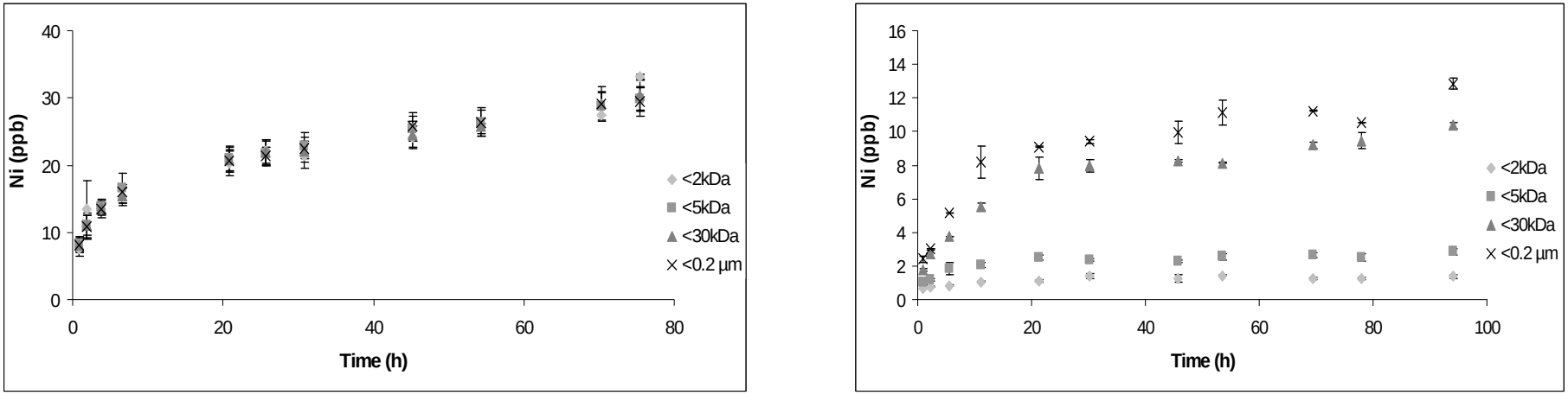

Figure IV. 7. Rubidium, Li and Ni concentrations at acid pH (pH = 4) (a) and at neutral pH (pH = 7.2) (b) for the four cut thresholds (black stars correspond to the fraction below 0.2 µm; grey triangles correspond to the fraction below 30 kDa; grey squares correspond to the fraction below 5 kDa, while grey diamond-shape symbols correspond to the fraction below 2 kDa).

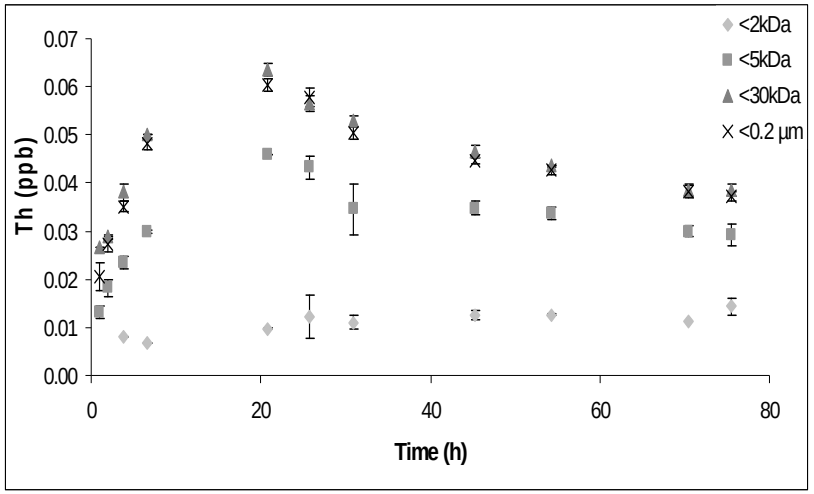
Th (ppb)
Time (h)
<2kDa
<5kDa
<30kDa
<0.2 µm

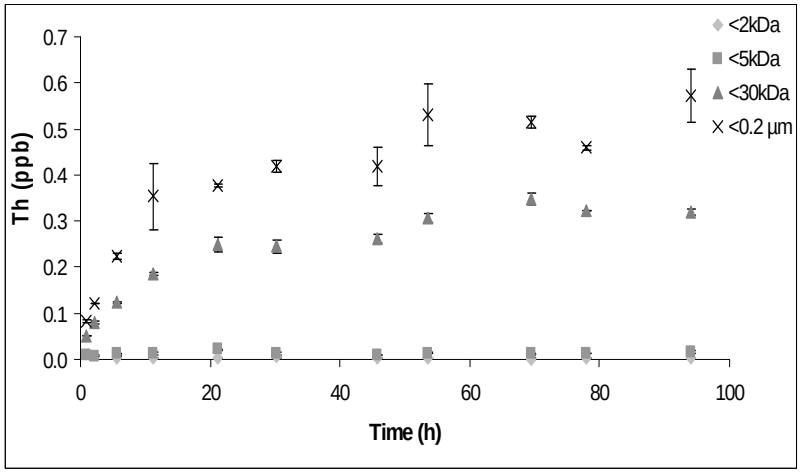
Th (ppb)
Time (h)
<2kDa
<5kDa
<30kDa
<0.2 µm

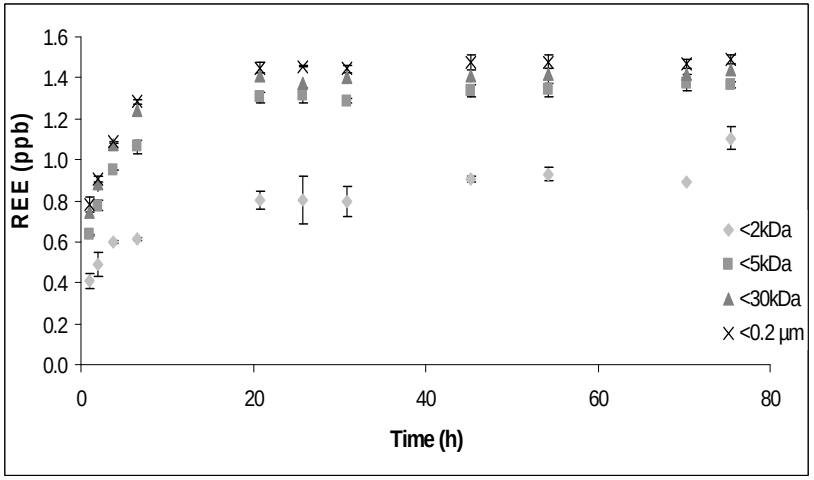
REE (ppb)
Time (h)
<2kDa
<5kDa
<30kDa
<0.2 µm

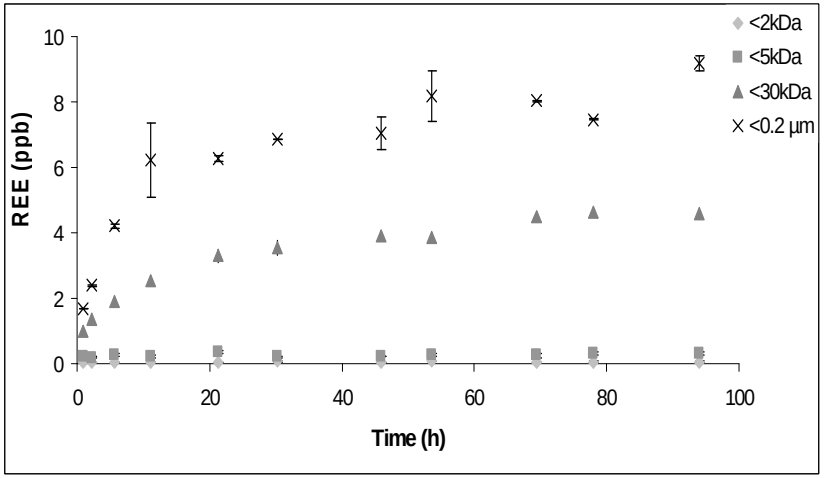
REE (ppb)
Time (h)
<2kDa
<5kDa
<30kDa
<0.2 µm

(a) (b)

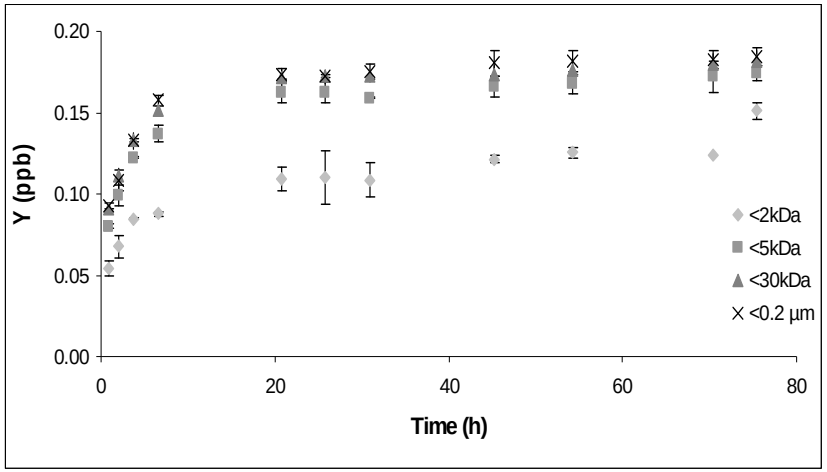
Y (ppb)
Time (h)
<2kDa
<5kDa
<30kDa
<0.2 µm

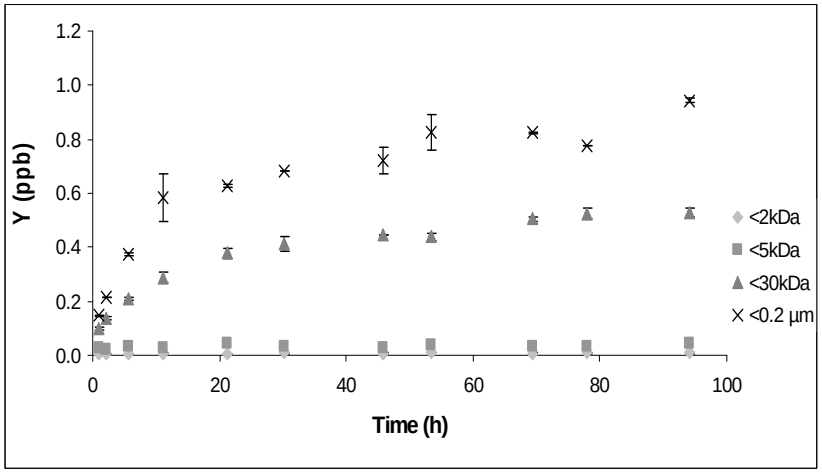
Y (ppb)
Time (h)
<2kDa
<5kDa
<30kDa
<0.2 µm

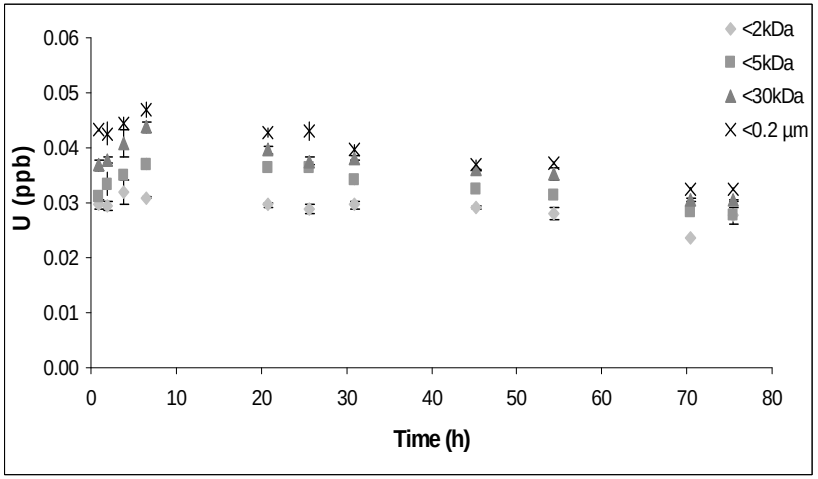
U (ppb)
Time (h)
<2kDa
<5kDa
<30kDa
<0.2 µm

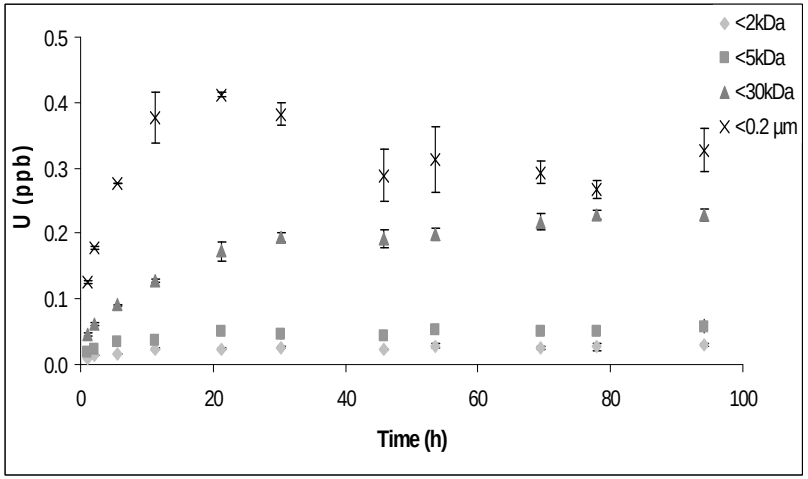
U (ppb)
Time (h)
<2kDa
<5kDa
<30kDa
<0.2 µm

(a) (b)

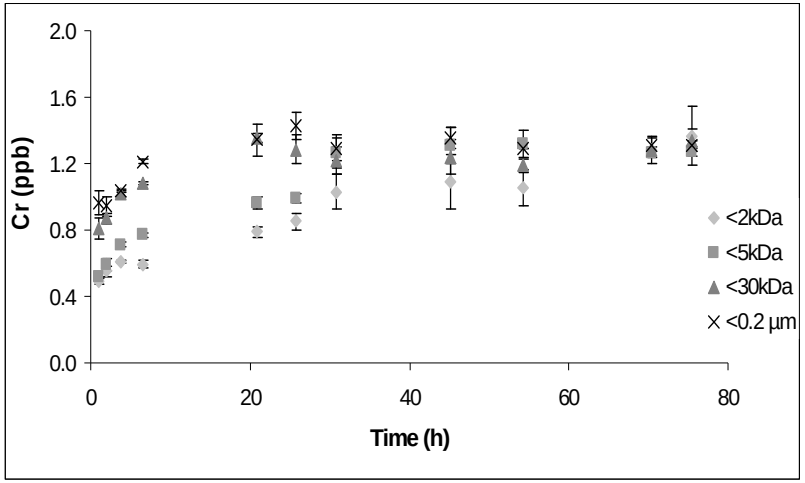
Cr (ppb)
Time (h)
<2kDa
<5kDa
<30kDa
<0.2 µm

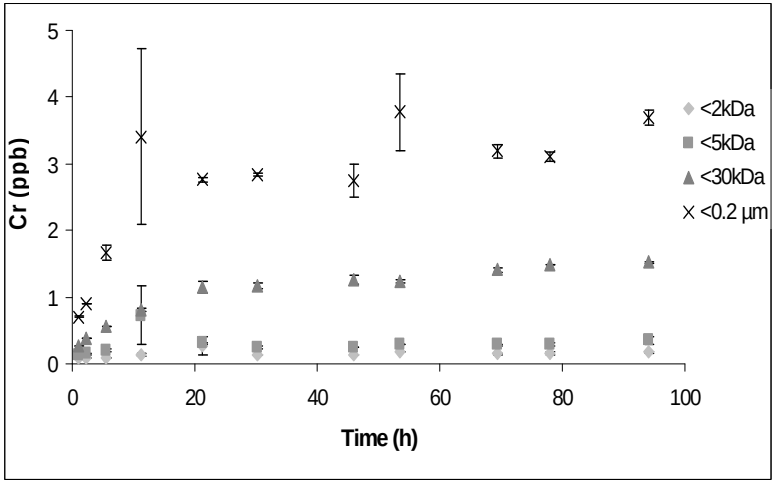
Cr (ppb)
Time (h)
<2kDa
<5kDa
<30kDa
<0.2 µm

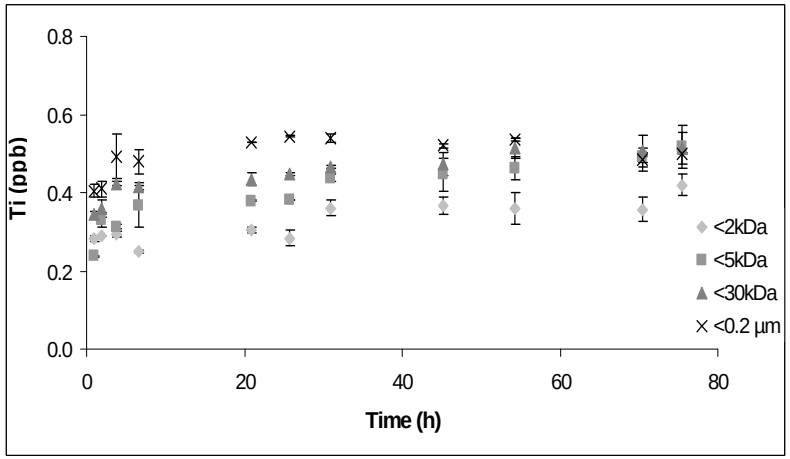
Ti (ppb)
Time (h)
<2kDa
<5kDa
<30kDa
<0.2 µm

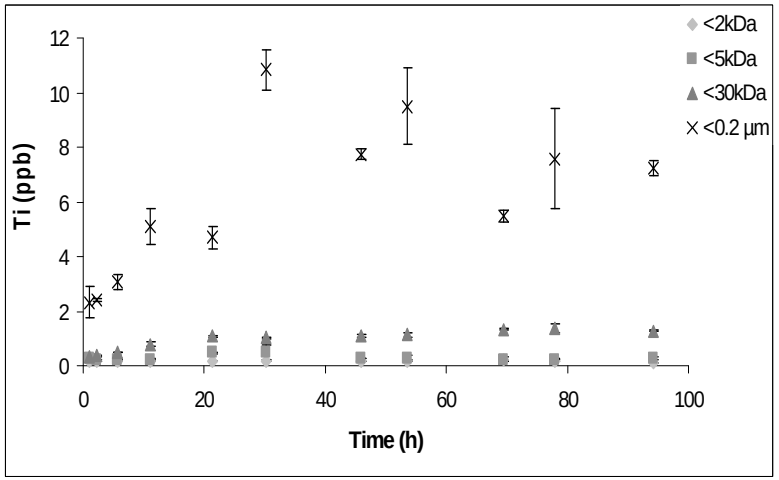
Ti (ppb)
Time (h)
<2kDa
<5kDa
<30kDa
<0.2 µm

(a) (b)

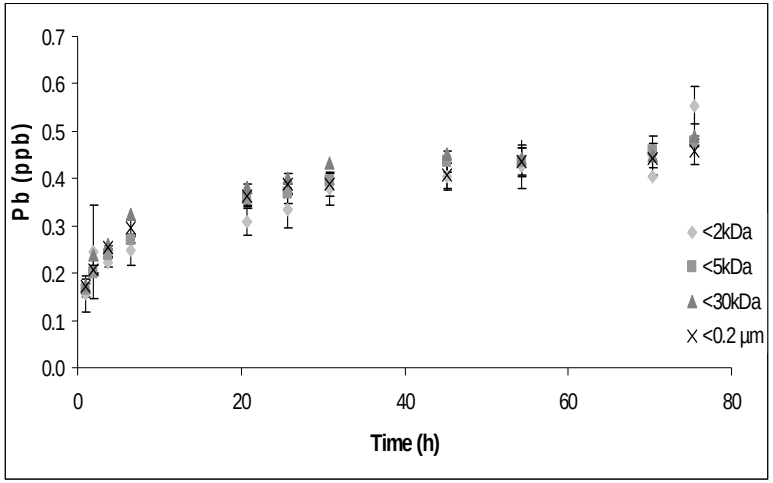
Pb (ppb)
Time (h)
<2kDa
<5kDa
<30kDa
<0.2 µm

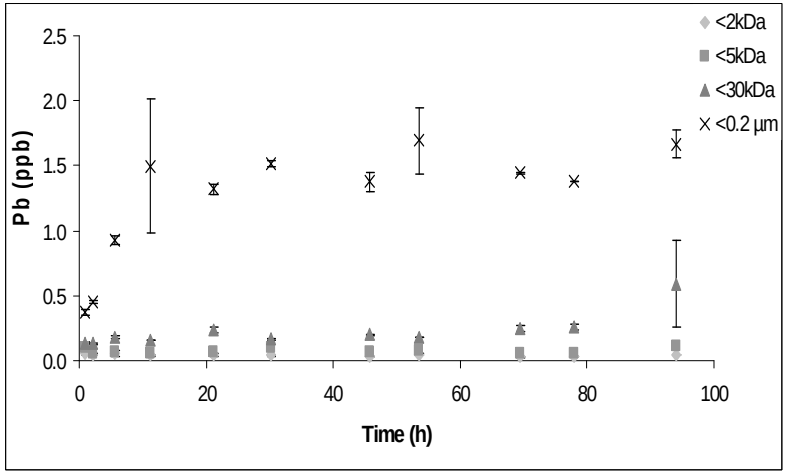
Pb (ppb)
Time (h)
<2kDa
<5kDa
<30kDa
<0.2 µm

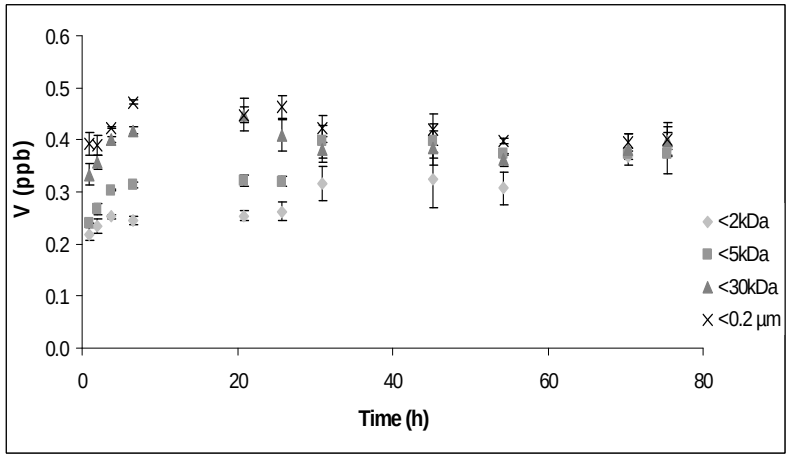
V (ppb)
Time (h)
<2kDa
<5kDa
<30kDa
<0.2 µm

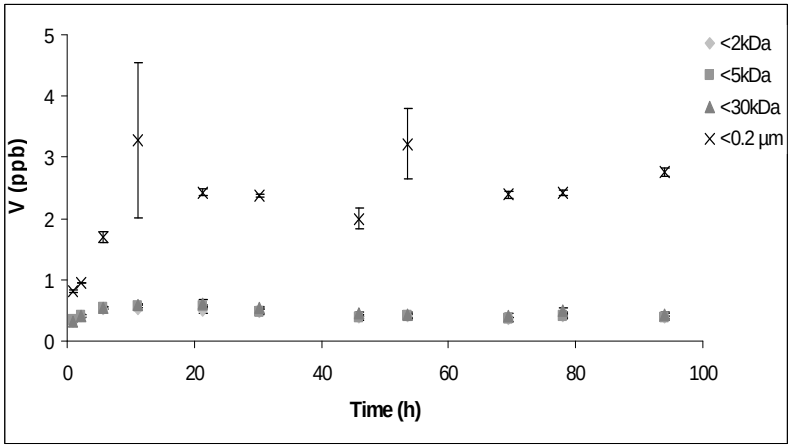
V (ppb)
Time (h)
<2kDa
<5kDa
<30kDa
<0.2 µm

(a) (b)

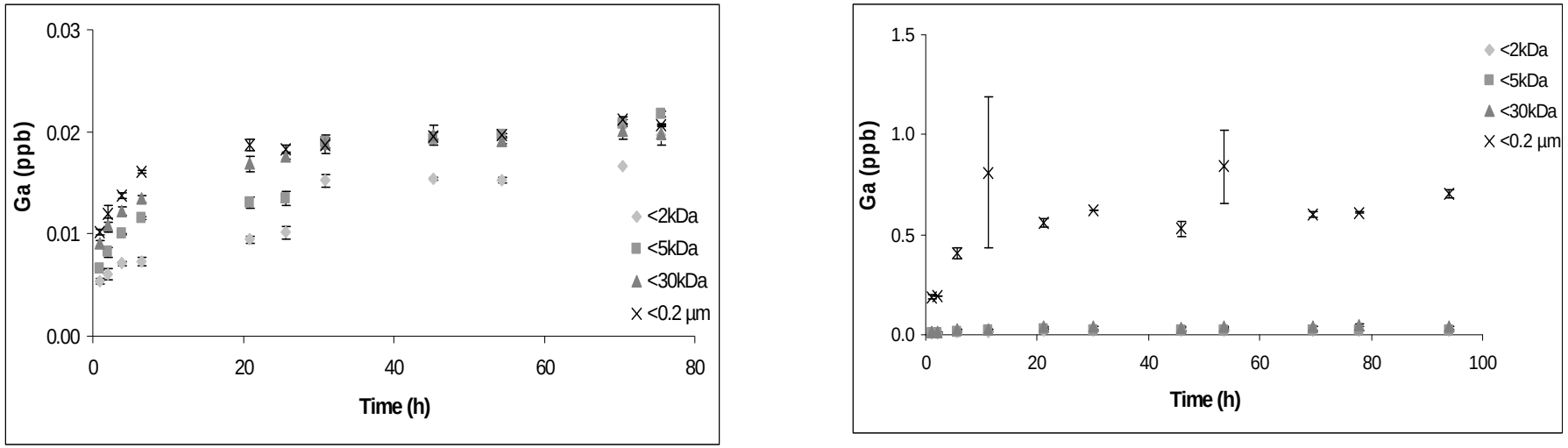

(a) (b)

Figure VI. 8 : Th, REE, Y, U, Cr, Ti, Pb, V and Ga concentrations at acid pH (pH = 4) (a) and at neutral pH neutral (pH = 7.2) (b) for the four cut thresholds (black stars correspond to the fraction below 0.2 µm; grey triangles correspond to the fraction below 30 kDa; grey squares correspond to the fraction below 5 kDa, while grey diamond-shape symbols correspond to the fraction below 2 kDa).

IV. Discussion

1. Nature of the colloidal pool

Iron and aluminium nanoparticles were released at high pH indicating that Fe and Al might interfere in the formation of ternary clay surfaces - oxyhydroxides - humic substance systems at pH = 4 (Wiseman and Püttmann, 2006). Iron and aluminium nanoparticles could form aggregates with mineral particles for pH below their zero point of charge and/or behave as interparticle bonds between humic substances and mineral particles. Aggregation of poorly crystalline Fe oxyhydroxides onto clays face-surfaces displays larger and more reactive surface areas than well crystallized Fe oxyhydroxides (Duiker et al., 2003) and enhances the humic substance adsorption onto clay particles However, pH rise could decrease the interparticle bond stability by enhancing the electro-negativity of both humic molecules and mineral surfaces, notably for pH upper than Fe- and Al- nanoparticles pHzpc.

The degree of solubility must also influence this association. At high pH, the proton-binding sites were sufficiently dissociated to develop a significant charge. The electrostatic interactions between the charges repelled humic substances from the Fe- and Al-nanoparticles. At acidic pH, the surface charge became probably less negative, the humic substances were more hydrophobic, and aggregation took place (Liu and Gonzales, 1999; Tipping, 2002). At acidic pH, the aggregation onto the mineral surface is also increased by the H-bonding increase. Therefore, a strong humic substance aggregation implies a decrease of their solubility at acidic pH. The solubility is also dependent on the humic substance charge. A higher positive charge results indeed in a higher solubility, since compounds are more fully hydrated (Tipping, 2002). Among humic substances, the density of proton-dissociating groups is stronger for humic acids than fulvic acids. Moreover, fulvic acid carboxyl groups are stronger acids (Tipping, 2002). As a result, humic acids present lower charge and solubility than fulvic acid. As a consequence, fulvic acids should therefore preferentially solubilized than humic acids at acidic pH, as previously demonstrated by numerous studies involving various types of solids (Murphy and Zachara, 1995; You et al., 1999; 2006; Hur and Schlautman, 2003; Weng et al., 2007). In the present experiment at pH = 7.2, high molecular-weight organic molecules can be considered as humic acids. These organic molecules contain a large fraction of TE compared to low molecular-weight organic molecules (Figures IV. 3 and 8). We therefore propose that these associated TE could act as 'bridges' between mineral

surfaces and humic compounds, favouring also the humic acid preferential adsorption onto mineral particles.

The consequences of the humic acid preferential adsorption can explain the aromaticity distribution at acidic pH following three points. (i) At pH = 4, humic acids being preferentially adsorbed onto mineral surface, small aromatic organic molecules such as fulvic acids enriched the small fractions and conspicuously the fractions <5 kDa. (ii) The presence in fractions >5 kDa of weakly aromatic molecules as cellulose or certain proteins, underlined by the lack of humic acids at pH 4, might also explain the global aromaticity decrease in fractions <30 kDa and <0.2 µm. (iii) The molecular size and shape of humic substances is usually explained by two concepts. Firstly, humic substances are considered as linear macromolecular polyelectrolytes that can form molecular aggregates under specific experimental conditions, principally acid pH and high ionic strength (Swift, 1999; Senesi, 1999). Secondly, humic substances are represented as supramolecular assemblies (molecular aggregates) of small molecules without macromolecular character, joined together by weak attraction forces (Wershaw, 1999; Piccolo, 2001; Simpson et al., 2001). Considering the humic substances, in major part, as supramolecular assemblies, Pédrot et al. (submitted 2009a) recently proposed that at acidic pH, a disruption of the DOM associations might involve the release of small, but highly aromatic organic molecules. Thus, this destabilisation of supramolecular assemblies resulted thus in a higher aromaticity in fractions <5 kDa.

2. Trace elements-colloid association

Solubilization kinetics and concentration distribution related to size-fractions allowed determining TE carrier phases. Two groups of colloid-carried elements could be thus distinguished. The first one is composed of Ca, Sr, Ba, Mn, Mg, Co and Zn. The increase of their concentration at low pH, as well as their lack of fractionation indicated that their concentrations were probably controlled by weak interactions (ion exchange or electrostatic attraction) with surface. The decreasing pH involved a concomitant H^+ competition increase and decrease of the surface electro-negativity that repelled such cations, which were thus leached, and partially released in solution. Besides, the majority of these elements correspond to elements occurring in the exchangeable and acidic soluble fraction of the sequential extraction. At pH = 7.2, the low TE concentrations displayed in soil correspond to cations solubilized as complexed with released colloidal DOC or iron nanoparticles (Citeau et al., 2003; Weng et al., 2005). Maguire et al. (1992) provided evidence that humic substance

addition in clay systems enhanced the desorption of TE weakly bound to clay surfaces. The strong solubilization of this first group of elements was therefore induced by mechanisms involving electrostatic interactions through pH change and humic substances solubility degree.

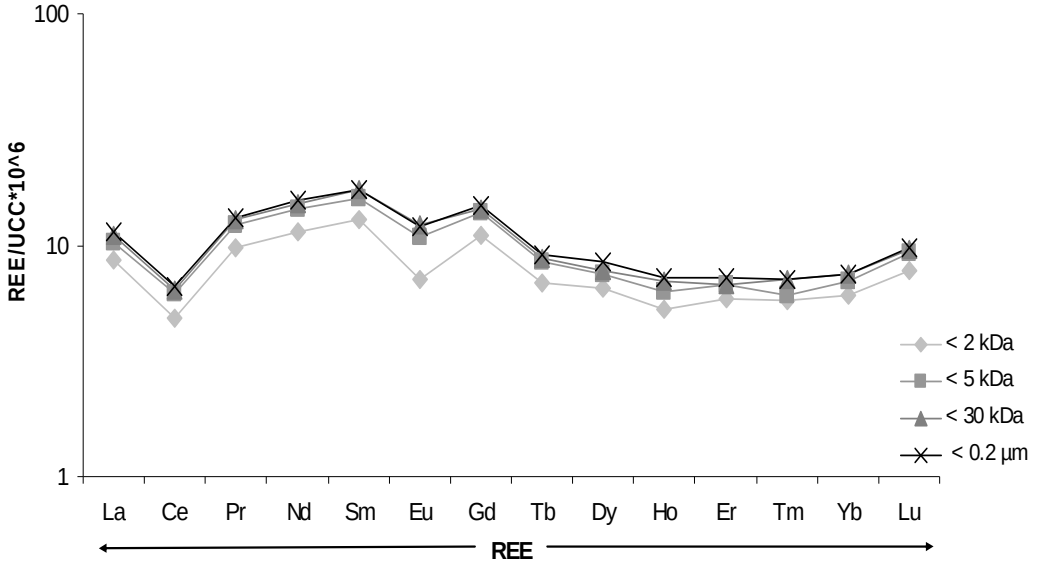

(a)

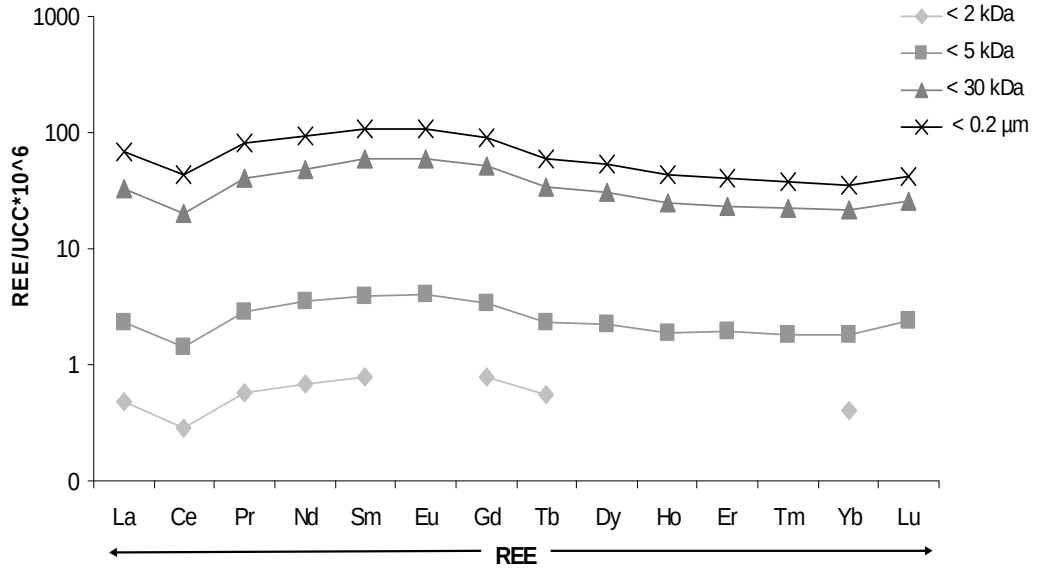

(b)

Figure IV. 9. Upper continental crust (UCC) normalized (Taylor and McLennan, 1985) REE patterns of soil solution at acid pH (pH = 4) (a) and at neutral pH (pH = 7.2) (b) for the four cut-thresholds (black stars correspond to the fraction below 0.2 µm; grey triangles correspond to the fraction below 30 kDa; grey squares correspond to the fraction below 5 kDa, while grey diamond-shape symbols correspond to the fraction below 2 kDa).

The second group is composed by Th, REE, Y, U, Ti, Pb, V, Ga and Cr. These elements exhibited a strong fractionation in the distribution of their concentration according to pore-

size cuts. Thorium, REE, Y, U and Cr seemed to strongly interact with DOC and especially with heavy and aromatic organic molecules such as humic acids. Tyler and Olsson (2001) showed that the pH rise involved the solubilization of Cr(III)-humic compounds complexes through a study of TE solubilization following $CaCO_3$ addition to an acidic soil. Lanthanides and related elements such as Th, are either strongly bound to humic substances in organic-rich soil solutions (Viers et al., 1997; Dupré et al., 1999; Dia et al., 2000, Pédrot et al., 2008), or complexed to carbonates when alkaline conditions (pH > 8) prevail (Tang and Johannesson, 2003; Pourret et al., 2007d). Rare earth element complexation to organic colloids implies the development of REE pattern exhibiting a specific shape in solution, namely, a middle rare earth element (MREE) downward concavity (Davranche et al., 2005, Yamamoto et al., 2006; 2008; Pourret et al., 2007c; Pédrot et al., 2008). In the present study, this specific MREE downward concavity shape remained unchanged through pH and size-fraction changes (Figure IV. 9) reinforcing the hypothesis that REE and Th were bound and released in solution carried by colloidal humic substances. By contrast, Ti, Pb, V and Ga seemed to strongly interact with Fe- and Al- nanoparticles. Their concentrations increased at high pH with the nanoparticle release. Solubilized Ti concentrations could also partly result from very stable nano- TiO_2 oxides released in solution (Zhang et al., 2007; Fang et al., 2009).

Although V is usually found at low concentrations in waters, rocks, and soils, vanadium has been found to be naturally associated with humic substances (Lu and Johnson, 1998; Tyler and Olsson, 2001; Tyler, 2004). However, in the present study, V was mainly present in fraction >30 kDa, enriched in Fe and Al nanoparticles. Therefore, V seems to be rather associated to mineral than organic colloids. This strong association of V with Fe-colloids was already reported by recent findings in a boreal river by Dahlqvist et al. (2007). Concerning the Pb behaviour, Klitzke et al. (2008) demonstrated that the concentration of colloidal Fe and Pb were correlated from pH ranging from 5 to 7. To explain this finding, they suggested the presence of colloidal Fe-oxides or colloidal Fe organic complexes at circumneutral pH, as highlighted in this study. Therefore, the occurrence of Fe-rich inorganic colloids was the key parameter controlling the Pb mobilization. There are only very few data available concerning the Ga behaviour in soil regards to pH. The Ga behaviour has to be related to that of Al since they are, from a chemical point of view, chemically related (Tyler and Olsson, 2001). Tyler (2004) demonstrated, working on the TE vertical distribution in a Haplic Podzol, that Ga could interact with Fe, through soluble Fe(III) compounds enriched in Ga. This observation is in good agreement with the present study in which the release kinetics of Ga and Fe-Al nanoparticles were similar.

3. pH controls on the nature of released colloids and carried TE distribution

The composition of the soil solution was strongly dependent on pH. At pH = 4, Ca, Sr, Ba, Mn, Mg, Co and Zn were strongly solubilized by mechanisms involving electrostatic interactions through the increase of proton concentration and humic acid sorption onto mineral surfaces. Colloids were weakly released in the soil solution and trace elements occurred mostly at 'truly' dissolved state (fraction <2 kDa) (Figure IV. 4, IV. 5, IV. 6 and IV. 8). As shown by the aromaticity value distribution (Figure IV. 2), fractions <5 kDa was composed of strongly complexing humic substances including both fulvic acids and low molecular-weight organic molecules released by the destabilization of the supramolecular humic acid structure. By contrast, at pH = 7.2, high molecular-weight colloids (>5 kDa) were released. These latter are supposed to be composed by association of humic acids and nano-oxides that bind especially Th, REE, Y, U, Cr, Ti, Pb, V and Ga (Figure IV. 3, IV. 4 and IV. 8).

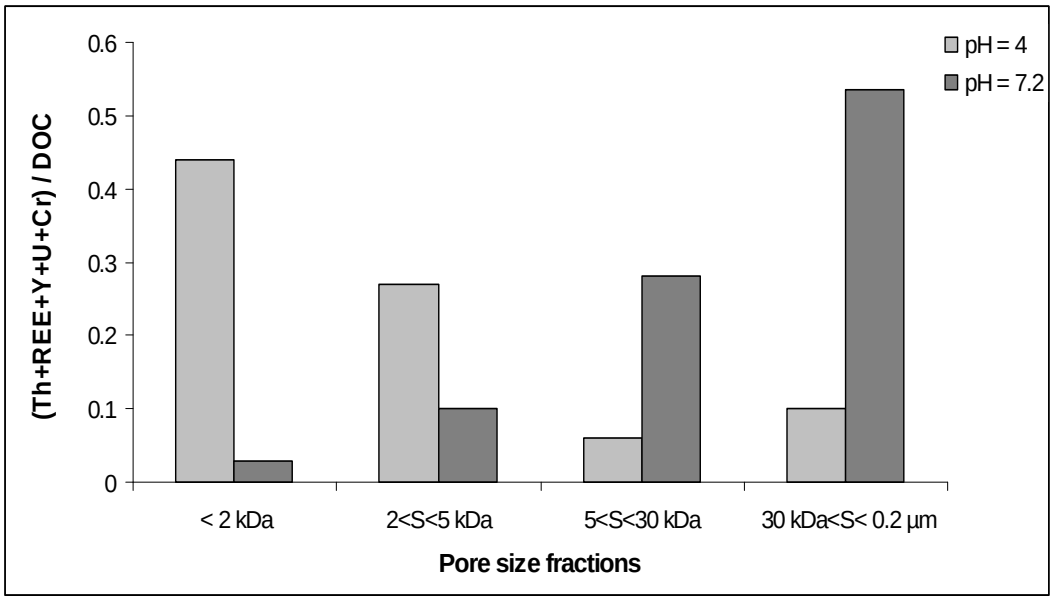

Figure IV. 10. Trace elements mobilized by organic colloids / DOC ratio at the end of the experiment (S corresponds to the molecular weight of the sample compounds).

By governing the detachment of colloids, pH controls the nature of the released colloids, and thus the TE concentration and distribution. The amount of TE bound to organic molecules (expressed as TE/DOC ratio) was modified according to pH (Figure IV. 10). At pH = 4, fractions <5 kDa were composed of TE-rich fulvic acids and low molecular-weight humic acids, although fractions >5 kDa were composed of TE-poor heavy organic molecules characterized by low aromaticity (cellulosis or hydrophilic proteins). At the opposite, at pH = 7.2, fractions >5 kDa were enriched in TE-rich heavy aromatic organic molecules, such as humic acids. Thus, pH controls the nature of the colloidal carriers of TE in the soil solution

with small and labile organic molecules at acidic pH and heavy organic molecules at circumneutral pH.

To sum up, pH controls strongly the mobility of TE by controlling, (i) the detachment of colloids (nature, size and quantity) and their mobility, and (ii) the chemical state of TE (truly dissolved or carried by colloids and/or mineral surfaces). Thus, pH exerts a double control on the composition of the dissolved phase of the soil solutions.

V. Conclusions

This study involving sequential extraction completed by soil/water interaction experiments at two contrasted pH and coupled with ultrafiltration led to several conclusions: (i) the released colloids were mostly composed of heavy humic substances with little nanooxides. Such colloidal release can be due to an increase of the humic substance solubility, following a combined decrease of both the aggregation and the stabillity of ternary systems (with interparticle bonds between particulate mineral surfaces, oxides and humic substances). (ii) pH controlled the nature, size and mobility of humic substances occurring in soil, since involved in their flocculation, spatial arrangement and solubility degree (dissolved state or adsorbed at mineral surfaces). (iii) The TE concentration distributions of the resulting soil solutions were closely related to pH. (iv) However, all TE did not behave in the same way regards to pH, leading to the identification of several groups of elements according to their chemical state - their affinity or not for the colloidal pool - within the solution regards to pH. Therefore, pH had an impact on the TE release both by increasing competition between TE and protons, and by influencing the detachment of the colloidal carriers of TE themselves. A pH increase promoted the combined release of colloids and associated TE, which therefore remained in solution carried by the colloidal pool. (v) While the TE closely associated to the colloidal pool seemed to be strongly bound to humic substances, several trace metals (Ga, Ti, V and Pb) remained however, mobilized by nanooxides. Therefore, the respective nature of the colloidal carrier phases, and the elemental specific affinities for them, put strong constrains on the colloidal transport of elements within soil. Further studies dedicated to the understanding of the Fe-humic substance interactions and their impact on the Fe and associated trace metals solubility should be undertaken.

Chapitre V : Interactions Fe - matière organique et biodisponibilité des nanoparticules de Fe

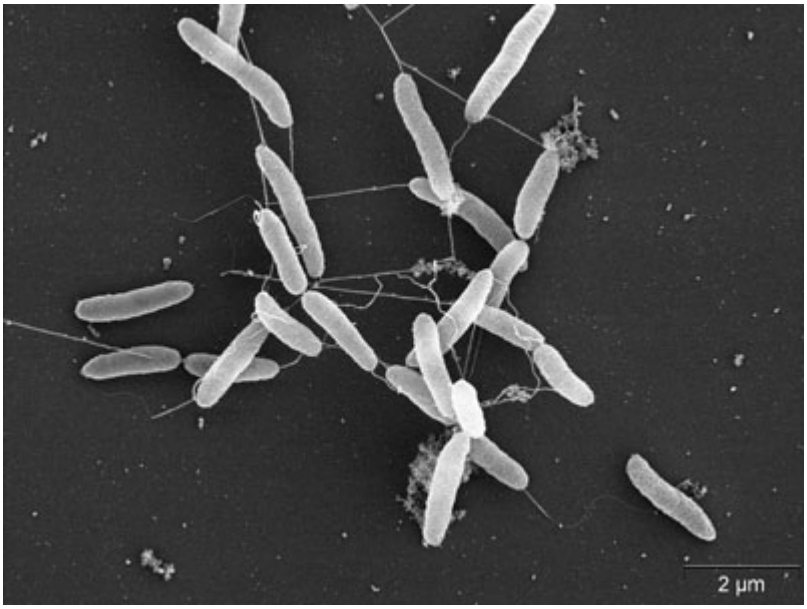

Photo par microscopie électronique à balayage de *Shewanella putrefaciens*
(Source : http://genome.jgi-psf.org/she_m/she_m.home.html).

Ce chapitre est organisé en deux parties. (A) La première traite des interactions entre le fer et les substances humiques (SH). L'objectif est de déterminer l'impact des substances humiques sur les réactions d'oxydation et d'hydrolyse du fer. (B) La deuxième partie traite de la biodisponibilité de colloïdes Fe-matière organique. L'objectif est de déterminer l'impact de tels colloïdes sur l'utilisation du fer comme accepteur d'électrons par les bactéries ferro-réductrices (exemple de Shewanella putrefaciens).

I. Introduction

En théorie, dans la majorité des eaux de surfaces (pH 6 à 9), la concentration du Fe(III) libre et complexé dans la phase dissoute devrait être faible en réponse aux réactions d'hydrolyse et de précipitation. Toutefois, sur le terrain, les concentrations mesurées du Fe(III) dissous dans les eaux de surface s'avèrent être plus importantes que les concentrations prédites à l'équilibre avec une phase cristalline. La présence de ce fer dissous additionnel a été largement attribuée à la complexation organique du Fe(III) (Perdue et al., 1976 ; Koenings, 1976) et/où à la présence de nanoparticules de fer amorphe, stabilisées par la matière organique. Mais l'importance relative de ces formes est peu connue. De récentes études sur la spéciation du fer dans les eaux naturelles (Eyrolle et al., 1996; Rose et al., 1998 ; Olivié-Lauquet et al., 1999 ; Benedetti et al., 2003 ; Gaffney et al., 2008 ; Lofts et al., 2008) suggèrent que le fer présent dans la phase colloïdale peut être présent sous forme libre (complexation organique de Fe^{2+} ou Fe^{3+}) et/ou sous forme de nanoparticules. En effet, la présence de colloïdes mixtes substances humiques-Fe(III) a été supposée dans plusieurs études de milieux riches en matière organique (Rose et al., 1998; Pokrovsky et al., 2005; You et al., 2006; Dahlqvist et al., 2007). Ainsi, Pédrot et al. (2008), dans une étude d'ultrafiltration de solution de sol, ont pu observer une distribution préférentielle du fer. Le fer était présent essentiellement dans le plus haut seuil de coupure entre 30 kDa et 0.2 µm. Cette fraction concentrait de nombreux éléments traces (Ti, V, Pb). Pédrot et al. (soumis, 2009b) ont également mis en évidence un relargage de fortes concentrations en fer dans ce même seuil de coupure par augmentation de pH due à la désorption, des solides du sol, d'une phase humique intimement associée à des nanoparticules de fer. De plus, Gaffney et al., (2008) ont demontré qu'un rapport (Fe/COD) élevé (de l'ordre de 1/3) permet la formation d'oxyhydroxydes de Fe de taille <0.2 µm, stabilisés par la matière organique. En fait, les substances humiques inhiberaient la formation des oxydes de fer mais permettraient la formation de nanoparticules de fer associées à la matière organique. Des observations par microscopie électronique à transmission (MET) conduites sur des échantillons d'eaux de rivières (Allard et al., 2004) et de solutions de sols soumis à des alternances redox (Thompson et al., 2006) confortent cette hypothèse.

Dans les sols naturels, les oxyhydroxydes de Fe sont souvent formés par oxydation-hydrolyse du Fe(II) en conditions biotiques ou abiotiques (Ehrenreich et Widdel, 1994; Emmerson et Moyer, 1997; Cornell et Schwertmann, 2003). Le Fe(II) provient de l'altération des roches et minéraux du sol ou est produit *in situ* par réduction microbienne de Fe(III)

(Todorova et al., 2005). Dans le cas des environnements temporairement anoxiques, certains microorganismes sont capables de réduire les oxyhydroxydes de fer par un processus de respiration dissimilatrice couplé à l'oxydation de la matière organique (donneur d'électrons) (Eq. 1) (Lovley et al., 1987; Lovley et Philipps, 1988; Roden et Lovley, 1993; Drever, 1997, Lovley, 2000, Zachara et al., 2001; 2002; Roden, 2006).

$$CH_2O + 4\ Fe(OH)_3 + 8\ H^+ \leftrightarrow CO_2 + 4\ Fe^{2+} + 11H_2O \qquad (1)$$

Cette réaction est réalisée grâce aux bactéries dites ferro-réductrices et dépend du type d'oxyde, de sa cristallinité et de son degré de substitution, les bactéries utilisant préférentiellement les oxyhydroxydes de fer mal cristallisés (lépidocrocite) aux formes plus cristallisées (goethite, hématite) (Lovley et Philips, 1986a; Ehrlich, 1990).

Les zones humides de bas de versant sont ainsi des zones propices à la fois à la réduction de Fe(III) mais aussi à la formation de colloïdes mixtes Fe-SH. Les zones humides allient, en effet, de fortes concentrations en Fe^{2+} et en concentrations en matières organiques (notamment SH) à des oscillations des conditions redox, liées à la submersion temporaire ou permanente des sols. Dans les zones humides, la source majeure de Fe (dans les horizons organiques) serait donc principalement constituée de colloïdes mixtes impliquant du Fe et de la matière organique. L'une des questions fondamentales posées par cette observation est de savoir si ce Fe colloïdal est la source Fe majoritairement impliquée dans le cycle du Fe dans les zones humides. Dans cette hypothèse, le stock de Fe cristallisé des sols n'est pas mobilisé.

L'objectif de la première partie de cette étude est donc de synthétiser des particules de fer (lépidocrocite) et des colloïdes mixtes (SH-nanooxydes de fer). Dans le but d'observer l'impact des SH sur la vitesse d'oxydation du Fe(II) et sur la nature et la taille des oxydes, une étude de la cinétique d'oxydation du Fe(II) en présence et absence de SH sera réalisée. L'hypothèse testée étant que les colloïdes mixtes ainsi formés pourraient concentrer une fraction importante du Fe dans l'horizon organique des zones humides. Ce piégeage du Fe dans la matrice organique influencerait la biodisponibilité du Fe pour les microorganismes, notamment dans les processus de réduction. La discussion des données expérimentales obtenues dans ce cadre fait l'objet de la première partie de ce chapitre intitulé 'Interactions fer – matière organique'.

L'objectif de la deuxième partie de cette étude est de tester la biodisponibilité lors de la réduction bactérienne de ces colloïdes mixtes Fe-SH, en comparaison à celle de colloïdes de fer. La présentation des résultats obtenus et leur discussion font l'objet de la deuxième partie de ce chapitre intitulé 'Biodisponibilité des nanoparticules de fer'.

II. Interactions fer – matière organique

L'objectif de cette étude était donc de fabriquer des colloïdes de fer (lépidocrocite) et des colloïdes mixtes (SH-nanooxydes de Fe) en suivant la cinétique d'oxydation du Fe(II) dans le but d'observer l'impact des SH sur la vitesse d'oxydation du Fe(II) et sur la nature et la taille des oxydes potentiellement formés. Ceci a consisté, à ajouter en condition oxique, du Fe^{2+} progressivement en présence ou non de substances humiques, en maintenant le pH à 6.5 par l'addition d'une solution de NaOH.

1. Matériels et méthodes

a. Synthèse des colloïdes de fer et des colloïdes mixtes SH-Fe

Une solution de Fe(II) à 261 $mg.L^{-1}$ a été préparée, à partir de $FeCl_2$, dans $9.3.10^{-4}$ M de HCl. La solution de Fe^{2+} a été ajoutée au cours du temps à une vitesse de 0.05 $mL.min^{-1}$, au moyen d'une burette automatique (Titrino 794, Metrohm), soit à une solution synthétique composée d'une solution de NaCl à 0.01 M préparée à partir d'eau désionisée (MilliQ system, Millipore^{TM}), soit à une solution colloïdale organique composée d'AH (60 $mg.L^{-1}$ de COD) ou d'AF (55 $mg.L^{-1}$ de COD), pour obtenir une solution finale à 18 $mg.L^{-1}$ de Fe. En parallèle, le pH a été continuellement maintenu à 6.5 par l'addition d'une solution de NaOH 0.01 M, par une seconde burette automatique programmée à un pH stationnaire de 6.5. La température a été maintenue à 25°C (±0.5) tout au long des expériences par l'utilisation d'un thermostat. Après la fin de l'addition de la solution Fe^{2+} (t = 7200 s), la solution Fe-matière organique a été laissée en contact avec l'atmosphère à pH 6.5 durant 9000 s, afin de déterminer la fin d'ajout de NaOH dans la solution et observer la remontée du potentiel redox. La synthèse des colloïdes de fer a été réalisée cinq fois et la synthèse des colloïdes mixtes a été tripliquée.

Les AH ont été obtenus à partir d'AH commerciaux Aldrich^{TM} (Aldrich^{TM}, H1, 675-2) extrais et purifiés suivant le protocole décrit par Vermeer et al. (1998). Les AH obtenus présentent la composition élémentaire suivante (en pourcentage massique) : C=55,8 %, O=38,9 %, H=4.6 %, N=0.6 % et possèdent une masse moléculaire moyenne de 23 kDa (Vermeer et al., 1998).

Les acides fulviques (AF) ont été obtenus à partir d'AF commerciaux standardisés (Elliot Soil, 3S102F, IHSS). Ils présentent la composition élémentaire suivante (en pourcentage massique) : C=49.8 %, O=44.3 %, H=4.3 %, N=3.2 %.

b. Analyses physico-chimiques

Durant la cinétique d'oxydation du Fe, deux échantillons ont été prélevés à t = 8200 s et t = 16000 s. Les échantillons ont été filtrés à 0.2 µm (Sartorius Minisart), puis un aliquote de ces échantillons a été ultrafiltré à 1 kDa à l'aide d'un système d'ultrafiltration (Model 8050, Millipore^{TM}) équipé d'une membrane de 1 kDa (Millipore^{TM}).

La concentration en carbone organique dissous a été mesurée au moyen d'un analyseur de carbone Shimadzu TOC-5050A. Les concentrations en Fe^{2+} et Fe^{3+} ont été mesurées selon la méthode colorimétrique à l'orthophénantroline 1.10 (ANFOR NF T90-017) (AFNOR, 1997). L'orthophénantroline forme avec le Fe(II) un complexe coloré stable qui empêche l'oxydation du Fe(II) en Fe(III). La concentration en Fe(II) a ensuite été déterminée par spectrophotométrie UV (UVIKON XS, Bio-Tek). Pour la mesure du Fe^{3+}, du chlorhydrate d'hydroxylamine (réducteur) a été ajouté afin de réduire le Fe^{3+} en Fe^{2+}. La concentration en Fe^{3+} est donc mesurée indirectement et correspond à la concentration en Fe_{tot} (Fe^{2+} + Fe^{3+} réduit en Fe^{2+}) soustraite de la concentration en Fe^{2+} mesurée.

Les concentrations en anions majeurs (Cl^-, SO_4^{2-} et NO_3^-) ont été mesurées par chromatographie ionique (Dionex DX120). Les concentrations en O_2 ont été suivies au moyen d'une électrode (Fisher Scientific Bioblock) au cours de trois cinétiques de synthèse de colloïdes de fer et deux cinétiques de synthèse de colloïdes Fe-matière organique Le potentiel redox a été suivi tout au long des cinétiques au moyen d'une électrode de Pt (Malter Pt 4805 DXK-S8/225). La mesure de potentiel redox a été corrigée par rapport à l'électrode normale à hydrogène à 25°C.

Lorsque les concentrations en Fe dissous étaient très basses, des mesures de Fe_{tot} ont été réalisées par ICP-MS (Agilent 4500), en utilisant l'indium comme standard interne. Un standard international (SLRS-4) a été utilisé pour vérifier la validité et la reproductibilité des résultats.

c. Cinétiques et stœchiométrie

La réaction d'oxydation/hydrolyse de Fe^{2+} est la suivante :

$$Fe^{2+} + 1/4\ O_2 + 2\ OH^- \rightarrow FeOOH + 1/2\ H_2O \quad (2)$$

À partir de cette équation (Eq. 2), il est possible de déterminer la vitesse de consommation des hydroxyles afin de déterminer la vitesse de la réaction d'oxydation/hydrolyse de Fe^{2+}. Cette vitesse v(t) est moyennée à chaque période de 200 s et calculée comme suit :

$$v(t) = (N(OH^-) - N(H^+)) / N(Fe^{2+}) \quad (3)$$

ou $N(H^+)$ et $N(OH^-)$ représentent le nombre de moles de H^+ et OH^- ajouté durant la période de 200 s considérée, et $N(Fe^{2+}) = 7.77*10^{-7}$ représente le nombre de moles de Fe^{2+} ajouté durant 200 s pour t < 7200 s. La stœchiométrie finale de la réaction est également calculée en utilisant le nombre d'OH^- ajoutés durant l'addition de Fe^{2+}, après soustraction de l'effet de l'acide déjà présent dans la solution de $FeCl_2$.

Dans un système où la réaction d'oxydation/hydrolyse de Fe^{2+} (Eq. 2) se produit, la stœchiométrie finale de la réaction devrait être égale à 2, et par conséquent si les ions Fe^{2+} introduits sont oxydés instantanément, v(t) est égal à 2.

d. Diffraction des rayons X (DRX) et microscopie à transmission électronique (MET)

Les colloïdes de fer synthétisés en conditions abiotiques ont été analysés par DRX afin de déterminer la nature des oxydes de fer formés. Ils ont été réalisés avec un diffractomètre Philips X'Pert diffractometer utilisant une source Cu opérant à 45 kV et 40 mA et un détecteur Kevex Si (Li). L'échantillon a été analysé en mode balayage à 0.04°/30s de 10° à 60° (2Θ). En fin d'expérience, plusieurs échantillons de colloïdes de Fe et de colloïdes mixtes Fe-AH ont été observés au microscope électronique à transmission Geol (voltage 120 kV). Les échantillons de colloïdes ont été directement déposés sur un film de carbone amorphe reposant lui-même sur une grille de Cu de 300 mesh (Oxford instrument, S162-3).

2. Résultats

a. Cinétique d'oxydation

Les concentrations en O_2 lors des différentes synthèses sont représentées sur la figure V. 1. Les concentrations en O_2 étaient de l'ordre de 8 $mg.L^{-1}$, ce qui est en accord avec la solubilité de l'oxygène dans l'eau à 25°C. Les fluctuations observées peuvent être attribuées à l'électrode et aux effets de matrice (les concentrations les plus basses étant enregistrées dans

les solutions de substances humiques). Cependant, les concentrations en O_2 sont toujours restées >5 $mg.L^{-1}$, indiquant un milieu oxique tout au long des expériences.

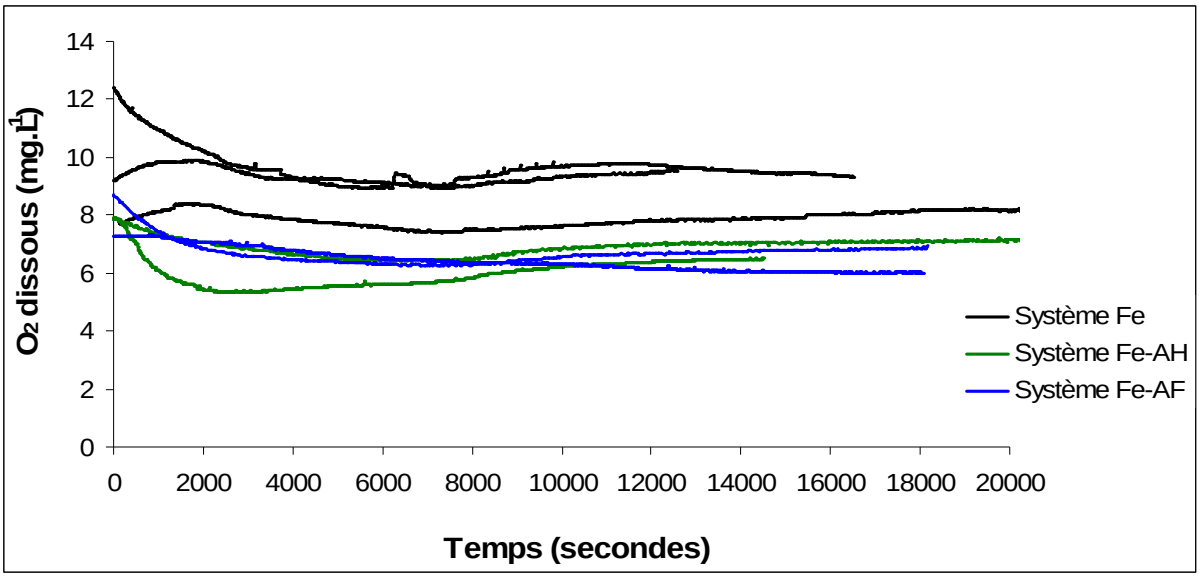

Figure V. 1. Concentration en O_2 en fonction du temps.

b. Cinétique d'oxydation/hydrolyse du Fe^{2+}

La figure V. 2 présente le suivi des volumes de NaOH ajoutés et du potentiel redox au cours de la cinétique d'oxydation/hydrolyse du Fe(II). Trois phases peuvent être observées :

- phase 1 : l'Eh chute très rapidement pour presque atteindre 250 mV, pour une faible quantité ajoutée de NaOH. Cette phase correspond à une augmentation de la concentration en Fe^{2+} dans la solution.
- phase 2 : l'Eh rebondit en concomitance avec une accélération du volume de NaOH ajouté. La vitesse d'ajout se stabilise et l'Eh re-diminue lentement. Cette phase correspond à la formation des oxydes de fer (réaction 2).
- phase 3 : lors de la fin de l'ajout de Fe^{2+} (7200 s), le volume de NaOH ajouté diminue fortement puis se stabilise pour atteindre en moyenne 6.41 ±0.08 ml en fin d'expérience. En parallèle, l'Eh remonte pour atteindre plus de 300 mV en fin d'expérience.

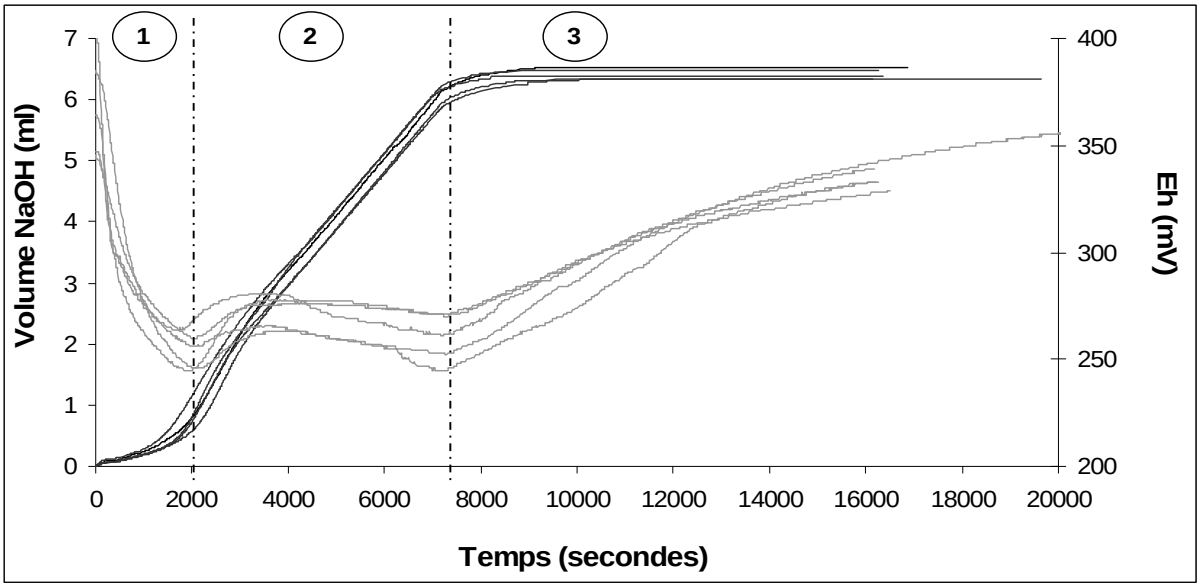

Figure V. 2. Volume de NaOH ajouté et potentiel redox au cours du temps. Les lignes noires correspondent aux volumes de NaOH ajoutés en ml et les lignes grises correspondent aux potentiels redox en mV. Les lignes verticales en pointillés délimitent les différentes phases observées.

c. Cinétique d'oxydation/hydrolyse du Fe^{2+} en présence de substances humiques

La figure V. 3 présente les cinétiques d'ajout de NaOH et de Eh pour les expériences en présence de substances humiques. Trois phases ont également été observées dans les cinétiques obtenues.

- la phase 1 : l'Eh est descendu très rapidement en parallèle à une faible quantité ajoutée de NaOH. Cette phase correspond à une augmentation de la concentration en Fe^{2+} dans la solution. Dans la solution d'AF, l'Eh diminue moins fortement et la quantité ajoutée de NaOH est plus élevée dès le début de l'expérience.

- la phase 2 : l'Eh continue de diminuer lentement alors que le volume ajouté de NaOH augmente.

- la phase 3 : lors de la fin de l'ajout de Fe^{2+} (7200 s), le volume de NaOH ajouté chute puis se stabilise pour atteindre 4.81 ±0.03 ml en moyenne en présence d'AH et 5.40 ±0.10 ml en présence d'AF. En parallèle, l'Eh remonte rapidement pour les AH et plus faiblement pour les AF.

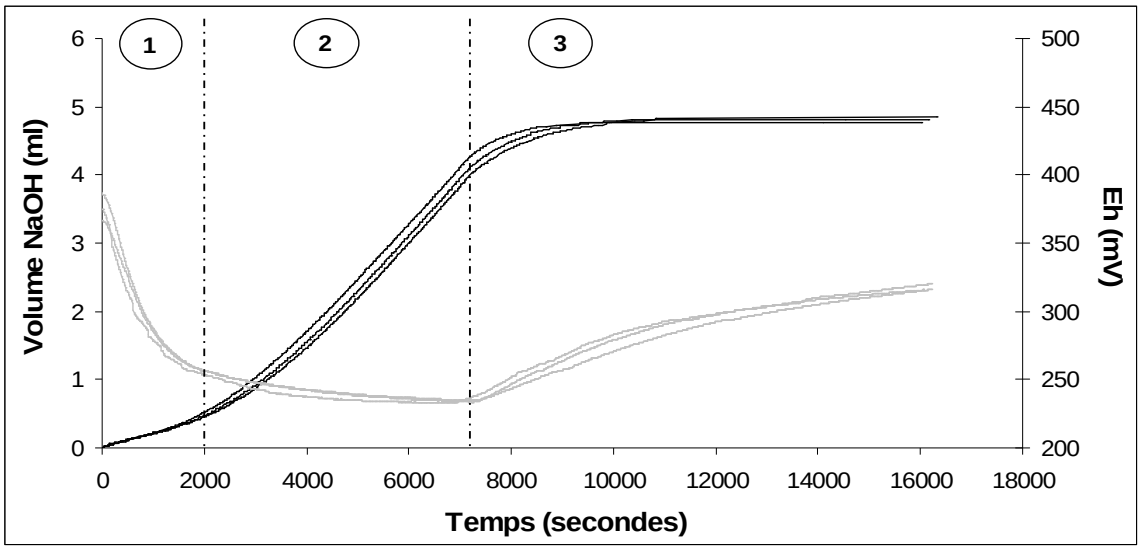

(a)

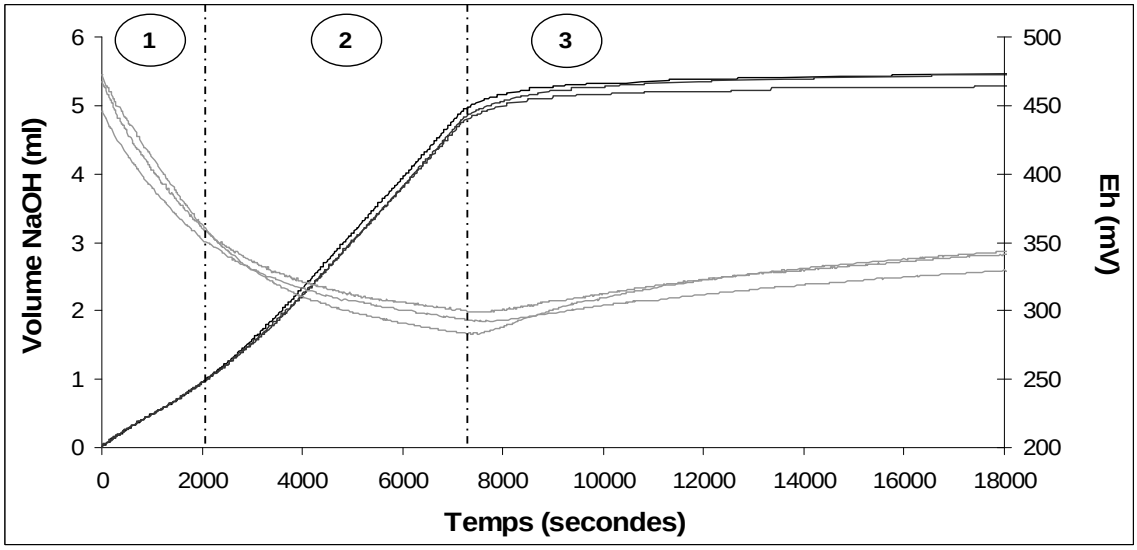

(b)

Figure V. 3. Volume de NaOH ajouté et potentiel redox au cours du temps pour les expériences avec AH (a) et les expériences avec AF (b). Les lignes noires correspondent aux volumes de NaOH ajoutés en ml et les lignes grises correspondent aux potentiels redox en mV. Les lignes verticales en pointillés délimitent les différentes phases observées.

d. Comparaison des cinétiques d'oxydation/hydrolyse du Fe^{2+} en présence ou non de substances humiques

L'observation des vitesses de consommation d'hydroxyles permet de montrer des différences entre les cinétiques d'oxydation/hydrolyse du Fe(II) en présence ou non de substances humiques (figure V. 4).

Durant la première phase (t <2000 s), v(t) est inférieure à la valeur de référence de 2. En absence de substances humiques, v(t) augmente rapidement pour atteindre 3.5 entre t = 2000 s et t = 4000 s. Ensuite, v(t) se stabilise à des valeurs proches de 2 à la fin de l'ajout de Fe^{2+} (t = 7200 s). Enfin, v(t) diminue rapidement pour atteindre une valeur <0.1 dès 9200 s.

En présence de substances humiques, entre t = 2000 s et t = 4000 s, v(t) augmente plus lentement et dépasse faiblement la valeur de référence de 2, pour ensuite fluctuer autour de cette valeur jusqu'à la fin de l'ajout de Fe^{2+} à t = 7200 s. Ensuite, v(t) diminue rapidement pour atteindre une valeur <0.1 dès 9200 s en présence d'AF et dès 11000 s en présence d'AH. La stœchiométrie finale de la synthèse des particules de Fe (FeOOH) atteint en moyenne 2.09, en absence de substances humique et elle est en moyenne de 1.73 et 1.52 en présence d'AF et d'AH respectivement. Ainsi, comme l'on peut l'observer sur la figure V. 4, une plus grande proportion de nanoparticules de Fe a été formée (d'après la réaction 2) en présence d'AF qu'en présence d'AH (concentration théorique en FeOOH de 18.9 $mg.L^{-1}$ sans substances humiques, 15.6 $mg.L^{-1}$ en présence d'AF et 13.7 $mg.L^{-1}$ en présence d'AH).

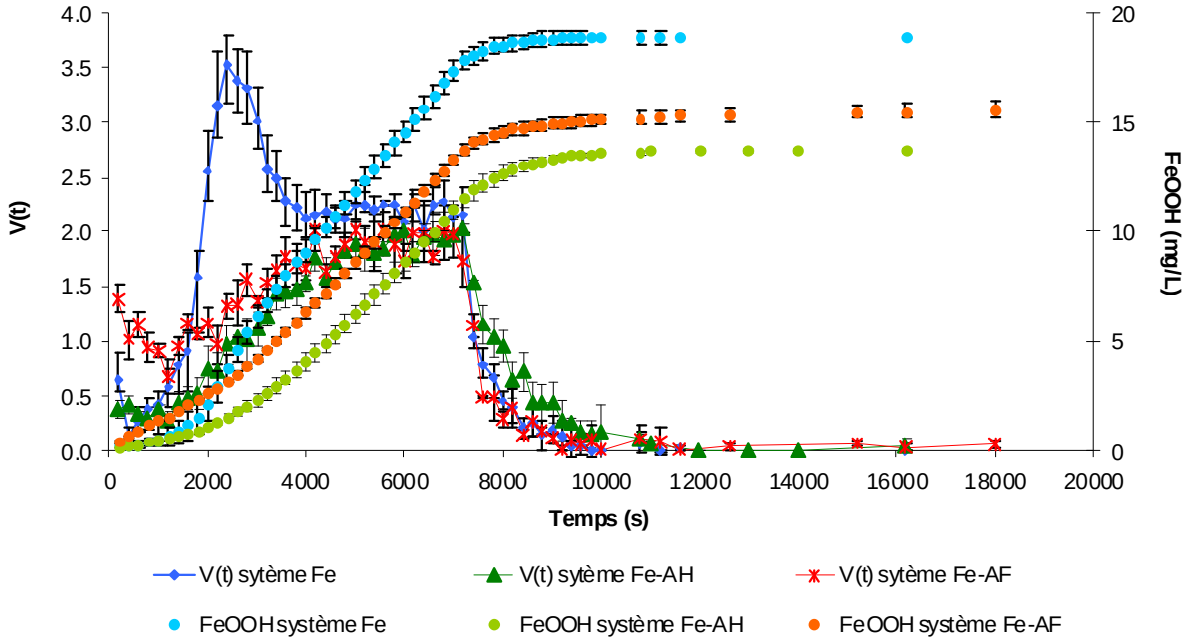

Figure V. 4. Cinétiques de consommation d'hydroxyles et de formation de FeOOH en absence et en présence de substances humiques.

e. Suivi des concentrations en Fe^{2+} et Fe^{3+}

À partir de t = 7200s, la concentration de Fe en solution devrait être approximativement de 18 $mg.L^{-1}$ dans les différentes expériences. Le tableau V.1. résume les concentrations en Fe(II) et en Fe(III) obtenues à t = 8200 s et t = 16000 s dans la phase dissoute (< 0.2 µm). Les données indiquent une absence de Fe ionique à t = 8200 s et une concentration inférieure aux limites de quantification de la méthode colorimétrique à t = 16000 s dans le système sans substances humiques. Pour les expériences Fe-SH, une ultrafiltration à 1 kDa a été réalisée pour déterminer la quantité de Fe libre. À t = 8200 s, les analyses des concentrations en Fe_{tot} <1 kDa ont du être réalisées par ICP-MS. En effet, les concentrations dans la fraction <1 kDa

étaient très faibles à t = 8200 s (< 1 $mg.L^{-1}$) et donc inférieures aux limites de quantification de la méthode colorimétrique à t = 16000 s. Le Fe mesuré dans la phase < 0.2 µm correspond donc au Fe lié aux substances humiques. Dans le système Fe-AH, les concentrations en Fe de la phase < 0.2 µm représente en moyenne 33 % à t = 8200 s (5.9 $mg.L^{-1}$ par rapport à 18 $mg.L^{-1}$ de référence) et 28 % à t = 16000 s dont 50 % sous forme Fe(II) et 50 % sous forme Fe(III). Ainsi, les concentrations diminuent sensiblement au cours de l'expérience mais la répartition Fe(II) - Fe(III) reste similaire.

Tableau V. 1. Valeurs des concentrations en Fe(II) et Fe_{tot} (Fe(II) + Fe(III)) en $mg.L^{-1}$ à t = 8200 s et t = 16000 s dans les différents systèmes expérimentaux.

		8200 s	16000 s	
Système Fe	Fe(II) <1 kDa	0.4 ± 0.2	< LQ	n = 5
	Fe(tot) <1 kDa	0.5 ± 0.1	< LQ	
	Fe(II) dissous	0.3 ± 0.1	< LQ	
	Fe(tot) dissous	0.6 ± 0.4	< LQ	
Système Fe - AH	Fe(II) <1 kDa	0.4 ± 0.3	< LQ	n = 3
	Fe(tot) <1 kDa	0.5 ± 0.1	< LQ	
	Fe(II) dissous	2.9 ± 0.4	2.4 ± 0.2	
	Fe(tot) dissous	5.9 ± 1	4.9 ± 0.9	
Système Fe - AF	Fe(II) <1 kDa	< LQ	< LQ	n = 3
	Fe(tot) <1 kDa	0.2 ± 0.1	< LQ	
	Fe(II) dissous	NA	NA	
	Fe(tot) dissous	3.9 ± 0.5	3 ± 0.3	

3. Discussion

a. Impact des substances humiques sur l'oxydation de Fe(II)

Dans le système sans substances humiques, la cinétique de consommation d'hydroxyles révèle un démarrage lent, en accord avec un pH légèrement acide et une absence de Fe dans la solution. Ainsi, comme l'indique la forte diminution de l'Eh durant les 2000 premières secondes, la solution s'est concentrée en ions Fe(II), n'oxydant qu'une faible partie des ions Fe^{2+} ajoutés. Puis à t = 2000 s, v(t) augmente fortement, dépassant largement la valeur de référence de 2 (Eq. 2), indiquant une accélération de l'oxydation des ions Fe^{2+} accumulés durant les 2000 premières secondes. Ce phénomène d'auto-accélération catalytique de l'oxydation des ions Fe^{2+} a déjà été observé antérieurement (Tamura et al., 1980; Tüfekci et Sarikaya, 1996; Fakih et al., 2008). Ce phénomène se produirait par la formation de nuclei d'oxyhydroxydes de Fe qui fourniraient les sites de surfaces favorables aux réactions auto-

catalytiques d'oxydation. Une étude récente a apporté la preuve d'un transfert d'électrons possible entre Fe(II) est Fe(III) au niveau de la surface de l'oxyde (Williams et Scherer, 2004). Ainsi, au cours de la croissance des oxyhydroxydes de Fe, les ions Fe^{2+} accumulés ont été rapidement consommés, comme le souligne le rebond de l'Eh. Ensuite l'Eh a diminué très lentement et v(t) s'est stabilisée à une valeur proche de 2 (Eq. 3) indiquant une oxydation rapide des ions Fe^{2+} à la surface des particules de Fe jusqu'à la fin de l'addition de $FeCl_2$ à t = 7200 s. Puis, une remontée de l'Eh a suivi, v(t) diminuant rapidement pour atteindre une valeur quasi-nulle à t = 9200 s, indiquant la fin de la réaction d'oxydation/hydrolyse.

En présence de substances humiques, l'évolution du volume de NaOH ajouté et de l'Eh sont sensiblement différentes. Des disparités entre les évolutions en présence d'AH et d'AF apparaissent également. Tout d'abord, la cinétique d'oxydation/hydrolyse de Fe(II) en présence d'AH démarre lentement, plus lentement que dans le système sans SH. A l'inverse, la cinétique d'oxydation/hydrolyse de Fe(II) en présence d'AF démarre plus rapidement avec un volume de NaOH ajouté plus important dès le début de l'expérience (Figures V. 2 et V. 3). Dans le système Fe-AF, moins d'ions Fe^{2+} s'accumulent donc alors que dans le système Fe-AH au contraire, les ions Fe^{2+} s'accumulent fortement. Durant cette première phase, l'Eh chute à des valeurs plus faibles en présence d'AH qu'en présence d'AF. Cependant dans les deux systèmes, l'effet auto-catalytique de l'oxydation et de l'hydrolyse du Fe est moins marqué. Ainsi, v(t) augmente linéairement pour atteindre péniblement l'équilibre stationnaire (valeur de 2) à la fin de l'ajout de $FeCl_2$ à t = 7200 s. Les mesures de l'Eh continuent à être en adéquation avec les vitesses de consommation d'hydroxyles. Le rebond de l'Eh en absence de SH ne se produit pas dans ces deux systèmes. Les processus de sorption et les réactions d'oxydation et d'hydrolyse de Fe conduisent à une stabilisation de Eh autour de 220 mV pour les AH et 250 mV pour les AF.

Les processus de sorption des ions Fe^{2+} et Fe^{3+} sur les groupements fonctionnels des SH ont ainsi ralenti la vitesse d'oxydation et réduit les réactions d'hydrolyse de Fe, ce qui explique des vitesses de consommation d'hydroxyles moins rapides et une vitesse stationnaire atteinte moins rapidement. Tout comme proposé par Fakih et al. (2008) dans une étude de la cinétique d'oxydation du Fe(II) en solutions concentrées de bactéries, les nuclei d'oxyhydroxydes formés durant la première phase (< 2000 s), qui induisent le phénomène autocatalytique, semble être moins réactifs et/ou moins facilement accessibles aux ions Fe libres pour leur hydrolyse, lorsqu'ils sont insérés dans la matrice humique.

b. Contrôle de la taille : particules-nanoparticules

Dans le système sans SH, la stœchiométrie finale de la réaction est de 2.09, en accord avec la formation d'un oxy-hydroxyde de Fe (Eq. 2). Les données montrent une absence de Fe dans la phase dissoute (< 0.2 µm) indiquant la formation d'oxydes de Fe. Les observations au MET des colloïdes de fer sont présentées sur la figure V. 5.

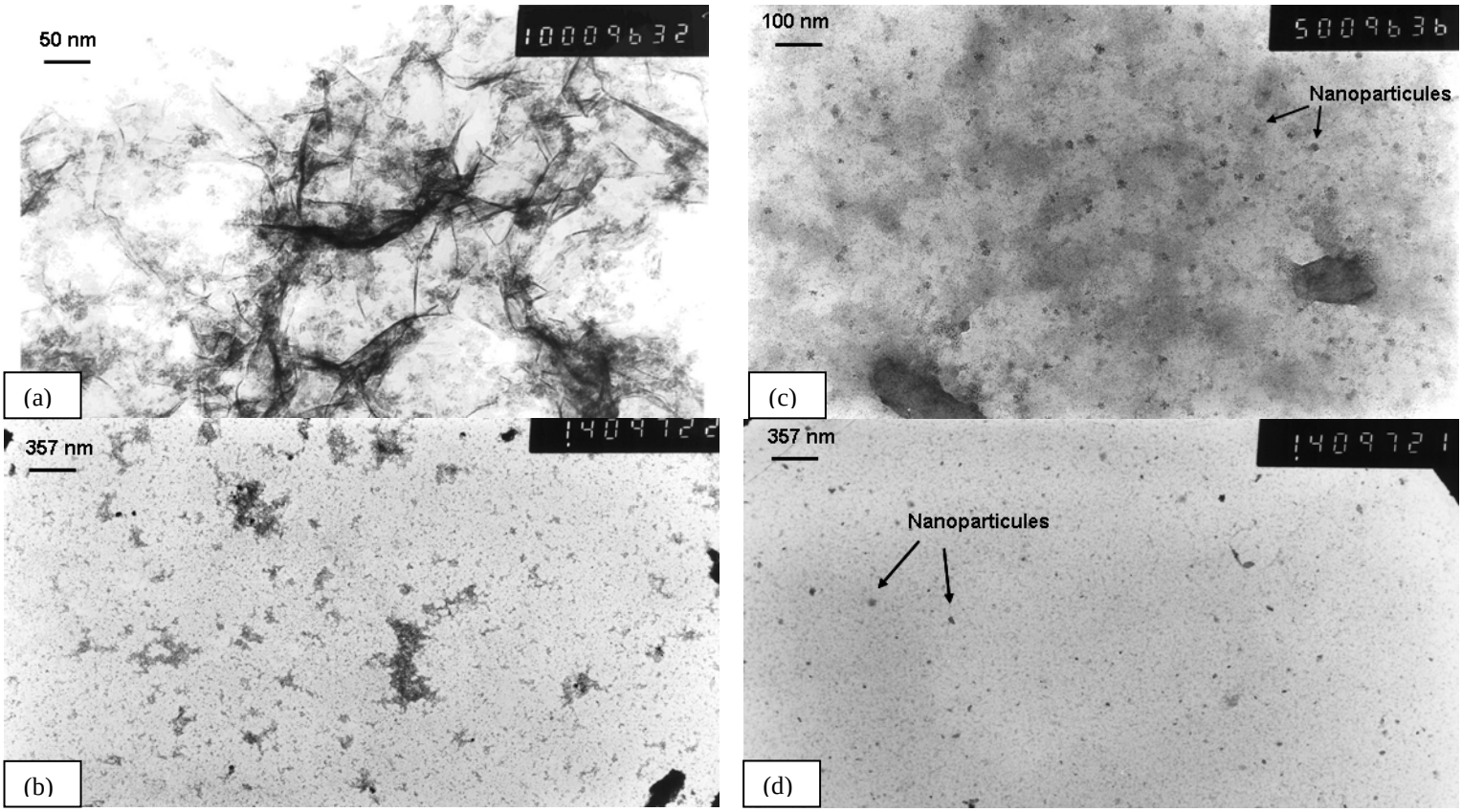

Figure V. 5. Photographie au MET de nano/particules de Fe : (a) et (b) solution Fe uniquement et (c) et (d) solution Fe-AH.

Les particules sont disposées en amas de feuilles fines agrégées dans des structures macroscopiques. La taille caractéristique de chaque amas est de 300 ±100 nm. En raison de leur très faible épaisseur, les particules ne sont pas complètement opaques aux électrons. De ce fait, de nombreuses "aiguilles" correspondant aux bords de particules sont observées dans la figure V. 5. La taille de ces "aiguilles" est de 120 ±50 nm de longueur et au maximum 10 nm de large. Ces résultats sont en accord avec d'autres observations réalisées dans une étude de cinétique d'oxydation du Fe^{2+} en présence de bactéries (Fakih et al., 2008). Les particules ont été identifiées par DRX comme étant de la lépidocrocite moyennement cristallisée (Figure V. 6). Des cristaux similaires de lépidocrocite ont déjà été observés dans des environnements

naturels, ou produits en laboratoire dans des conditions physico-chimiques similaires où les ions Fe^{2+} avaient été oxydés à pH neutre ou légèrement acide (Schwertmann et Taylor, 1979; Fortin et al., 1993; Châtellier et al., 2001; 2004).

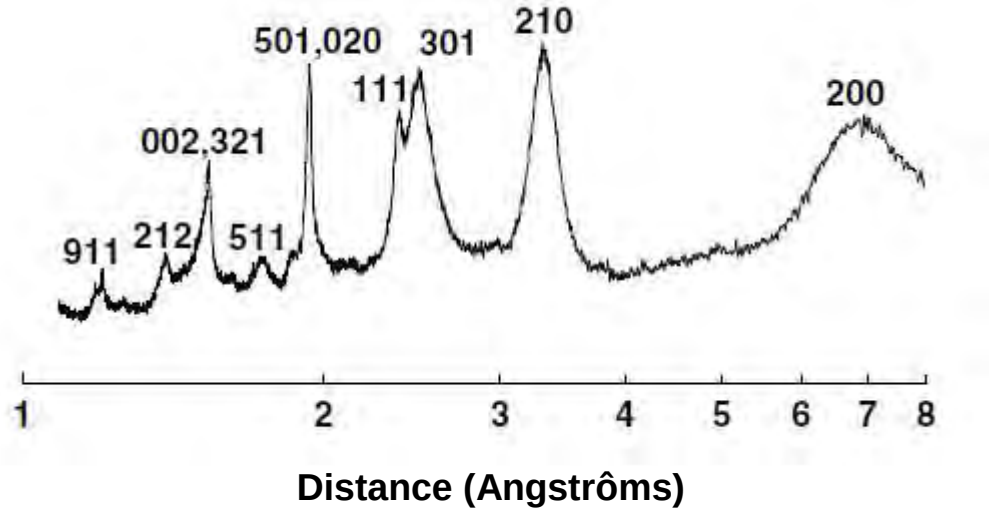

Figure V. 6. Spectre DRX des oxydes de Fe formés dans le système abiotique. L'identification des pics hkl correspond à celle de Cornell et Schwertmann (2003).

Dans le système Fe-SH, la stœchiométrie finale de la réaction est de 1.73 pour le système Fe-AF et 1.52 pour le système Fe-AH. La réaction d'oxydation/hydrolyse du Fe(II) reste donc incomplète. De plus, les AH semblent inhiber plus fortement la formation d'oxydes de Fe que les AF. Les concentrations en Fe^{2+} et Fe^{3+} mesurées dans la phase dissoute confirment le fait que les réactions sont incomplètes. Théoriquement, après l'ajout de $2.8.10^{-5}$ moles de Fe, la concentration en Fe devrait correspondre à 18 $mg.L^{-1}$ de FeOOH. Selon l'équation 2, la concentration en FeOOH en fin d'expérience est approximativement de 13.7 $mg.L^{-1}$ et de 15.6 $mg.L^{-1}$ dans le système Fe-AH et Fe-AF, respectivement. De plus dans le système Fe-AH, 28 % du Fe (4.9 ± 0.9 $mg.L^{-1}$) ne participent pas à la formation d'oxydes mais sont présents à 50 % sous forme Fe^{2+} et 50 % sous forme Fe^{3+} en fin d'expérience. Cette quantité ajoutée à la concentration théorique de formation de FeOOH (Eq. 2) indique une concentration totale de 18.6 $mg.L^{-1}$ correspondant à la concentration théorique de 18 $mg.L^{-1}$. Une proportion significative du Fe ne précipite donc pas sous forme d'oxyhydroxydes, mais est adsorbée à la surface des SH sous forme de Fe(II) et/ou Fe(III). Tipping et al. (2002) a montré grâce à la modélisation que la concentration maximale de Fe(III) adsorbable à la surface des SH était de l'ordre de 1.10^{-4} $mol.g^{-1}$ de C à pH 7, soit pour notre étude une concentration théorique qui devrait être de 6.10^{-6} mol de Fe pour 56.8 $mg.L^{-1}$ de COD (concentration atteinte en fin d'expérience). Or la concentration de Fe atteint $7.57.10^{-6}$ mol de Fe. Cette concentration est

proche de la valeur maximale de sorption déterminée par Tipping et al. (2002). Ce Fe adsorbé aux SH ne participe pas à la formation d'oxyhydroxydes car la réaction d'hydrolyse est inopérante si le Fe est complexé. En effet, le complexe Fe-ligand doit se dissocier pour qu'une réaction de coordination ait lieu avec un ligand OH^- (Rose et Waite, 2002). Ainsi, comme suggéré par Pullin et Cabaniss (2003), la matière organique ralentit et diminue la formation de particules de Fe en stabilisant une fraction du Fe par complexation.

Des observations au MET du système Fe-AH ont été réalisées (Figure V. 5). Les observations suggèrent la formation de nanoparticules de Fe réparties de manière diffuse au sein de la matrice humique. La taille des nanoparticules est en moyenne de 30 ±15 nm, de forme sphérique majoritairement. Les nanoparticules de Fe sont ainsi très peu développées et piégées dans la matrice organique formant un réseau Fe-Matière organique comme précédemment suggéré par Perret et al. (1994) et Taillefert et al. (2000). Comme montré par Gaffney et al. (2008) la matière organique joue donc un rôle clé dans la croissance-développement des cristaux d'oxyhydroxydes de Fe en inhibant leur développement. D'après une récente étude de Baalousha (2009) sur l'impact de la matière organique sur l'agrégation et la désagrégation des nanoparticules de Fe, la matière organique à forte concentration (rapport AH/Fe > 0.5) induirait la désagrégation ou inhiberait l'agrégation des nanoparticules de Fe en fonction des conditions physico-chimiques. Le processus serait produit par l'augmentation de la charge de surface induite par la sorption des molécules humiques. Ainsi, dans cette étude, une partie du Fe(II) apporté serait tout d'abord complexée, puis les premiers nuclei d'hydroxyles se formeraient. Cependant, la présence des SH ne permettrait pas ou peu l'agrégation de particules de Fe par augmentation significative des forces de répulsion entre elles. Il en résulterait la formation de nombreux amas diffus dans la matrice organique. À l'inverse, dans une matrice ne contenant pas de SH, le pHzpc (zéro point charge) étant proche du pH du milieu (pHzpc = 6-8), peu de forces de répulsion existent entre les nanoparticules ce qui facilite la formation d'amas de taille micrométrique.

4. Conclusions

Les SH influent sur l'oxydation et l'hydrolyse du Fe puisque :

- (1) elles diminuent et ralentissent l'oxydation du Fe(II) en stabilisant une fraction du Fe par complexation
- (2) elles inhibent le développement des particules d'oxyhydroxyde de Fe, en réduisant la taille de ces particules à l'échelle du nanomètre et en inhibant leur agrégation.

En contrôlant la taille des particules formées, les SH agissent indirectement sur la mobilité des oxydes de fer et des éléments traces associés, en les rendant plus mobiles. De récentes études sur des solutions de sols ou des eaux de surface montrent le rôle, parfois majeur, joué par des phases ferriques colloïdales sur la mobilisation d'éléments traces (Pokrovsky et Schott, 2002; Lyvén et al., 2003; Pokrovsky et al., 2006, Dahlqvist et al., 2007; Pédrot et al., 2008; soumis 2009b).

De plus, la sorption d'ions Fe(II) par la matière organique pourrait ainsi favoriser la sous-estimation de la réactivité du Fe dans les processus de mobilisation des éléments ou encore surestimer le potentiel de sorption d'éléments lors de modélisation si l'analyse des concentrations de Fe(II) n'était pas réalisée. La fraction complexée (Fe^{2+} et Fe^{3+}) est probablement biologiquement disponible pour les organismes. En effet, des études ont montré la capacité des substances humiques à réduire le Fe(III) complexé régénérant du Fe(II) biodisponible lors de processus de réduction abiotique photochimique ou non-photochimique (Voelker et Sulzberger, 1996; Voelker et al., 1997; Rose et Waite, 2002; Pullin et Cabaniss, 2003a). À l'inverse, la production de Fe(II) par ces processus environnementaux peut éventuellement permettre la formation de nanoparticules de Fe (Pullin et Cabaniss, 2003b).

III. Biodisponibilité des nanoparticules de fer

1. Le contexte

Précédemment, il a été montré que la présence de substances humiques agit sur l'oxydation du Fe(II) et la nature des particules de Fe en résultant. Les substances humiques inhibent, en effet, la formation des oxydes de Fe et induisent, par contre, la formation de nanoparticules sphériques (30 ±15 nm de diamètre) de Fe diffuses dans la matrice humique. Les colloïdes mixtes ainsi formés peuvent ainsi concentrer une fraction importante du Fe dans les zones humides. De plus, ce Fe colloïdal, amorphe, développant de grandes surfaces spécifiques est probablement plus réactif et biodisponible que les oxydes de Fe bien cristallisés conservés dans ces mêmes zones humides. La question se pose donc de savoir si les bactéries ferro-réductrices sont capables ou non d'utiliser le Fe colloïdal inclus dans des matrices organiques est de déterminer quelle peut être la bioréductibilité des ces nanoparticules comparée à celle d'oxyhydroxydes formés dans un contexte dépourvu de substances humiques.

L'objectif de cette partie est donc de déterminer la capacité de ces nanoparticules de Fe incluses dans une matrice organique à être utilisées comme accepteur d'électrons par une espèce de bactérie ferro-réductrice, *Shewanella putrefaciens*. Des expériences de bioréduction de suspensions de Fe(III) présent sous forme particulaire (lépidocrocite) et sous forme de colloïdes mixtes Fe-AH ont donc été réalisées pour apporter des éléments de réponse à ces questions.

2. *Matériels et méthodes*

a. Synthèse des colloïdes de fer et des colloïdes mixtes AH-Fe

Les colloïdes de Fe et les colloïdes mixtes AH-Fe ont été synthétisés en suivant le protocole décrit dans la première partie de ce chapitre. Le rapport Fe/AH est approximativement de 1/3 avec une concentration finale de 56.8 $mg.L^{-1}$ de COD et une concentration en Fe de 18 $mg.L^{-1}$.

b. Culture bactérienne

1. Choix de la bactérie Shewanella putrefaciens

Shewanella putrefaciens est une bactérie déjà très largement étudiée (Lovley et al., 1996 ; Ona-Nguema et al., 2000 ; Roden, 2003) en raison de ses capacités à réduire le Fe(III) en milieu anaérobie. De plus, aéobie-tolérante, sa culture peut être réalisée en milieu aérobie, à pH neutre et température ambiante (croissance optimale entre 25°C et 35°C). La souche utilisée dans cette étude provient de la collection du Centre de Ressources Biologiques de l'Institut Pasteur (CIP 80.40, équivalence ATCC 8071).

2. Culture

Dans un premier temps, les bactéries ont été cultivées sur plaque d'Agar 24h à 30°C. Ensuite, 100 ml de milieu de pré-culture liquide 'Luria Bertani Broth' ($20g.L^{-1}$) ont été inoculés et placés dans un incubateur (Ecotron HT) à 25°C pendant 24h sous agitation constante (130 $tr.min^{-1}$). Dans une troisième étape, 10 ml de cette pré-culture ont été à nouveau inoculés dans 1L du même milieu de culture et incubés dans les mêmes conditions pendant 24 h. Ces 24 h correspondent à l'optimum de croissances des bactéries. Les bactéries ont ensuite été lavées 3 fois avec le milieu réactionnel de l'expérience de bio-réduction du

Fe(III) puis centrifugées à 4°C et 7500 tr.min^{-1}. Le culot bactérien a ensuite été re-dilué dans environ 100 ml de milieu réactionnel.

3. Évaluation de la concentration bactérienne

De manière à connaître les quantités bactériennes inoculées, des mesures de densité optique, à λ=600nm, ont été réalisées. La concentration bactérienne de la solution initiale a été estimée en effectuant une mesure du poids sec. Pour cela, 10ml de solution bactérienne du milieu de pré-culture ont été lavés 3 fois avec de l'eau distillée ultra-pure par centrifugation, puis repris dans de l'eau distillée ultra-pure et séchés dans une étuve à 70°C pendant une semaine. En estimant le poids d'une bactérie à 7.10^{-13}g (Claessens et al. 2006), il a alors été possible de calculer la concentration bactérienne et de réaliser une gamme de concentrations en fonction de la valeur de la densité optique mesurée.

c. Principe expérimental

Afin de comparer les cinétiques de réduction de la lépidocrocite et des colloïdes Fe-AH, il était impératif de débuter les expériences avec les mêmes concentrations en Fe et bactéries. La concentration en Fe a été fixée à 18mg.L^{-1} et celle des bactéries à 3,8.10^{7} cellules.ml^{-1}. La lépidocrocite ou les colloïdes Fe-AH ainsi que les bactéries ont été inoculés dans un milieu réactionnel composé de : 10mM de lactate de sodium (donneur d'électrons), 10 mM de tampon HEPES (tampon pH), 28mM de NH_4Cl et 1 mM de CaCl dihydraté (Hyacinthe et al., 2008). Les suspensions ainsi préparées ont ensuite été placées en chambre anaérobie pour maintenir les conditions d'anaérobiose nécessaires à la réduction du Fe.

d. Analyses physico-chimiques

Durant les cinétiques de réduction du Fe, plusieurs échantillons ont été prélevés et ont été filtrés à 0.2 µm au moyen de filtres en acétate de cellulose (Sartorius Minisart). Les concentrations en Fe^{2+} et Fe^{3+} ont été mesurées selon la méthode colorimétrique à l'orthophénantroline 1.10 (ANFOR NF T90-017) (AFNOR, 1997) (cf. partie I).

Les concentrations en O_2 ont été suivies au moyen d'une électrode (Fisher Scientific Bioblock) durant les cinétiques de réduction du Fe(III). Le potentiel redox a été suivi tout au long des cinétiques au moyen d'une électrode Eh (Schott Platin Elektrode BlueLine 31 RX).

La mesure de potentiel redox a été corrigée par rapport à l'électrode normale à hydrogène à 25°C.

3. Résultats

L'évolution des concentrations en Fe(II) et Fe total de la phase dissoute en fonction du temps est reportée sur la figure V. 7.

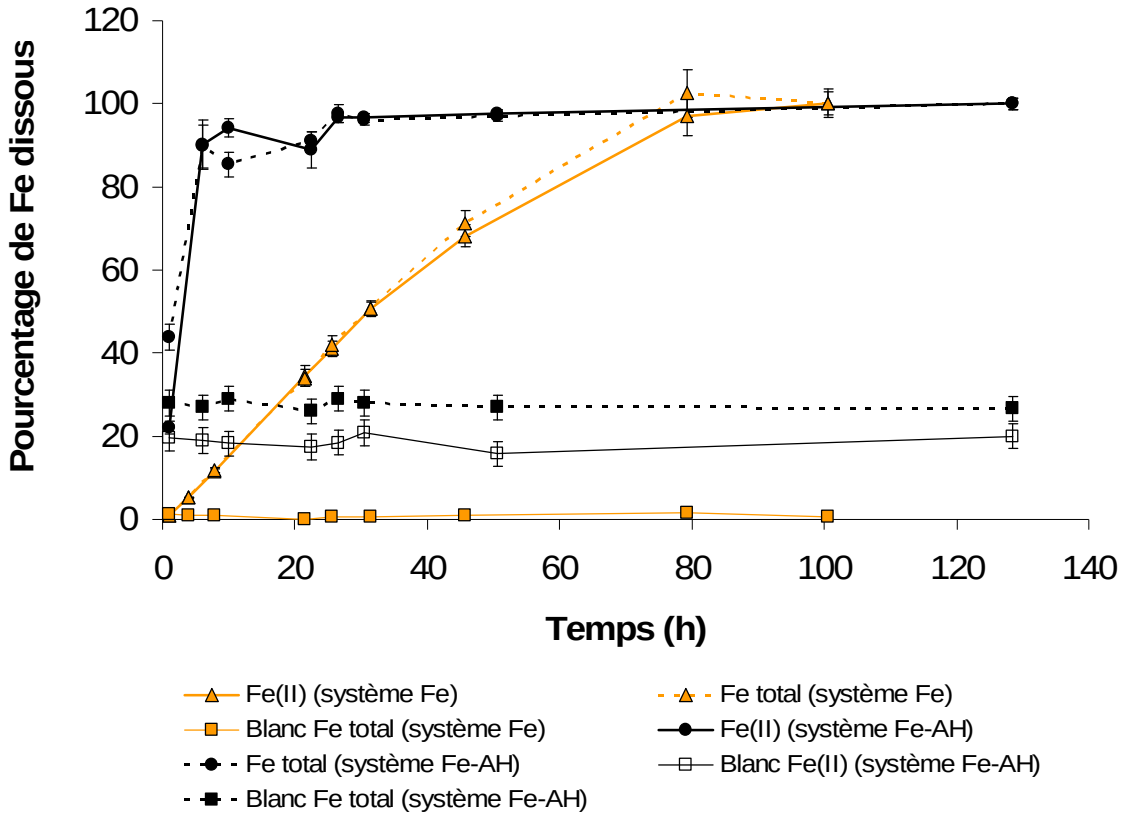

Figure V. 7. Pourcentage de Fe(II) et Fe_{tot} solubilisé en fonction du temps par bioréduction de lépidocrocite (Système Fe) et de colloïdes Fe-AH (Système Fe-AH).

Les concentrations mesurées en Fe(II) sont similaires aux concentrations en Fe_{tot}, indiquant que le Fe est sous forme de Fe^{2+} dans la solution. Dans les cinétiques de contrôle en absence de bactéries, les concentrations en Fe_{tot} dans la phase dissoute sont nulles dans le système sans acides humiques, et sont approximativement de 5,3 $mg.L^{-1}$ de Fe en présence de substances humiques dès le début de l'expérience, restant stables tout au long de l'expérience. Dans le système biotique Fe et Fe-AH, les cinétiques de réductions peuvent être découpées en 3 phases : (a) une phase rapide de réduction du Fe(III) (0,28 $mg.L^{-1}.h^{-1}$ sur les 40 premières heures pour la lépidocrocite et 2.12 $mg.L^{-1}.h^{-1}$ sur les 6 premières heures pour les colloïdes

Fe-MO), (b) une phase de réduction un peu plus lente (0,18 $mg.L^{-1}.h^{-1}$, de 40 h à 80 h pour la lépidocrocite et 0,06 $mg.L^{-1}.h^{-1}$ de 6 h à 30 h pour les colloïdes Fe-MO), et (c) l'atteinte d'un plateau correspondant à la réduction totale du Fe(III) initial. Ainsi, la cinétique de réduction des colloïdes Fe-MO est beaucoup plus rapide que celle de la lépidocrocite. En effet, 90 % du Fe(III) des colloïdes Fe-MO ont été réduits en 8 h par les bactéries, alors qu'il faut approximativement 70 h dans le système Fe pour atteindre ce niveau de solubilisation.

4. Discussion

a. Réduction abiotique

En absence d'acides humiques et de bactéries, la réduction du Fe est inopérante. En condition abiotique mais en présence d'acides humiques, la concentration en Fe, de 3.4 ±0.3 $mg.L^{-1}$ de Fe^{2+} et de 5.3 ±0.4 $mg.L^{-1}$ de Fe_{tot}, est constante tout au long de l'expérience. Lors de la précédente étude sur la cinétique d'oxydation du Fe^{2+} en présence de substances humiques (voir ci-dessus la première partie du chapitre), 4.9 ±0.9 $mg.L^{-1}$ de Fe était sous forme d'ions complexés aux acides humiques. Ainsi, la quantité de Fe ionique complexé aux AH reste égale à la concentration de Fe ionique initial complexé aux substances humiques. De plus, cette concentration stable tout au long de l'expérience indique qu'aucune réaction de réduction ne s'est produite.

b. Réduction biotique

En présence de bactéries, le Fe à la fois sous forme particulaire ou inséré dans des colloïdes mixtes Fe-AH, a été réduit à 100 %. Les bactéries ont donc permis la bioréduction totale du Fe(III) dans ces expériences.

Cependant, en absence d'acides humiques, la vitesse de réduction est plus faible, 100 % du Fe(III) est réduit en 80 h contre 10 h en présence d'acides humiques. En appliquant une cinétique réactionnelle de pseudo 1er ordre, la constante de vitesse (k) de réduction de Fe(III) est de $k = 6.10^{-4}$ min^{-1} pour le système Fe seul (80 h) et de $k = 4{,}9.10^{-3}$ min^{-1} pour le système Fe-AH (10 h). Chen et al. (2003) ont estimé des constantes de vitesse de réduction de Fe(III) par *Schewanella putrefaciens* en présence de différentes substances organiques. Ces valeurs fluctuent entre $2{,}3.10^{-3}$ min^{-1} et $6{,}2.10^{-2}$ min^{-1} respectivement pour une matière organique faiblement aromatique (<15 %) et des acides humiques de sol (>40 % d'aromaticité). Ces

valeurs sont donc proches des valeurs de la littérature. L'écart observé pour les acides humiques peut être expliqué par la différence de concentration bactérienne entre notre étude $3.7*10^7$ cellules.ml^{-1} et celle de Chen et al. (2003), 10^8 cellules.ml^{-1}. Les nanoparticules de Fe piégées dans les colloïdes mixtes Fe-AH sont donc réduites plus rapidement et donc plus facilement que les particules de lépidocrocite.

Plusieurs études ont montré que la matière organique naturelle favorisait la bioréduction du Fe pour des pH neutres à légèrement acides (Lovley et al., 1996; Royer et al., 2002; Chen, 2003). De plus, les bactéries ferro-réductrices réduisent plus rapidement les oxydes de Fe amorphes et le Fe(III) contenus dans les argiles que les oxydes de fer cristallisés (Lovley et Phillips, 1986 ; Roden et Zachara, 1996 ; Kostka et al., 1999 ; Roden, 2003 ; Royer et al., 2004). Les différences de vitesses de réduction entre le système Fe et Fe-AH peuvent être expliquées par plusieurs éléments :

(a) Roden et Zachara (1996) et Royer et al. (2002) ont démontré que le Fe^{2+} issu des réactions de bioréduction se réabsorbait massivement à la surface des oxydes de Fe. Cette réabsorption induit un ralentissement, voire un arrêt de la réduction microbienne. En présence de substances humiques, une partie des ions Fe^{2+} produits par la bioréduction est complexée par les groupements fonctionnels de surface des acides humiques ; ce qui limite fortement leur réabsorption sur les sites réactifs des oxydes.

(b) Dans les colloïdes mixtes Fe-AH, une partie du Fe(III) se trouve sous forme ionique complexée. Or, ce Fe est facilement utilisable (Urrutia et al., 1999), notamment en début d'expérience, ce qui explique les fortes concentrations en Fe de la phase <0.2 µm dès les premières heures de début de l'expérience.

(c) La chute de la vitesse de réduction peut également provenir des différences intrinsèques entre les particules de Fe. De récentes études soulignent en effet, que même si la vitesse de dissolution des oxydes de Fe (ou la vitesse de réduction) n'apparaît pas contrôlée par la réactivité chimique intrinsèque du minéral (comme ses propriétés thermodynamiques liées à la cristallinité) (Roden, 2003 ; Taillefert et al., 2007), elle serait plutôt liée à la surface spécifique développée par l'oxyhydroxyde. En effet, la réaction chimique de réduction serait fortement affectée par le nombre de sites de surface réactifs (Taillefert et al., 2007). Ainsi, le Fe(III) de la lépidocrocite, disposant d'une plus faible surface spécifique en formant notamment de petits agrégats micrométriques, serait moins bioréductible. La taille, la forme et la densité de l'oxyhydroxyde, influencées par la présence d'acides humiques lors de sa formation seraient donc des facteurs de contrôle de sa vitesse de réduction, gouvernant la 'zone de surface' bioréductible (Bonneville et al., 2006).

Le contact entre la bactérie et la surface de l'oxyde est en effet primordial dans le processus de réduction. La réduction des oxyhydroxydes de Fe par *Shewanella putrefaciens* se produit en majorité par un transfert d'électrons à l'interface minéral/membrane cellulaire (Das et Caccavo, 2000; Bonneville et al., 2004) et demande ainsi une adhésion à la surface de l'oxyhydroxyde. En présence de substances humiques, le transfert d'électrons nécessaire à la réduction de Fe(III) pourrait être assuré par les substances humiques elles-mêmes. Lovley et al. (1996) a proposé que les substances humiques agissent comme transporteur d'électrons entre les microorganismes et le Fe(III). Ce processus utiliserait comme ponts électroniques, soit les groupements fonctionnels quinoniques (Lovley et al., 1996; Scott et al., 1998), soit les groupements aromatiques et polyphénoliques des substances humiques (Chen et al., 2003). Ces groupements fonctionnels seraient réduits temporairement en effectuant le transport de l'électron jusqu'au Fe(III) qui serait l'accepteur final de l'électron. Le mécanisme proposé autoriserait ainsi le transfert d'électrons sans la nécessité d'un contact direct entre la membrane cellulaire et l'oxyde. Ceci augmenterait ainsi considérablement la vitesse de réduction et l'étendue de la zone de réduction par cellule en se dispensant du besoin d'un contact direct entre le Fe(III) et la membrane cellulaire.

5. Conclusion

La capacité des nanoparticules de Fe, incluses dans des colloïdes mixtes Fe-SH, à être utilisées comme accepteur d'électrons a été démontrée dans cette étude expérimentale. Les colloïdes mixtes Fe-AH sont réduits environ 10 fois plus rapidement que les nanoparticules de Fe de lépidocrocite agrégées. Ces résultats démontrent une bioréductibilité plus importante des nanoparticules de Fe en présence de substances humiques. Cette augmentation de la bioréductibilité semble être liée à la présence d'acides humiques qui (a) indirectement contrôleraient la taille, forme et densité des oxyhydroxydes (voir chapitre V, I) et (b) adsorberaient directement le Fe sous forme Fe^{2+} et Fe^{3+} et favoriseraient le transfert d'électrons entre la cellule bactérienne et le Fe(III) en jouant le rôle de ponts électroniques.

IV. Conclusion

Les travaux décrits dans ce chapitre confortent l'importance majeure de la formation de colloïdes mixtes Fe-SH dans les environnements de surface, notamment dans les milieux riches en matière organique, soumis à des alternances de conditions redox. Les expérimentations conduites dans cette étude ont montré qu'en l'absence de SH, les particules

de Fe formées étaient de la nano-lépidocrocite qui s'agrège en amas de taille micrométrique. Il a aussi été établi qu'en présence de SH, l'accélération auto-catalytique de la formation d'oxydes était fortement ralentie. Les particules de Fe ainsi formées sont de taille nanométrique, insérées de manière diffuse dans la matrice humique. De plus, dans ce cas, une fraction du fer ne participe pas à la formation de nanoparticules par la formation de complexes SH-Fe(II) et SH-Fe(III), notamment dans le système incluant des AH. Les SH tendent donc ainsi à ralentir et diminuer l'amplitude des réactions d'oxydation-hydrolyse du Fe, et impactent directement la taille des oxydes de fer formés en inhibant le développement des nuclei d'hydroxydes formés et en diminuant les phénomènes d'agrégation des nanoparticules de Fe.

Lors d'expériences de réductions biotiques par les bactéries ferro-réductrices *Schewanella putrefaciens*, la biodisponibilité de ces nanoparticules de Fe à être utilisées comme accepteur d'électrons a ensuite été testée en comparaison avec celle de particules de lépidocrocite formées en absence de substances humiques. Les résultats ont montré une cinétique de bioréduction 10 fois plus rapides avec les nanoparticules de Fe incluses dans des colloïdes mixtes SH-Fe qu'avec des nanoparticules de Fe en contexte inorganique. Ces résultats suggèrent donc une biodisponibilité accrue des nanoparticules de Fe pour la réduction, liée à la présence d'acides humiques qui contrôlent (1) indirectement la taille, forme et densité des oxyhydroxydes formés, et (2) directement la capacité des acides humiques à adsorber le Fe sous forme Fe^{2+} et Fe^{3+} et le transfert d'électrons entre la cellule bactérienne et le Fe(III) par la présence de groupements fonctionnels jouant le rôle de ponts électroniques.

Ces résultats nous engagent à porter un intérêt encore plus vif aux zones de bas de versant. En effet, ces zones, outre le fait d'être siège de dynamiques redox importantes, impliquant éléments métalliques et matière organique, et d'activité bactérienne intense, sont des zones majeures de production de colloïdes mixtes Fe-matière organique, de par la proximité de la surface de la zone de battement de la nappe. Le potentiel redox y fluctue selon la fréquence des oscillations de la nappe et la durée de la saturation hydrique du sol. De plus, 70 à 90 % du COD présent dans les zones humides sont représentés par les substances humiques (Thurman, 1985). Ainsi, ces zones représentent de véritables réacteurs biogéochimiques où les réactions d'oxydation/hydrolyse et formation de colloïdes mixtes SH-Fe sont catalysées et amplifiées. Ces zones en étant soumises à des changements fréquents des paramètres physico-chimiques, liés aux changements de l'état de saturation hydrique du sol notamment, représentent aussi des zones privilégiées de libération de colloïdes et d'éléments

associés. La libération de colloïdes mobiles dans les sols et les eaux souterraines étant majoritairement induite par des changements dans la chimie de la solution. Ces zones sont par conséquent les plus susceptibles d'être le siège de fabrication et de libération de ces nanoparticules colloïdales dans les eaux de surface. Ceci suggère l'importance de futures investigations dans ces zones pour déterminer jusqu'à quel point les colloïdes organiques peuvent être un facteur de contrôle prédominant de la mobilité du Fe, notamment au travers de la genèse et de la capacité de sorption de ces nanoparticules vis-à-vis du Fe(II). En effet, une forte proportion de Fe lié à des SH sous la forme Fe(II) (> 20 % du Fe total lié) a déjà été observée dans le milieu naturel (Gaffney et al., 2008) comme observée dans cette étude.

Conclusions Générales et Perspectives

I. Conclusions

1. Principaux résultats

Les différents travaux ont permis d'apporter de nombreux éléments de réponse quant au rôle des colloïdes dans la mobilisation des éléments traces. Cette étude a permis : a) de décrire le rôle des colloïdes dans la mobilisation des éléments traces dans des zones de haute production de nanoparticules que sont les zones humides et b) de déterminer la nature des colloïdes porteurs et vecteurs d'éléments traces dans ces zones humides. Dans le chapitre II, il a été démontré à partir d'expériences de lixiviation de sol que les éléments traces ont un comportement variable entre eux vis-à-vis des colloïdes. Certains éléments sont fortement complexés par le compartiment colloïdal (Al, Cr, U, Mo, Pb, Ti, Th, Fe, et les REE), d'autres apparaissent plus modérément complexés (Cu, Cd, Co, et le Ni) alors qu'une autre partie de ces éléments n'interagit pas avec les colloïdes (Li, B, K, Na, Rb, Si, Mg, Sr, Ca, Mn, Ba et le V). Les colloïdes complexants sont représentés en majorité par des acides humiques riches en nanoparticules de Fe. Ce fer colloïdal mobilise une fraction importante du Pb, Ti, et U. Ainsi, les acides humiques permettent directement ou indirectement le transport colloïdal de nombreux éléments traces, par complexation directe ou indirecte en stabilisant la phase porteuse ferrique Enfin, ces données expérimentales ont montré que les REE, essentiellement mobilisées par les acides humiques, présentent un spectre de concentrations de forme concave, spécifique de leur complexation par les substances humiques (SH) qui exercent donc un contrôle majeur sur leur spéciation et fractionnement. De plus, la distribution des REE dans les environnements organiques est fortement influencé par le rapport Substances Humiques/Métaux (mol/mol), paramètre clé de contrôle de la forme de leur spectre.

Les deuxièmes résultats marquants de cette étude concernent le rôle du pH et de la force ionique sur la conformation des colloïdes organiques. Ce travail a permis, par le suivi de la taille, de l'aromaticité et des teneurs en REE utilisées comme traceur des matières organiques de déterminer l'impact majeur du pH sur la stabilité structurale des substances humiques, et par conséquent sur la distribution organique et élémentaire dans la phase dissoute. Les résultats ont notamment confirmé la présence d'associations supramoléculaires de petites molécules organiques dans la phase dissoute. Une fraction des SH présente une structure dynamique, qui évolue selon le pH. De faibles pH induisent une déstabilisation de la structure

des SH ; ce qui enrichit la solution en petites molécules plus labiles. Cette déstabilisation a un impact sur la distribution des éléments traces dans la solution de sol, comme l'atteste la distribution des terres rares, et inversement, le degré de déstabilisation des SH semble être influencé par la charge en ions métalliques présente dans la solution.

Une étude de l'influence du pH sur la libération de colloïdes et sur la composition élémentaire de la phase dissoute est venue compléter ces résultats. La figure VI. 1 reprend les principaux résultats de cette étude. La charge colloïdale et élémentaire dans la phase dissoute varie fortement entre les deux pH étudiés. Lors d'une diminution du pH, la concentration de plusieurs éléments chimiques a très fortement augmenté, pouvant représenter une fraction importante de la concentration totale du sol. En revanche, la concentration d'autres éléments augmente lors de l'augmentation du pH, en association avec une augmentation de la quantité de colloïdes dans la solution de sol. Deux phases porteuses colloïdales ont été identifiées au cours de l'augmentation du pH: (a) la première correspond à des substances humiques et véhicule la majorité des éléments associés à la phase colloïdale, et (b) la deuxième est constituée de nano-oxydes. Le fractionnement du COD joue donc un rôle clé sur la concentration élémentaire de la solution de sol lors de changements de conditions de pH.

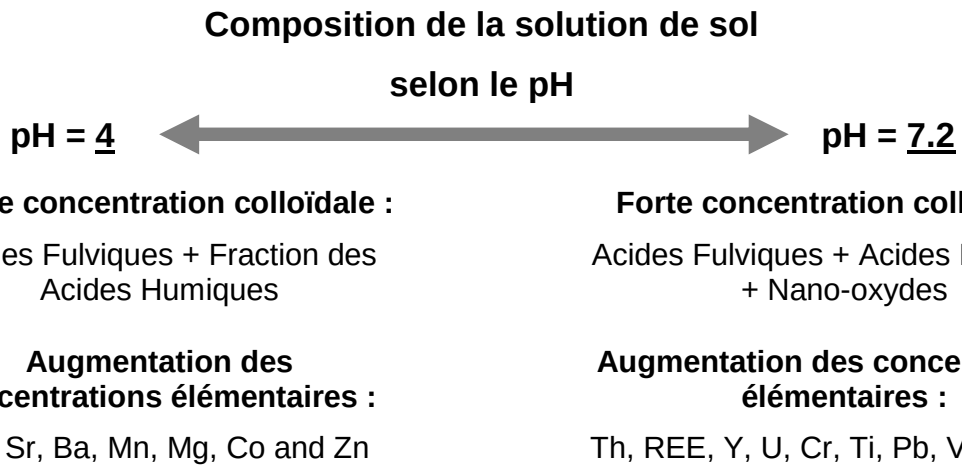

Figure **VI.1**. Principaux résultats de l'étude dédiée à l'influence du pH sur la libération de colloïdes et sur la composition élémentaire de la phase dissoute

La dernière partie de ce travail s'est concentrée sur la formation et la biodisponibilité des colloïdes mixtes Fe-matière organique. Cette étude repose sur deux types d'expériences, des cinétiques d'oxydation de Fe^{2+} en présence ou non de SH et des expériences de bioréduction des colloïdes mixtes Fe-MO. Les premières séries d'expériences ont été réalisées afin de synthétiser des colloïdes mixtes Fe-MO et d'évaluer l'impact de la MO sur la nature

des oxydes de Fe(III) formés. Dans un deuxième temps, ces colloïdes mixtes ont été réduits en présence de bactéries ferro-réductrices, *Shewanella putrefaciens*. Cette étude a montré que les SH tendent à ralentir et diminuer les réactions d'oxydation-hydrolyse du Fe. Elles agissent également directement sur la taille des oxydes de fer formés par inhibition des nuclei d'hydroxydes de Fe(III) et diminution de l'agrégation des nanoparticules de Fe. Le Fe est ainsi présent, soit sous forme ionique complexée aux substances humiques, soit sous forme de nanoparticules majoritairement sphériques de 30 ±15 nm de diamètre, inclus dans la matrice organique. L'étude de la capacité de ces nanoparticules de Fe à être utilisées comme accepteur d'électrons par *Schewanella putrefaciens* a montré une cinétique de réduction 10 fois plus rapides pour les colloïdes mixtes Fe-MO que pour des particules ferriques sensu stricto de lépidocrocite. Les nanoparticules mixtes Fe-MO sont donc plus facilement bioréductibles que les particules de Fe.

2. Implications

Ces résultats mettent en avant le contrôle majeur exercé par les phases colloïdales sur la composition élémentaire des solutions de sols. Le pH apparaît être le facteur de contrôle majeur de la distribution et de la nature des colloïdes et des éléments traces associés. Tout changement du pH agit directement sur la composition colloïdale et élémentaire des solutions de sols. De plus, le pH apparaît être un acteur non négligeable dans la conformation même des substances humiques, identifiées comme les principales molécules organiques actives dans la mobilisation des éléments traces. Les SH peuvent être formées de molécules organiques de faibles poids moléculaires associées par des liaisons électrostatiques faibles très sensibles aux diminutions du pH. Un changement du pH du milieu tend ainsi à augmenter la solubilité des colloïdes et des éléments associés. Le stock et la biodisponibilité des éléments traces du sol sont ainsi fortement accrus.

Dans cette étude, les colloïdes observés étaient de natures organiques ou mixtes avec la présence de nanoparticules de fer intimement liées aux molécules organiques. Ces derniers peuvent être produits par oxydation du Fe(II) en présence de substances humiques, comme démontré dans le chapitre V. Ainsi, dans les zones riches en matière organique et soumises à des périodes de réduction (saturation hydrique du sol) comme les zones humides, ce type de colloïdes mixtes Fe-MO peut donc être produit en fonction de l'hydropériode. Les colloïdes mixtes Fe-SH modifient la mobilité du Fe en agissant sur la taille des oxyhydroxydes piégés dans la matrice organique et en augmentant leur bioréductibilité. Ainsi, lors des périodes de

réduction, ce Fe colloïdal serait réduit préférentiellement et cela au détriment des oxydes de Fe plus cristallisés du sol. Ainsi, seule une fraction du fer serait alternativement réduite puis ré-oxydée selon les conditions de saturation du milieu, permettant ainsi le stock de phases ferriques moins biodisponibles dans le sol. De nombreuses études (McBride, 1994; Zachara et al., 2001; Cornell et Schwertmann, 2003) ont montré que la dynamique du Fe est contrôlée par le pH, l'Eh, et l'activité microbienne. Nos travaux ajoutent à ces paramètres la forme du Fe, colloïdale ou particulaire. Cette forme est elle-même sous la dépendance des concentrations en ligands organiques et des alternances aérobiose/anaérobiose. La matière organique colloïdale joue ainsi un rôle clé sur les cycles biogéochimiques des éléments.

Enfin, la formation de colloïdes organo-métalliques soustrait des éléments à la solution ‘vraie’ du sol et modifie les équilibres minéraux-solutions (Boudot et al., 2000; Lucas, 2001). Ce processus peut agir directement sur les processus de pédogénèse si la capacité de la matière organique à piéger le Fe devient importante. En effet, le stade final de la pédogénèse dépend de la capacité de migration et d’exportation des colloïdes mixtes Fe-SH, elle-même soumise aux changements de la chimie des solutions de sols. L'exportation du Fe et des SH empêchant la stabilité des minéraux argileux pourrait favoriser la déstructuration du sol, la migration de colloïdes et à terme, la formation de podzols.

II. Perspectives de ces travaux

1. À court terme

Les travaux menés durant cette thèse permettent de dégager un certain nombre de perspectives de recherche à court et à plus long terme. Au nombre de celles-ci, puisque les expérimentations se sont essentiellement basées sur un sol de zone humide de bas de versant, il pourrait être intéressant d’étudier le comportement des colloïdes et des éléments associés de sols provenant d’autres écosystèmes, comme des sols de zone humides forestiers, des sols agricoles ou encore des sols enclins à des modifications biogéochimiques suite au réchauffement climatique comme les sols d’environnements boréaux. Dans ce cadre, l’intensité et la nature du relargage colloïdal de ces sols, ainsi que leur lien intrinsèque avec la spéciation des éléments traces pourraient être étudiés. Ces études permettraient de distinguer la nature des colloïdes selon la nature du sol et les conséquences en terme de spéciation et (bio)disponibilité des éléments traces associés.

Les résultats présentés dans le chapitre 3 ont montré le double impact du pH sur la composition colloïdale et élémentaire de la solution du sol générée. Étendre la gamme de force ionique permettrait de connaitre l'impact de la force ionique sur la composition de la solution de sol, et ainsi de mieux déterminer et hiérarchiser les conditions physico-chimiques clés gouvernant la libération des colloïdes et des éléments traces associés.

Concernant l'étude des interactions Fe-matière organique, il serait intéressant de pouvoir plus finement imager les nanoparticules de Fe par des observations par MET couplé à l'EDS (Energy Dispersive X-ray Spectroscopy), ou encore par des analyses par Spectroscopie Mössbauer afin de déterminer le degré d'oxydation et l'environnement électronique local du fer dans la matrice humique. De plus, puisque nous avons montré, à plusieurs reprises que les nanoparticules de Fe peuvent piéger certains éléments traces comme le Pb ou le Ti, une caractérisation plus fine par EXAFS permettrait de déterminer le voisinage atomique du Fe et de ces éléments traces afin de mieux déterminer si ces éléments traces sont plus spécifiquement liés aux nanoparticules ou aux substances humiques. Il pourrait être intéressant de définir la capacité de complexation en éléments traces de ces nanoparticules de Fe, notamment lors de leur formation, afin de déterminer l'impact de ces nanoparticules de Fe, plus mobiles, sur le transport d'éléments traces dans les sols et les hydrosystèmes.

2. À moyen et plus long termes

Les résultats expérimentaux présentés dans cette étude permettront d'enrichir les bases de données concernant les complexes organiques d'éléments traces. Ceci dans l'objectif de tester, valider ou améliorer les modèles de complexation des éléments traces par la matière organique, notamment au niveau de leur capacité à prédire le comportement des éléments traces dans des eaux riches en matière organique. La présence de nanoparticules de Fe, stabilisées par la matrice humique, doit être prise en compte dans les modèles de complexation étant donné leur potentiel de mobilisation de certains éléments traces.

Il serait aussi intéressant d'étudier les cinétiques d'oxydation du Fe et la formation des colloïdes mixtes en milieu naturel pour mieux définir l'occurrence et la persistance temporelle des colloïdes mixtes Fe-matière organique, notamment au cours d'une année hydrologique. De plus, des expériences in situ pourraient être menées afin de mieux déterminer la biodisponibilité du Fe(III) suivant la nature et la cristallinité des oxyhydroxydes formés dans le milieu naturel (goethite, ferryhydrite ou nanoparticules liées à la matière organique). Enfin, le fait que la matière organique impacte la formation des oxydes de Fe en diminuant

notamment leur nucléation/cristallinité, augmente aussi potentiellement leur mobilité et leur surface spécifique. Il pourrait ainsi être intéressant de déterminer l'importance de ces nanoparticules sur l'adsorption des éléments traces métalliques et sur leur mobilité dans le milieu naturel.

Annexes

La partie annexes se décompose d'une part des supporting information des précédents articles (chapitre II et III) et d'autre part de deux articles supplémentaires. Le premier article correspond à un article soumis à la revue 'Chemical Geology': Davranche, M.; Gruau, G.; Grybos, M.; Pédrot, M.; Dia, A. : 'Rare earth elements as fingerprint of soil components activation'. Le deuxième article correspond à un article révisé (corrections mineures) soumis à la revue 'Geoderma': Grybos, M.; Davranche, M.; Gruau, G.; Petitjean, P.; Pédrot, M. : 'Increasing pH drives organic matter solubilization from wetland soils under reducing conditions'.

I. Annexe 1 : Supporting information : Chapitre II

1. Soil sample

The soil sample was collected from the organic horizon at a maximum depth of 10 cm. It was then dried at 40 °C for 72 h and the agglomerates were hand broken. Particles larger than 2 mm were removed by sieving. All the here below described experiment were conducted using the soil fraction smaller than 2-mm-size. The granulometric composition of the soil was determined at the Arras INRA laboratory (France) (Table II. S1). The total organic carbon content was determined at the Nancy SARM laboratory (France), using an oxygen combustion method with a CS Analyser (LECO SC 144DRPC) (Table S1). The soil organic matter content was estimated by multiplying the organic carbon concentration of the soil sample with the Van Bemmelen factor (Nelson and Sommers, 1982). The upper soil in the Mercy wetland is considered as an organic acid soil dominated by silt (total silt = 60.7%, organic matter = 10.12%, pH = 5.9). This soil contains more humic acids than fulvic ones, which implies a slow degradation of organic matter characterized by a humic acid versus fulvic acid ratio of 1.85.

Table II. S1. Granulometric composition, pH, cationic exchange capacity (CEC) of soil expressed in meq/100 g and organic carbon content.

Clay (<2 µm)	33.5 %
Silt (2-20 µm)	46 %
Coarse Silt (20-50 µm)	14.7 %
Sand (50-200 µm)	3.4 %
Coarse Sand (> 200 µm)	2.4 %
pH Water	5.9
CEC meq/100g	4.7
Fe_2O_3	2.61 %
Total Organic Carbon	5.87 %

2. Soil porosity

Table II. S2. Effective soil porosity in the column.

Soil volume	100 cm^3
Total water addition / saturation	56.3 ml
Free water	2.9 ml

3. Dataset

Table II. S3. Major-, Trace-element and DOC concentrations of samples during the experiment at the different chosen cut thresholds.

	Li	B	Na	Mg	Al	Si	K	Ca	Ti	V	Cr	Mn	Fe	Co
2 kDa	6.64	32.59	30595	35232	138.1	5038	10347	24542	0.78	0.90	0.69	60.82	171.9	4.147
	3.66	28.44	20681	9425	79.7	2613	5425	6494	0.61	0.39	0.39	16.61	72.1	1.674
	3.51	24.82	22975	8263	67.5	1772	5086	5490	0.33	0.36	0.30	16.77	51.8	1.223
	3.47	20.35	23550	7524	68.4	1794	5038	5137	0.62	0.39	0.34	20.02	51.6	1.071
	3.38	20.00	28384	6872	65.2	1633	4635	4593	0.29	0.37	0.28	24.54	35.9	1.132
	3.07	17.93	30474	5864	61.8	1651	4143	3884	0.39	0.36	0.24	26.90	31.8	1.074
	3.02	12.10	31917	5314	84.0	1603	3947	3546	0.65	0.39	0.31	31.41	63.1	1.261
	2.69	10.69	31242	5375	123.9	1167	3803	3501	0.42	0.39	0.40	36.51	111.3	1.428
	2.35	7.52	30444	4591	127.9	998	3258	3016	0.42	0.35	0.40	36.37	90.8	1.437
	2.54	7.23	35693	4759	85.1	1060	3490	3018	0.18	0.38	0.22	41.96	19.2	1.377
5 kDa	5.92	32.78	32191	32021	194.5	5139	9743	23399	0.88	0.98	0.86	58.79	213.5	4.219
	3.59	27.85	20652	9645	142.1	2267	5491	6737	0.67	0.47	0.61	18.08	120.6	1.976
	3.49	22.36	21391	8537	115.5	1603	5165	5907	0.51	0.40	0.46	18.04	93.0	1.466
	3.50	20.58	22769	7990	109.4	1654	5218	5809	0.55	0.44	0.60	22.01	76.4	1.419
	3.33	19.78	26549	6952	109.2	1412	4616	4956	0.50	0.39	0.45	26.18	75.0	1.416
	2.99	16.28	29118	5940	123.2	1321	4192	4022	0.73	0.40	0.43	29.81	73.9	1.505
	2.98	11.14	31254	6877	127.7	1294	3998	4737	0.54	0.49	0.56	41.44	84.0	1.970
	2.64	8.35	30103	6075	133.9	1194	3853	4167	0.50	0.45	0.51	44.70	74.2	2.035
	2.81	7.25	32341	5578	128.8	982	3983	3782	0.52	0.43	0.56	46.73	72.3	2.116
	2.72	5.80	32965	5260	138.1	1062	3787	3557	0.46	0.45	0.75	52.82	58.0	2.457
30 kDa	6.13	33.16	33281	32574	308.1	5127	9726	23729	1.39	1.27	1.33	61.21	346.0	4.600
	3.97	27.56	21406	11230	353.8	2290	5995	7716	1.23	0.61	1.25	21.67	354.3	2.536
	3.77	23.12	20987	9647	323.9	1749	5500	7076	1.10	0.52	1.08	21.77	333.2	2.004
	3.59	20.69	21651	8849	309.7	1463	5235	6100	1.17	0.47	1.11	25.45	297.2	1.894
	3.18	19.69	26798	7140	293.7	1465	4466	5168	1.04	0.43	1.02	29.46	301.8	1.943
	3.02	15.91	27028	6938	324.7	1323	4451	4976	1.26	0.43	1.18	36.22	314.2	2.220
	2.91	11.92	30321	6111	341.1	1183	4156	4505	1.41	0.44	1.10	42.05	311.4	2.535
	2.73	10.16	34618	5814	341.9	1038	3845	4218	1.08	0.42	1.06	50.01	245.0	2.896
	2.46	7.66	33406	5314	317.3	950	3515	3847	1.21	0.40	0.98	50.29	248.4	2.848
	2.37	5.87	36128	5015	325.0	1042	3289	3696	1.13	0.43	1.15	58.85	229.0	3.425
0.2 µm	6.04	34.57	32149	32653	341.9	5153	9274	23267	2.74	1.26	1.32	58.50	557.1	4.353
	3.85	27.12	21596	10860	403.6	2109	5600	8235	3.29	0.76	1.29	21.46	720.5	2.468
	3.81	21.97	19455	9884	387.0	1678	5517	7597	2.88	0.67	1.24	22.82	685.7	2.079
	3.60	20.60	23675	8825	384.3	1542	5252	6692	3.27	0.65	1.20	26.28	631.6	1.944
	3.46	19.23	26868	7890	408.5	1483	4813	6157	2.80	0.66	1.24	32.67	659.0	2.135
	3.00	15.46	27617	7209	422.3	1389	4577	5268	3.43	0.66	1.26	37.19	654.6	2.261
	2.84			6372	448.8	1368	4211	4786		0.67	1.29	43.16	673.6	2.627
	2.60	10.30	32448	6015	442.1	1206	3910	4432	3.10	0.60	1.19	48.58	589.2	2.797
	2.50	8.96	33150	5471	461.3	1057	3591	4102	2.85	0.63	1.19	51.94	563.1	2.948
	2.37	6.69	35698	5291	453.5	1117	3435	3942	2.81	0.65	1.24	61.08	546.3	3.598

ppb	Ni	Cu	Zn	Rb	Sr	Ba	La	Ce	Pr	Nd	Sm	Eu	Gd	Tb
2 kDa	9.99	4.05	24.06	10.86	116.97	38.28	0.2762	0.3480	0.0809	0.3566	0.0717	0.0116	0.0468	0.0050
	5.03	3.12	8.93	6.06	33.49	11.48	0.1559	0.1974	0.0451	0.2016	0.0388	0.0070	0.0272	0.0029
	4.22	2.65	7.81	5.82	29.84	10.46	0.1135	0.1377	0.0316	0.1451	0.0264	0.0050	0.0184	0.0019
	4.13	2.61	5.77	5.71	28.71	9.88	0.1163	0.1464	0.0332	0.1455	0.0285	0.0054	0.0212	0.0023
	4.46	2.69	5.28	5.53	25.70	9.21	0.1035	0.1313	0.0302	0.1381	0.0250	0.0047	0.0203	0.0021
	4.57	2.39	5.10	5.00	21.79	7.89	0.0970	0.1135	0.0255	0.1169	0.0216	0.0044	0.0167	0.0017
	4.61	2.62	4.94	4.90	20.25	7.36	0.1595	0.2066	0.0466	0.2038	0.0402	0.0083	0.0296	0.0032
	4.58	2.61	5.38	4.14	17.45	5.98	0.2002	0.2673	0.0600	0.2539	0.0523	0.0099	0.0375	0.0040
	4.75	2.46	7.58	3.66	15.15	5.14	0.2026	0.2708	0.0604	0.2602	0.0515	0.0100	0.0368	0.0040
	3.32	2.03	4.41	4.06	15.36	5.08	0.0520	0.0623	0.0152	0.0607	0.0129	0.0023	0.0090	0.0008
5 kDa	11.23	5.05	23.05	10.43	126.66	38.33	0.4263	0.5519	0.1277	0.5438	0.1085	0.0198	0.0718	0.0075
	6.75	4.09	12.05	6.08	35.69	11.76	0.2937	0.3871	0.0892	0.3896	0.0767	0.0138	0.0519	0.0052
	6.02	3.81	11.95	5.82	31.80	10.95	0.2316	0.3026	0.0679	0.2948	0.0589	0.0102	0.0409	0.0042
	6.51	3.89	7.74	5.82	30.55	10.60	0.2341	0.3059	0.0696	0.2991	0.0578	0.0110	0.0407	0.0041
	5.77	3.76	6.45	5.53	27.05	9.59	0.2385	0.3150	0.0725	0.3108	0.0602	0.0113	0.0430	0.0045
	6.32	3.48	6.76	5.05	23.76	8.65	0.2458	0.3240	0.0728	0.3197	0.0637	0.0117	0.0454	0.0048
	7.73	3.85	7.58	4.94	23.09	7.36	0.2003	0.2606	0.0577	0.2611	0.0527	0.0099	0.0369	0.0039
	6.91	3.49	6.71	4.91	20.66	6.72	0.1920	0.2537	0.0561	0.2485	0.0505	0.0095	0.0350	0.0037
	6.86	3.56	9.65	4.62	18.73	6.18	0.1904	0.2544	0.0560	0.2460	0.0500	0.0100	0.0364	0.0039
	6.64	3.30	7.67	4.52	17.88	5.83	0.1907	0.2517	0.0552	0.2432	0.0525	0.0105	0.0367	0.0041
30 kDa	13.33	6.63	28.64	10.43	116.04	39.71	0.7192	0.9270	0.2164	0.9266	0.1843	0.0341	0.1276	0.0132
	10.60	5.50	16.00	6.53	40.56	14.31	0.8130	1.0844	0.2538	1.0905	0.2159	0.0411	0.1508	0.0158
	9.58	5.19	15.23	6.14	36.07	13.39	0.7695	1.0282	0.2392	1.0156	0.2017	0.0381	0.1465	0.0154
	9.49	5.09	10.50	5.85	33.18	12.21	0.7696	1.0406	0.2415	1.0122	0.2027	0.0396	0.1459	0.0157
	9.07	4.84	9.56	5.30	28.75	11.22	0.8036	1.0653	0.2413	1.0493	0.2195	0.0422	0.1470	0.0159
	11.00	5.16	9.79	5.11	26.92	10.60	0.8709	1.1869	0.2715	1.1509	0.2324	0.0451	0.1669	0.0184
	9.95	5.12	8.97	4.88	24.43	9.70	0.9172	1.2595	0.2895	1.2501	0.2530	0.0482	0.1787	0.0193
	9.81	5.00	0.35	4.62	23.58	9.29	0.9919	1.3126	0.2950	1.2758	0.2624	0.0493	0.1812	0.0194
	9.65	4.60	10.99	4.15	20.80	7.96	0.8450	1.1711	0.2674	1.1416	0.2361	0.0459	0.1671	0.0189
	10.25	4.65	10.89	4.09	19.80	7.74	0.9142	1.2704	0.2913	1.2403	0.2560	0.0492	0.1825	0.0210
0.2 µm	12.60	6.44	27.44	10.08	116.74	40.98	0.9143	1.1756	0.2587	1.0840	0.2174	0.0408	0.1479	0.0156
	10.29	5.87	15.78	6.32	40.86	15.43	1.0483	1.3909	0.3105	1.3175	0.2596	0.0510	0.1756	0.0192
	9.82	5.43	16.10	6.23	37.88	14.62	1.0351	1.3593	0.3051	1.3014	0.2678	0.0508	0.1759	0.0192
	9.73	5.29	10.97	5.90	34.39	13.28	1.0004	1.3385	0.2955	1.2434	0.2564	0.0485	0.1769	0.0193
	9.89	5.38	10.33	5.66	31.37	12.52	1.0739	1.4445	0.3207	1.3385	0.2687	0.0528	0.1881	0.0207
	10.57	5.06	9.40	5.05	26.95	10.88	1.0692	1.4250	0.3131	1.3148	0.2664	0.0523	0.1867	0.0206
	10.40	5.43	10.07	4.84	24.60	10.11	1.1425	1.5124	0.3335	1.4194	0.2863	0.0545	0.2002	0.0220
	9.79	5.04	9.82	4.40	22.57	9.18	1.0848	1.4510	0.3213	1.3424	0.2791	0.0529	0.1955	0.0222
	9.93	4.86	12.37	4.21	20.86	8.35	1.0433	1.4059	0.3097	1.3009	0.2639	0.0504	0.1907	0.0213
	10.51	4.89	11.11	4.12	19.97	8.11	1.1247	1.5080	0.3342	1.3980	0.2844	0.0552	0.2084	0.0234

ppb	Dy	Ho	Er	Tm	Yb	Lu	Pb	Th	U	DOC (ppm)	Times (min)	Pore volumes
2 kDa	0.0245	0.0047	0.0138	0.0022	0.0134	0.0026	0.135	0.025	0.068	61.31	57	2.83
	0.0143	0.0030	0.0087	0.0012	0.0086	0.0017	0.095	0.014	0.047	29.82	124	5.76
	0.0107	0.0020	0.0060	0.0009	0.0062	0.0011	0.085	0.009	0.039	24.08	202	8.47
	0.0113	0.0024	0.0067	0.0010	0.0062	0.0011	0.080	0.011	0.042	22.88	295	11.52
	0.0095	0.0021	0.0057	0.0009	0.0062	0.0011	0.078	0.007	0.038	22.14	423	14.92
	0.0089	0.0018	0.0050	0.0008	0.0052	0.0010	0.075	0.009	0.035	19.58	555	18.15
	0.0159	0.0032	0.0090	0.0013	0.0089	0.0017	0.123	0.023	0.048	20.68	705	21.49
	0.0203	0.0039	0.0117	0.0017	0.0104	0.0018	0.122	0.012	0.054	19.40	875	24.63
	0.0213	0.0040	0.0115	0.0017	0.0109	0.0018	0.129	0.012	0.050	13.97	1087	27.99
	0.0051	0.0010	0.0035	0.0005	0.0033	0.0006	0.046	0.006	0.025	10.83	1430	32.80
5 kDa	0.0375	0.0073	0.0218	0.0031	0.0191	0.0035	0.194	0.040	0.052	67.84	57	2.83
	0.0271	0.0053	0.0139	0.0021	0.0146	0.0027	0.143	0.025	0.055	34.40	124	5.76
	0.0209	0.0043	0.0123	0.0018	0.0119	0.0019	0.137	0.020	0.050	27.88	202	8.47
	0.0216	0.0046	0.0126	0.0017	0.0118	0.0022	0.145	0.021	0.053	26.91	295	11.52
	0.0232	0.0048	0.0129	0.0018	0.0132	0.0023	0.122	0.021	0.055	25.26	423	14.92
	0.0246	0.0049	0.0145	0.0020	0.0136	0.0024	0.151	0.022	0.059	24.29	555	18.15
	0.0208	0.0041	0.0119	0.0019	0.0124	0.0020	0.134	0.019	0.047	21.24	705	21.49
	0.0197	0.0040	0.0119	0.0018	0.0116	0.0021	0.135	0.017	0.046	19.71	875	24.63
	0.0216	0.0042	0.0129	0.0018	0.0124	0.0022	0.133	0.019	0.048	17.55	1087	27.99
	0.0213	0.0040	0.0123	0.0019	0.0115	0.0024	0.119	0.018	0.049	15.69	1430	32.80
30 kDa	0.0646	0.0124	0.0362	0.0054	0.0338	0.0062	0.226	0.132	0.109	86.92	57	2.83
	0.0768	0.0148	0.0422	0.0058	0.0392	0.0071	0.264	0.177	0.138	52.25	124	5.76
	0.0737	0.0140	0.0408	0.0056	0.0376	0.0072	0.269	0.167	0.133	40.86	202	8.47
	0.0792	0.0148	0.0421	0.0060	0.0377	0.0068	0.232	0.176	0.133	37.96	295	11.52
	0.0773	0.0152	0.0429	0.0063	0.0395	0.0070	0.253	0.181	0.139	37.42	423	14.92
	0.0905	0.0166	0.0481	0.0067	0.0440	0.0078	0.309	0.199	0.141	32.57	555	18.15
	0.0977	0.0180	0.0509	0.0070	0.0456	0.0080	0.313	0.215	0.150	35.45	705	21.49
	0.1034	0.0187	0.0534	0.0076	0.0507	0.0069	0.321	0.192	0.157	31.02	875	24.63
	0.0946	0.0171	0.0477	0.0071	0.0453	0.0081	0.307	0.184	0.139	27.14	1087	27.99
	0.1027	0.0190	0.0542	0.0079	0.0484	0.0088	0.309	0.195	0.148	26.08	1430	32.80
0.2 µm	0.0781	0.0141	0.0410	0.0059	0.0383	0.0067	0.368	0.174	0.437	112.66	57	2.83
	0.0945	0.0178	0.0504	0.0070	0.0476	0.0084	0.580	0.216	0.427	62.61	124	5.76
	0.0987	0.0178	0.0499	0.0069	0.0466	0.0079	0.590	0.217	0.340	54.23	202	8.47
	0.0947	0.0177	0.0507	0.0066	0.0459	0.0082	0.593	0.220	0.300	48.34	295	11.52
	0.1029	0.0190	0.0528	0.0075	0.0490	0.0084	0.631	0.232	0.279	48.27	423	14.92
	0.0994	0.0189	0.0533	0.0076	0.0480	0.0085	0.600	0.214	0.277	46.67	555	18.15
	0.1103	0.0203	0.0570	0.0075	0.0500	0.0089	0.640	0.232	0.280	45.41	705	21.49
	0.1083	0.0198	0.0571	0.0073	0.0492	0.0087	0.591	0.217	0.248	37.29	875	24.63
	0.1046	0.0198	0.0544	0.0076	0.0487	0.0086	0.558	0.202	0.229	31.91	1087	27.99
	0.1148	0.0209	0.0605	0.0084	0.0547	0.0088	0.621	0.204	0.230	32.16	1430	32.80

Whatever was the considered fraction, alkaline, alkaline-earth metals and other trace element such as Mn, Si and B showed very stable concentrations in solutions (Figure II. 8 where K, Ca, Sr, Mg and Na concentrations are reported through time).The concentrations strongly decreased at the beginning of the experiment, and then decreased more slowly, except for the Na and the Mn ones. This suggests that the 'truly' dissolved elements were more easily leachable at the beginning of the experiment.

Concentrations of Ni, Co, Cu and Zn concentrations became stable during the experiment after a strong decrease registered during the first steps of the experiment (Figure II. 8). The below 2 kDa fraction (so-called soluble) displayed relatively high concentrations all over the experiment. This group of elements is characterized by strong interactions with DOC since their concentrations increased with the DOC ones. However, this was not true at the beginning of the experiment since a large amount of small compounds (lower than 2-kDa-molecular weight) was leached.

Al, Fe, Cr, Mo, Ti, U, Th, Pb and REE concentrations decreased regularly according to the cut threshold at each sampling point (See Th, REE, Pb, U, Al, Fe, Cr and Ti concentrations as reported in Figure II. 9). Their concentrations in the fractions lower than 2 kDa and 5 kDa were low. However, higher than 5 kDa compounds were strongly complexed to these trace elements. This group was characterized by strong interactions with DOC since the concentrations of these trace elements increased with the DOC concentrations displaying high positive correlation coefficients ($0.89 < r^2 < 0.99$). These experimental data showed that some trace elements such as Ni, Co, REE and Th were mostly carried by DOC suggesting that DOC-mediated complexation can be very strong in such DOC-rich environment (Figure II. 10).

II. Annexe 2 : Supplementary information Chapitre III

1. Soil sample

The granulometric composition of the soil was determined at the National Analytical INRA Soil Laboratory (France) (Table S1). The organic carbon content was determined at the CNRS Analytical Research Facility - SARM - (France), using an oxygen combustion method with a CS Analyser (LECO SC 144DRPC) (Table S1). The soil organic matter content was estimated by multiplying the organic carbon concentration of the analysed soil sample by the Van Bemmelen factor of 1.724 (Nelson and Sommers, 1982). The upper soil in the Mercy wetland is considered as an organic acid soil dominated by silt (total silt = 60.7%, organic matter = 10.12%, pH = 5.9). This soil contains more humic acids than fulvic ones, which implies a slow degradation of organic matter characterized by a humic acid versus fulvic acid ratio of 1.85.

Table III. S1. Granulometric composition (%), pH, cationic exchange capacity (CEC) of soil expressed in meq/100 g and organic carbon content (%).

Clay (<2 µm)	33.5 %
Silt (2-20 µm)	46 %
Coarse Silt (20-50 µm)	14.7 %
Sand (50-200 µm)	3.4 %
Coarse Sand (> 200 µm)	2.4 %
pH Water	5.9
CEC meq/100g	4.7
Fe_2O_3	2.61 %
Total Organic Carbon	5.87 %

2. Solution analyses

Selected pH was monitored using an automatic pH stat titrator (Titrino 794, Metrohm) with 0.1 M NaOH or HCl solutions. Total acid and base solution additions were considered as negligible since they represented less than 1% of the total volume of solution. pH was measured with a combined Mettler InLab® electrode after a calibration performed with WTW standard solutions (pH= 4.01 and 7.00 at 25 °C). The accuracy of the pH measurement was ±

0.05 pH units. Dissolved organic carbon (DOC) was analysed on a Total Organic Carbon analyser (Shimadzu TOC-5050A). Accuracy of DOC measurement was estimated at ± 3 % (by using standard solution of potassium hydrogen phtalate). Major anions (Cl^-, SO_4^{2-} and NO_3^-) concentrations were measured by ion chromatography (Dionex DX-120): the uncertainty on the data was below 4%. Major cation and trace element concentrations were determined by ICP-MS (Agilent 4500), using indium as an internal standard. The international geostandard SLRS-4 was used to check the validity and reproducibility of the data. All measurements were made in triplicate. Typical uncertainties including all error sources were below ± 5 % for all the analyzed trace elements, whereas for major cations, the uncertainty lied between 2 % and 5 %, depending on the concentration (Yéghicheyan et al., 2001; Davranche et al., 2004).

III. Annexe 3 : Rare earth elements as a fingerprint of soil components solubilization

Article soumis à la revue '*Chemical Geology'*, auteurs : Mélanie Davranche, Marlgorzata Grybos, Gérard Gruau, Mathieu Pédrot, Aline Dia

ABSTRACT

The coupling of rare earth elements (REE) patterns shapes obtained from soil incubations under various chemical conditions were discussed to identify the soil phases preferentially activated by induced chemical reactions. For this purpose, an organic-rich wetland soil sample was incubated under anaerobic condition at both pH 5 and without pH buffer. The REE patterns developed in the soil solution were compared to the REE patterns obtained through either aerobic incubations at pH 3 and 7 or a chemical reduction experiment (using hydroxylamine). REE patterns in anaerobic and aerobic experiments at pH 7 exhibited the same middle rare earth element (MREE) downward concavity significant of the complexation of REE with soil organic matter (OM). By contrast, under acidic condition, the REE pattern exhibited a positive Eu anomaly due to the dissolution of soil feldspar. Finally, REE pattern obtained from the chemical reducing experiment showed an intermediary flat shape corresponding to a mixing between the soil organic and mineral phases dissolution. The comparison of the various REE pattern shapes allowed to conclude that (i) biological reduction of wetland soil involved amorphous Fe(III) colloids linked to OM and, (ii) that the REE mobility was controlled by the dynamic of OM in wetland soil. They also evidence the potential of REE to be use as a tracer of the soil phases involved in the various chemical processes running in solid/solution interface

Key-words: rare earth elements, soil, reductive dissolution, Fe-oxyhydroxides, organic matter, tracer

1. Introduction

One of the key issues addressed by environmental geochemistry is to understand the processes that control the chemistry of ground-, surface and soil waters. In this regard, the fourteen stable rare earth elements (REE) are of unique value. The coherence of their chemical properties leads to characteristic REE signatures or fingerprints in solutions in which a given process dominates. In the past, REE were therefore largely used as

hydrological and hydrochemical tracers in the studies of rivers, lakes, groundwater and geothermal fluids (e.g. Elderfield and Greaves, 1982; Johannesson et al., 1995; Braun et al., 1998; Dia et al., 2000; Aubert et al., 2001) or in the study of groundwater-rock interactions (Smedley, 1991; Fee et al., 1992, Johannesson et al.,1997a; 1997b, Dia et al., 2000; Möller et al., 2000; Worrall and Pearson, 2001).

In soil, REE are sourced in the chemical and physical weathering of rocks and rock-forming minerals (e.g., Sholkovitz, 1995; Gaillardet at al., 2003). Physicochemical processes leading to the mobilization and retention of REE during alteration is well-documented (e.g., Nesbitt et al., 1979; Braun et al., 1998; Steinman and Stille, 1997). The retention of REE in the soil profile are mainly controlled by three factors, (i) the stability of the primary REE-carrying minerals, (ii) the presence of secondary phases as clays and Fe- and Mn-oxyhydroxides (Koeppenkastrop and de Carlo, 1992; Coppin et al. 2002) and (ii) the concentration of colloidal organic matter (OM) (Tang and Johannesson 2003; Grybos et al., 2007; Pourret et al., 2007c). Considering that each soil phases (mineral or organic) displays (ii) various surface properties, such as specific area, surface sites density and nature (hydroxyl, carboxylic, phenolic…) and (ii) their own REE distribution inherited from the rock weathering, their mobilization through various chemical reactions (dissolution, colloidal release….) may involve the development of various shaped REE patterns in the soil solutions. Experimental studies already demonstrated that (i) REE complexed with colloidal OM (humate) exhibited a middle rare earth element (MREE) downward concavity (Davranche et al., 2005; Yamamoto et al., 2006; Pourret et al., 2007c), that (ii) REE adsorbed onto clays were fractionated, heavy rare earth elements (HREE) being more sorbed than light rare earth elements (LREE) (Coppin et al., 2002) and that (iii) REE adsorption and co-precipitation with MnO_2 and Fe(III)-oxide involved the development of a Ce anomaly on the REE pattern (Bau et al., 1999; Otha and Kawabe, 2001, Davranche et al., 2004, 2005). From granite weathering products studies, Aubert et al. (2001) and Compton et al. (2003) provided evidence that (i) REE pattern of feldspar and plagioclase show a strong positive Eu anomaly, a slight enrichment in LREE and a slight depletion in the HREE and (ii) that REE pattern of apatite displayed a strong negative Eu anomaly and are enriched in MREE and depleted in LREE. These features were already used (i) to elucidate the origin and the migration behaviour of REE in various soil system (e.g. Braun et al., 1998; Aubert et al., 2001; Compton et al. 2003; Ndjigui et al., 2008), (ii) to differentiate pedologic processes (Aide and Smith-Aide, 2003; Laveuf et al., 2008), (iii) to reconstruct the history of soil genesis (Mourier et al., 2008).

In the present study, we assess that REE fractionation from the different soil phases may also be used to identify the response of the soil system to a particular chemical process such as reductive and/or acidic dissolution. The objectives of this study were to demonstrate that the REE fractionation developed in the soil solution in response to a specific chemical 'forcing' could be used to (i) identify the REE source and (ii) to precise the nature and state of the involved soil phases. To test this assumption, REE concentration distributions obtained from a wetland soil submitted to anaerobic and aerobic incubations at various pH values were studied.

2. Materials and Methods

All chemicals used were of analytical grade, and all the experimental solutions were prepared with doubly deionised water (MilliQ system, Millipore™). All containers were previously soaked in 10 % Ultrapure HNO_3 for 48 h at 60 °C, then rinsed with MilliQ water for 24 h at 60 °C to remove all possible contamination sources.

a. Soil sampling and descriptions

Soil was sampled into the uppermost organo-mineral horizon (Ah) from a planosol (according to the WRB international classification) of the Mercy wetland located in the Kervidy-Coët Dan subcatchments in Brittany, Western France (Curmi et al., 1997). The bedrock of the catchments is made of fissured and fractured upper Proterozoic schist (Dabard et al., 1996). The soils, developed into a loamy material derived from bedrock weathering and eolian Quaternary deposits, exhibit facies variations, which are locally dominated by silt, clay or sandstone materials (Pellerin and Van Vliet-Lanoë, 1994). This wetland soil was selected since several authors identified and studied, from both field and laboratory works, an organic matter (OM) release concomitant to the soil Fe(III)-oxides reduction (Dia et al., 2000; Olivié-Lauquet et al., 2001, Grybos et al., 2007; submitted 2009). Approximately 10 kg of soil were collected from the surface layer (0-10 cm), sieved at 2-mm and stored at 4°C. After soil sample fusion with $LiBO_2$ and acidic dissolution with HNO_3, the major element composition was determined at the CRPG laboratory in Nancy, France, by inductively-coupled plasma atomic emission spectrometry (ICPAES, Jobin-Yvon JY 70) (Table AIII. 1). The organic carbon content was determined at the CNRS Analytical Research Facility - SARM - (France), using an

oxygen combustion method with a CS Analyser (LECO SC 144DRPC) (Tab 2). Soil is acidic with a pH of 5.5.

Table AIII. 1. Soil sample major element and OM proportions and total REE concentration ($\mu g.g^{-1}$).

Major elements (%)								∑REE* ($\mu g.g^{-1}$)	OC* (%)
Si	**Al**	**Fe**	**Mn**	**Mg**	**Ca**	**Na**	**K**		
28	3.5	1.03	0.01	0.28	0.13	0.14	1.00	128.27	9.3

*∑REE : sum of rare earth elements

OC : organic carbon

The sample was sequentially leached in three steps following the modified BCR extraction scheme used for operational speciation of metals (Mossop, 2002). The protocol is described in Table AIII. 2. The BCR sequential extraction scheme was applied to 1 g of dried soil sample and the extractions were conducted in centrifuge tube (polypropylene, 15 mL).

Table AIII 2. The modified BCR sequential extraction scheme used for operational speciation of metals.

Step	Soil phases	Extractant	Shaking time and temperature
F1	Water and acid soluble and exchangeable	40 mL 0.11 M CH_3COOH	16 h at room temperature
F2	Reducible	40 mL 0.5 M $NH_2OH.HCl$ (pH 2)	16 h at room temperature
F3	Oxidizable	10 mL 8.8 M H_2O_2(pH 2) 10 mL 8.8 M H_2O_2(pH 2) 50 mL 1 M NH_4Oac (pH 2)	1 h at room temperature 1 h at 85 °C 16 h at room temperature
F4	Residual	15 mL aqua regia 10 mL aqua regia	Heating to dryness

b. Experimental set-up

The experimental procedure was based on a series of 5 laboratory experiments each designed to involve a precise chemical process in the soil sample, namely OM desorption, Fe(III)-oxides reduction and mineral dissolution. This procedure was developed to identify in each experiment, the mechanism by which REE were released in the soil solution and to determine the exact nature and state of the involved soil phases. Two experiments under

aerobic conditions were performed at pH 3 and 7 (Aerobic experiment at pH 3 and Aerobic experiment at pH 7) to stimulate soil mineral dissolution and OM desorption, respectively. Two experiments under anaerobe were also carried out. In one of this experiment, pH was left to shift in response to the reducing conditions (Anaerobic without pH buffer experiment). Therefore, both soil Fe(III)-oxides dissolution and OM desorption mechanism were involved (Grybos et al., 2007). In the other anaerobic experiment, pH was adjusted and monitored at 5 (Anaerobic experiment at pH 5), value which drastically limited OM desorption. The major stimulated mechanism was therefore biological soil Fe(III)-oxides reduction. Finally, a chemical reduction experiment (Chemical reduction experiment) was designed to stimulate soil Fe(III)-oxides abiotic reduction within the incubated soil.

All experiments were prepared following the same protocol as previously described in Grybos et al. (2007; submitted 2009). Briefly, about 95 g of sieved soil were mixed with a synthetic solution containing 0.48 mmol l^{-1} of NO_3^-, 0.85 mmol l^{-1} of Cl, and 0.1 mmol l^{-1} of SO_4^{2-} These concentrations correspond to the anionic composition of the soil-solution during autumn (period of water table rise) in the Mercy wetland. All experiments were performed with a (dry) soil/solution ratio of 1/20 (soil moisture = 43% in weight). Incubation experiments were carried out with a batch Prelude reactor (Guerin, Biolafite), equipped with an on-line systems for monitoring pH, Eh, temperature, and N_2 flux, as well as a data logger and monitored using the ADAGIOTM program (Guerin, Biolafite) (Grybos et al. 2007; submitted 2009). The reactor was placed in a thermostatically-controlled water bath at 30°C to ensure a constant temperature. For all experiments, soil suspension was stirred during 5 h under aerobic conditions.

For aerobic and anaerobic experiments at pH 3, 5 and 7, the pH was adjusted and kept constant manually by acid/base addition (0.5M HCl, 0.5M NaOH). For anaerobic experiments, anaerobe was induced by passing a continuous nitrogen stream through the soil suspension. A high nitrogen flow rate was maintained during the first 2 h at 2 l min^{-1}, and then reduced to about 0.2 l min^{-1}. Only Eh was allowed to vary in response to the biogeochemical reactions. Finally, for the chemical reduction experiment, Fe(III)-oxides dissolution was induced by a 4.6 10^{-4} M hydroxylamine ($NH_2OH.HCl$) addition, whose concentration corresponds to the soil oxidation capacity, calculated from the soil total Fe concentration (Davranche and Bollinger 2000 a-b). Hydroxylamine buffered the pH of the soil suspension at 3. Monitoring of pH, for each series of experiment, was performed with the one-line Biolafitte system using a Malter HA 405-DPA-SC-S8/225 electrode. The accuracy of the pH measurement was ±0.05.

Approximately 20 ml of soil suspension was drawn off daily with a sterile syringe (under N_2 gas in the anaerobic treatments), centrifuged for 10 min at 1950g, and filtered through a 0.2 µm cellulose acetate membrane filter (Millipore).. The sample was then divided into several aliquots for the determination of dissolved organic carbon (DOC), Fe_T and Fe(II), and major and trace cations. For the anaerobic experiments, sampling and treatment for Fe(II) analysis was performed under a slow flow of nitrogen to prevent Fe(II) oxidation.

c. Soil solution analyses

Dissolved organic carbon (DOC) was determined in triplicate on a Shimadzu 5050 TOC analyzer. For the present study, the relative standard deviation (RSD) was systematically less than 2%. DOC measurements were corrected using ultrapure water blanks (blank level < 0.2 mg L^{-1}). The accuracy of DOC concentration measurements was estimated at ±5%, as determined by repeated analyses of freshly prepared standard solutions (potassium biphtalate).

Iron (II) was analysed using the 1.10 phenantroline colorimetric method, AFNOR NF T90-017 (AFNOR, 1997), using a UV-visible spectrophotometer (UVIKON XS, Bio-Tek) with a precision of 5%. Major cation and trace element were determined by ICP-MS (HP 4500, Agilent Technologies HP4500) using indium as an internal standard. Prior to ICP-MS analysis, samples were digested with 14 N HNO_3 at 100°C, then evaporated to complete dryness and taken up in 0.4 N HNO_3 to avoid interference with OM during mass analysis. The international geostandard SLRS-3 was used to check the accuracy and reproducibility of the results. Typical uncertainties including all error sources were below ± 5 % for all the trace elements, whereas for major cations, the uncertainty lay between 2 % and 5 %, depending on the concentration (Yéghicheyan et al., 2001; Davranche et al., 2005).

3. Results

a. Selective extractions

The proportions of Al, Fe_T and ∑REE (sum of the rare earth elements) in each fraction of the selective extraction procedure were reported in Figure AIII. 1. In the studied organo-mineral soil, Al is mainly present in the residual fraction (96.5 % in residual fraction, 1.5% in reducible fraction and 1.8 % in oxidizable fraction), namely linked to soil minerals such as

clays or primary minerals provided by the alteration of the bed rock. In temperate soils, Al does not occur as oxides but is mainly fixed in clays minerals (e.g. Allen and Hajek, 1989 ; Schulze, 1989). This method indicates that 23 % of Fe is contained in the reducible fraction (probably as Fe-oxyhydroxides), 24% in the oxidizable fraction (as organic complexes or as sulphides) and 52% in the residual fraction (as well crystallized Fe(III)-oxides or in clays and/or primary minerals). REE occurred mainly in the residual fraction (78 %), as previously shown by Yan et al. (1999) and Leybourne and Johannesson (2008) from two different extractions methods. REE were also distributed at 13 % in the reducible fraction, probably bound to Fe-oxyhydroxides and 8 % in the oxidizable fraction probably complexed with organic matter. However, it is important to note that REE in the reducible fraction could be bound to Fe-oxyhydroxides as trivalent ion and/or as complexed ions such as REE-organic complexes.

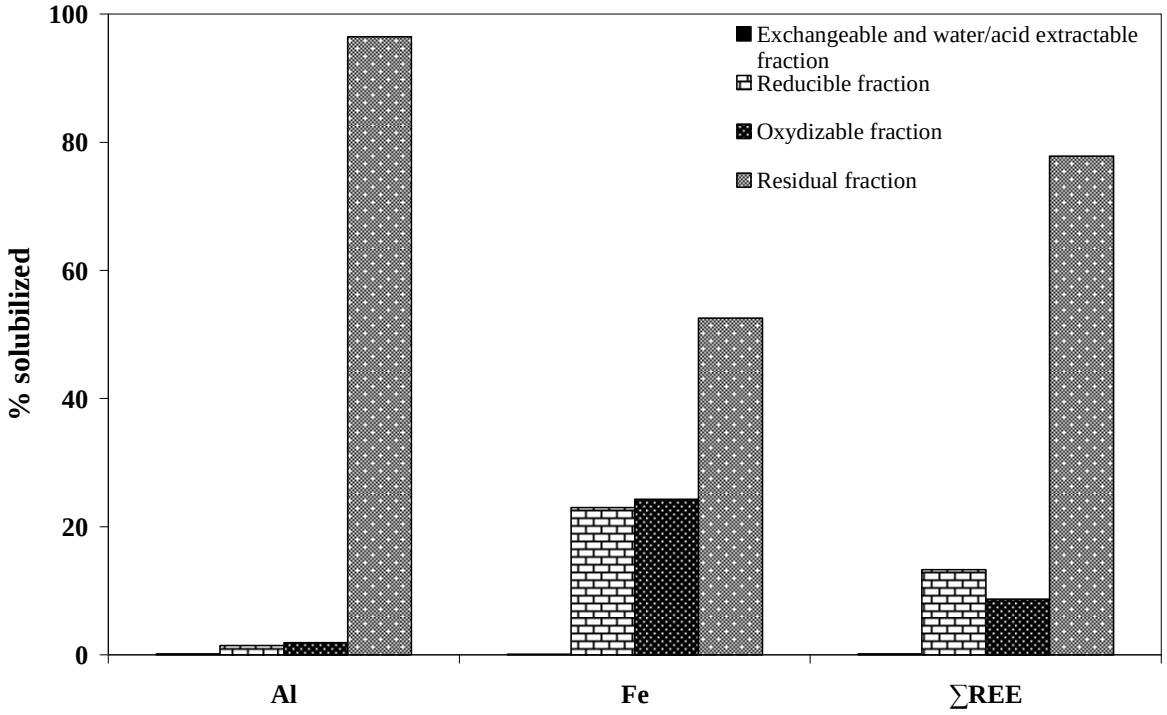

Figure AIII. 1. Al, Fe_T and ∑REE proportions in the different fractions of the selective extraction procedure.

The REE patterns obtained in the solution of each fractions of the selective extraction procedure are plotted in the Figure AIII. 2. The first three fractions exhibited a REE pattern with a MREE (middle rare earth element) downward concavity (i.e. (La/Sm<1 and (Gd/Yb>1) (Figure AIII. 2 and 3). Same REE pattern shape were obtained by Yan et al. (1999), from sequential extraction performed on clays-rich tills samples, in their amorphous Fe- and Mn-oxyhydroxides fraction. This feature has been already observed in complexation experiments of REE with humic acid (Davranche et al., 2005; Yamamoto et al., 2006; Pourret et al.,

2007c) and seems to be a specific shape of pattern of REE bound to organic matter. This pattern shape therefore confirms that REE in the reducible fraction occurred mainly as organic complexes themselves bound or coated onto soil Fe-oxyhydroxides. The REE pattern of the residual fraction present a flatter shape strongly different as compared to the previously described pattern, with La/Sm and Gd/Yb ratio around 1 against a La/Sm ratio between 0.4 and 1.2 and a Gd/Yb ratio around 3 for the three other fractions. Subsequently, in the residual fraction, REE were not bound to organic matter but were probably provided by the dissolution of soil minerals components.

b. Soil solution chemistry of incubation experiments

For the clarity of the manuscript, only concentrations at equilibrium are presented (Table AIII. 3). The equilibrium concentrations of C (solubilized organic carbon), Al, Fe_T, ∑REE (the sum of rare earth elements) for each series of experiment are plotted in Figure AIII. 3.

Table AIII. 3. Concentrations ($mol.L^{-1}$) of C (organic carbon), Al, Fe_T, ∑REE (sum of rare earth elements) at equilibrium for each experiment.

	Concentration ($mol.L^{-1}$)					
Experiments	**C**	**Al**	**Fe_T**	**∑REE**	**∑REE/C (x 10^{-5})**	**REE bound to OM (%)**
Aerobic at pH 7	$1.18\ 10^{-2}$	$4.24\ 10^{-5}$	$7.71\ 10^{-5}$	$1.40\ 10^{-8}$	1.19	100
Aerobic at pH 3	$3.37\ 10^{-3}$	$4.14\ 10^{-4}$	$1.79\ 10^{-5}$	$1.56\ 10^{-7}$	4.64	26
Anaerobic without pH buffer	$1.78\ 10^{-2}$	$6.49\ 10^{-5}$	$2.24\ 10^{-4}$	$2.07\ 10^{-7}$	1.17	102
Anaerobic at pH 5	$1.44\ 10^{-2}$	$4.59\ 10^{-5}$	$3.98\ 10^{-3}$	$2.15\ 10^{-7}$	1.49	80
Chemical reduction	$2.90\ 10^{-2}$	$7.27\ 10^{-4}$	$4.77\ 10^{-3}$	$9.18\ 10^{-7}$	3.17	38

Aerobic experiment at pH 7 was designed to promote soil OM desorption. This experiment allowed the determination of the proportion of REE bound to organic matter (Grybos et al., 2007), $1.4\ 10^{-6}$ mol ∑REE mol^{-1}C. Considering that this proportion represented the amount of REE bound to OM in the soil, it was possible to calculate the proportion of REE complexed by OM in each experiment (Table AIII. 3). In the Aerobic experiment at pH 7, Al and Fe were slightly released and corresponded to ions complexed with OM desorbed from the soil components. Despite a pH value of 7, Fe and Al occurred in solution since their complexation by OM prevented their re-adsorption onto soils components.

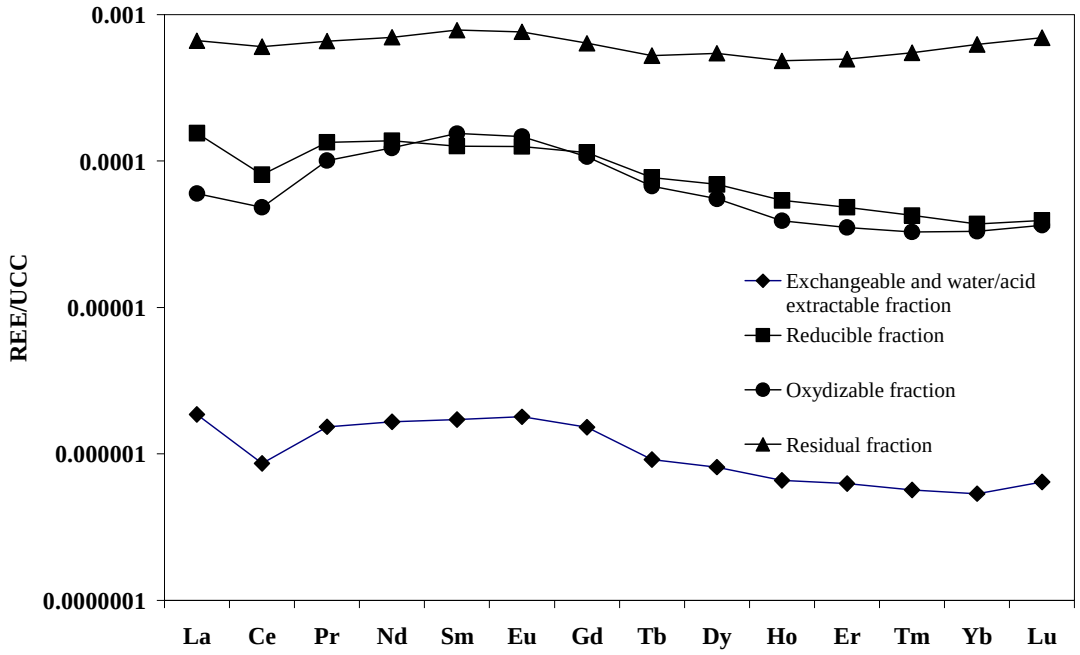

Figure AIII. 2. Upper continental crust (UCC) normalized REE patterns in the solution of each fraction recovered for the soil selective extraction procedure.

Aerobic experiment at pH 3 was designed to promote the acidic dissolution of soil minerals. The dissolution occurrence was confirmed by the Al concentration of 4.1 10^{-4} M against 1.5 10^{-5} to 6.5 10^{-5} M for experiments carried out at higher pH. Acidic conditions probably also stimulated the dissolution of the Fe(III)-oxides. However, Fe in solution could also correspond to Fe bound to OM. Although OM concentration was the lower among the series of experiments (3.4 10^{-3}M of C against 1.18 10^{-2} to 2.90 10^{-2} M for the other experiments), it was still significant. Gu et al. (1994) and Avena and Koopal (1998) provided evidence that OM adsorption was more important at acidic pH where minerals surfaces were positively charged and OM was as anionic species. Therefore, OM released in the Aerobic at pH 3 experiment corresponded to OM probably released from the acidic dissolution of soil mineral surfaces. Regards to these results, most part of REE was supplied by soil minerals dissolution. Only 26 % of REE were estimated to be bound to OM (Table AIII. 3). Moreover, acidic pH prevented REE readsorption on the solid surfaces although their site densities and surface areas were increased by dissolution.

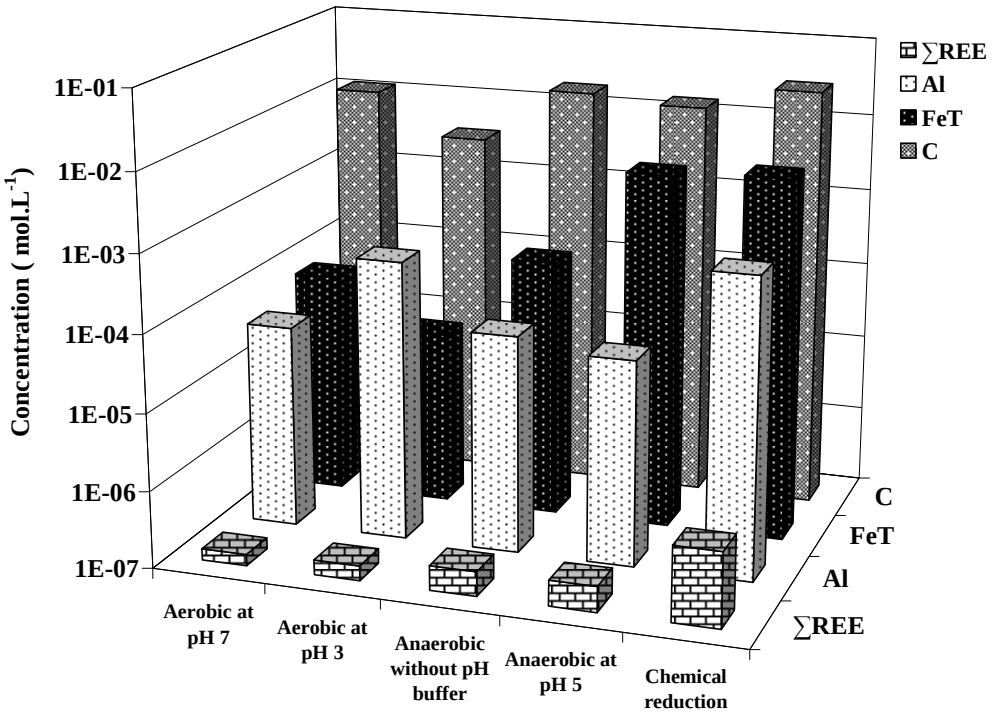

Figure AIII. 3. Concentrations (in mol.L-1) of C (organic carbon), Al, FeT, ∑REE (sum of rare earth elements), in the aerobic experiment at pH 3 and 7 (Aerobic at pH 3 and Aerobic at pH 7), in the anaerobic experiment at uncontrolled pH and pH 5 (Anaerobic without pH buffer and Anaerobic at pH 5) and in the chemical reduction experiment (Chemical reduction).

Anaerobic experiments were designed to promote soil Fe(III)-oxides reductive dissolution. In both anaerobic experiments, solubilized Al concentration was low suggesting that soil mineral dissolution was not or slightly activated. Both Fe(III)-oxides dissolution and OM desorption were proceeded when pH was not buffered. Around 100 % of the solubilized REE were estimated to be bound to OM (Table AIII. 3). In the Anaerobic experiment at pH 5, only Fe(III)-oxides reductive dissolution is promoted, since pH 5 prevented OM desorption. However, high OM concentrations were nevertheless released into the soil solution. This OM corresponded to the OM solubilized by the only reductive dissolution of soil Fe(III)-oxides (Grybos et al., submitted 2009). About 80 % of REE were estimated to be released by OM solubilization (Table AIII. 3).

The Chemical reduction experiment was performed with hydroxylamine ($NH_2OH.HCl$) as reducing agent. Hydroxylamine buffered the soil suspension at pH 3. Subsequently, not only reductive dissolution of soil Fe(III)-oxides, but also acidic dissolution of soil mineral components was promoted. The mineral dissolution was assessed by an Al concentration reaching 7.27 10^{-4} M, which was the higher Al concentration obtained in the series of experiments. The acidic pH should have limited OM solubilization, however, the concentration of OM released here is the higher obtained. If pH 3 effectively prevented OM

desorption, the combination of the hydroxylamine addition and the acidic pH promoted the reductive dissolution of Fe(III)-oxides and the acidic dissolution of minerals which both involved OM release in the solution. Despite OM concentration, only 38 % of REE were estimated to be solubilized by the OM release in the chemical reduction experiment (Table AIII. 3).

c. Rare earth elements patterns

Upper continental crust (UCC) normalized REE pattern for the soil solution of each incubation experiment were plotted in Figure AIII. 4. The three soil solution corresponding to the Aerobic experiment at pH 7 and both Anaerobic experiments at pH 5 and without buffer pH exhibited similar REE pattern. They presented a MREE downward concavity (i.e. (La/Sm<1 and (Gd/Yb>1) (Figure AIII. 4). The REE pattern obtained for the chemical reduction experiment exhibited a flatter shape traduced by a La/Sm ratio >1 (Figure AIII. 5). However, as observed for the previously described patterns, the Gd/Yb ratio was > 1, the combination of both ratios provide evidence that, in the chemical reduction experiment, LREE (light rare earth elements) were more solubilized than HREE (heavy rare earth elements). The negative Ce anomaly was more developed than those obtained for the anaerobic and pH 7 aerobic experiments ($Ce/Ce^* \approx 0.77$ against 0.83 for the anaerobic and pH 7 aerobic experiments) (Figure AIII. 6). REE pattern developed in the soil solution of the Aerobic at pH 3 experiment exhibited a very different shape and MREE downward concavity did not appeared (Figure AIII. 4). Gd/Yd and La/Sm ratio were high with values upper to 2.5 suggesting that LREE were more solubilized than HREE (Figure AIII. 5). The negative Ce anomaly is the most developed among the series of experiments ($Ce/Ce^* \approx 0.69$) (Figure AIII. 6). A positive Eu anomaly ($Eu/Eu^* = 1.46$) is also developed on this REE pattern as displayed in Figure AIII. 4 and AIII. 6. In Figure AIII. 5 where the Gd/Yb ratio was reported relative to the La/Sm ratio, two groups of pattern shape might be distinguished. The first group corresponds to Aerobic experiment at pH 7 and both Anaerobic at pH 5 and without pH buffer experiments with La/Sm<1 and Gd/Yb>1. The second group was associated to a flatter shape with La/Sm and Gd/Yb>2.5 and correspond to the Aerobic experiment at pH 3. Pattern developed from the Chemical reduction experiment was intermediary with La/Sm<2.5 and Gd/Yb>1.

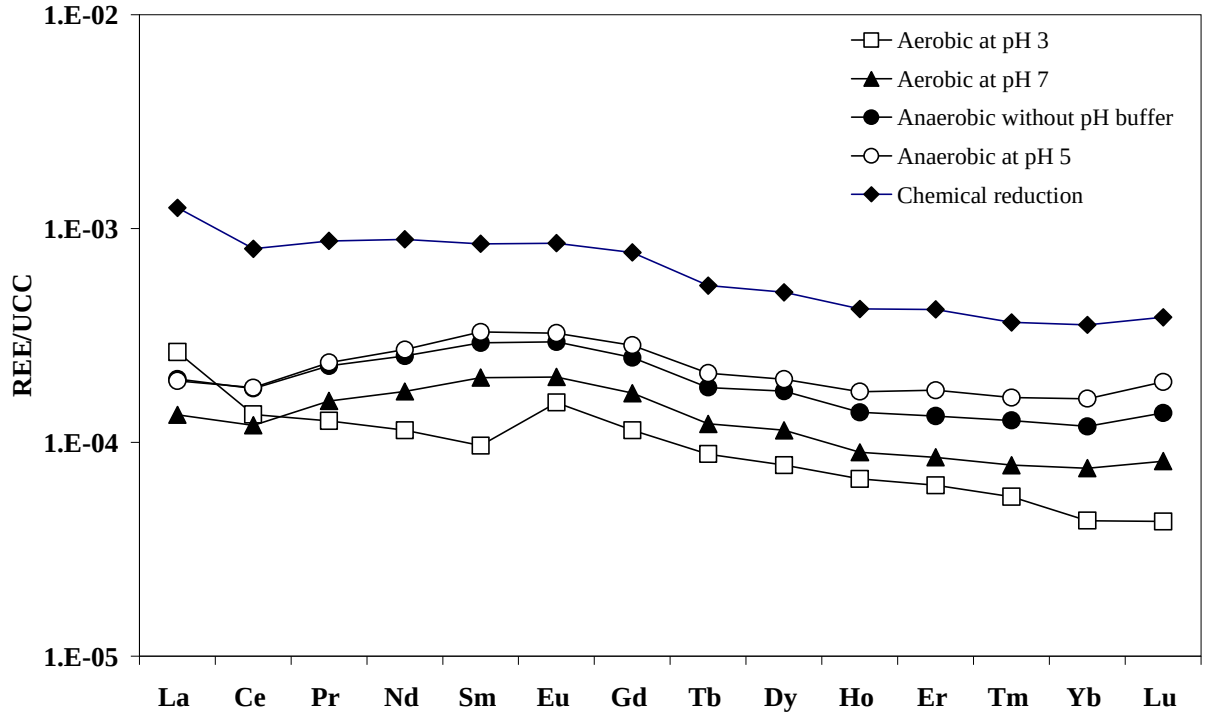

Figure AIII. 4. UCC (upper continental crust) normalized patterns of REE in the soil solution of each soil incubation experiments at steady state.

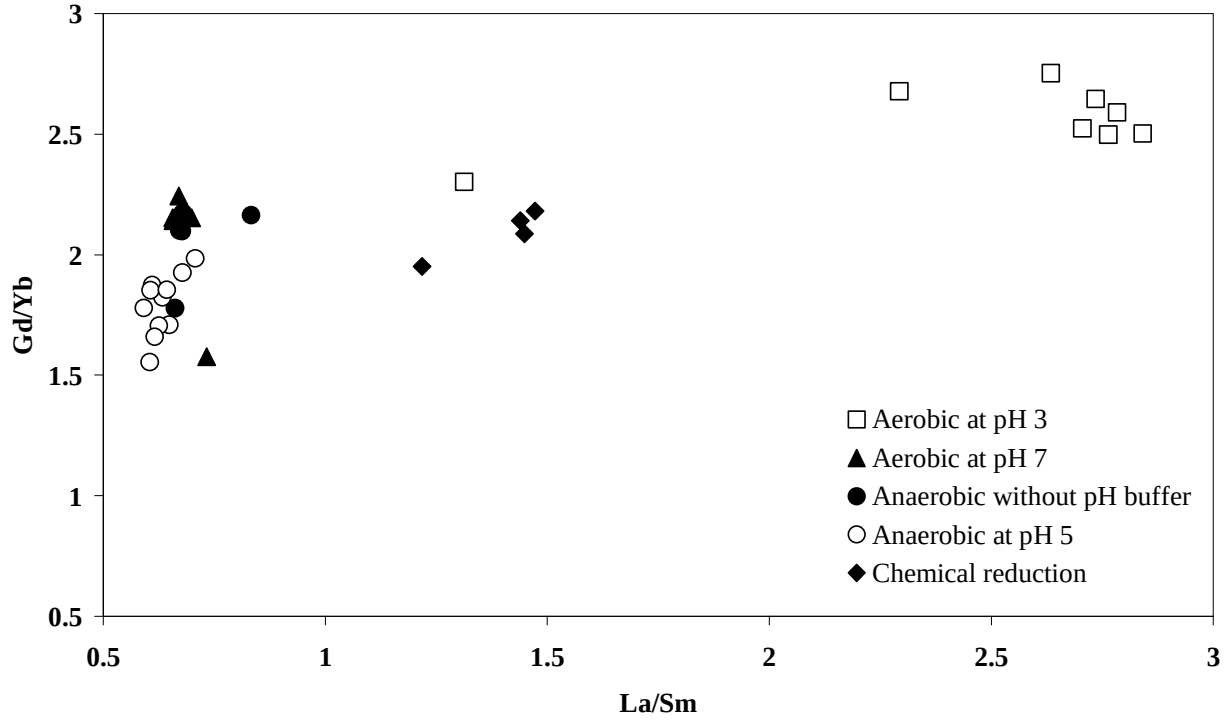

Figure AIII. 5. Gd/Yb reported relative to La/Sm of REE pattern of soil solution for each soil incubation experiments. The different point corresponds to samples recovered through the running time-experiment.

4. Discussion

a. REE patterns shapes and the resulting involved soil components

Anaerobic experiments. Whatever were the pH values, the REE patterns exhibited downward concavity allowing to conclude that REE speciation was dominated by complexation to OM (Davranche et al., 2005; Yamamoto et al., 2006; Pourret et al., 2007c) (Figure AIII. 4). Mass calculations also suggested that REE were probably totally bound to the OM present in the soil solution (Table AIII. 3). However, the anaerobic soil experiments might to involve two chemical mechanisms, (i) the reductive dissolution of soil Fe-oxyhydroxides and, (ii) the subsequent OM release. In consequence, the soil Fe-oxyhydroxides dissolution should have influenced the solution REE pattern. Yet, the obtained REE pattern was similar to the pattern resulting from the aerobic at pH 7 experiments where the only OM solubilization is promoted (Figure AIII. 4). It is important to note that the Fe-oxyhydroxides dissolution and pH increase in response to the redox reactions are known to promote themselves OM solubilization (Grybos et al., submitted 2009). Moreover, the present selective extractions provided evidence that REE occurring in the reductive fraction were as REE-organic matter complexes themselves bound to reducible Fe-oxyhydroxides (Figure AIII. 1). In this organic-rich wetland soil submitted to regular oxidation and reduction alternations, bacterially-reducible Fe is probably amorphous Fe(III) linked to organic matter. Roden and Zachara (1996) provided evidence that biotic reductive dissolution of amorphous Fe(III) was 20 to 100 times faster than for goethite and hematite respectively. Moreover, Olomu et al. (2005) show that Fe solubilized from eight waterlogged soil experiments was almost bound to organic matter. Peiffer et al. (1999) also demonstrated that, at the boundary between oxic and anoxic pore water from an organic-rich wetland soil, the oxidation of Fe(II) result in the formation of small Fe(III)-oxides colloids stabilized by surficially bound organic matter (able to pass through a 0.45 μm dialysis membrane). Pédrot et al. (2008) from reduction/re-oxidation wetland soil experiments obtained the formation of such Fe(III)-organic matter colloids and estimated their size range in between 0.2 μm and 30 kDa. Thompson et al. (2006), from TEM/EDS observations identified, these colloids release from redox oscillations as <160 nm and composed of an organic matrix embedded with nanoscale Fe-mineral particles. Therefore, in both presented anaerobic soil incubations, autochthonous reducing bacteria probably mainly reduced such amorphous Fe(III)-oxides strongly bound to organic matter which itself complexed REE. A direct consequence is the development of a

solution REE pattern which exhibited a downward concavity fingerprinting a REE organic matter complexation (Davranche et al., 2005; Yamamoto et al., 2006; Pourret et al., 2007c).

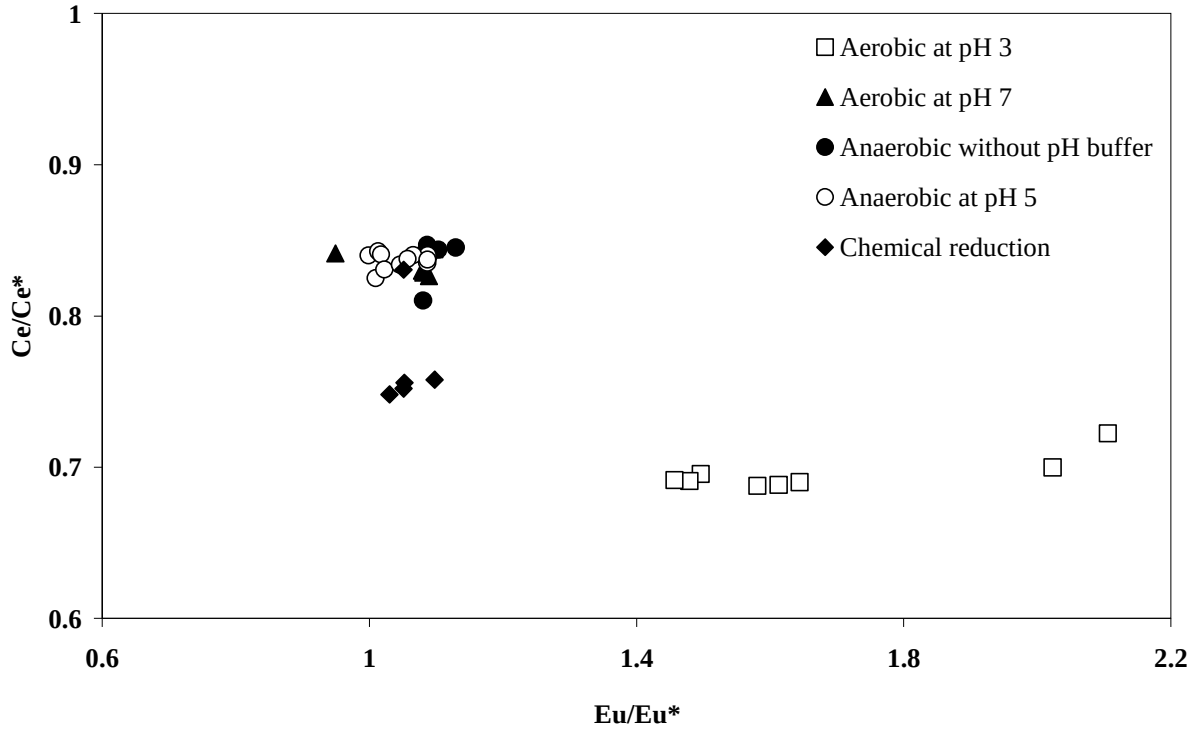

Figure AIII. 6. Ce anomaly (Ce/Ce*) reported relative to Eu anomaly (Eu/Eu*) developed in soil solution for each soil incubation experiments. The different point correspond to samples recovered through the running time-experiment.

Aerobic at pH 3 experiment. The REE pattern in solution resulting from the aerobic experiment at pH 3 was strongly different from REE pattern recovered from the other experimental conditions (Figure AIII. 4-6). Any downward concavity was observed while a slight enrichment in LREE and depletion in HREE appeared, and a positive Eu anomaly developed. Mass calculation estimated that only 26% of REE in solution were bound to the solubilized organic matter. Although the chosen pH promoted cation desorption from solid surface, the REE concentration in solution was the lowest obtained among the various conducted series of experiments. The here displayed REE pattern differs also strongly from the REE pattern developed in the F1 fraction of the sequential extractions performed on the soil sample which was supposed to induce the 'water and acid exchangeable' REE solubilization (Figures AIII. 1 and AIII. 2). The REE concentration in the F1 fraction is strongly lower than the REE concentration recovered in the aerobic at pH 3 experiments (1.25 10^{-9} mol L^{-1} against 4.64 10^{-5} mol L^{-1}). All these observations suggest that in the aerobic at pH3 experiment, REE desorption from soil solids surface was not the main mechanism that controlled the REE concentration in solution. The development of the positive Eu anomaly is

a significant and interesting point that could be used to explain the results. Aubert et al., (2001) and Compton et al. (2003) provided evidence that K-feldspar and plagioclase grains from fresh and altered granite showed a strong positive Eu anomaly, a slight enrichment in LREE and a depletion in HREE. Aubert et al. (2001) observed a corresponding positive Eu anomaly in the suspended and dissolved load of spring- and stream-waters and soil solution developed from an altered granite (Strenbach catchment, France). Moreover, the dissolution of plagioclase in this system was previously evidence by STEM analyses (Probst et al., 2000). From these data, Aubert et al. (2001) concluded that weathering of feldspars and plagioclase is an important process controlling the mobilization and fractionation of REE in soil and surrounding waters. It is important to note that Aubert et al. (2001) studies were carried out on a natural system where soil pHs were acidic averaging 4.5 (Strenbach catchment, France). Moreover, several authors showed that plagioclase are rapidly altered during granite weathering (Taylor and McLennan, 1985, 1988; Condie et al., 1995; White et al., 2001). Yan et al. (1999) who studied the geochemistry of REE in clay-rich till by applying sequential leaching method on tills samples, obtained also REE pattern with prominent Eu anomaly in the residual fraction of their extraction scheme. They attributed this Eu anomaly to the dissolution of feldspars and plagioclases which represent in average 18 wt.% of their sediment samples. Leybourne and Johannesson (2008) also suggested the Eu is retained preferentially in clays mineral during weathering of host rock. This literature data allow suggesting that the acidic pH applied in the present soil incubation experiment promoted the dissolution of plagioclase, K-feldspar or clays present in the soil sample. This hypothesis is reinforced by the strong concentration of Al ($4.14*10^{-4}$ $mol.L^{-1}$) released in the soil solution in this experiment. Moreover, this planosol sample is developed from alluvium and colluvium (Curmi at al., 1997) which is partly derived from the weathering of the underlying schist basement known to contain plagioclase and/or feldspar (Dabard et al., 1996).

The residual fraction of the sequential extractions does not exhibit the same Eu anomaly. However, this fraction is assumed to represent the soil resistant minerals, namely quartz, heavy minerals, well-crystallised minerals such as clays, feldspar, etc…This residual fraction is therefore the result of several minerals dissolution. REE pattern could be thus either the weighted sum of the different patterns corresponding to each mineral or, the pattern of the mineral in the higher proportion. This mineral mixing probably hid the Eu anomaly developed on the REE pattern of the K-feldspar or plagioclase in the residual fraction.

The development of a negative Ce anomaly on the REE pattern of the Aerobic experiment at pH 3 was evidenced by calculation (Figure AIII. 6). This calculation estimated that the Ce

anomaly was, in such experiment, the most negative obtained among the series of experiments. However, the observation of the REE pattern showed that soil solution is enriched in La as compared to Ce and Pr (Figure AIII. 4). This La enrichment could over estimated the Ce anomaly value. In consequence, this parameter was not discussed here.

Chemical reduction. In the chemical reduction experiment both reductive dissolution of soil Fe-oxyhydroxides and acidic dissolution of soil mineral (pH 3) were promoted. The mechanism of chemical reductive dissolution was strongly different from the bacteria-mediated reduction process. The chemical reductants, here hydroxylamine, adsorbed onto the hydrous oxide surface, exchange electrons with a Fe(III) surface center of the oxide. The electron transfer leads to an oxidized reactant and a surface Fe(II) atom that is easily detached from the surface. The dissolution is directly related to the surface concentration of the reductant (Dos Santos Afonso et al., 1990; Suter et al., 1991; Stumm and Sulzberger, 1992). Chemical reduction was therefore susceptible to dissolve Fe(III)-oxides colloids surficially coated by organic matter but also more crystallized Fe(III)-oxides particle able to adsorb reductants. In consequence, four main sources of REE could be identified in the chemical reduction experiment, (i) the mixed Fe(III)-organic matter colloids produced in the soil by oxic-anoxic conditions alternations (Peiffer et al., 1999 ; Olomu et al., 2005 ; Pédrot et al., 2008), (ii) the Fe(III)-oxides particles (probably more crystallized) weakly useable by Fe-reducing bacteria, (iii) the OM matter coated on the soil Fe(III)-oxides colloids/particles and (iv) the soil minerals themselves. The solubilization of this multiple REE sources is illustrated by the strong concentrations of REE, Fe, C and Al in the soil solution and the low calculated proportion of REE bound to OM (38%). This result reflected a stronger dissolution of Fe(III) colloids or particles and Al(III) from primary or secondary soil minerals. This REE multiple sources is also recorded by an intermediary REE pattern displaying Gd/Yb, La/Sm ratio and Ce and Eu anomaly values ranged between the value corresponding to the Aerobic experiment at pH 7 (REE source: OM) and Aerobic experiment at pH 3 (main REE source: soil minerals) (Figure AIII. 4-6).

b. REE pattern as fingerprint of peculiar soil component activation

The source of REE in soil is the primary minerals originally from the native rock-weathering. However, the factors responsible of the REE retention in soil is not well understood but may be related to the preferential sorption onto Fe(III)-oxides (Koeppenkastrop and De carlo, 1993; White et al., 2000), clays minerals (Coppin et al. 2002)

as well as colloidal OM (Tang and Johannesson 2006; Grybos et al., 2007; Pourret et al., 2007c). The dissolution of each soil phases may induce the solubilization of associated REE (adsorbed or substituted) into the soil solution. In the present study, the REE patterns developed in the soil solution in response to the reductive dissolution were indeed strongly different from the REE pattern obtained from the soil acidic dissolution. The difference was assigned to the nature of the dissolved soil components such as colloid or particle of Fe(III) or, alumino-silicates. Therefore, the comparison between the REE patterns from each type of experiment allowed to precise (i) the nature and chemical form of involved Fe(III)-pool and (ii) the impact of OM on the REE distribution. Thereby, it appeared that the biological reduction of wetland soil (namely organic-rich soil) does not concern crystallized Fe(III)-oxide particles but more probably amorphous OM bound Fe(III)-colloids. Moreover, as previously demonstrated by Grybos et al. (2007) the present result provide a new evidence of the control of the REE mobility by the OM dynamic in wetland soil.

5. Conclusions

Chemical and biological reductive dissolution of soil and their consequence on the ions mobility was largely studied in laboratory (e.g. Dos Santos Afonso et al., 1990; Suter et al., 1991; Stumm and Sulzberger, 1992; Davranche and Bollinger, 2000a-b, 2001; Roden and Zachara, 1996, Roden 2003). To discriminate between the possible involved chemical mechanism, the experimental system was often extremely simplified, a reducing agent (chemical reductants or reducing bacteria) and synthetic or extracted from the natural system Fe-oxyhydroxides were mixed together. If such followed experimental methodology allows describing and evaluating the major parameters implicated in the reaction (bacteria cell density, ionic strength, temperature…), it presents the great disadvantage to ignore the influence of the other natural soils phases (either organic or mineral). Thereby, the impact of organic matter on the mobilization of ions in wetland soil under reductive conditions was regularly by-passed. However, Thompson et al. (2006) provide evidence that proton production/consumption associated with Fe redox cycling has important implications for mobilization organic colloid-borne trace elements; and Grybos et al. (2007) demonstrated that the soil colloidal OM is one of the major factor implicated in the mobilization of ions from organic soil. The present studied showed that the REE pattern development in soil solution in response to specific chemical reactions could be a way to identify the involved soil phases. Due to their surface properties and their REE concentration inherit from the native-rock

weathering, soil secondary, primary minerals and OM are susceptible to exhibit their own REE pattern. Since each phases could be activated by a specific chemical process, the resulting REE pattern could then traduced the nature of the phases or their mixing activated by this specific chemical process. In the present study, the comparison between REE patterns of the soil solution obtained from three soil incubations under anaerobic and aerobic (pH 3 and 7) conditions allowed the identification of the nature and the form of the involved soil phases when reductive dissolution is running. It appeared that under reductive conditions, the autochthonous reducing bacteria used preferentially small Fe(III)-oxides colloids stabilized by surficially bound organic matter as compared to stabilized (more crystallized) Fe-oxide particles. The REE charge of the preserved primary mineral and crystallized soil particles are preferentially released under strong acidic conditions.

The present study showed the potential of REE to be used as a tracer of chemical processes in soil. However, it is important to note that this potential is only revealed when contrasted REE pattern shape could be identified when coupling the experiments performed under various chemical conditions.

Acknowledgments

We thank the technical staff in Rennes, both at Géosciences-Rennes for their assistance during preparation and chemical analyses. This research was funded mainly by the French CPER program "Dévelopement de la recherche sur la maîtrise de la qualité de l'eau en Bretagne" jointly funded by the city of Rennes and the French ministry of Education and Research and the French ANR ‘Programme Jeunes chercheuses - jeunes chercheurs : Rare earth elements partitioning at solid-water interface: Impact on REE geochemical behaviour and tracing properties'.

IV. Annexe 4 : Increasing pH drives organic matter solubilization from wetland soils under reducing conditions

Article soumis à la revue *'Geoderma', auteurs :* Malgorzata Grybos[1], Mélanie Davranche*, Gérard Gruau, Patrice Petitjean and Mathieu Pédrot

Abstract

In wetlands, large quantities of dissolved organic matter (DOM) are solubilized under reducing conditions. Controlled incubations of a wetland soil were performed under aerobic and anaerobic conditions to investigate the extent to which the following processes account for this phenomenon: i) production of organic metabolites by microbes during soil reduction; ii) release of organic matter (OM) from Mn- and Fe-oxyhydroxides that undergo reductive dissolution; and iii) desorption of OM from soil minerals due to pH changes. Anaerobic incubation releases 2.5% of the total soil organic carbon (OC) as dissolved organic carbon (DOC), and is accompanied by a pH rise from 5.5 to 7.4 and by the soil Mn- and Fe-reduction. The three above processes all take place. However, anaerobic incubation at a constant pH of 5.5 (preventing OM desorption) releases only 0.5% of the total soil OC, while aerobic incubation at pH 7.4 (preventing Mn- and Fe-reduction) releases 1.7% of the total soil OC. By contrast, aerobic incubation at pH 5.5 (preventing both Mn- and Fe-reduction and pH rise) does not solubilize any DOC. The DOC released is markedly aromatic, indicating little contribution from microbial metabolites, but, rather, the presence of microbes leading to OM mineralization. The pH rise is the key factor controlling OM solubilization under reducing conditions. This rise of pH accounts for > 60% of the total released DOC, which is not due to reductive dissolution as such.

Key-words: organic matter, pH, reductive dissolution, Mn- Fe- oxyhydroxides, DOC

1. Introduction

Water-table rise in wetland areas often leads to water saturation of the uppermost organic-rich soil horizons, which involves the release of large quantities of dissolved organic matter (DOM) into the soil solution. Studies investigating the dynamics of DOM release in wetlands under field conditions report positive correlations between DOM, Mn(II) and Fe(II)

concentrations (Hagedorn et al., 2000; Olivié-Lauquet et al., 2001; Gruau et al., 2004). This suggests that the establishment of soil conditions able to reduce Mn and Fe could be a key factor in enhancing DOM release in wetlands.

What are the inter-relationships between the processes of Mn and Fe reduction and DOM release? At least three hypotheses can be proposed: (i) reductive dissolution leading to release of organic matter (OM) bound to Mn- and Fe-oxyhydroxides; (ii) pH change accompanying reduction reactions involving OM desorption; (iii) production of DOM during reduction of microbial biomass present in soil. The first hypothesis ("dissolution") assumes that the solubilized DOM is derived from OM originally bound onto Mn- and Fe-oxyhydroxides. Indeed, along with clay minerals (Jardine et al., 1989; Kahle et al., 2003; Fiedler and Kalbitz, 2003), Mn- and Fe-oxyhydroxides strongly adsorb OM (Tipping & Heaton, 1983; Gu et al., 1994; Avena and Koopal, 1999, Chorover & Amistadi, 2001). However, when soils become water saturated, the microorganisms that normally use oxygen as the terminal electron acceptor for OM oxidation will change over to other electron acceptors such as manganese and iron. This results in the reductive dissolution of Mn- and Fe-oxyhydroxides (Stumm and Sulzberger, 1992), followed by a release of associated substances (adsorbed, coated and substituted) (Davranche and Bollinger, 2000a-b, 2001), including the OM (Quantin et al., 2001; Zachara et al., 2001).

The second hypothesis (desorption) assumes that DOM release occurs in response to pH change. Reduction reactions consume protons, which may increase the pH of the soil solution (Ponnamperuma et al., 1966; Stumm and Sulzberger, 1992). Thompson et al. (2006) have provided evidence that proton production/consumption associated with Fe-redox cycling has important implications for the mobilization of colloid-borne trace elements and sorbed contaminants. The capacity of mineral phases to adsorb OM strongly decreases with increasing pH (Gu et al., 1994; Vermeer et al., 1997; Avena and Koopal, 1999). At low pH, protonated hydroxyl groups generate a positive charge on the mineral surfaces, which induces adsorption of negatively charged organic molecules and promotes surface complex formation. Changing from neutral to basic conditions, (i) deprotonation of the hydroxyl groups at mineral surfaces decreases the positive net surface charge and (ii) organic molecules become more electronegative. Hence, mineral surfaces and OM repel each other and thus limit surface complex formation. Therefore, DOM is released into solution (Avena and Koopal, 1998). In this case, the released DOM will be made up of OM derived from adsorbent soil minerals (i.e. Mn- and Fe-oxyhydroxides, clay minerals, etc.), and not just the OM from Mn- and Fe-oxyhydroxides as in the "dissolution" hypothesis.

Finally, the third hypothesis (microbial) assumes that DOM release is due to the production of soluble organic metabolites by the soil microbial biomass (Christ and David, 1996). Recent studies have shown that microbial metabolites may account for a significant proportion of soil DOM (Kalbitz et al., 2000). According to these studies, the microbial metabolite fraction of DOM is composed of smaller and less reactive molecules than the humic acid fraction. Several authors have also shown that microbial activity is stimulated by pH increase (Andersson and Nilsson, 2001).

It is difficult to assess the effect of microbial metabolite production, pH changes and reductive dissolution on DOM release because these processes operate simultaneously as the soil becomes reduced. In this study, to evaluate the effects of these processes separately, we use soil incubation experiments under anaerobic and aerobic conditions with or without buffered pH.

2. Materials and Methods

V. Soil sampling and soil characteristics

The soil sample was collected from the upper soil organo-mineral horizon (Ah) from a planosol (according to the WRB classification, (ISSS-ISRIC-FAO, 1998)) of the Mercy wetland located in the Kervidy-Coët Dan subcatchment in Brittany, Western France. This wetland has been intensively surveyed from the hydrological, pedological and geochemical points of view (Durand and Torres, 1996; Mérot et al., 1995; Curmi et al., 1998; Dia et al., 2000; Olivié-Lauquet et al., 2001). Wetlands in the Kervidy-Coët Dan subcatchment cover 15% of the total surface-area (5 km^2). The natural hydraulic gradients between upland and bottomland domains, as well as the poor natural drainage in the overall area, lead to seasonal waterlogging (between November-December and March-April) of the bottomland domains, with the development of hydromorphic soils (Curmi et al., 1998; Bourrié et al., 1999). Approximately 10 kg of soil were collected from the surface layer (0-10 cm), sieved at 2-mm and stored at 4°C. After soil sample fusion with $LiBO_2$ and acid digestion with HNO_3, the major element composition was determined at the CRPG laboratory in Nancy, France, by inductively-coupled plasma atomic emission spectrometry (ICPAES, Jobin-Yvon JY 70) (Table AIV. 1). The organic carbon content was determined at the CNRS Analytical Research Facility - SARM - (France), using an oxygen combustion method with a CS Analyzer (LECO SC 144DRPC) (Table AIV. 2). The soil organic matter content was estimated by multiplying

the organic carbon concentration of the analysed soil sample by the Van Bemmelen factor of 1.724 (Nelson and Sommers, 1982), yielding a value of 10.12 % (anhydrous basis) (Table AIV. 1). The upper soil in the Mercy Wetlands is considered as an organic acid soil dominated by silt: Total Silt = 60.7%, pH = 5.9. This soil is richer in humic than in fulvic acids, which implies a relatively slow degradation of organic matter with a fulvic to humic acid ratio of 0.54.

Table AIV. 1. Chemical composition of soil sample.

	SiO_2	Al_2O_3	Fe_2O_3	MnO	MgO	CaO	Na_2O	K_2O	OM
%	59.2	13.7	4.71	0.01	0.48	0.14	0.14	2.27	10.12

The Fe and Mn distribution in soil phases was determined following the three-step BCR extraction scheme (Mossop, 2003) (Table AIV. 2). This method indicates that 23 % of Fe is contained in the reducible fraction (probably as Fe-oxyhydroxides), 24% in the oxidizable fraction (as organic complexes or as sulphides) and 52% in the residual fraction (as well crystallized Fe(III)-oxides or in clays and/or primary minerals). Mn is mainly distributed in the exchangeable and reducible fractions (27.3 and 28.6 %, respectively). Only 8% of Mn is present in the oxidizable fraction, being bound to organic matter or as sulphides.

Table AIV. 2. BCR sequential extraction scheme and proportion of Fe and Mn distributed in each soil phase

Soil phases	Extractant	Shaking time and temperature *	% Mn	% Fe
Water- and acid-soluble and exchangeable	40 mL 0.11 M CH_3COOH	16 h at room temperature	27.3	0.1
Reducible	40 mL 0.5 M $NH_2OH.HCl$ (pH 2)	16 h at room temperature	28.6	23.0
Oxidizable	10 mL 8.8 M H_2O_2(pH 2) 10 mL 8.8 M H_2O_2(pH 2) 50 mL 1 M NH_4Oac (pH 2)	1 h at room temperature 1 h at 85 °C 16 h at room temperature	8.4	24.3
Residual	15 mL aqua regia 10 mL aqua regia	Heating to dryness	35.8	52.6

*. The BCR sequential extraction procedure was applied in triplicate to 1 g of dried soil sample.

c. Experimental set-up

The experimental procedure was based on a series of four laboratory experiments (1) anaerobic without pH buffer, (2) anaerobic at pH 5.5, (3) aerobic at pH 7.4, (4) aerobic at pH

5.5. Additional abiotic incubations were performed with a soil sample sterilised using sodium azide (NaN_3) under aerobic conditions at pH 7.4 and pH 5.5. Soil suspensions were prepared at 1/20 dry soil/solution ratio by mixing approximately 95 g of soil with a solution containing 0.48, 0.85 and 0.1 mol L^{-1} of NO_3^-, Cl^- and SO_4^{2-}, respectively, to mimic the anion composition of the soil solution in the Mercy wetland system during autumn (period of water-table rise). The suspension was placed in an air-tight, 1-litre batch Prelude reactor (Guerin, Biolafite) in a water bath at 30°C. The suspension was continuously stirred, with a stream of $N_2 \pm O_2$ gas continuously supplied via an auto-gas injection system at 2 l min^{-1} for the first 2 h and then at 0.2 l min^{-1}. The Eh and pH of the suspension were monitored with combination electrodes (Malter Pt 4805 DXK-S8/225 and Malter HA 405-DPA-SC-S8/225, respectively). For experiments at controlled pH, the pH was adjusted by addition of 0.5 M HCl or 0.5 M NaOH. Approximately 20 ml of soil suspension was drawn off daily with a sterile syringe (under N_2 gas in the anaerobic treatments), centrifuged for 10 min at 1950g, and filtered through a 0.2 µm cellulose acetate membrane filter (Millipore). The samples were analysed for dissolved organic carbon (DOC), nitrate, Fe(II), total Fe and total Mn as well as UV absorbance as described below.

d. Soil solution analyses

Dissolved organic carbon (DOC) was determined in triplicate on a Shimadzu 5050 TOC analyzer. For the present study, the relative standard deviation (RSD) was systematically less than 2%. DOC measurements were corrected using ultrapure water blanks (blank level < 0.2 mg L^{-1}). The accuracy of DOC concentration measurements was estimated at ±5%, as determined by repeated analyses of freshly prepared standard solutions (potassium biphtalate).

Iron (II) was analysed using the 1.10 phenantroline colorimetric method, AFNOR NF T90-017 (AFNOR, 1997), using a UV-visible spectrophotometer (UVIKON XS, Bio-Tek) with a precision of 5%. Total Fe and Mn concentrations were determined by ICP-MS (HP 4500, Agilent Technologies HP4500) using indium as an internal standard. Prior to ICP-MS analysis, samples were digested with 14 N HNO_3 at 100°C, then evaporated to complete dryness and taken up in 0.4 N HNO_3 to avoid interference with OM during mass analysis. The international geostandard SLRS-3 was used to check the accuracy and reproducibility of the results. Typical uncertainties including all error sources were below ± 5 % for Fe and Mn.

Nitrate concentrations were analysed by ionic chromatography (Dionex, DX120), with a precision of about ±4%.

SUVA (Specific UltraViolet Absorbance) - strongly correlated with aromaticity percentage of the organic matter (Aromaticity = 6.52 * SUVA + 3.63) (Weishaar et al., 2003) - was used as an indicator of the chemical composition of dissolved organic carbon. $SUVA_{254}$ is defined as the UV absorbance of a water sample at 254 nm normalized to the DOC concentration, expressed in milligrams per litre per metre (±5%. precision). UV absorbance measurements were performed on an UVIKON XS (Bio-Tek) spectrophotometer with distilled water as blank. We tested for potential interference from inorganic species (Weishaar et al., 2003), but failed to detect any NO_3^- absorbance influence at λ=254 nm. Interference of Fe absorbance at λ=254 nm was taken into consideration and corrected.

3. Results

a. Anaerobic experiment without pH buffer

In the anaerobic experiment without pH buffer, Eh decreases rapidly from 500 mV to 100 mV during the first 100 h. After 280 h, Eh decreases more slowly and falls to approximately –50 mV (Figure AIV. 1a). Over the first 200 h, the pH increases from 5.5 to ca. 7.4, and then remains constant during the last 80 h of incubation (Figure AIV. 1a). The NO_3^- concentration decreases rapidly to reach 0 at 50 h (Figure AIV. 1b). The NO_3^- decrease is followed by a rapid increase of Fe and Mn concentrations (Figure AIV. 1b). Mn and Fe solubilization is rapid between 90 and 160 h. Out of the total amount of Fe and Mn released during the experiment, 80% is solubilized during the run time. After 160 h, the Fe and Mn concentrations remain constant at 0.25 mmol L^{-1} and 7.28 µmol L^{-1}, respectively. From 90 hours to the end of the experiment, 100% of the Fe in solution is in the form Fe(II).

OM is strongly solubilized into solution, with the DOC concentration reaching 10.3 mmol L^{-1} after 280 h of incubation. As shown in Figure AIV. 1b, DOC starts to increase after about 40 h of anaerobic incubation. The increase is rapid from 40 to about 140 h, slower between 140 and 250 h, and very slow after 250 h. The aromaticity of the released DOC increases from 22 to 35% within the first 110 h of incubation then remains constant at 34.5±1.2% (Figure AIV. 4).

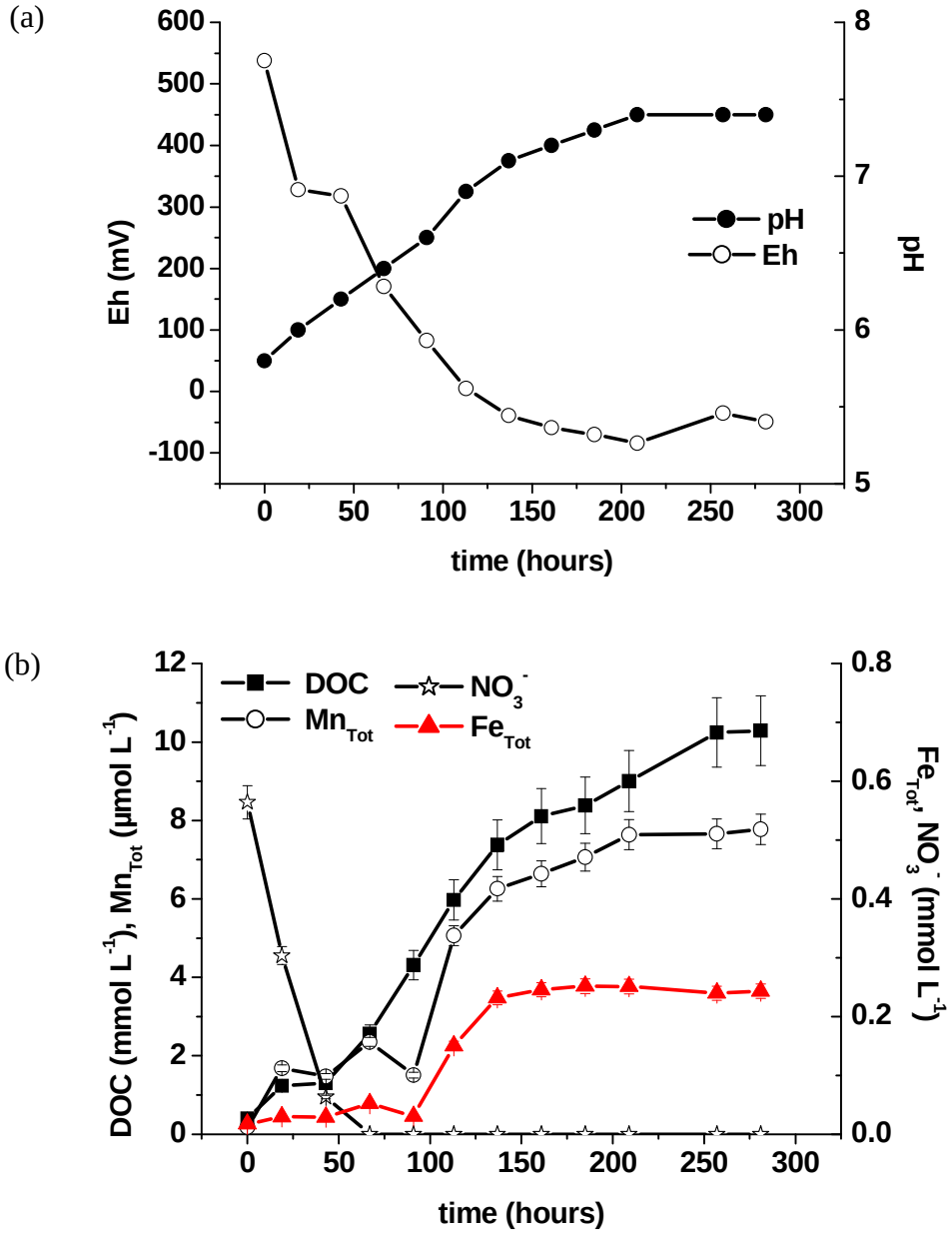

Figure AIV. 1. Time-variation of Eh and pH (a), and dissolved organic carbon (DOC), Fe_{Tot}, Mn_{Tot} and NO_3^- concentrations (b) for anaerobic experiment without pH buffer.

b. Anaerobic experiment at pH-5.5

A rapid decrease of Eh is produced during the first 100 h of soil incubation, followed by a slow decrease down to 75 mV after 280 h (Figure AIV. 2a). During the first 70 h of incubation, there is little or no reductive dissolution of Fe-oxyhydroxides. Afterwards, dissolved Fe increases exponentially until the end of the experiment, reaching 4.53 mmol L^{-1} (Figure AIV. 2b). Proton addition shifts the chemical equilibrium towards production of Fe(II). Periodic Fe(II) measurements show that 100% of solubilized Fe is present as Fe(II).

Mn concentration increases continuously during the incubation without reaching equilibrium (Figure AIV. 2b).

The initial DOC concentration is 0.46 mmol L^{-1}, which is close to the initial concentration of the anaerobic experiment without pH buffer. DOC concentration increases as soon as the setting up of anaerobic conditions, and increases until the end of the experiment (Figure AIV. 2b), reaching 8.94 mmol L^{-1}. The aromaticity of DOC increases from 22 to 33% between 0 and 50 h, and then remains constant at 32.1±0.6% (Figure AIV. 4).

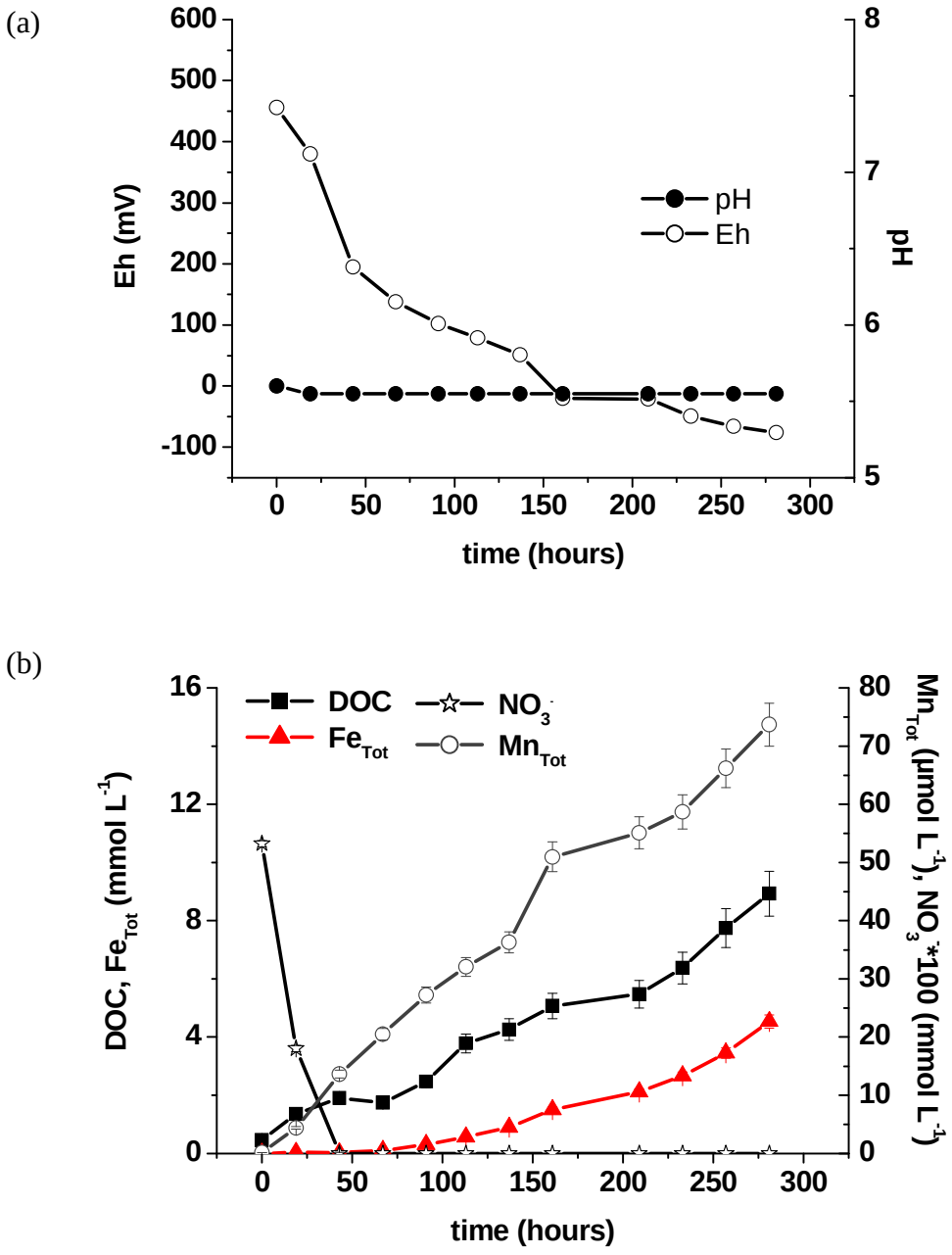

Figure AIV. 2. Time-variation of (a) Eh and pH, (b) dissolved organic carbon (DOC), FeTot, MnTot and NO3- concentrations for anaerobic experiment at pH 5.5.

c. Aerobic experiment at pH 7.4 and 5.5

In both aerobic experiments, Fe is poorly solubilized (7.1±1.8 µmol l^{-1} and 3.5±1.8 µmol l^{-1}, respectively) (Figure AIV. 3) and occurs in the Fe(III) state.

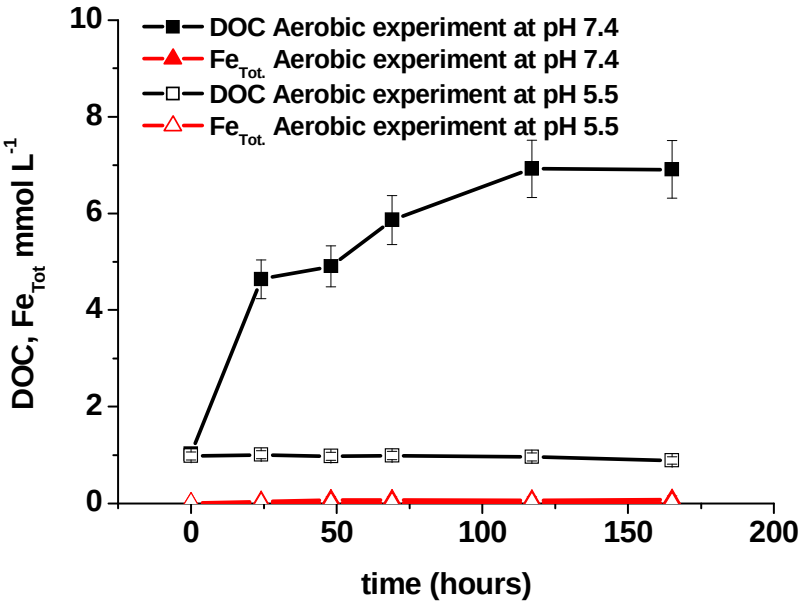

Figure AIV. 3. Time-variation of dissolved organic carbon (DOC) and $Fe_{Tot.}$ concentration during anaerobic experiments at pH 7.4 and pH 5.5.

In the aerobic experiment at pH 7.4, DOC concentrations increase rapidly during the first 25 h of incubation, from 1.02 to 4.64 mmol.L^{-1}, then more slowly between 25 and 120 h to reach 6.92 mmol L^{-1}. Subsequently, DOC concentration remains constant at 6.9±0.17 mmol.L^{-1} until the end of the experiment (Figure AIV. 3). In the aerobic experiment at pH 5.5, DOC increases rapidly to reach a constant level at 0.98±0.02 mmol L^{-1} after 120 h of incubation. Then, DOC starts to decrease to 0.88 mmol.L^{-1} (Figure AIV. 3).

The aromaticity of DOC in the aerobic experiment at pH 7.4 increases during the first 40 h, from 26 to 36.4%, then remains constant at 36.7±1.0% until the end of the experiment. In the aerobic experiment at pH-5.5, DOC maintains a constant aromaticity of 25±0.9% during the first 120 h, which decreases to 23±0.02% at the end of the experiment (Figure AIV. 4).

The final DOC concentration is 9.95 mmol.L^{-1} and 2.46 mmol.L^{-1} in the abiotic experiment at pH-7.4 and the aerobic experiment at pH-5.5, respectively.

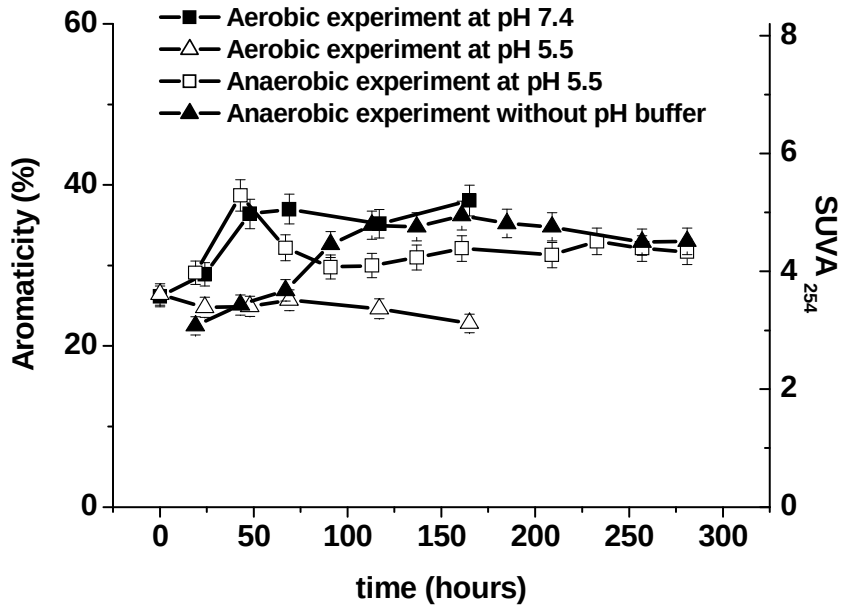

Figure AIV. 4. Time-variation of $SUVA^{254}$ and aromaticity of dissolved organic matter (DOC) in the corresponding experiments.

4. Discussion

The experimental approach used here demonstrates that OM can be mobilized under reducing conditions in wetland soils, as previously shown by several field studies, (Hagedorn et al., 2000; Olivié-Lauquet et al., 2001; Gruau et al., 2004). In anaerobic experiments, most of this release is concomitant with Fe and Mn solubilization, as encountered during field studies (e.g. Gruau et al., 2004). At the beginning of anaerobic soil incubation, all the Fe present in solution is in the Fe(III) state, most probably as soluble Fe(III)-organic complexes. Soil extractions experiment show that about 24% of Fe is present in the oxidizable fraction, probably bound to organic matter. However, after reduction of NO_3^-, solubilized Fe is in the Fe(II) state, indicating that soil Fe-oxyhydroxides have been reductively dissolved (Figure AIV. 1b). Moreover, Eh-pH values (-75 mV; pH=7.4, after 280 hours) correspond to the critical Eh-pH for Fe reduction in soils, as shown by several authors; these values are situated around 300 mV at pH 5, between 300 and 100 mV at pH 6-7, and around -100 mV at pH 8 (Gotoh and Patrick, 1974; Patrick and Henderson, 1981; Patrick and Jugsujinda, 1992). The fall in Eh is accompanied by a continuous pH increase from 5.5 to 7.4 (Figure AIV. 1a). An enhancement of pH is commonly observed in acidic waterlogged soils, produced by the consumption of protons required for the reduction of NO_3^-, Mn and Fe (Ponnamperuma, 1972; McBride, 1994; Quantin et al., 2001). However, in the present experiments, the soil buffer capacity might be modified by the flushing out of the CO_2 due to the continuous

stirring of soil suspensions. Nevertheless, the experimental final pH is close to field pH values (between 6.5 and 6.9) measured during the flooding period (Dia et al., 2000; Olivié-Lauquet et al., 2001).

The anaerobic experiment without pH buffer demonstrates that the setting up of reducing conditions favouring the reductive dissolution of Mn- and Fe-oxyhydroxides can lead to the mobilization of DOC in wetland soils. This experiment also shows that the reduction process is accompanied by a marked increase of soil pH.

a. Role of microbial metabolites

Microbial metabolites are poor in aromatic carbon, and are associated with an aromaticity of generally less than 16%. By contrast, soil humic substances (i.e. dominant source of DOC in soils; see Kalbitz et al., 2000) are enriched in aromatic carbon, and thus display higher aromaticity (35%) (Chin et al., 1994; Weishaar et al., 2003). As shown in Fig. 4, the final aromaticity of DOC is between 23 and 37%, thus corresponding to dissolved humic substances (Chin et al., 1994; Weishaar et al., 2003). The lowest values are obtained either in experiments carried out or beginning at pH 5.5. At this pH, the desorption of OM is not promoted, and only exchangeable and probably hydrophilic organic molecules with lower aromaticity are released into the soil solution. The highest aromaticity was obtained in the aerobic experiment at pH 7.4, although metabolite production under aerobic conditions is known to be more pronounced than under anaerobic conditions.

The second indication provided by our study is that, in the aerobic experiment at pH 5.5 (no pH rise, no Fe(III) reduction), the DOC concentration remains constant during the first 120 h of incubation (Fig. 3). Therefore, no significant microbial metabolite production and/or OM decomposition occurs. DOC decrease can lead to OM mineralization. Consequently, in the aerobic experiment at pH 7.4, DOC solubilization is mainly the result of OM desorption from soil solid phases in response to the imposed pH (7.4).

Therefore, in the anaerobic experiment without pH buffer, the released DOC consists primarily of soil humic substances with little or no contribution from microbial metabolites.

b. Reductive dissolution of Mn- and Fe-oxyhydroxides versus pH rise

The kinetics of DOC release in the anaerobic experiment without pH buffer is more closely linked to the variation of pH with time than Fe solubilization kinetics (Figure AIV. 1a

and AIV. 1b). In particular, i) when Fe(II) concentration starts to build up (90 h; Figure AIV. 1b), DOC has already increased by a factor of 5, and ii) DOC concentration is enhanced after Fe reaches a steady state (at 140 h), (Figure AIV. 1b).

According to figure AIV. 1, pH rise might be a key factor controlling the onset of DOC solubilization in the anaerobic experiment without pH buffer. The influence of pH on DOC release has been observed in several field and laboratory studies. Avena and Koopal (1998), Kaiser and Zech (1999) show that high pH promotes OM desorption from Mn- and Fe-oxyhydroxides. Whitehead et al. (1981) and Kalbitz et al. (2000) report a positive correlation between DOC and pH in organic soil horizons. But what are the possible reactions that can induce a rise in pH (Figure AIV. 1a)? The reduction of nitrate and Fe(III) involves two proton-consuming reactions that take place in the anaerobic experiment without pH control/?buffer. However, all the NO_3^- is reduced after ca. 70 h, while Fe(III) reduction ceases after ca. 140 h (Figure AIV. 1b). Why does the pH continue to increase (by ca. 0.4 pH units) after 140 h? Reduction of SO_4^{2-} could result in proton consumption. However, the SO_4^{2-} concentration stays constant throughout the incubation time (reducing conditions never becoming favourable for sulphate reduction - data not shown). Another possible explanation is that Mn(IV) reduction takes place after 140 h, consuming protons between 140 h and 280 h. Dissolved Mn concentrations increase by almost 20% in the anaerobic experiment without pH buffer after about 140 h. Mn(IV) is more reactive with organic compounds than Fe(III), and reduction of Mn(IV) occurs before Fe(III). In this way, 28.6 % of total soil Mn is present in the reducible fraction obtained by the extraction procedure, probably as Mn oxides. However, under near-neutral pH conditions, several organic compounds (such as oxalate, pyruvate and syringic acid) could reduce Mn(IV), while Fe remains oxidized (Stone and Morgan, 1984; Lovley and Phillips, 1988; Lovley et al., 1994). Reduction of Mn(IV) by Fe(II) at pH 7 has also been documented, and could be an alternative mechanism for Mn reduction (Lovley and Phillips, 1988; Myers and Nealson, 1988; Nealson and Myers, 1992).

It is also possible that Fe(III) reduction still occurs after 140 h of incubation, although Fe(II) concentration in soil solution appears to reach a steady state. After 140 h, Fe(II) concentration might be controlled by the precipitation of Fe(II)-bearing minerals such as green rust $Fe_6(OH)_{12}SO_4.3H_2O$ (log Ksp = -127.5) (Hansel et al., 1994) and/or Fe(II)-hydroxide (log Ks = -14.7). To evaluate this hypothesis, we make use of the geochemical modelling program PHREEQC (version 2.12.5) (Parkhurst and Appelo, 1999). Mineral saturation indexes are calculated using the chemical composition of the experimental solution after 280 h. Calculated saturation indexes (SI) are -5.41 for green rust and -1.79 for Fe(II)

hydroxide. The experimental solution is therefore under-saturated with respect to these two mineral phases. Between 90 and 140 h, reduction of both the Mn and Fe takes place simultaneously with pH rise and contributes to some extent to the total amount of DOC finally released.

Two approaches are used to quantify the proportion of DOC released by each mechanism. In the first approach, the results of the aerobic experiment at pH-7.4 are used to quantify the amount of DOC that can be solubilized due solely to the rise in pH. This amount is compared to the amount of DOC released in the anaerobic experiment without pH buffer. In the second approach, results from the anaerobic experiment at pH-5.5 are used to calculate the amount of DOC released by the reductive dissolution of Mn- and Fe-oxyhydroxides alone. When the Fe(II) concentration is equal to the final Fe(II) concentration, in the anaerobic experiment without pH control/?buffer, we compare the amount of DOC solubilized with the total amount of DOC released. Finally, the fraction of released DOC calculated from the anaerobic at pH-5.5 experiment is compared with the fraction based on the aerobic experiment at pH 7.4 (Table AIV. 3).

Table AIV. 3. Dissolved organic carbon (DOC) solubilized in anaerobic and aerobic experiments.

	Concentration (mmol L^{-1})					OM solubilized by		
Experiments	**Fe(II)**	**Initial DOC**	**Final DOC**	**Delta DOC**	**%**	**Fe reduction**	**OM desorption**	**Microbial activity**
Anaerobic without pH buffer	0.25	0.04	10.30	9.89	100	X	X	X
Anaerobic at pH 5.5	0.25	0.45	2.20	1.74	17.64	X	-	X
Aerobic at pH7.4	0	1.02	6.74	5.90	59.61	-	X	X
Aerobic at pH 5.5	0	0.98	0.88	(-) 0.10	(-)10	-	-	X

The solubilized DOC concentration is 10.3 mmol L^{-1} in the anaerobic experiment without pH buffer, as against 6.92 mmol L^{-1} in the aerobic experiment at pH 7.4. In the anaerobic experiment without pH buffer, the amount of released DOC due to pH rise corresponds to 60% of the total solubilized DOC. The final concentration of Fe(II) in the anaerobic experiment without pH buffer is 0.25 mmol L^{-1} wheareas, in the anaerobic experiment at pH 5.5, this Fe(II) concentration is attained after 80 h of incubation. The amount of DOC solubilized at this time (80 h) corresponds to 1.75 mmol L^{-1}. Thus, 18% of the total amount of DOC present at the end of the anaerobic experiment without pH buffer would appear to be released by the dissolution of Mn- and Fe-oxyhydroxides.

Therefore, reductive dissolution of Mn- and Fe-oxyhydroxides is much less important than pH in controlling DOC release. Reductive dissolution accounts for only 18% of the total amount of DOC, as against 60% brought about by the pH increase. The pH increase involving OM desorption could thus be considered as the determining parameter in the degradation of the OM-mineral association. Thomson et al. (2006) drew a similar conclusion from a study of colloid mobilization during oscillations of Fe-redox conditions. They showed that pH exerted a major control on colloid dispersion during the redox cycle, masking any direct influence that reductive dissolution of Fe(III)-cementing agents might have on colloid dispersion.

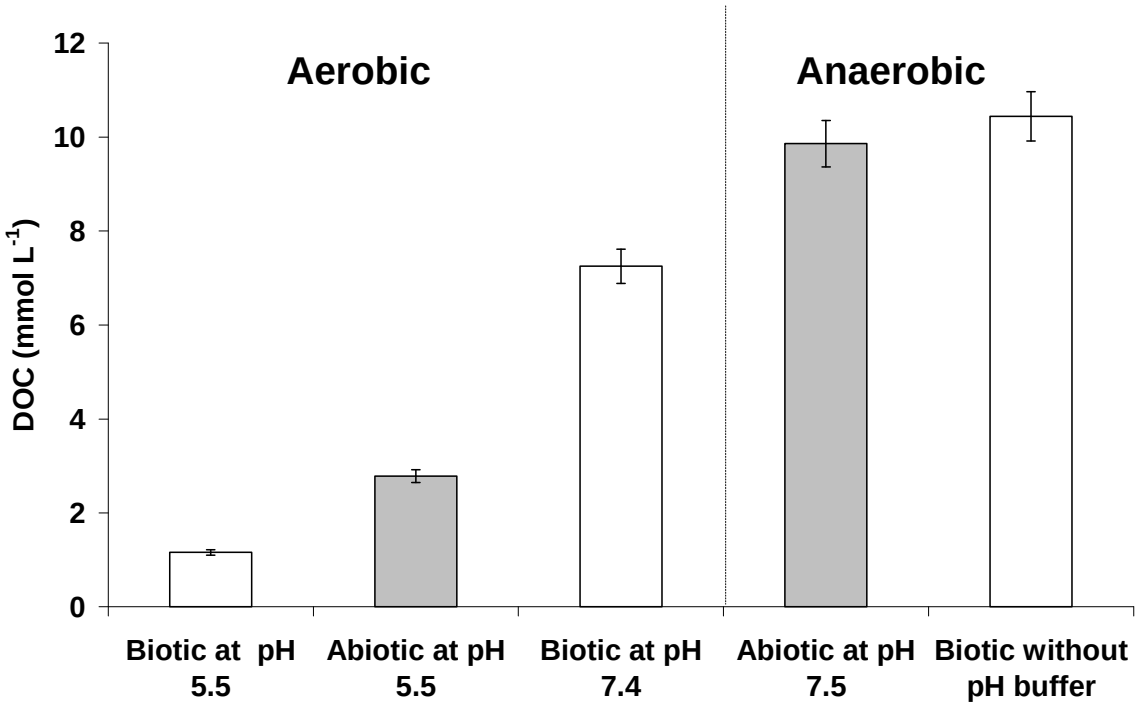

Figure AIV. 5. Amounts of dissolved organic carbon (DOC) solubilized under biotic and abiotic conditions at pH-5.5 and pH-7.4 compared to DOC solubilized in the anaerobic experiment without pH buffer (biotic).

Several reasons could explain the remaining 22%. It is possible that the Fe(II) content of the experimental solution does not accurately represent the amount of Fe-oxyhydroxides actually dissolved under our experimental reducing conditions. Besides, since there appears to be no precipitation of green rust and/or (Fe(II)hydroxide in our experiments, some of the Fe(II) could be readsorbed onto the soil solid phase (Stumm and Sulzberger, 1992; Davranche and Bollinger, 2000b). Another possible explanation is that, in the aerobic experiment at pH 7.4, the DOC concentrations are underestimated because of higher OM mineralization under aerobic conditions. As shown in figure AIV. 5, less DOC is released under biotic than under abiotic conditions (>30%), suggesting a process of OM mineralization under biotic conditions

that could lead to an under-estimation of the DOC released by desorption from mineral phases.

c. Implications regarding DOC mobility in wetlands

It appears that pH plays a dominant role in controlling the mobility of DOC in wetlands, so several implications, including the source of the mobilized DOC, should be considered. Assuming that reductive dissolution of Mn- and Fe-oxyhydroxides is the dominant mechanism, then the source of DOC would be mainly the OM bound to soil Mn- and Fe-oxyhydroxides. On the other hand, if the dominant mechanism is OM desorption due to rising pH imposed by redox reactions, the source of DOC should not only be the OM bound to the Mn- and Fe-oxyhydroxides, but also OM adsorbed onto other soil minerals such as clays. However, it is important to note that the impact of each release process (reductive dissolution or pH rise) is a function of the ratio of Mn- and Fe-oxyhydroxides to clay in the soil. The varying nature of the DOC sources could lead to differences in the composition of DOC (Hagedorn et al., 2000). Studies of DOC adsorption onto minerals have shown that minerals rich in surface hydroxyl groups, such as Fe-oxyhydroxides, preferentially adsorb high molecular-weight humic substances. The binding of DOC to the Fe-oxyhydroxides surfaces is strong and rapid due to the high density of carboxylic and phenolic groups on humic substances (Avena and Koopal, 1999; Maurice et al., 2002). Conversely, OM with lower aromaticity and more marked hydrophobic behaviour would be preferentially adsorbed onto soil minerals such as clays or talc that are less hydrophilic or hydrophobic (Sallez et al., 2000). Therefore, the reductive dissolution of Fe-oxyhydroxides would solubilize OM with a higher density of carboxylic and phenolic groups than if desorption took place owing to pH increase. The capacity of organic molecules to complex metals is positively correlated with the density of carboxylic and phenolic groups. Hence, the source of released OM will affect the cycling and transport of metals at the wetland/river interface. Our results demonstrate that competitive and fractional adsorption studies of DOC in wetland soils should not be restricted merely to Mn- and Fe-oxyhydroxides, but should be extended to a wider range of soil minerals.

Wider implications concern the increased levels of DOC in surface waters observed across large areas of Europe and North America (e.g. Skjelkvale et al., 2005, Monteith et al., 2007) with consequences for both local water quality and regional carbon balances. This DOC trend is related to declining sulphur deposition in surface waters (reduces the magnitude of

recovery from acidification in terms of rising alkalinity and pH (Clark et al., 2005). The present results provide clear evidence that pH increase is the key factor in DOC release from soil. Any chemical process that increases soil solution pH might involve the solubilization of organic matter.

5. Conclusions

The present experimental approach is used to unravel the nature of the mechanisms involved in the mobilization of DOC under reducing conditions in wetlands soils. Three mechanisms are tested: i) production of soluble organic metabolites by reducing bacteria; ii) release of OM bound to reductively dissolved Mn- and Fe- oxyhydroxides; iii) desorption of OM sorbed onto soil minerals due to pH rise during reduction.

Anaerobic incubation of a natural wetland soil provides evidence that reducing conditions in wetlands can lead to the release of DOC. This process is clearly associated with a pH increase (from 5.5 to 7.4) as well as the reduction of Mn and Fe. According to our observations, about 2.5% of the total soil OC content is released as DOC. During soil incubation favouring Mn and Fe reduction without pH increase (soil anaerobic experiment at a constant pH of 5.5), the amount of DOC released corresponds to about 0.5% of the total soil OC. Finally, the amount of DOC released during soil incubation promoting solely pH increase (soil aerobic experiment at pH 7.4) corresponds to 1.7% of the total soil OC content.

UV absorbance analyses indicate that the DOC released in the experiments exhibits the characteristics of humic substances (no significant trace of bacterial metabolites).

Our results suggest that the process of DOC release in wetlands is not predominantly caused by the reductive dissolution of Mn- and Fe-oxyhydroxides and subsequent release of associated OM. The dominant process appears to be desorption due to the pH rise imposed by redox reactions, (>60% of the total amount of released DOC).

Acknowledgments

We thank the technical staff both at Géosciences-Rennes and INRA Science du Sol for their assistance during sample preparation and chemical analyses. Dr M.S.N. Carpenter is acknowledged for English corrections. This research was funded mainly by the French CPER programme "Dévelopement de la recherche sur la maîtrise de la qualité de l'eau en Bretagne" jointly funded by the city of Rennes and the French Ministry of Education and Research.

Références bibliographiques

A

Aide, M, Smith-Aide, C., 2003. Assessing soil genesis by rare earth elements analysis. Soil Science Society of America Journal 67, 1470-1476.

AFNOR, 1997. Qualité de l'Eau, méthodes d'analyses 2, élément majeurs; autres éléments et composés minéraux. ANFOR, editor. Paris.

Allard, T., Menguy, N., Salomon, J., Calligaro, T., Weber, T., Calas, G., Benedetti, M.F., 2004. Revealing forms of iron in river-borne material from major tropical rivers of the Amazon Basin (Brazil). Geochimica et Cosmochimica Acta 68, 3079-3094.

Allen, B. L., Hajek, B. F., 1989. Mineral occurrence in soil environnement. In minerals in soil environments, eds J. B. Dixon and S. B. Weed. Soil Science Society of America, Madison, Wisconsin, USA.

Amal, R., Raper, J.A., Waite, T.D., 1992. Effect of fulvic acid adsorption on the aggregation kinetics and structure of hematite particles. Journal of Colloid and Interface Science 151, 244-257.

Amoozegar-Fard, A., Fuller, W.H., Warrick, A.W., 1984. An approach to predicting the movement of selected polluting metals in soils, Journal of Environmental Quality 13, 290-297.

Andersson, S., Nilsson, S.I., 2001. Influence of pH and temperature on microbial activity, substrate availability of soil-solution bacteria and leaching of dissolved organic carbon in a mor humus. Soil Biology & Biochemistry 33, 1181-1191.

Artinger, R., Buckau, G., Geyer, S., Fritz, P., Wolf, M., Kim, J.I., 2000. Characterization of groundwater humic substances: influence of sedimentary organic carbon. Applied Geochemistry 15, 97-116.

Aubert, D., Stille, P., Probst, A., 2001. REE fractionation during granite weathering and removal by waters and suspended loads: Sr and Nd isotopic evidence, Geochimica Cosmochimica Acta 65 387–406.

Avena, M.J., Koopal, L.K., 1998. Desorption of humic acids from an iron oxide surface. Environmental Science & Technology 32, 2572-2577.

Avena, M.J., Koopal, L.K., 1999. Kinetics of Humic Acids Adsorption at Solid-Water Interfaces. Environmental Science & Technology 33, 2739-2744.

Avena, M.J., Vermeer, A.W.P., Koopal, L.K., 1999. Volume and structure of humic acids studied by viscometry: pH and electrolyte concentration effects. Colloids and Surfaces A: Physicochemical and Engineering Aspects 151, 213-224.

Avena, M.J., Wilkinson, K.J., 2002. Disaggregation kinetics of a peat humic acid: Mechanism and pH effects. Environmental Science & Technology 36, 5100-5105.

B

Baalousha, M., 2009. Aggregation and disaggregation of iron oxide nanoparticles: Influence of particle concentration, pH and natural organic matter. Science of The Total Environment 407, 2093-2101.

Baigorri, R., Fuentes, M., Gonzalez-Gaitano, G., Garcia-Mina, J.M., 2007. Analysis of molecular aggregation in humic substances in solution. Colloids and Surfaces A: Physicochemical and Engineering Aspects 302, 301-306.

Baize, D., 1997. Teneurs en éléments traces métalliques dans les sols (France). Références et stratégies d'interprétation. INRA Editions, Paris.

Balcke, G.U., Kulikova, N.A., Hesse, S., Kopinke, F.-D., Perminova, I.V., Frimmel, F.H., 2002. Adsorption of humic substances onto kaolin clay related to their structural features. Soil Science Society of America Journal 66, 1805-1812.

Bau, M., 1999. Scavenging of dissolved yttrium and rare earths by precipitating iron oxyhydroxide: experimental evidence for Ce oxidation, Y-Ho fractionation, and lanthanide tetrad effect. Geochimica Cosmochimica Acta 63, 67-77.

Benedetti, M.F., vanRiemsdik, W.H., Koopal, L.K., 1996. Humic substances considered as a heterogeneous donnan gel phase. Environmental Science & Technology 30, 1805-1813.

Benedetti, M.F., Ranville, J.F., Allard, T., Bednar, A.J., Menguy, N., 2003. The iron status in colloidal matter from the Rio Negro, Brasil. Colloids and Surfaces A: Physicochemical and Engineering Aspects 217, 1-9.

Bidoglio, G., Grenthe, I., Qi, P., Robouch, P., Omentto, N., 1991. Complexation of Eu and Tb with fulvic acids as studied by time-resolved laser-induced fluorescence. Talanta 38, 999-1008.

Bonneville, S., Van Cappellen, P., Behrends, T., 2004. Microbial reduction of iron(III) oxyhydroxides: effects of mineral solubility and availability. Chemical Geology 212, 255-268.

Bonneville, S., Behrends, T., Cappellen, P.V., Hyacinthe, C., Röling, W.F.M., 2006. Reduction of Fe(III) colloids by *Shewanella putrefaciens*: a kinetic model. Geochimica et Cosmochimica Acta 70, 5842-5854.

Boudot, J.-P., Maitat, O., Merlet, D., Rouiller, J., 2000. Soil solutions and surface water analysis in two contrasted watersheds impacted by acid deposition, Vosges mountains, N.E. France: interpretation in terms of Al impact and nutrient imbalance. Chemosphere 41, 1419-1429.

Bourrié, G., Maitre V., Curmi P., 1994. Mise en évidence de deux dynamiques saisonnières du fer dans les sols hydromorphes en climat tempéré. Compte rendus de l'Académie des Sciences, Séries IIA. Earth and Planetary Science 318, 87-92.

Bourrié, G., Trolard, F., Jaffrezic, J.M., Robert G.A., Maitre, V., Abdelmoula, M., 1999. Iron control by equilibria between hydroxy-Green Rusts and solutions in hydromorphic soils. Geochimica et Cosmochimica Acta 63, 3417-3427.

Bradl, H.B., 2004. Adsorption of heavy metal ions on soils and soils constituents. Journal of Colloid and Interface Science 277, 1-18.

Brady, N.C., Weil, R.R., 1996. The nature and properties of soils. Prentice-Hall International (UK) Limited, London.

Braun, J.J., Viers, J., Dupré, B., Polvé, M., Ndam, J., Muller, J.P., 1998. Solid/liquid fractionation in the laterite system of Goyoum, East Cameroon: The implication for the present dynamics of the soil covers of the humid tropical regions. Geochimica Cosmochimica Acta 62, 273-299.

Brown, G.E., 1990. Spectroscopic studies of chemisorption reaction mechanisms at oxide-water interfaces. Reviews in Mineralogy and Geochemistry 23, 309-363.

Bryan, S.E., Tipping, E., Hamilton-Taylor, J., 2002. Comparison of measured and modelled copper binding by natural organic matter in freshwaters. Comparative Biochemistry and Physiology Part C: Toxicology & Pharmacology 133, 37-49.

Buffle, J., Wilkinson, K.J., Stoll, S., Filella, M., Zhang, J., 1998. A generalized description of aquatic colloidal interactions: the three-colloidal component approach. Environmental Science & Technology 32, 2887-2899.

C

Châtellier, X., Fortin, D., West, M.M., Leppard, G.G., Ferris, F.G., 2001. Effect of the presence of bacterial surfaces during the synthesis of Fe oxides by oxidation of ferrous ions. European Journal of Mineralogy13, 705-714.

Châtellier, X., West, M.M., Rose, J., Fortin, D., Leppard, G.G., Ferris, F.G., 2004. Characterization of iron-oxides formed by oxidation of ferrous ions in the presence of various bacterial species and inorganic ligands. Geomicrobiology Journal 21, 99 - 112.

Chen, J., Gu, B.H., Royer, R.A., Burgos, W.D., 2003. The roles of natural organic matter in chemical and microbial reduction of ferric iron. Science of The Total Environment 307, 167-178.

Chin, Y.-P., Aiken, G., O'Loughlin, E., 1994. Molecular weight, polydispersity, and spectroscopic properties of aquatic humic substances. Environmental Science & Technology 28, 1853-1858.

Chorover, J., Amistadi, M.K., 2001. Reaction of forest floor organic matter at goethite, birnessite and smectite surfaces. Geochimica et Cosmochimica Acta 65, 95-109.

Christ, M.J., David, M.B., 1996. Temperature and moisture effects on the production of dissolved organic carbon in a spodosol. Soil Biology & Biochemistry 28, 1191-1199.

Christl, I., Kretzschmar, R., 2001. Interaction of copper and fulvic acid at the hematite-water interface. Geochimica et Cosmochimica Acta 65, 3435-3442.

Chuan, M.C., Shu, G.Y., Liu, J.C., 1996. Solubility of heavy metals in a contaminated soil: Effects of redox potential and pH. Water Air and Soil Pollution 90, 543-556.

Citeau, L., Lamy, I., van Oort, F., Elsass, F., 2003. Colloidal facilitated transfer of metals in soils under different land use. Colloids and Surfaces A: Physicochemical and Engineering Aspects 217, 11-19.

Citeau, L., 2004. Étude des colloïdes naturels présents dans les eaux gravitaires de sols contaminés : relation entre nature des colloïdes et réactivité vis-à-vis des métaux (Zn, Cd, Pb, Cu). Thèse de doctorat, Institut National d'Agronomie Paris-Grignon (France).

Claessens, J., van Lith, Y., Laverman, A.M., Van Cappellen, P., 2006. Acid-base activity of live bacteria: Implications for quantifying cell wall charge. Geochimica et Cosmochimica Acta 70, 267-276.

Clark, M., Chapman, P.J., Adamson, J.K., Lane, S.N., 2005 Influence of drought-induced acidification on the mobility of dissolved organic carbon in peat soils. Global Change Biology 11, 791–809.

Compton, J. S., White, R. A., Smith, M., 2003. Rare earth element behaviour in soils and salt pan sediments of a semi-arid granitic terrain in the Western Cape, South Africa. Chemical Geology 201, 239-255.

Condie, K.C., Dengate, J., Cullers, R.L., 1995. Behavior of rare earth elements in a paleoweathering profile on granodiorite in the Front Range, Colorado, USA. Geochimica Cosmochimica Acta 59, 279–294

Cooke, J.D., Hamilton-Taylor, J., Tipping, E., 2007. On the acid-base properties of humic acid in soil. Environmental Science & Technology 41, 465-470.

Coppin, F., Berge,r G., Bauer, A., Castet, S., Loubet, M. 2002. Sorption of lanthanide on smectite and kaolinite. Chemical Geology 182, 57-68.

Cornell, R.M., Schwertmann, U., 2003. The iron oxides: structure, properties, reactions, occurence and uses. VCH. Weinheim.

Cornu, S., Montagne, D., Conil, P., 2004. Comparaison d'extractions séquentielles et cinétiques pour la spéciation de As dans des sols sableux contaminés. Comptes Rendus Géosciences 336, 1007-1015.

Curmi, P., Durand, P., Gascuel-Odoux, C., Hallaire, V., Mérot, P., Robin, P., Trolard, F., Walter, C., Bourrié, G., 1995. Le programme CORMORAN-INRA: de l'importance du milieu physique dans la régulation biogéochimique de la teneur en nitrate des eaux superficielles. Journal Européen d'Hydrologie 26, 37-56.

Curmi, P., Bidois, J., Bourrié, G., Cheverry, C., Durand, P., Guasguel-Odoux, C., Germon, J. C., Hallaire, V., Hénault, C., Jaffrezic, A., Mériat, P., Trolard, F., 1997. Rôle du sol sur la circulation et la qualité des eaux au sein de paysages présent en domaine hydromorphe. Etude et gestion des sols 4, 95-111.

Curmi, P., Durand, P., Gascuel-Odoux, C., Mérot, P., Walter, C., Taha, A., 1998. Hydromorphic soils, hydrology and water quality: spatial distribution and functional modelling at different scales. Nutrient Cycling in Agroecosystems 50, 127-142.

D

Dabard, M.P., Loi, A., Peucat, J.J., 1996. Zircon typology combined with Sm-Nd whole rock isotope analysis to study Brioverian sediments from the armorican Massif. Sedimentary Geology 101, 243–260

Dahlqvist, R., Benedetti, M.F., Andersson, K., Turner, D., Larsson, T., Stolpe, B., Ingri, J., 2004. Association of calcium with colloidal particles and speciation of calcium in the Kalix and Amazon rivers. Geochimica Et Cosmochimica Acta 68, 4059-4075.

Dahlqvist, R., Andersson, K., Ingri, J., Larsson, T., Stolpe, B., Turner, D., 2007. Temporal variations of colloidal carrier phases and associated trace elements in a boreal river. Geochimica et Cosmochimica Acta 71, 5339-5354.

Dai, M., Martin, J.-M., Cauwet, G., 1995. The significant role of colloids in the transport and transformation of organic carbon and associated trace metals (Cd, Cu and Ni) in the Rhone delta (France). Marine Chemistry 51, 159-175.

Das, A., Caccavo, F., 2000. Dissimilatory Fe(III) oxide reduction by Shewanella alga BrY requires adhesion. Current Microbiology 40, 344-7.

Davies, G., Ghabbour, E.A., 1998. Humic Substances : structure, properties and uses. Cambridge : Royal Society of Chemistry.

Davis, J.A., Kent, D.B., 1990. Surface complexation modeling in aqueous geochemistry. Reviews in Mineralogy and Geochemistry 23, 177-260.

Davison, W., 1993. Iron and manganese in lakes. Earth-Science Reviews 34, 119-163.

Davranche, M., Bollinger, J-C., 2000a. Heavy metals desorption from synthesized and natural Fe and Mn oxyhydroxides: effect of reductive conditions. Journal of Colloid and Interface Science 227, 531-539

Davranche, M., Bollinger, J-C., 2000b. Release of heavy metals from iron oxyhydroxides under reductive conditions: metal/solid interaction. Journal of Colloid and Interface Science 232, 165-173.

Davranche, M., Bollinger, J-C., 2001. A desorption/dissolution model for metal release from polluted soil under reductive conditions. Journal of Environmental Quality 30, 1581-1586.

Davranche, M., Pourret, O., Gruau, G., Dia, A., 2004. Impact of humate complexation on the adsorption of REE onto Fe oxyhydroxide. Journal of Colloid and Interface Science 277, 271-279.

Davranche, M., Pourret, O., Gruau, G., Dia, A., Le Coz-Bouhnik, M., 2005. Adsorption of REE(III)-humate complexes onto MnO2: Experimental evidence for cerium anomaly and lanthanide tetrad effect suppression. Geochimica et Cosmochimica Acta 69, 4825-4835.

Dehaan, H., Jones, R.I., Salonen, K., 1987. Does ionic strength affect the configuration of aquatic humic substances, as indicated by gel filtration? Freshwater Biology 17, 453-459.

Dia, A., Gruau, G., Olivie-Lauquet, G., Riou, C., Molenat, J., Curmi, P., 2000. The distribution of rare earth elements in groundwaters: assessing the role of source-rock composition, redox changes and colloidal particles. Geochimica et Cosmochimica Acta 64, 4131-4151.

Donisa, C., Mocanu, R., Steinnes, E., 2003. Distribution of some major and minor elements between fulvic and humic acid fractions in natural soils. Geoderma 111, 75-84.

Dos Santos Afonso, M., Morando, P. J., Blesa, M. A., Banwart, S., Stumm, W., 1990. The reductive dissolution of iron oxides by ascorbate : The role of carboxylate anions in accelerating reductive dissolution. Journal of Colloid and Interface Science 138, 74-82.

Drever, J.I., Vance, G.F., 1994. Role of soil organic acids in mineral weathering process. In: E.D. Pittman and M.D. Lewan (Editors), Organic Acids in Geological Processes.

Drever, J.I., 1997. The geochemistry of natural waters : surface and groundwaters environments. Prentice Hall (Third edition).

Duiker, S.W., Rhoton, F.E., Torrent, J., Smeck, N.E., Lal, R., 2003. Iron (hydr)oxide crystallinity effects on soil aggregation. Soil Science Society of America Journal 67, 606-611.

Dupré, B., Viers, J., Dandurand, J.-L., Polvé, M., Benezeth, P., Vervier, P., Braun, J.-J., 1999. Major and trace elements associated with colloids in organic-rich river waters: ultrafiltration of natural and spiked solutions. Chemical Geology 160, 63-80.

Durand, P., Juan Torres, J.L., 1996. Solute transfer in agricultural catchments: the interest and limits of mixing models. Journal of Hydrology 181, 1-22.

E

Ehrenreich, A., Widdel, F., 1994. Anaerobic oxidation of ferrous iron by purple bacteria, a new-type of phototrophic metabolism. Applied and Environmental Microbiology 60, 4517-4526.

Ehrlich, H.L., 1990. Geomicrobiology. Marcel Dekker, Inc., New York.

Elderfield, H., Greaves, M. J., 1982. The rare-earth elements in seawater. Nature 296, 214-219.

Emmerson, D., Moyer, C.L., 1997. Isolation and characterization of novel iron-oxidizing bacteria that grow at circumneutral pH. Applied and Environmental Microbiology 63, 4784-4792.

Esquenet, C., 2003. Propriétés structurales et dynamiques des solutions de polyélectrolytes rigides et semirigides et de polysaccharides associatifs. Université Joseph Fourier - Grenoble I, Grenoble (France).

Eyrolle, F., Benedetti, M.F., Benaim, J.Y., Fevrier, D., 1996. The distributions of colloidal and dissolved organic carbon, major elements, and trace elements in small tropical catchments. Geochimica et Cosmochimica Acta 60, 3643-3656.

F

Fakih, M., Châtellier, X., Davranche, M.l., Dia, A., 2008. *Bacillus subtilis* bacteria hinder the oxidation and hydrolysis of Fe^{2+} ions. Environmental Science & Technology 42, 3194-3200.

Fang, J., Shan, X.-q., Wen, B., Lin, J.-m., Owens, G., 2009. Stability of titania nanoparticles in soil suspensions and transport in saturated homogeneous soil columns. Environmental Pollution 157, 1101-1109.

Fee, J.A., Gaudette, H.E., Lyons, W.B., Long, D.T., 1992. Rare earth element distribution in the lake Tyrrell groundwaters, Victoria, Australia. Chemical Geology 96, 67-93.

Felbeck, G.T., 1971. Chemical and biological characterization of humic matter. *In* Soil Biochemistry 2. A.D. McLoren and J. Skeyins (eds.). Marcel Dekker, New York.

Fiedler, S., Kalbitz, K. 2003. Concentrations and properties of dissolved organic matter in forest soils as affected by the redox regime. Soil Science 168, 793–801.

Flaig, W., 1964. Effects of micro-organisms in the transformation of lignin to humic substances. Geochimica et Cosmochimica Acta 28, 1523-1535.

Fortin, D., Leppard, G.G., Tessier, A., 1993. Characteristics of lacustrine diagenetic iron oxyhydroxides. Geochimica et Cosmochimica Acta 57, 4391-4404.

G

Gaffney, J.W., White, K.N., Boult, S., 2008. Oxidation state and size of Fe controlled by organic matter in natural waters. Environmental Science & Technology 42, 3575-3581.

Gaillardet, J., Viers, J., Dupré, B., 2003. Trace elements in rivers. In 'Treatise on Geochemistry: Surface and Ground Water, Weathering, and Soils', Eds. H. D. Holland and K. K. Turekian, Editor Elsevier.

Geckeis, H., Rabung, T., Manh, T.N., Kim, J.I., Beck, H.P., 2002. Humic colloid-borne natural polyvalent metal ions; Dissociation experiment. Environmental Science & Technology 36, 2946-2952.

Gerth, J., 1990. Unit-cell dimensions of pure and trace metal-associated goethites. Geochimica et Cosmochimica Acta 54, 363-371.

Gerritse, R.G., 1996. Column- and catchment-scale transport of cadmium: effect of dissolved organic matter. Journal of Contaminant Hydrology 22, 145-163.

Girard, M.C., Walter, C., Remy, J.C., Berthelin, J., Morel, J.L., 2005. Sols et Environnement. Dunod, Paris.

Gonet, S.S., Wegner, K., 1996. Viscosimetric and chromatographic studies of soil humic acids. Environment International 22, 485-488.

Gotoh, S., Patrick, J.W.H. 1974. Transformation of iron in a waterlogged soil as affected by redox potential and pH. Soil Science Society of America Journal 38, 66-71.

Gounaris, V., Anderson, P.R., Holsen, T.M., 1993. Characteristics and environmental significance of colloids in landfill leachate. Environmental Science & Technology 27, 1381-1387.

Grolimund, D., Borkovec, M., Barmettler, K., Sticher, H., 1996. Colloid-facilitated transport of strongly sorbing contaminants in natural porous Media: A Laboratory Column Study. Environmental Science & Technology 30, 3118-3123.

Grolimund, D., Elimelech, M., Borkovec, M., Barmettler, K., Kretzschmar, R., Sticher, H., 1998. Transport of in situ mobilized colloidal particles in packed soil columns. Environmental Science & Technology 32, 3562-3569.

Grosbois, C., Courtin-Nomade, A., Martin, F., Bril, H., 2007. Transportation and evolution of trace element bearing phases in stream sediments in a mining - Influenced basin (Upper Isle River, France). Applied Geochemistry 22, 2362-2374.

Gruau, G., Dia, A., Olivié-Lauquet, G., Davranche, M., Pinay, G., 2004. Controls on the distribution of rare earth elements in shallow groundwaters. Water Research 38, 3576-3586.

Grybos, M., Davranche, M., Gruau, G., Petitjean, P., 2007. Is trace metal release in wetland soils controlled by organic matter mobility or Fe-oxyhydroxides reduction? Journal of Colloid and Interface Science 314, 490-501.

Grybos, M., Davranche, M., Gruau, G., Petitjean, P., Pédrot, M., 2009. Increasing pH drives organic matter solubilization from wetland soils under reducing conditions. Geoderma, submitted.

Gu, B., Schmitt, J., Chen, Z., Liang, L., McCarthy, J.F., 1994. Adsorption and desorption of natural organic matter on iron oxide: mechanisms and models. Environmental Science & Technology 28, 38-46.

H

Hagedorn, F., Kaiser, K., Feyen, H., Schleppi, P. 2000. Effect of redox conditions and flow

processes on the mobility of dissolved organic carbon and nitrogen in a forest soil. Journal of Environmental Quality 29, 288-297.

Hansen, H.C.B., Borggaard, O.K, Sorensen, J. 1994. Evolution of the free energy of formation of Fe(II)-Fe(III) hydroxide-sulphate (green rust) and its reduction of nitrite. Geochimica et Cosmochimica Acta 58, 2599-2608.

Hayes, M.H.B., McCarthy, P., Malcolm, R.L., Swift, R.S., 1989. Humic Substances II: In search of structure, Wiley, New York.

Hayes, M.H.B., Bolt, G.H., 1991. Soil colloids and the soil solution. In: Interactions at the soil colloid - soil solution interface. Bolt GH, de Boodt, Hayes MHB, McBride MB (eds), Kluwer Academic Publishers, The Netherlands, 1-34.

Heidmann, I., Christl, I., Kretzschmar, R., 2005. Sorption of Cu and Pb to kaolinite-fulvic acid colloids: Assessment of sorbent interactions. Geochimica et Cosmochimica Acta 69, 1675-1686.

Hiemstra, T., Van Riemsdijk, W.H., Bolt, G.H., 1989. Multisite proton adsorption modeling at the solid/solution interface of (hydr)oxides: A new approach: I. Model description and evaluation of intrinsic reaction constants. Journal of Colloid and Interface Science 133, 91-104.

Hiemstra, T., Van Riemsdijk, W.H., 1996. A surface structural approach to ion adsorption: The Charge Distribution (CD) model. Journal of Colloid and Interface Science 179, 488-508.

Hiemstra, T., Venema, P., Riemsdijk, W.H.V., 1996. Intrinsic proton affinity of reactive surface groups of metal (hydr)oxides: the bond valence principle. Journal of Colloid and Interface Science 184, 680-692.

Honeyman, B.D., 1999. Geochemistry: Colloidal culprits in contamination. Nature 397, 23-24.

Hummel, W., Glaus, M.A., Van Loon, L.R., 1995. Binding of radionuclides by humic substances: the "conservative roof" approach. Proceeding of an NEA Workshop, 14-16 September 1994. OECD Documents, Bas Zurzach, Switzerland.

Hummel, W., Glaus, M.A., Van Loon, L.R., 2000. Trace metal-humate interactions. II. The "conservative roof" model and its application. Applied Geochemistry 15, 975-1001.

Hur, J., Schlautman, M.A., 2003. Molecular weight fractionation of humic substances by adsorption onto minerals. Journal of Colloid and Interface Science 264, 313-321.

Hyacinthe, C., Bonneville, S., Van Cappellen, P., 2008. Effect of sorbed Fe(II) on the initial reduction kinetics of 6-line ferrihydrite and amorphous ferric phosphate by *Shewanella putrefaciens*. Geomicrobiology Journal 25, 181-192.

I

Imai, A., Fukushima, T., Matsushige, K., Kim, Y.-H., Choi, K., 2002. Characterization of dissolved organic matter in effluents from wastewater treatment plants. Water Research 36, 859-870.

Ingri, J., Widerlund, A., Land, M., Gustafsson, O., Andersson, P., Ohlander, B., 2000. Temporal variations in the fractionation of the rare earth elements in a boreal river; the role of colloidal particles. Chemical Geology 166, 23-45.

ISSS-ISRIC-FAO. 1998. World reference basis for soil resources. World Soil Resources Reports FAO Rome, 84.

J

Jaffrézic, A., 1997. Géochimie des éléments métalliques, des nitrates et du carbone organique dissous dans les eaux et les sols hydromorphes. Agriculture intensive et qualité des eaux dans les sols humides en Bretagne. Thèse de doctorat, Université de Rennes 1 (France).

Jardine, P.M., Weber, N.L., McCarthy, J.F. 1989. Mechanism of dissolved organic carbon adsorption on soil. Soil Science Society of America Journal 53, 1378-1385.

Johannesson, K.H., Stetzenbach, K.J., Hodge, V.F., 1995. Speciation of the rare earth element neodymium in groundwaters of the Nevada Test Site and Yucca Mountain and implications for actinide solubility. Applied Geochemistry 10, 565-572.

Johannesson, K.H., Stetzenbach, K.J., Hodge, V.F., Kreamer, D.K., Zhou, X., 1997a. Delineation of ground-water flow systems in the southern Great Basin using aqueous rare earth element distributions, Ground Water 35, 807–819.

Johannesson, K.H., Stetzenbach, K.J., Hodge, V.F., 1997b. Rare earth elements as geochemical tracers of regional groundwater mixing, Geochimica Cosmochimica Acta 61, 3605–3618.

Johannesson, K.H., Tang, J., Daniels, J.M., Bounds, W.J., Burdige, D.J., 2004. Rare earth element concentrations and speciation in organic-rich blackwaters of the Great Dismal Swamp, Virginia, USA. Chemical Geology 209, 271-294.

K

Kahle, M., Kleber, M., Jahn, R. 2003. Retention of dissolved organic matter by illitic soils and clay fractions: Influence of mineral phase properties. Journal of Plant Nutrition and Soil Science 166, 737-741.

Kaiser, K., Zech, W. 1999. Release of Natural Organic Matter Sorbed to Oxides and a Subsoil. Soil Science Society of America Journal 63, 1157-1166.

Kalbitz, K., Solinger, S., Park, J.H., Michalzik, B., Matzner, E., 2000. Controls on the dynamics of dissolved organic matter in soils: A review. Soil Science 165, 277-304.

Kang, K.-H., Shin, H.S., Park, H., 2002. Characterization of humic substances present in landfill leachates with different landfill ages and its implications. Water Research 36, 4023-4032.

Kaplan, D.I., Bertsch, P.M., Adriano, D.C., Miller, W.P., 1993. Soil-borne mobile colloids as influenced by water flow and organic carbon. Environmental Science & Technology 27, 1193.

Kaplan, D.I., Bertsch, P.M., Adriano, D.C., 1997. Mineralogical and physicochemical differences between mobile and nonmobile colloidal phases in reconstructed pedons. Soil Science Society of America Journal 61, 641-649.

Karathanasis, A.D., 1999. Subsurface migration of copper and zinc mediated by soil colloids. Soil Science Society of America Journal 63, 830-838.

Kedziorek, M.A.M., Bourg, A.C.M., 1996. Acidification and solubilisation of heavy metals from single and dual-component model solids. Applied Geochemistry 11, 299-304.

Kedziorek, M.A.M., Dupuy, A., Bourg, A.C.M., Compere, F., 1998. Leaching of Cd and Pb from a polluted soil during the percolation of EDTA: laboratory column experiments modeled with a non-equilibrium solubilization step. Environmental Science & Technology 32, 1609-1614.

Kersting, A.B., Efurd, D.W., Finnegan, D.L., Rokop, D.J., Smith, D.K., Thompson, J.L., 1999. Migration of plutonium in ground water at the Nevada Test Site. Nature 397, 56-59.

Kipton, H., Powell, J., Town, R.M., 1992. Solubility and fractionation of humic acid - Effect of pH and ionic medium. Analytica Chimica Acta 267, 47-54.

Klitzke, S., Lang, F., Kaupenjohann, M., 2008. Increasing pH releases colloidal lead in a highly contaminated forest soil. European Journal of Soil Science 59, 265-273.

Koenings, J.P., 1976. In situ experiments on the dissolved and colloidal state of iron in an acid bog lake. Limnology and Oceanography 21, 674-683.

Koeppenkastrop, D., De Carlo, E.H., 1992. Sorption of rare-earth elements from seawater onto synthetic mineral particles: An experimental approach. Chemical Geology 95, 251-263.

Kononova, M., 1966. Soil organic matter, Oxford.

Kostka, J.E., Haefele, E., Viehweger, R., Stucki, J.W., 1999. Respiration and dissolution of iron(III)-containing clay minerals by bacteria. Environmental Science & Technology 33, 3127-3133.

Kretzschmar, R., Robarge, W.P., Weed, S.B., 1993. Flocculation of kaolinitic soil clays - Effects of humic substances and iron-oxides. Soil Science Society of America Journal 57, 1277-1283.

Kretzschmar, R., Sticher, H., 1997. Transport of humic-coated iron oxide colloids in a sandy soil: influence of Ca^{2+} and trace metals. Environmental Science & Technology 31, 3497-3504.

Kretzschmar, R., Sticher, H., 1998. Colloid transport in natural porous media: influence of surface chemistry and flow velocity. Physics and Chemistry of The Earth 23, 133-139.

Kretzschmar, R., Borkovec, M., Grolimund, D., Elimelech, M., 1999. Mobile subsurface colloids and their role in contaminant transport. Advances in Agronomy, Vol 66. Academic Press Inc, San Diego.

Kurek, E., Czaban, J., Bollag, J.-M., 1982. Sorption of cadmium by microorganisms in competition with other soil constituents. Applied and Environmental Microbiology 43, 1011-1015.

L

Langmuir, D., 1997. Aqueous environmental geochemistry. Prentice Hall, Upper Sadle River, New Jersey.

Laveuf, C., Cornu, S., Juillot, F., 2008. Rare earth elements as tracers of pedogenetic processes. Comptes Rendus des Geosciences 340, 523-532.

Lebart, L., Morineau, A., Piron, M., 2000. Statistique exploratoire multidimensionnelle. Dunod, Paris.

Leybourne, M. I., Johanesson, K. H., 2008. Rare earth elements (REE) and yttrium in strem waters, strem sediments, and Fe-Mn oxyhydroxides: Fractionation, speciation, and controls aver REE+Y patterns in the surface environment. Geochimica Cosmochimica Acta 72, 5962-5983.

Li, L., Zhao, Z., Huang, W., Peng, P., Sheng, G., Fu, J., 2004. Characterization of humic acids fractionated by ultrafiltration. Organic Geochemistry 35, 1025-1037.

Liu, A., Gonzalez, R.D., 1999. Adsorption/Desorption in a system consisting of humic acid, heavy metals, and clay minerals. Journal of Colloid and Interface Science 218, 225-232.

Lofts, S., Tipping, E., Hamilton-Taylor, J., 2008. The chemical speciation of Fe(III) in freshwaters. Aquatic Geochemistry 14, 337-358.

Logan, E.M., Pulford, I.D., Cook, G.T., MacKenzie, A.B., 1997. Complexation of Cu^{2+} and Pb^{2+} by peat and humic acid. European Journal of Soil Science 48, 685-696.

Lovley, D.R., Phillips, E.J.P., 1986. Availability of ferric iron for microbial reduction in bottom sediments of the freshwater tidal Potomac river. Applied and Environmental Microbiology 52, 751-757.

Lovley, D.R., Stolz, J.F., Nord, G.L., Phillips, E.J.P., 1987. Anaerobic production of magnetite by a dissimilatory iron-reducing microorganism. Nature 330, 252-254.

Lovley, D.R., Phillips, E.J.P., 1988. Novel mode of microbial energy metabolism: organic carbon oxidation coupled to dissimilatory reduction of iron or manganese. Applied and Environmental Microbiology 54, 1472-1480.

Lovley, D.R., Chapelle, F.H., Woodward, J.C. 1994. Use of dissolved H_2 concentrations to determine distribution of microbially catalyzed redox reactions in anoxic groundwater. Environmental Science & Technology 28, 1250-1210.

Lovley, D.R., Coates, J.D., Blunt-Harris, E.L., Phillips, E.J.P., Woodward, J.C., 1996. Humic substances as electron acceptors for microbial respiration. Nature 382, 445-448.

Lovley, D.R., 2000. Iron(III) and Mn(IV) reduction. In: Lovley, D.R. (Ed.), Environmental microbe-metal interactions. ASM Press, Washington, D.C.

Lu, X., Johnson, W.D., Hook, J., 1998. Reaction of vanadate with aquatic humic substances: an ESR and V NMR study. Environmental Science & Technology 32, 2257-2263.

Lucas, Y., 2001. The role of plants in controlling rates and products of weathering: importance of biological pumpinp. Annual Review of Earth and Planetary Sciences 29, 135-163.

Lützenkirchen, J., 1999. The Constant Capacitance Model and variable ionic strength: an evaluation of possible applications and applicability. Journal of Colloid and Interface Science 217, 8-18.

Lyvén, B., Hassellov, M., Turner, D.R., Haraldsson, C., Andersson, K., 2003. Competition between iron- and carbon-based colloidal carriers for trace metals in a freshwater assessed using flow field-flow fractionation coupled to ICPMS. Geochimica et Cosmochimica Acta 67, 3791-3802.

M

McBride, M.B. 1994. Environmental Chemistry of Soils. Oxford University Press, New York.

McCarthy, J.F., Zachara, J.M., 1989. Subsurface transport of contaminants. Environmental Science & Technology 23, 496-502.

McCarthy, P., Clapp C.E., Malcom R.L., Bloom P.R., 1990. Humic substances in soil and crop sciences: selected readings. Madison, Wisconsin, Soil Science Society of America.

McCarthy, J.F., Williams, T.M., Liang, L., Jardine, P.M., Jolley, L.W., Taylor, D.L., Palumbo, A.V., Cooper, L.W., 1993. Mobility of natural organic matter in a study aquifer. Environmental Science & Technology 27, 667-676.

McCarthy, P., 2001. The Principles of Humic Substances. Soil Science 166, 738-751.

McCarthy, J.F., McKay, L.D., 2004. Colloid transport in the subsurface: past, present, and future challenges. Vadose Zone Journal 3, 326-337.

McGechan, M.B., Lewis, D.R., 2002. Transport of particulate and colloid-sorbed contaminants through soil, Part 1: general principles. Biosystems Engineering 83, 255-273.

Maguire, S., Pulford, I.D., Cook, G.T., Mackenzie, A.B., 1992. Cesium sorption desorption in clay humic-acid systems. Journal of Soil Science 43, 689-696.

Malcolm, R.L., 1990. The uniqueness of humic substances in each of soil, stream and marine environments. Analytica Chimica Acta 232, 19-30.

Martyniuk, H., Wieckowska, J., 2003. Adsorption of metal ions on humic acids extracted from brown coals. Fuel Processing Technology 84, 23-36.

Maurice, P.A., Cabaniss, S.E., Drummond, J., Ito, E. 2002. Hydrogeochemical controls on the variations in chemical characteristics of natural organic matter at a small freshwater wetland. Chemical Geology 187, 59-77.

Meier, M., Namjesnik-Dejanovic, K., Maurice, P.A., Chin, Y.-P., Aiken, G.R., 1999. Fractionation of aquatic natural organic matter upon sorption to goethite and kaolinite. Chemical Geology 157, 275-284.

Mercier, F., Moulin, V., Barre, N., Casanova, F., Toulhoat, P., 2001. Study of the repartition of metallic trace elements in humic acids colloids: potentialities of nuclear microprobe and complementary techniques. Analytica Chimica Acta 427, 101-110.

Mérot, P., Durand, P., Morisson, C., 1995. Four-component hydrograph separation using isotopic and chemical determinations in an agricultural catchment in western France. Physics and Chemistry of The Earth 20, 415-425.

Miano, T.M., Piccolo, A., Celano, G., Senesi, N., 1992. Infrared and fluorescence spectroscopy of glyphosate-humic acid complexes. Science of The Total Environment 123-124, 83-92.

Mitsch, W.J., Gosselink, J.G., 2000. Wetlands. John Wiley & Sons, Inc, New York (Third edition).

Miyajima, T., Kanegae, Y., Yoshida, K., Katsuki, M., Naitoh, Y., 1992. A Donnan model for the analysis of metal complexation of weak-acidic polyelectrolytes -- an approach to the quantitative analytical treatment of the metal complexation equilibria of humic substances. Science of The Total Environment 117-118, 129-137.

Molénat, J., Durand, P., Gascuel-Odoux, C., Davy, P., Gruau, G., 2002. Mechanisms of nitrate transfer from soil to stream in an agricultural watershed of french Brittany. Water, Air, & Soil Pollution 133, 161-183.

Möller, P., Dulski, P., Bau, M., Knappe, A., Pekdeger, A., Sommervon, J., 2000. Anthropogenic gadolinium as a conservative tracers in hydrology. Journal of Geochemical Exploration 69–70, 409– 414.

Monteith, D.T., Stoddard, J.L., Evans, C.D., de Wit, H.A., Forsius, M., Høgasen, T., Wilander, A., Skjelkvale, B. L., Jeffries, D. S., Vuorenmaa, J., Keller, B., Kopacek, J., Vesely J. 2007. Dissolved organic carbon trends resulting from changes in atmospheric deposition chemistry. Nature 450, 537–541.

Mossop, K.F., Davidson, C.M., 2003. Comparison of original and modified BCR sequential extraction procedures for the fractionation of copper, iron, lead, manganese and zinc in soils and sediments. Analytica Chimica Acta 478, 111-118.

Mourier, B., Poulenard, J., Chauvel, C., Faivre, P., Carcaillet, C. 2008. Distinguish subalpine soil types using extractible Al and Fe fractions and REE geochemistry. Geoderma 1145, 107-120.

Murphy, E.M., Davis, S.N., Long, A., Donahue, D., Jull, A.J.T., 1989. Characterization and isotopic composition of organic and inorganic carbon in the Milk river aquifer. Water Resources Research 25, 1893-1905.

Murphy, E.M., Zachara, J.M., Smith, S.C., Phillips, J.L., 1992. The sorption of humic acids to mineral surfaces and their role in contaminant binding. The Science of the Total Environment, 117-118, 413-423.

Murphy, E.M., Zachara, J.M., Smith, S.C., Phillips, J.L., Wietsma, T.W., 1994. Interaction of hydrophobic organic-compounds with mineral-bound humic substances. Environmental Science & Technology 28, 1291-1299.

Murphy, E.M., Zachara, J.M., 1995. The role of sorbed humic substances on the distribution of organic and inorganic contaminants in groundwater. Geoderma 67, 103-124.

Myers, C.R., Nealson, K.H. 1988. Microbial reduction of manganese oxides: interaction with iron and sulfur. Geochimica et Cosmochimica Acta 52, 2727-2732.

N

Nealson, K.H., Myers, C.R. 1992. Microbial reduction of manganese and iron: new approach to carbon cycling. Applied and Environmental Microbiology 58, 439-443.

Nelson, D.W., Sommers, L.E., 1982. Methods of soil analysis, Part 2. Chemical and microbiological properties. American Society of Agronomy, Madison.

Nesbitt, H. W., 1979. Mobility and fractionation of Rare earth elements during weathering of a granodiorite. Nature 279, 206-210.

Nidjigui, P-D, Bilong, P., Bitom, D., Dia, A., 2008. Mobilization and redistribution of major and trace elements in two weathering profiles developed on serpentinites in the Lomié ultramafic complex, South-East Cameroon. Journal of Africa Earth Science 50, 305-328.

Nirel, P.M.V., Morel, F.M.M., 1990. Pitfalls of sequential extractions. Water Research 24, 1055-1056.

Nirel, P.M.V., Morel, F.M.M., 1991. Comments on "Pitfalls of sequential extractions". Water Research 25, 115-117.

O

Ohno, T., Fernandez, I.J., Hiradate, S., Sherman, J.F., 2007. Effects of soil acidification and forest type on water soluble soil organic matter properties. Geoderma 140, 176-187.

Ohta, A., Kawabe, I., 2001. REE(III) adsorption onto Mn dioxide (δ-MnO2) and Fe oxyhydroxide: Ce(III) oxidation by δ-MnO2. Geochimica Cosmochimica Acta 65, 695-703.

Oliva, P., Viers, J., Dupré, B., Fortune, J.P., Martin, F., Braun, J.J., Nahon, D., Robain, H., 1999. The effect of organic matter on chemical weathering: study of a small tropical watershed: Nsimi-Zoetele site, Cameroon. Geochimica et Cosmochimica Acta 63, 4013-4035.

Olivié-Lauquet, G., Allard, T., Benedetti, M., Muller, J.-P., 1999. Chemical distribution of trivalent iron in riverine material from a tropical ecosystem: a quantitative EPR study. Water Research 33, 2726-2734.

Olivié-Lauquet, G., Gruau, G., Dia, A., Riou, C., Jaffrezic, A., Henin, O., 2001. Release of Trace Elements in Wetlands: Role of Seasonal Variability. Water Research 35, 943-952.

Olomu, M.O., Racz, G.J., Cho, C.M., 1973. Effect of flooding on the Eh, pH, and concentrations of Fe and Mn in several Manitoba soils. Soil Science Society of America Journal 37, 220-224.

Ona-Nguema, G., Abdelmoula, M., Jorand, F., Benali, O., Gehin, A., Block, J.C., Genin, J.M.R., 2000. Microbial reduction of lepidocrocite gamma-FeOOH by *Shewanella putrefaciens*; The formation of green rust. 5th International Symposium on the Industrial Applications of the Mossbauer Effect. Kluwer Academic Publ, Virginia Beach, Virginia.

P

Parkhurst, D.L., Appelo, C.A.J. 1999. PHREEQC (Version 2) - A computer program for speciation, batch-reaction, one-dimensional transport, and inverse geochemical calculations. U.S. Geological Survey Water-Resources Investigations Report.

Patrick, J.W.H., Henderson, R.E. 1981. A method for controlling redox potential in packed soil cores. Soil Science Society of America Journal 45, 35-38.

Patrick, J.W.H., Jugsujinda, A. 1992. Sequential reduction and oxidation of inorganic nitrogen, manganese, and iron in flooded soil. Soil Science Society of America Journal 56, 1071-1073.

Pédrot, M., Dia, A., Davranche, M., Bouhnik-Le Coz, M., Henin, O., Gruau, G., 2008. Insights into colloid-mediated trace element release at the soil/water interface. Journal of Colloid and Interface Science 325, 187-197.

Pédrot, M., Dia, A., Davranche, M. 2009a. Dynamic structure of humic substances and its impact on associated Rare Earth Element distribution in waters. Chemical Geology, submitted.

Pédrot, M., Dia, A., Davranche, 2009b. Double pH control on humic substance-borne trace element distribution in soil waters as inferred from ultrafiltration. Journal of Colloid and Interface Science, submitted.

Peiffer, S., Walton-Day, K., Macalady, D.L., 1999. The Interaction of natural organic matter with iron in a wetland (Tennessee Park, Colorado) receiving acid mine drainage. Aquatic Geochemistry 5, 207-223.

Pellerin, J., Van Vliet Lanoë, B., 1994. Cadre géomporphologique du bassin du Coët-Dan et du Haut Evel (Morbihan): Rapport sur les travaux de cartographie et de stratigraphie. Thèse de doctorat non-publié, Université de Brest (France).

Penrose, W.R., Polzer, W.L., Essington, E.H., Nelson, D.M., Orlandini, K.A., 1990. Mobility of plutonium and americium through a shallow aquifer in a semiarid region. Environmental Science & Technology 24, 228.

Perdue, E.M., Beck, K.C., Helmut Reuter, J., 1976. Organic complexes of iron and aluminium in natural waters. Nature 260, 418-420.

Perret, D., Newman, M.E., Nègre, J.-C., Chen, Y., Buffle, J., 1994. Submicron particles in the rhine river-I. Physico-chemical characterization. Water Research 28, 91-106.

Piccolo, A., 2001. The supramolecular structure of humic substances. Soil Science 166, 810-832.

Piccolo, A., Conte, P., Cozzolino, A., 2001. Chromatographic and spectrophotometric properties of dissolved humic substances compared with macromolecular polymers. Soil Science 166, 174-185.

Piccolo, A., Nardi, S., Concheri, G., 1996. Macromolecular changes of humic substances induced by interaction with organic acids. European Journal of Soil Science 47, 319-328.

Pokrovski, G.S., Schott, J., 1998. Experimental study of the complexation of silicon and germanium with aqueous organic species: implications for germanium and silicon transport and Ge/Si ratio in natural waters. Geochimica et Cosmochimica Acta 62, 3413-3428.

Pokrovsky, O.S., Schott, J., 2002. Iron colloids/organic matter associated transport of major and trace elements in small boreal rivers and their estuaries (NW Russia). Chemical Geology 190, 141-179.

Pokrovsky, O.S., Dupré, B., Schott, J., 2005. Fe-Al-organic colloids control of trace elements in peat soil solutions: Results of ultrafiltration and dialysis. Aquatic Geochemistry 11, 241-278.

Pokrovsky, O.S., Schott, J., Dupré, B., 2006. Trace element fractionation and transport in boreal rivers and soil porewaters of permafrost-dominated basaltic terrain in Central Siberia. Geochimica et Cosmochimica Acta 70, 3239-3260.

Ponnamperuma, F.N. 1972. The chemistry of submerged soils. Advances in Agronomy 24, 29-96.

Ponnamperuma, F. N.; Martinez, E.; Loy, T., 1966. Influence of redox potential and partial pressure of carbon dioxide on pH values and suspension effect of flooded soils. Soil Science 101, 421- 431.

Pourret, O., Dia, A., Davranche, M., Gruau, G., Henin, O., Angee, M., 2007a. Organo-colloidal control on major- and trace-element partitioning in shallow groundwaters: Confronting ultrafiltration and modelling. Applied Geochemistry 22, 1568-1582.

Pourret, O., Davranche, M., Gruau, G., Dia, A., 2007b. Organic complexation of rare earth elements in natural waters: Evaluating model calculations from ultrafiltration data. Geochimica et Cosmochimica Acta 71, 2718-2735.

Pourret, O., Davranche, M., Gruau, G., Dia, A., 2007c. Rare earth elements complexation with humic acid. Chemical Geology 243, 128-141.

Pourret, O., Davranche, M., Gruau, G., Dia, A., 2007d. Competition between humic acid and carbonates for rare earth elements complexation. Journal of Colloid and Interface Science 305, 25-31.

Probst, A., El Gh'Mari, A., Aubert, D., Fritz, B., McNutt, R., 2000. Strontium as a tracer of weathering processes in a silicate catchment polluted by acid atmospheric inputs, Strengbach, France. Chemical geology 170, 203-209.

Pullin, M.J., Cabaniss, S.E., 2003a. The effects of pH, ionic strength, and iron-fulvic acid interactions on the kinetics of non-photochemical iron transformations. II. The kinetics of thermal reduction. Geochimica et Cosmochimica Acta 67, 4079-4089.

Pullin, M.J., Cabaniss, S.E., 2003b. The effects of pH, ionic strength, and iron-fulvic acid interactions on the kinetics of non-photochemical iron transformations. I. Iron(II) oxidation and iron(III) colloid formation. Geochimica et Cosmochimica Acta 67, 4067-4077.

Q

Quantin, C., Becquer, T., Rouiller, J.H., Berthelin, J. 2001. Oxide weathering and trace metal release by bacterial reduction in a New Caledonia Ferralsol. Biogeochemistry 53, 323-340.

R

Ranville, J.F., Schmiermund, R., 1999. General aspects of aquatic colloids in environmental geochemistry. In: G.S. Plumlee and M.J. Logson, Editors, The Environmental Geochemistry of Mineral Deposits Part A: Processes, Techniques, and Health Issues, vol. 6A of Reviews in Economic Geology. Society of Economic Geologists, Chelsea.

Rauret, G., Rubio, R., Lopez-Sanchez, J.F., 1989. Optimization of Tessier procedure for metal solid speciation in river sediments. International Journal of Environmental Analytical Chemistry 36, 69-83.

Ren, S.Z., Tombacz, E., Rice, J.A., 1996. Dynamic light scattering from power-law polydisperse fractals: Application of dynamic scaling to humic acid. Physical Review E 53, 2980-2983.

Senesi, N., 1999. Aggregation Patterns and Macromolecular Morphology of Humic Substances: A Fractal Approach. Soil Science 164, 841-856.

Roden, E.E., Lovley, D.R., 1993. Dissimilatory Fe(III) reduction by the marine microorganism desulfuromonas-acetoxidans. Applied and Environmental Microbiology 59, 734-742.

Roden, E.E., Zachara, J.M., 1996. Microbial Reduction of Crystalline Iron(III) Oxides: Influence of Oxide Surface Area and Potential for Cell Growth. Environmental Science & Technology 30, 1618-1628.

Roden, E.E., 2003. Fe(III) Oxide Reactivity Toward Biological versus Chemical Reduction. Environmental Science & Technology 37, 1319-1324.

Roden, E.E., 2006. Geochemical and microbiological controls on dissimilatory iron reduction. Comptes Rendus Geosciences 338, 456-467.

Rose, J., Vilge, A., Olivié-Lauquet, G., Masion, A., Frechou, C., Bottero, J.-Y., 1998. Iron speciation in natural organic matter colloids. Colloids and Surfaces A: Physicochemical and Engineering Aspects 136, 11-19.

Rose, A.L., Waite, T.D., 2002. Kinetic Model for Fe(II) oxidation in seawater in the absence and presence of natural organic matter. Environmental Science & Technology 36, 433-444.

Roy, S.B., Dzombak, D.A., 1996. Colloid release and transport processes in natural and model porous media. Colloids and Surfaces A: Physicochemical and Engineering Aspects 107, 245-262.

Royer, R.A., Burgos, W.D., Fisher, A.S., Unz, R.F., Dempsey, B.A., 2002. Enhancement of biological reduction of hematite by electron shuttling and Fe(II) complexation. Environmental Science & Technology 36, 1939-1946.

Royer, R.A., Dempsey, B.A., Jeon, B.-H., Burgos, W.D., 2004. Inhibition of biological reductive dissolution of hematite by ferrous iron. Environmental Science & Technology 38, 187-193.

Ryan, J.N., Honeyman, B.D., Murphy, R., Shannon, R., 1995. V.M. Goldschmidt Conference, Geochemical Society, Pennsylvania State University.

Ryan, J.N., Elimelech, M., 1996. Colloid mobilization and transport in groundwater. Colloids and Surfaces A: Physicochemical and Engineering Aspects 107, 1-56.

S

Sallez, Y., Bianco, P., Lojou, E. 2000. Electrochemical behavior of c-type cytochromes at clay-modified carbon electrodes: a model for the interaction between proteins and soils. Journal of Electroanalytical Chemistry 493, 37-49.

Schindler, P., Kamber, H.R., 1968. Die acidität von silanolgruppen. Vorläufige Mitteillung. Helvetica Chimica Acta 51, 1781-1786.

Schlautman, M.A., Morgan, J.J., 1994. Adsorption of aquatic humic substances on colloidal-size aluminum oxide particles: Influence of solution chemistry. Geochimica et Cosmochimica Acta 58, 4293-4303.

Schroth, B.K., Sposito, G., 1998. Effect of landfill leachate organic acids on trace metal adsorption by kaolinite. Environmental Science & Technology 32, 1404-1408.

Schulze, D.G., 1989. An introduction to soil mineralogy. In: J.B. Dixon and S.B. Weed, Editors, Minerals in Soil Environments, Soil Science Society of America, Madison, Wisconsin (USA) 1–34.

Schwertmann, U., Taylor, R.M., 1979. Natural and synthetic poorly crystallized lepidocrocite. Clay Minerals 14, 285-293.

Schwertmann, U. and Cornell, R.M., 2000. Iron oxides in the laboratory. Second, Completely Revised and Extended Edition, Wiley-VCH.

Scott, D.T., McKnight, D.M., Blunt-Harris, E.L., Kolesar, S.E., Lovley, D.R., 1998. Quinone moieties act as electron acceptors in the reduction of humic substances by humics-reducing microorganisms. Environmental Science & Technology 32, 2984-2989.

Seaman J.C., Bertsch P.M., Miller W.P., 1995. Chemical controls on colloid generation and transport in a sandy aquifer. Environmental Science & Technology 29, 1808-1815.

Selim H.M., Buchter B., Hinz C., Ma L., 1992. Modeling the transport and retention of cadmium in soils: multireaction and multicomponent approaches. Soil Science Society of America Journal 56, 1004-1015.

Sen, T.K., Mahajan, S.P., Khilar, K.C., 2002. Colloid-Associated contaminant transport in porous media: 1. Experimental studies. American Institute of Chemical Engineer Journal 48, 2366-2374.

Sen, T.K., Khilar, K.C., 2006. Review on subsurface colloids and colloid-associated contaminant transport in saturated porous media. Advances in Colloid and Interface Science 119, 71-96.

Senesi, N., 1999. Aggregation patterns and macromolecular morphology of humic substances: a fractal approach. Soil Science 164, 841-856.

Shi, Z., Allen, H.E., Di Toro, D.M., Lee, S.-Z., Flores Meza, D.M., Lofts, S., 2007. Predicting cadmium adsorption on soils using WHAM VI. Chemosphere 69, 605-612.

Shiller, A.M., 1997. Dissolved trace elements in the Mississippi River: seasonal, interannual, and decadal variability. Geochimica et Cosmochimica Acta 61, 4321-4330.

Shin, H.-S., Monsallier, J.M., Choppin, G.R., 1999. Spectroscopic and chemical characterizations of molecular size fractionated humic acid. Talanta 50, 641-647.

Sholkovitz, E.R., 1995. The aquatic chemistry of rare earth elements in rivers and estuaries. Aquatic Geochemistry 1, 1-34.

Sigg, L., Behra, P., Stumm, W., 2000. Chimie des milieux aquatiques: chimie des eaux naturelles et des interfaces dans l'environnement. Dunod, Paris.

Simpson, A.J., Kingery, W.L., Shaw, D.R., Spraul, M., Humpfer, E., Dvortsak, P., 2001. The application of H-1 HR-MAS NMR spectroscopy for the study of structures and associations of organic components at the solid - Aqueous interface of a whole soil. Environmental Science & Technology 35, 3321-3325.

Skjelkvale B.L., Stoddard J.L., Jeffries D.S., Torseth K., Hogasen T., Bowman J. Mannio J., Monteith D.T., Mosello R., Rogora M.,Rzychon D., Vesely J., Wieting J., Wilander A., Worsztynowicz, A., 2005. Regional scale evidence for improvements in surface water chemistry 1990–2001. Environmental Pollution 137, 165–176.

Smedley, P.L., 1991. The geochemistry of rare earth elements in groundwater from the Carnmenellis area, southwest England. Geochimica Cosmochimica Acta 55, 2767–2779.

Sonke, J.E., Salters, V.J.M., 2006. Lanthanide-humic substances complexation. I. Experimental evidence for a lanthanide contraction effect. Geochimica et Cosmochimica Acta 70, 1495-1506.

Sparks, D.L, 1995. Environmental soil chemistry. Academic Press, London.

Sposito, G., 1984. The Surface Chemistry of Soils, Oxford University Press, New York.

Steinmann, P., Shotyk, W., 1997. Chemical composition, pH, and redox state of sulfur and iron in complete vertical porewater profiles from two Sphagnum peat bogs, Jura Mountains, Switzerland. Geochimica et Cosmochimica Acta 61, 1143-1163.

Steinmann, M., Stille, P., 1997. Rare earth element behaviour and Pb, Sr, Nd isotope systhematics in a heavy metal contaminated soil. Applied Geochemistry 12, 607-624.

Stern, J.C., Sonke, J.E., Salters, V.J.M., 2007. A capillary electrophoresis-ICP-MS study of rare earth element complexation by humic acids. Chemical Geology 246, 170-180.

Stevenson, F.J., 1994. Humus Chemistry. Genesis, composition, reactions, 2nd Ed. John Wiley & Sons, New York.

Stone, A.T., Morgan, J.J. 1984. Reduction and dissolution of manganese (III) and manganese (IV) oxides by organics. 2. Survey of the reactivity of organics. Environmental Science & Technology 18, 617-624.

Strobel, B.W., Borggaard, O.K., Hansen, H.C.B., Andersen, M.K., Raulund-Rasmussen, K., 2005. Dissolved organic carbon and decreasing pH mobilize cadmium and copper in soil. European Journal of Soil Science 56, 189-196.

Stumm, W., Sulzberger, B., 1992. The cycling of iron in natural environments: Considerations based on laboratory studies of heterogeneous redox processes. Geochimica Cosmochimica Acta 56, 3233-3257.

Stumm, W., Morgan, J.J., 1996. Aquatic Chemistry. Wiley Intersciences, New York.

Suteerapataranon, S., Bouby, M., Geckeis, H., Fanghanel, T., Grudpan, K., 2006. Interaction of trace elements in acid mine drainage solution with humic acid. Water Research 40, 2044-2054.

Suter, D., Banwart, S., Stumm, W., 1991. Dissolution of hydrous iron (III) oxides by reductive mechanisms. Langmuir 7, 809-813.

Sutton, R., Sposito, G., 2005. Molecular structure in soil humic substances: the new view. Environmental Science & Technology 39, 9009-9015.

Swift, R.S., 1999. Macromolecular properties of soil humic substances: fact, fiction, and opinion. Soil Science 164, 790-802.

T

Taillefert, M., Lienemann, C.-P., Gaillard, J.-F., Perret, D., 2000. Speciation, reactivity, and cycling of Fe and Pb in a meromictic lake. Geochimica et Cosmochimica Acta 64, 169-183.

Taillefert, M., Beckler, J.S., Carey, E., Burns, J.L., Fennessey, C.M., DiChristina, T.J., 2007. Shewanella putrefaciens produces an Fe(III)-solubilizing organic ligand during anaerobic respiration on insoluble Fe(III) oxides. Journal of Inorganic Biochemistry 101, 1760-1767.

Tamura, H., Kawamura, S., Hagayama, M., 1980. Acceleration of the oxidation of Fe2+ ions by Fe(III)-oxyhydroxides. Corrosion Science 20, 963-971.

Tang, J., Johannesson, K.H., 2003. Speciation of rare earth elements in natural terrestrial waters: assessing the role of dissolved organic matter from the modeling approach. Geochimica et Cosmochimica Acta 67, 2321-2339.

Tanizaki, Y., Shimokawa, T., Yamazaki, M., 1992. Physico-chemical speciation of trace elements in urban streams by size fractionation. Water Research 26, 55-63.

Taylor, S.R., McLennan, S.M., 1985. The continental crust: its composition and evolution. Blackwell, Oxford.

Taylor, S.R., McLennan, S.M., 1988. The significance of the rare earths in geochemistry and cosmochemistry. In: K.A. Gschneidner and L. Eyring, Editors, Handbook on the Physics and Chemistry of Rare Earths vol. 11, Chap. 79, North-Holland, Amsterdam, 485–578.

Thompson, A., Chadwick, O.A., Boman, S., Chorover, J., 2006. Colloid mobilization during soil iron redox oscillations. Environmental Science & Technology 40, 5743-5749.

Thurman, E.M., 1985. Organic geochemistry of natural waters. In: Nijhoff/Junk (Ed.), Dordrechtthe, Netherlands.

Tiller, C.L., O'Melia, C.R., 1993. Natural organic matter and colloidal stability: models and measurements. Colloids and Surfaces A: Physicochemical and Engineering Aspects 73, 89-102.

Tipping, E., Heaton, M.J. 1983. The adsorption of aquatic humic substances by two oxides of manganese. Geochimica et Cosmochimica Acta 47, 1393-1397.

Tipping, E., 2002. Cation binding by humic substances. In: Press, C.U. (Ed.), New-York.

Tipping, E., Rey-Castro, C., Bryan, S.E., Hamilton-Taylor, J., 2002. Al(III) and Fe(III) binding by humic substances in freshwaters, and implications for trace metal speciation. Geochimica et Cosmochimica Acta 66, 3211-3224.

Todorova, S.G., Siegel, D.I., Costello, A.M., 2005. Microbial Fe(III) reduction in a minerotrophic wetland - geochemical controls and involvement in organic matter decomposition. Applied Geochemistry 20, 1120-1130.

Tombacz, E., 1999. Colloidal properties of humic acids and spontaneous changes of their colloidal state under variable solution conditions. Soil Science 164, 814-824.

Tombacz, E., Meleg, E., 1990. A theoretical explanation of the aggregation of humic substances as a function of pH and electrolyte concentration. Organic Geochemistry 15, 375-381.

Tombácz, E., Szekeres, M., Baranyi, L., Michéli, E., 1998. Surface modification of clay minerals by organic polyions. Colloids and Surfaces A: Physicochemical and Engineering Aspects 141, 379-384.

Tüfekci, N., Sarikaya, H.Z., 1996. Catalytic effects of high Fe(III) concentrations on Fe(II) oxidation. Water Science and Technology 34, 389-396.

Tyler, G., 2004. Vertical distribution of major, minor, and rare elements in a Haplic Podzol. Geoderma 119, 277-290.

Tyler, G., Olsson, T., 2001. Concentrations of 60 elements in the soil solution as related to the soil acidity. European Journal of Soil Science 52, 151-165.

U

Urrutia, M.M., Roden, E.E., Zachara, J.M., 1999. Influence of aqueous and solid-phase Fe(II) complexants on microbial reduction of crystalline iron(III) oxides. Environmental Science & Technology 33, 4022-4028.

V

Van Beinum, W., Hofmann, A., Meeussen, J.C.L., Kretzschmar, R., 2005. Sorption kinetics of strontium in porous hydrous ferric oxide aggregates: I. The Donnan diffusion model. Journal of Colloid and Interface Science 283, 18-28.

Van Bodegom, P., Broekman, R., Dijk, J., Bakker, C., Aerts, R., 2005. Ferrous iron stimulates phenol oxidase activity and organic matter decomposition in waterlogged wetlands. Biogeochemistry 76, 69-83.

Van Hees, P.A.W., Lundstrom, U.S., 2000. Equilibrium models of aluminium and iron complexation with different organic acids in soil solution. Geoderma 94, 201-221.

Vermeer, A.W.P., Riemsdijk, W.H., Koopal, L.K. 1997. Adsorption of humic acid to mineral particles. 1. Specific and electrostatic interactions. Langmuir 14, 2810-2819.

Vermeer, A.W.P., van Riemsdijk, W.H., Koopal, L.K., 1998. Adsorption of humic acid to mineral particles. 1. Specific and electrostatic interactions. Langmuir 14, 2810-2819.

Vermeer, A.W.P., McCulloch, J.K., van Riemsdijk, W.H., Koopal, L.K., 1999. Metal ion adsorption to complexes of humic acid and metal oxides; Deviations from the additivity rule. Environmental Science & Technology 33, 3892-3897.

Viers, J., Dupré, B., Polve, M., Schott, J., Dandurand, J.-L., Braun, J.-J., 1997. Chemical weathering in the drainage basin of a tropical watershed (Nsimi-Zoetele site, Cameroon) : comparison between organic-poor and organic-rich waters. Chemical Geology 140, 181-206.

Vilks, P., Cramer, J.J., Bachinski, D.B., Doern, D.C., Miller, H.G., 1993. Studies of colloids and suspended particles, Cigar Lake uranium deposit, Saskatchewan, Canada. Applied Geochemistry 8, 605-616.

Violleau, D., 1999. Intérêt du fractionnement et de l'extraction des matières organiques naturelles d'eaux de surface pour l'étude de leurs propriétés structurales et de leur pouvoir complexant vis-à-vis du cuivre. Thèse de doctorat, Université de Poitiers (France).

Voelker, B.M., Sulzberger, B., 1996. Effects of fulvic acid on Fe(II) oxidation by hydrogen peroxide. Environmental Science & Technology 30, 1106-1114.

Voelker, B.M., Morel, F.M.M., Sulzberger, B., 1997. Iron redox cycling in surface waters: effects of humic substances and light. Environmental Science & Technology 31, 1004-1011.

Voegelin, A., Barmettler, K., Kretzschmar, R., 2003. Heavy metal release from contaminated soils: comparison of column leaching and batch extraction results. Journal of Environmental Quality 32, 865-875.

W

Waksman, S.A., 1932. Principles of soil microbiology. Williams & Wilkins Co. Baltimore.

Warren, L.A., Haack, E.A., 2001. Biogeochemical controls on metal behaviour in freshwater environments. Earth-Science Reviews 54, 261-320.

Weber, T., 2006. Étude expérimentale et modélisation des modes d'association du fer avec la matière organique naturelle. Thèse de doctorat, Université Paris VI (France).

Weng, L.P., Koopal, L.K., Hiemstra, T., Meeussen, J.C.L., Van Riemsdijk, W.H., 2005. Interactions of calcium and fulvic acid at the goethite-water interface. Geochimica et Cosmochimica Acta 69, 325-339.

Weng, L.P., Van Riemsdijk, W.H., Hiemstra, T., 2007. Adsorption of humic acids onto goethite: Effects of molar mass, pH and ionic strength. Journal of Colloid and Interface Science 314, 107-118.

Weishaar, J.L., Aiken, G.R., Bergamaschi, B.A., Fram, M.S., Fujii, R., Mopper, K., 2003. Evaluation of specific ultraviolet absorbance as an indicator of the chemical composition and reactivity of dissolved organic carbon. Environmental Science and Technology 37, 4702-4708.

Wershaw, R.L., 1999. Molecular aggregation of humic substances. Soil Science 164, 803-813.

White, F., Bullen, T.D., Schulz, M.S., Blum, A.E., Huntington, T.G., Peters, N.E, 2001. Differential rates of feldspar weathering in granitic regoliths. Geochimica Cosmochimica Acta 65, 847–869.

Whitehead, D.L., Dibb H., Hartley D. 1981. Extractant pH and the release of phenolic compounds from soils, plant roots and leaf litter. Soil Biology & Biochemistry 13, 343-348.

Williams, A.G.B., Scherer, M.M., 2004. Spectroscopic evidence for Fe(II)-Fe(III) electron transfer at the iron oxide-water interface. Environmental Science & Technology 38, 4782-4790.

Wiseman, C.L.S., Püttmann, W., 2006. Interactions between mineral phases in the preservation of soil organic matter. Geoderma 134, 109-118.

Wong, J.W.C., Li, K.L., Zhou, L.X., Selvam, A., 2007. The sorption of Cd and Zn by different soils in the presence of dissolved organic matter from sludge. Geoderma 137, 310-317.

Worrall, F., Pearson, D.G., 2001. The development of acidic groundwaters in coal-bearing strata: Part I. Rare earth element fingerprinting. Applied Geochemistry 16, 1465-1480.

Y

Yamamoto, Y., Takahashi, Y., Shimizu, H., 2005. Systematics of stability constants of fulvate complexes with rare earth ions. Chemistry Letters 34, 880-881.

Yamamoto, Y., Takahashi, Y., Shimizu, H., 2006. Interpretation of REE patterns in natural water based on the stability constants. Geochimica et Cosmochimica Acta 70, A717.

Yamamoto, Y., Takahashi, Y., Shimizu, H., 2008. Systematics on the stability constants of REE-humic complexes at various metal loading levels. 8th Annual V M Goldschmidt Conference. Pergamon-Elsevier Science Ltd, Vancouver, CANADA, pp. A1051-A1051.

Yan, X. P., Kerrich, R., Hendry, M. J., 1999. Sequential leachates of multiple grain size fractions from a clay-rich till, Saskatchewan, Canada: implications for controls on the rare earth element geochemistry of porewaters in an aquitard. Chemical Geology 158, 53-79.

Yee, N., Fowle, D.A., Ferris, F.G., 2004. A Donnan potential model for metal sorption onto *Bacillus subtilis*. Geochimica et Cosmochimica Acta 68, 3657-3664.

Yéghicheyan, D., Carignan, J., Valladon, M., Coz, M.B., Cornec, F.L., Castrec-Rouelle, M., Robert, M., Aquilina, L., Aubry, E., Churlaud, C., Dia, A., Deberdt, S., Dupre, B., Freydier, R., Gruau, G., Henin, O., Kersabiec, A.-M., Mace, J., Marin, L., Morin, N., Petitjean, P., Serrat, E.,

2001. A Compilation of silicon and thirty one trace elements measured in the natural river water reference material SLRS-4 (NRC-CNRC). Geostandards and Geoanalytical Research 25, 465-474.

You, S.-J., Yin, Y., Allen, H.E., 1999. Partitioning of organic matter in soils: effects of pH and water/soil ratio. The Science of The Total Environment 227, 155-160.

You, S.-J., Thakali, S., Allen, H.E., 2006. Characteristics of soil organic matter (SOM) extracted using base with subsequent pH lowering and sequential pH extraction. Environment International 32, 101-105.

Z

Zachara, J.M., Fredrickson, J.K., Smith, S.C., Gassman, P.L., 2001. Solubilization of Fe(III) oxide-bound trace metals by a dissimilatory Fe(III) reducing bacterium. Geochimica et Cosmochimica Acta 65, 75-93.

Zachara, J.M., Kukkadapu, R.K., Fredrickson, J.K., Gorby, Y.A., Smith, S.C., 2002. Biomineralization of poorly crystalline Fe(III) oxides by dissimilatory metal reducing bacteria (DMRB). Geomicrobiology Journal 19, 179 - 207.

Zhang, X., Sun, H., Zhang, Z., Niu, Q., Chen, Y., Crittenden, J.C., 2007. Enhanced bioaccumulation of cadmium in carp in the presence of titanium dioxide nanoparticles. Chemosphere 67, 160-166.

Zmirou, D., Bard, D., Dab, W., Dor, F., Goldberg, M., Hubert, P., Potelon J.L., Quénel, P., 2000. Quels risques pour notre santé? Syros, Paris.

Zuyi, T., Taiwei, C., Jinzhou, D., XiongXin, D., Yingjie, G., 2000. Effect of fulvic acids on sorption of U(VI), Zn, Yb, I and Se(IV) onto oxides of aluminium, iron and silicon. Applied Geochemistry, **15**, 133-139.